

# Report on the Key Comparison

CCPR-K2.a-2003

## Spectral Responsivity in the Range of 900 nm to 1600 nm

### Final Report

November 30, 2009

Prepared by  
Steven W. Brown, Thomas C. Larason, and Yoshi Ohno  
Optical Technology Division  
National Institute of Standards and Technology (NIST)  
USA



## Table of Contents

1. Introduction.....	1
2. Organization of the Key Comparison .....	1
3. Characterization of the Transfer Detectors prior to the Key Comparison .....	4
3.1 Description of the NIST Spectral Comparator Facility .....	4
3.2 Spectral responsivity of transfer detectors .....	5
3.3 Spatial uniformity of responsivity .....	6
3.4 Linearity .....	6
3.5 Temperature dependence .....	6
3.6 Stability .....	6
4. Tabulated Results from Participating Laboratories .....	9
4.1 BNM-INM .....	10
4.2 CSIR.....	12
4.3 CSIRO.....	14
4.4 HUT .....	16
4.5 IFA-CSIC.....	18
4.6 KRISS .....	20
4.7 NIM.....	22
4.8 NMi-VSL .....	24
4.9 NPL .....	26
4.10 NRC .....	28
4.11 OMH .....	30
4.12 PTB .....	32
4.13 SMU.....	34
4.14 VNIIOFI.....	36
4.15 NIST (Pilot lab).....	38
5. Examination and Correction of the Data .....	46
5.1 Temperature correction to the transfer detector responsivities.....	46
5.2 Repeatability of the measurements at NIST .....	48
5.3 Stability of the transfer detectors .....	48
5.4 Instability and anomalous behavior of transfer detectors .....	51
5.5 Uncertainties associated with Laboratory-NIST transfer .....	55
5.5.1 <i>Repeatability of NIST measurement</i> .....	55
5.5.2 <i>Long-term stability of the comparison scale</i> .....	55
5.5.3 <i>Wavelength scale uncertainty</i> .....	56
5.5.4 <i>Bandwidth effect</i> .....	58
5.5.5 <i>Beam size</i> .....	60
5.5.6 <i>Alignment of detector</i> .....	63
5.5.7 <i>Summary of transfer uncertainties associated with photodiode characteristics</i> .....	63
6. Data Analysis .....	69
6.1 Analysis method.....	69
7. Results of the Comparison .....	72
7.1 Intermediate calculation results .....	72
7.2 Determination of the Key Comparison Reference Values.....	80

7.3 Birge Ratio .....	80
7.4 Summarized laboratory results with respect to the KCRV .....	81
8. Discussion of results .....	106
9. Conclusions.....	109
10. References.....	110
Appendix A. Degree of Equivalence Tables.....	111

### List of Tables

Table 2.1.	List of participants.
Table 2.2.	List of the rounds and photodiodes used.
Table 2.3.	List of transfer detectors and rounds that each detector participated in.
Table 4.1.1.	BNM-INM laboratory results for photodiode IGA001 (NIST04).
Table 4.1.2.	BNM-INM laboratory results for photodiode IGA002 (NIST08).
Table 4.1.3.	BNM-INM laboratory results for photodiode IGA003 (NIST10).
Table 4.2.1.	CSIR laboratory results for photodiode IGA010 (NIST04).
Table 4.2.2.	CSIR laboratory results for photodiode IGA011 (NIST08).
Table 4.2.3.	CSIR laboratory results for photodiode IGA012 (NIST15).
Table 4.3.1.	CSIRO laboratory results for photodiode IGA007 (NIST06).
Table 4.3.2.	CSIRO laboratory results for photodiode IGA008 (NIST14).
Table 4.3.3.	CSIRO laboratory results for photodiode IGA009 (NIST03).
Table 4.4.1.	HUT laboratory results for photodiode IGA004 (NIST06).
Table 4.4.2.	HUT laboratory results for photodiode IGA005 (NIST10).
Table 4.4.3.	HUT laboratory results for photodiode IGA006 (NIST15).
Table 4.5.1.	IFA laboratory results for photodiode IGA007 (NIST04).
Table 4.5.2.	IFA laboratory results for photodiode IGA008 (NIST03).
Table 4.5.3.	IFA laboratory results for photodiode IGA009 (NIST11).
Table 4.6.1.	KRISS laboratory results for photodiode IGA004 (NIST17).
Table 4.6.2.	KRISS laboratory results for photodiode IGA005 (NIST10).
Table 4.6.3.	KRISS laboratory results for photodiode IGA006 (NIST13).
Table 4.7.1.	NIM laboratory results for photodiode IGA007 (NIST04).
Table 4.7.2.	NIM laboratory results for photodiode IGA008 (NIST11).
Table 4.7.3.	NIM laboratory results for photodiode IGA009 (NIST09).
Table 4.8.1.	NMi-VSL laboratory results for photodiode IGA013 (NIST16).
Table 4.8.2.	NMi-VSL laboratory results for photodiode IGA014 (NIST02).
Table 4.8.3.	NMi-VSL laboratory results for photodiode IGA015 (NIST05).
Table 4.9.1.	NPL laboratory results for photodiode IGA001 (NIST07).
Table 4.9.2.	NPL laboratory results for photodiode IGA002 (NIST08).
Table 4.9.3.	NPL laboratory results for photodiode IGA003 (NIST14).
Table 4.10.1.	NRC laboratory results for photodiode IGA001 (NIST16).
Table 4.10.2.	NRC laboratory results for photodiode IGA002 (NIST14).
Table 4.10.3.	NRC laboratory results for photodiode IGA003 (NIST08).
Table 4.11.1.	OMH laboratory results for photodiode IGA004 (NIST07).
Table 4.11.2.	OMH laboratory results for photodiode IGA005 (NIST11).
Table 4.11.3.	OMH laboratory results for photodiode IGA006 (NIST15).

Table 4.12.1.	PTB laboratory results for photodiode IGA007 (NIST18).
Table 4.12.2.	PTB laboratory results for photodiode IGA008 (NIST11).
Table 4.12.3.	PTB laboratory results for photodiode IGA009 (NIST01).
Table 4.13.1.	SMU laboratory results for photodiode IGA004 (NIST07).
Table 4.13.2.	SMU laboratory results for photodiode IGA005 (NIST02).
Table 4.13.3.	SMU laboratory results for photodiode IGA006 (NIST10).
Table 4.14.1.	VNIIOFI laboratory results for photodiode IGA001 (NIST07).
Table 4.14.2.	VNIIOFI laboratory results for photodiode IGA002 (NIST14).
Table 4.14.3.	VNIIOFI laboratory results for photodiode IGA003 (NIST09).
Table 4.15.1	NIST results for detectors measured by BNM-INM.
Table 4.15.2	NIST results for detectors measured by CSIR.
Table 4.15.3	NIST results for detectors measured by CSIRO.
Table 4.15.4	NIST results for detectors measured by HUT.
Table 4.15.5	NIST results for detectors measured by IFA-CSIC.
Table 4.15.6	NIST results for detectors measured by KRISS.
Table 4.15.7	NIST results for detectors measured by NIM.
Table 4.15.8	NIST results for detectors measured by NMi-VSL.
Table 4.15.9	NIST results for detectors measured by NPL.
Table 4.15.10	NIST results for detectors measured by NRC.
Table 4.15.11	NIST results for detectors measured by OMH.
Table 4.15.12	NIST results for detectors measured by PTB.
Table 4.15.13	NIST results for detectors measured by SMU.
Table 4.15.14	NIST results for detectors measured by VNIIOFI.
Table 5.1.	Detector measurement temperatures ( $^{\circ}\text{C}$ ).
Table 5.2.	Repeatability of NIST measurements of the transfer detectors.
Table 5.3.	Uncertainty contribution $u_{\text{long}}(s_{\text{NIST}})$ from the longterm stability of the comparison scale.
Table 5.4	Transfer uncertainty contribution $u_{\text{w},p}^{\text{T}}$ associated with the wavelength scale uncertainty of NIST SCF.
Table 5.5	Transfer uncertainty contribution $u_{\text{bp},p}^{\text{T}}$ associated with the effect of bandpass of NIST SCF.
Table 5.6	Relative difference (%) in measured responsivity for different beam sizes compared to the 1 mm diameter beam used at NIST
Table 5.7	Transfer uncertainty contribution $u_{\text{bs},ij}^{\text{T}}$ (%) associated with the differences in beam size used by the participants and the spatial nonuniformity of transfer photodiodes
Table 5.8.1	BNM-INM additional transfer uncertainty contributions.
Table 5.8.2	CSIR additional transfer uncertainty contributions.
Table 5.8.3	CSIRO additional transfer uncertainty contributions.
Table 5.8.4	HUT additional transfer uncertainty contributions.
Table 5.8.5	IFA additional transfer uncertainty contributions.
Table 5.8.6	KRISS additional transfer uncertainty contributions.
Table 5.8.7	NIM additional transfer uncertainty contributions.
Table 5.8.8	NMi-VSL additional transfer uncertainty contributions.
Table 5.8.9	NPL additional transfer uncertainty contributions.
Table 5.8.10	NRC additional transfer uncertainty contributions.
Table 5.8.11	OMH additional transfer uncertainty contributions.

Table 5.8.12	PTB additional transfer uncertainty contributions.
Table 5.8.13	SMU additional transfer uncertainty contributions.
Table 5.8.14	VNIIOFI additional transfer uncertainty contributions.
Table 7.1.	BNM-INM intermediate calculation results (values in %).
Table 7.2.	CSIR intermediate calculation results (values in %).
Table 7.3.	CSIRO intermediate calculation results (values in %).
Table 7.4.	HUT intermediate calculation results (values in %).
Table 7.5.	IFA intermediate calculation results (values in %).
Table 7.6.	KRISS intermediate calculation results (values in %).
Table 7.7.	NIM intermediate calculation results (values in %).
Table 7.8.	NMi-VSL intermediate calculation results (values in %).
Table 7.9.	NPL intermediate calculation results (values in %).
Table 7.10.	NRC intermediate calculation results (values in %).
Table 7.11.	OMH intermediate calculation results (values in %).
Table 7.12.	PTB intermediate calculation results (values in %).
Table 7.13.	SMU intermediate calculation results (values in %).
Table 7.14.	VNIIOFI intermediate calculation results (values in %).
Table 7.15.	Combined uncertainty $u_c(\bar{A}_i)$ for each laboratory (no cut-off applied) [%].
Table 7.16.	Corresponding weights $w_i$ used in the calculation of the KCRV if no cut-off value is applied.
Table 7.17.	$u_{\text{cut-off}}$ at each wavelength [%].
Table 7.18.	Combined uncertainty $u_{c,\text{adj}}(\bar{A}_i)$ of each lab with cut-off applied [%].
Table 7.19.	Corresponding weights $w_i$ used in the calculation of the KCRV, with cut-off applied.
Table 7.20.	Birge ratios calculated with and without cutoff (CSIR and KRISS excluded).
Table 7.21.	The KCRV $\bar{A}_{\text{KCRV}}$ and its uncertainty $u(\bar{A}_{\text{KCRV}})$ and $U(\bar{A}_{\text{KCRV}})$ with $k=2$ .
Table 7.22.	Laboratory differences $d_i$ [%] from the KCRV, or unilateral Degree of Equivalence $D_i$ [%].
Table 7.23.	Standard uncertainties $u(d_i)$ in laboratory difference $d_i$ [%].
Table 7.24.	Expanded uncertainties $U(d_i)$ [%] in laboratory difference, or $U(D_i)$ [%] in DoE, with coverage factor $k=2$ .
Table 7.25.	Laboratories' reported uncertainties $u_i$ [%].
Table 7.26.	Laboratory name and associated figure label.
Table A1.	900 nm Unilateral and Bilateral Degrees of Equivalence (unit: %)
Table A2.	950 nm Unilateral and Bilateral Degrees of Equivalence (unit: %)
Table A3.	1000 nm Unilateral and Bilateral Degrees of Equivalence (unit: %)
Table A4.	1050 nm Unilateral and Bilateral Degrees of Equivalence (unit: %)
Table A5.	1100 nm Unilateral and Bilateral Degrees of Equivalence (unit: %)
Table A6.	1150 nm Unilateral and Bilateral Degrees of Equivalence (unit: %)
Table A7.	1200 nm Unilateral and Bilateral Degrees of Equivalence (unit: %)
Table A8.	1250 nm Unilateral and Bilateral Degrees of Equivalence (unit: %)
Table A9.	1300 nm Unilateral and Bilateral Degrees of Equivalence (unit: %)
Table A10.	1350 nm Unilateral and Bilateral Degrees of Equivalence (unit: %)

Table A11.	1400 nm Unilateral and Bilateral Degrees of Equivalence (unit: %)
Table A12.	1450 nm Unilateral and Bilateral Degrees of Equivalence (unit: %)
Table A13.	1500 nm Unilateral and Bilateral Degrees of Equivalence (unit: %)
Table A14.	1550 nm Unilateral and Bilateral Degrees of Equivalence (unit: %)
Table A15.	1600 nm Unilateral and Bilateral Degrees of Equivalence (unit: %)

## List of Figures

- Figure 2.1. InGaAs photodiode mounted in package used for the key comparison.
- Figure 3.1. Spectral responsivities of photodiodes used in the intercomparison separated by vendor.
- Figure 3.2. Responsivity spatial uniformity (0.2 % contours) of representative InGaAs photodetectors from (a) Ge Power Devices, (b) Fermionics, (c) EG&G Optoelectronics, and (d) Telcom Devices Corporation at 900 nm, 1250 nm and 1600 nm, respectively.
- Figure 3.3. Spectral responsivity linearity measured on the NIST Beam Conjoiner Facility.
- Figure 3.4. Average temperature dependence of the responsivity of the InGaAs transfer detectors over the range from 20 °C to 30 °C.
- Figure 5.1(a) Round 1 transfer detector stability.
- Figure 5.1(b) Round 2 transfer detector stability.
- Figure 5.1(c) Round 3 transfer detector stability.
- Figure 5.1(d) Round 4 transfer detector stability.
- Figure 5.2 (a). Stability of photodiodes over the course of the measurement comparison. Example results for Ge Power Devices photodiodes are shown.
- Figure 5.2 (b). Stability of photodiodes over the course of the measurement comparison. Example results for Fermionics photodiodes are shown.
- Figure 5.2 (c). Stability of photodiodes over the course of the measurement comparison. Example results for EGG Optoelectronics photodiodes are shown
- Figure 5.2 (d). Stability of photodiodes over the course of the measurement comparison. Example results for Telcom Devices photodiodes are shown.
- Figure 5.3. Change in the responsivity of NIST03 after Round 3.
- Figure 5.4. Spectral responsivity uniformity of NIST06 measured after Round 3.
- Figure 5.5. Laboratory results, plotted as difference from NIST, separated by vendor.
- Figure 5.6. An example of the wavelength scale calibration results for the NIST SCF in the near IR region.
- Figure 5.7 (a). Relative sensitivity coefficient for one of NIST working standard detectors (GPD).
- Figure 5.7 (b). Relative sensitivity coefficient for one of the Telcom Devices photodiodes
- Figure 5.8 (a). Relative errors due to bandwidth (4 nm) of the NIST SCF for a typical GPD photodiode.
- Figure 5.8 (b). Relative errors due to bandwidth (4 nm) of the NIST SCF for one of TDC photodiodes.
- Figure 5.9. Responsivity spatial nonuniformity of NIST#13 at 1600 nm.
- Figure 7.1. Weighting factors with no cut-off value applied to the data.

- Figure 7.2. Weighting factors with cut-off value applied to the data.
- Figure 7.3(a). Laboratory differences from the KCRV at 900 nm. Error bars correspond to uncertainties listed in Table 7.24
- Figure 7.3(b). Laboratory differences from the KCRV at 950 nm.
- Figure 7.3(c). Laboratory differences from the KCRV at 1000 nm.
- Figure 7.3(d). Laboratory differences from the KCRV at 1050 nm.
- Figure 7.3(e). Laboratory differences from the KCRV at 1100 nm.
- Figure 7.3(f). Laboratory differences from the KCRV at 1150 nm.
- Figure 7.3(g). Laboratory differences from the KCRV at 1200 nm.
- Figure 7.3(h). Laboratory differences from the KCRV at 1250 nm.
- Figure 7.3(i). Laboratory differences from the KCRV at 1300 nm.
- Figure 7.3(j). Laboratory differences from the KCRV at 1350 nm.
- Figure 7.3(k). Laboratory differences from the KCRV at 1400 nm.
- Figure 7.3(l). Laboratory differences from the KCRV at 1450 nm.
- Figure 7.3(m). Laboratory differences from the KCRV at 1500 nm.
- Figure 7.3(n). Laboratory differences from the KCRV at 1550 nm.
- Figure 7.3(o). Laboratory differences from the KCRV at 1600 nm.
- Figure 7.4(a). BNM-INM differences from the KCRV.
- Figure 7.4(b). CSIR differences from the KCRV.
- Figure 7.4(c). CSIRO differences from the KCRV.
- Figure 7.4(d). HUT differences from the KCRV.
- Figure 7.4(e). IFA differences from the KCRV.
- Figure 7.4(f). KRISS differences from the KCRV.
- Figure 7.4(g). NIM differences from the KCRV.
- Figure 7.4(h). NIST differences from the KCRV.
- Figure 7.4(i). NMI-VSL differences from the KCRV.
- Figure 7.4(j). NPL differences from the KCRV.
- Figure 7.2(k). NRC differences from the KCRV.
- Figure 7.4(l). OMH differences from the KCRV.
- Figure 7.4(m). PTB differences from the KCRV.
- Figure 7.4(n). SMU differences from the KCRV.
- Figure 7.4(o). VNIIOFI differences from the KCRV.
- Figure 8.1. Laboratory differences  $d_i$  [%] from the KCRV listed in Table 7.22.
- Figure 8.2. Magnification (-1.0 % to 1.0 %) of the Laboratory differences  $d_i$  [%] from the KCRV listed in Table 7.22.
- Figure 8.3. Laboratories' reported uncertainties  $u_i$  [%] listed in Table 7.25.
- Figure 8.4 (a). Comparison of the results between CCPR K2.a and CCPR K2.b (single photodiodes) at 900 nm.
- Figure 8.4 (b). Comparison of the results between CCPR K2.a and CCPR K2.b (single photodiodes) at 950 nm .
- Figure 8.4 (c). Comparison of the results between CCPR K2.a and CCPR K2.b (single photodiodes) at 1000 nm

## 1. Introduction

The Mutual Recognition Arrangement (MRA) for national measurements standards and for calibration and measurement certificates issued by National Metrology Institutes (NMIs) was signed in 1999 by the directors of the NMIs of 38 member states of the Metre Convention and representatives of two international organizations. The objectives of the MRA were to establish the degree of equivalence of national measurements standards maintained by NMIs; to provide for the mutual recognition of calibration and measurement certificates issued by NMIs; and to thereby provide governments and other parties with a secure technical foundation for wider agreements related to international trade, commerce and regulatory affairs.

Under the MRA, the metrological equivalence of national measurement standards is to be determined by a set of key comparisons chosen and organized by the Consultative Committees of the International Committee for Weights and Measures (Comité International des Poids et Mesures, CIPM) working closely with Regional Metrology Organizations (RMOs).

At the annual meeting of the Consultative Committee for Photometry and Radiometry (CCPR) in March 1997, several Key Comparisons were identified in the field of optical radiation metrology, one of which, K2, was spectral responsivity. The Key Comparison of Spectral Responsivity was divided into three separate comparisons covering different spectral regions: K2.a (900 nm to 1600 nm), K2.b (300 nm to 1000 nm), and K2.c (200 nm to 400 nm).

The NMI of the United States of America, the National Institute of Standards and Technology (NIST), was chosen as the Pilot Laboratory for K2.a. A small working group of NMIs participating in the Key Comparison was responsible for the organization of the Key Comparison and development of the Technical Protocol. The working group was comprised of representatives from the National Physical Laboratory, United Kingdom (NPL); the Physikalisch-Technische Bundesanstalt, Germany (PTB); the National Research Council, Canada (NRC), and the NIST. The Pilot Laboratory was responsible for purchasing and characterizing the transfer artifacts used in the Key Comparison.

## 2. Organization of the Key Comparison

15 laboratories including the pilot laboratory participated in this comparison. Table 2.1 shows the list of participants. The names of some of the laboratories have changed since the start of this comparison. In this document, the original names of the laboratories at the time of the start of this comparison are used.

The Key Comparison K2.a was designed to cover the spectral range from 900 nm to 1600 nm. Three transfer standard artifacts were sent to each participating laboratory. Laboratories were asked to make three independent measurements of each artifact, for a total of nine spectral responsivity measurements over the full spectral range. Participating laboratories were requested to make spectral responsivity measurements every 50 nm. An incoherent source, with incident power in the range from 1  $\mu$ W to 100  $\mu$ W and a beam diameter of 1 mm to 3 mm, was recommended. 5 mm diameter indium gallium arsenide (InGaAs) photodiodes with sapphire windows were selected as transfer artifacts. The photodiodes were mounted in 50.8 mm diameter circular holders (Fig.2.1). A thermistor was included in the mount in close proximity to the photodiode to monitor the temperature. Two standard BNC-type connections were provided on the back plate to measure the signal and the thermistor resistance.

The Comparison was organized in a star pattern. Transfer detectors were first measured at NIST, then sent to groups of participating laboratories. They were again measured upon their return to NIST. There were a total of four rounds in the Comparison. The comparison

measurements for the four rounds took place in the period from January 1999 to February 2001; each round took approximately 6 months to complete.

Each photodiode mount was engraved with a serial number starting with 'NIST' for record-keeping. To ensure the validity of the independent measurements by participating laboratories, a cover plate was placed over the mount serial number with a second serial number starting with 'IGA'. Records were kept of both IGA and NIST serial numbers for artifacts sent to each participating laboratory. Laboratories reported measurements for photodiodes with 'IGA' serial numbers. Table 2.2 shows the list of the rounds each laboratory participated in, the 'IGA' serial numbers of the transfer detectors measured by each laboratory, and the corresponding 'NIST' serial numbers. The transfer detectors, identified by their 'NIST' serial number, the manufacturer and the rounds that each photodiode participated in are listed in Table 2.3.

Table 2.1. List of participants

Laboratory	Contact Person(s) <sup>*6</sup>
BNM-INM/CNAM (France) <sup>*1</sup>	Jeanne-Marie Coutin
CSIR (South Africa) <sup>*2</sup>	Bertus Theron, Natasha Nel-Sakharova, Elsie Coetzee
CSIRO (Australia) <sup>*3</sup>	James Gardner, Peter Manson
HUT (Finland) <sup>*4</sup>	Erkki Ikonen, Farshid Manoocheri
IFA-CSIC (Spain)	Antonio Corrons
KRISS (South Korea)	Young Boong Chung, Seung Nam Park, Dong-Hoon Lee
NIST (USA) - Pilot	Steven Brown, Yoshi Ohno
NIM (China)	Lin YanDong
NMi-VSL (Netherlands)	Charles Schrama, Eric van der Ham
NPL (Great Britain)	Nigel Fox, Bill Hartree
NRC (Canada)	Phil Boivin, Charles Bamber
OMH (Hungary) <sup>*5</sup>	Gyula Dezsi, George Andor
PTB (Germany)	Lutz Werner
SMU (Slovakia)	Peter Nemecek
VNIIOFI (Russia)	Victor Sapritsky, Raisa Stolyarevskaya Boris Khlevnoy

\*1 now known as Laboratoire National de Métrologie et d'Essais / Institut National de Métrologie (LNE-INM).

\*2 now known as National Metrology Institute of South Africa (NMISA).

\*3 now known as National Metrology Institute of Australia (NMIA).

\*4 now known as Metrology Research Institute, Centre for Metrology and Accreditation (MIKES).

\*5 now known as Hungarian Trade Licensing Office (MKEH).

\*6 All the names are listed if the contact person changed during the course of the comparison including report preparation.

Table 2.2. List of the rounds and photodiodes used.

	Laboratory	IGA photodiode Serial number			NIST photodiode Serial number		
Round 1	NPL	01	02	03	07	08	14
	HUT	04	05	06	06	10	15
	IFA-CSIC	07	08	09	04	03	11
Round 2	BNM-INM	01	02	03	04	08	10
	OMH	04	05	06	07	11	15
	CSIRO	07	08	09	06	14	03
Round 3	NRC	01	02	03	16	14	08
	SMU	04	05	06	07	02	10
	NIM	07	08	09	04	11	09
Round 4	VNIOFI	01	02	03	07	14	09
	KRISS	04	05	06	17	10	13
	PTB	07	08	09	18	11	01
	CSIR	10	11	12	04	08	15
	NMi-VSL	13	14	15	16	02	05



Figure 2.1. InGaAs photodiode mounted in package used for the key comparison.

Table 2.3. List of transfer detectors and rounds that each detector participated in.

Manufacturer	NIST serial #	Round				Used in all Rounds
Fermionics	01				4	
Fermionics	02			3	4	
Fermionics	03	1	2		-	
Ge Power Devices	04	1	2	3	4	X
Ge Power Devices	05				4	
Ge Power Devices	06	1	2		-	
Ge Power Devices	07	1	2	3	4	X
EG&G Optoelectronics	08	1	2	3	4	X
EG&G Optoelectronics	09			3	4	
EG&G Optoelectronics	10	1	2	3	4	X
EG&G Optoelectronics	11	1	2	3	4	X
Telcom Devices Corp.	12					Never
Telcom Devices Corp.	13				4	
Telcom Devices Corp.	14	1	2	3	4	X
Telcom Devices Corp.	15	1	2		4	
Ge Power Devices	16			3	4	
Ge Power Devices	17				4	
Ge Power Devices	18				4	

### 3. Characterization of the Transfer Detectors prior to the Key Comparison

A total of 18 detectors from 4 different commercial vendors were used in the comparison. Prior to the start of the comparison, the detector spectral responsivities were measured and they were characterized for responsivity uniformity, linearity, stability, and temperature dependence. The polarization dependence was not measured.

#### 3.1 Description of the NIST Spectral Comparator Facility

Measurements were made on the Visible to Near-Infrared Spectral Comparator Facility (Vis/NIR SCF) [Larason 1998]. The facility was designed to measure the spectral power responsivity of test artifacts over the spectral range from 350 nm to 1800 nm. From 700 nm to 1800 nm, InGaAs photodiodes are typically used as working standard detectors. Prior to the start of the Key Comparison, the near infrared spectral responsivity scale was derived on a series of reference standard InGaAs detectors by comparison against a cryogenic radiometer [Shaw 2000].

A constant-voltage-controlled, 100 W quartz-tungsten halogen lamp was used as the excitation source of radiant flux. The source is imaged onto the entrance slit of a modified Cary-14 prism-grating monochromator. The monochromator uses a 30° fused silica prism in series with a 600 line per mm echelette grating. The monochromator slits are set for a 4 nm full-width half

maximum (FWHM) bandwidth. The instrument has a stray light rejection of approximately  $10^{-8}$ ; the exit beam is f/9. A circular 1.1 mm diameter aperture located just after the monochromator exit slit determines the beam size. The exit aperture is imaged onto the detector with 1:1 magnification using two 15.24 cm diameter spherical mirrors and two 7.62 cm diameter flat mirrors.

Two orthogonal linear positioning stages are used to translate the test and working standard detectors in front of the excitation source. Calibrations against the reference standard detectors are done using direct substitution; variations in the source intensity during a calibration are corrected using a beam splitter and monitor detector located after the monochromator. The detectors, translation stages and imaging optics are located inside a light-tight enclosure to eliminate ambient background light from the environment.

### 3.2 Spectral responsivity of transfer detectors

The spectral responsivity of each photodiode used in the comparison was measured just prior to the start of the comparison. In Fig. 3.1, the spectral responsivities of the detectors are shown, separated by vendor.

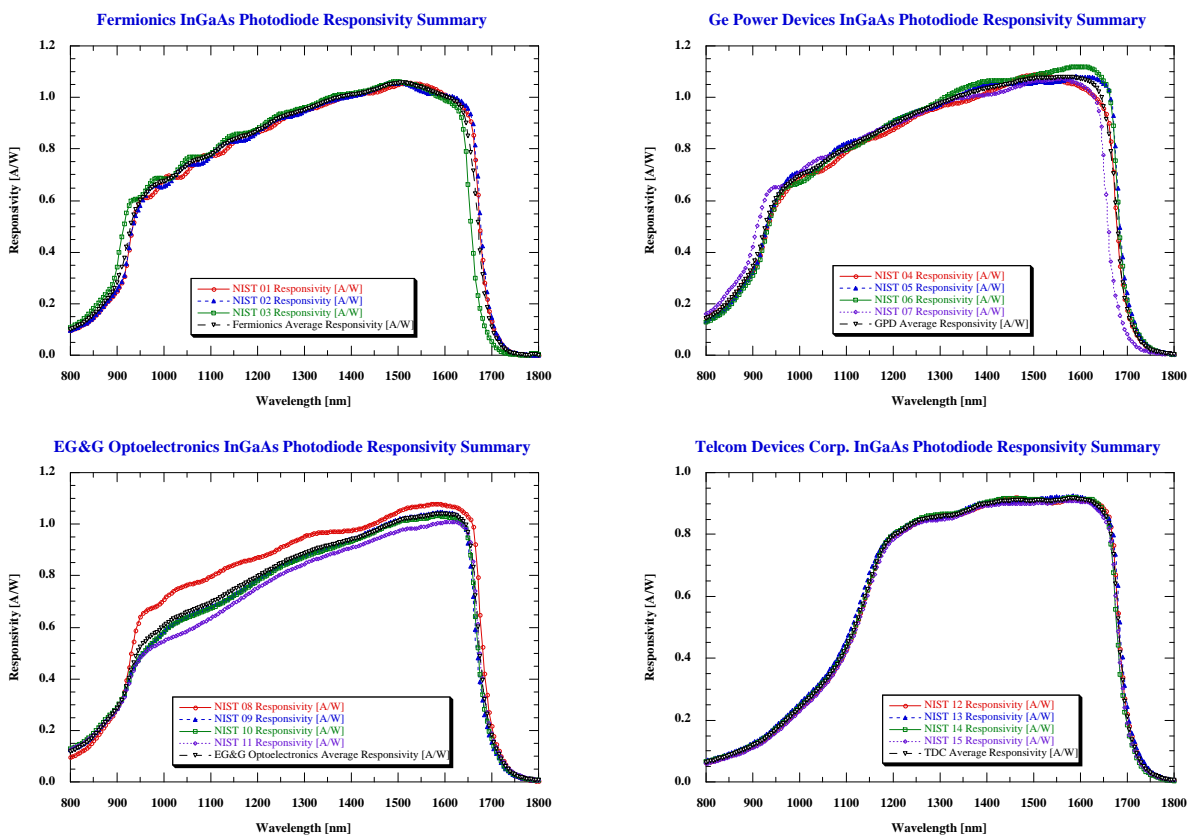


Figure 3.1. Spectral responsivities of photodiodes used in the intercomparison separated by vendor.

### 3.3 Spatial uniformity of responsivity

The spectral responsivity uniformity of each transfer artifact was measured at 900 nm, 1250 nm and 1600 nm. Representative results for one photodiode from each manufacturer are shown in Fig. 3.2. Note the large decrease in the photodiode responsivity uniformity at 900 nm and 1600 nm compared with the uniformity at 1250 nm. No corrections were made to the InGaAs photodiode responsivities to account for differences in incident beam sizes by participating laboratories.

### 3.4 Linearity

The linearity of all transfer and working standard InGaAs detectors was measured on the NIST Beam Conjoiner Facility [Yoon 2003]. In these measurements, the detectors were under-filled with broad-band illumination; the incident power was changed over 4 orders of magnitude (in the power range of interest for the comparison) using the flux addition method. No dependence on incident power was observed; typical results are shown in Fig 3.3. While noting the possibility of a spectral dependence to the linearity below 1000 nm [Fox 1993, Boivin 2000], no linearity correction was applied to the responsivity of the photodiodes.

### 3.5 Temperature dependence

A special thermo-electrically controlled copper mount was designed to measure the temperature dependence of the responsivity of the InGaAs transfer detectors. Using this mount, the spectral responsivities of several transfer artifacts were measured from 20 °C to 30 °C. The average temperature dependence of the responsivities of two photodiodes used in the comparison from each vendor is shown in Fig 3.4. The results for other photodiodes were similar. Because of the large observed temperature dependence, temperature corrections were applied to the data set (see Section 5.1) according to the recommendation by the K2.a Working Group.

### 3.6 Stability

Prior to the start of the comparison, the responsivities and uniformities of several photodiodes were measured, separated in time by 6 months, to assess their short-term stability and compatibility with the Key Comparison protocols. No changes within the measurement reproducibility were observed in any of the photodiodes over that time period. The stabilities of the transfer detectors were also monitored during the comparison (see Sections 5.3).

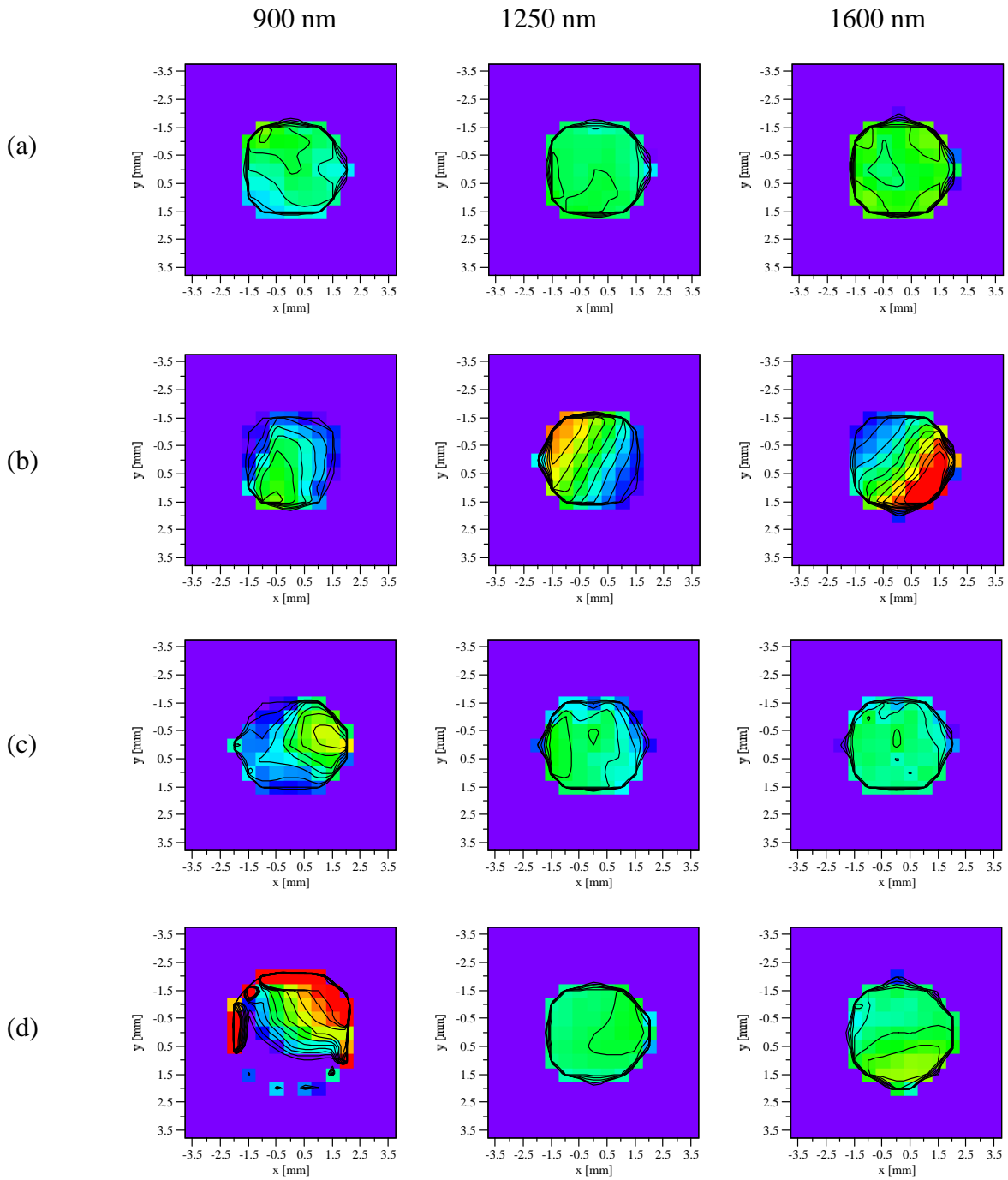
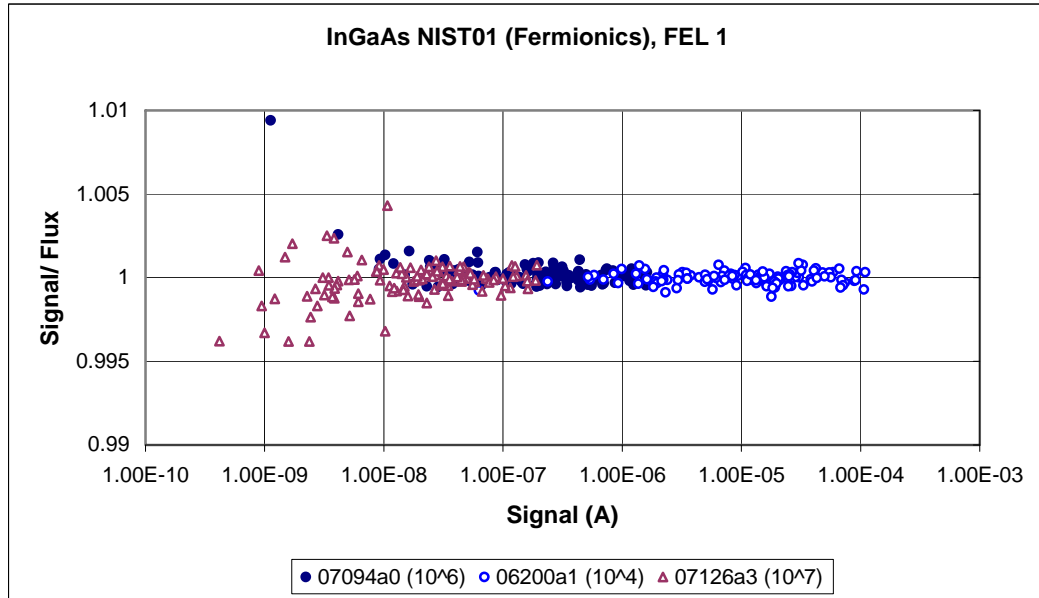
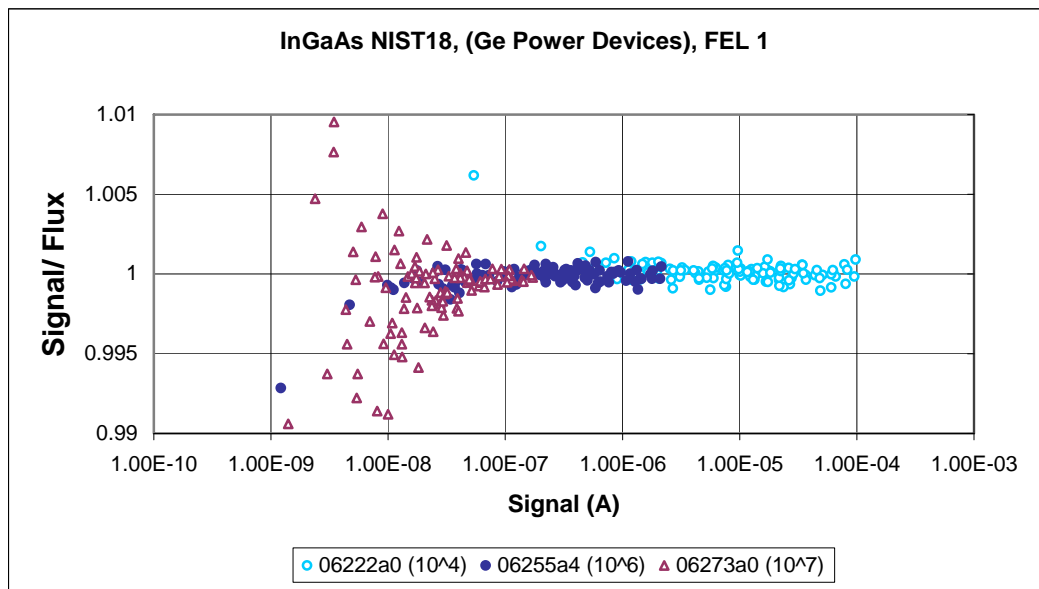


Figure 3.2. Responsivity spatial uniformity (0.2 % contours) of representative InGaAs photodetectors from (a) Ge Power Devices, (b) Fermionics, (c) EG&G Optoelectronics, and (d) Telcom Devices Corporation at 900 nm, 1250 nm and 1600 nm, respectively. All plots are on the same scale, from 99 % to 101 %, with 100 % at the center of the photodiode.



(a) Fermionics photodiode, typical shunt resistance, 15 MΩ.



(b) Ge Power Devices photodiode, typical shunt resistance, 2 MΩ.

Figure 3.3. Spectral responsivity linearity measured on the NIST Beam Conjoiner Facility.

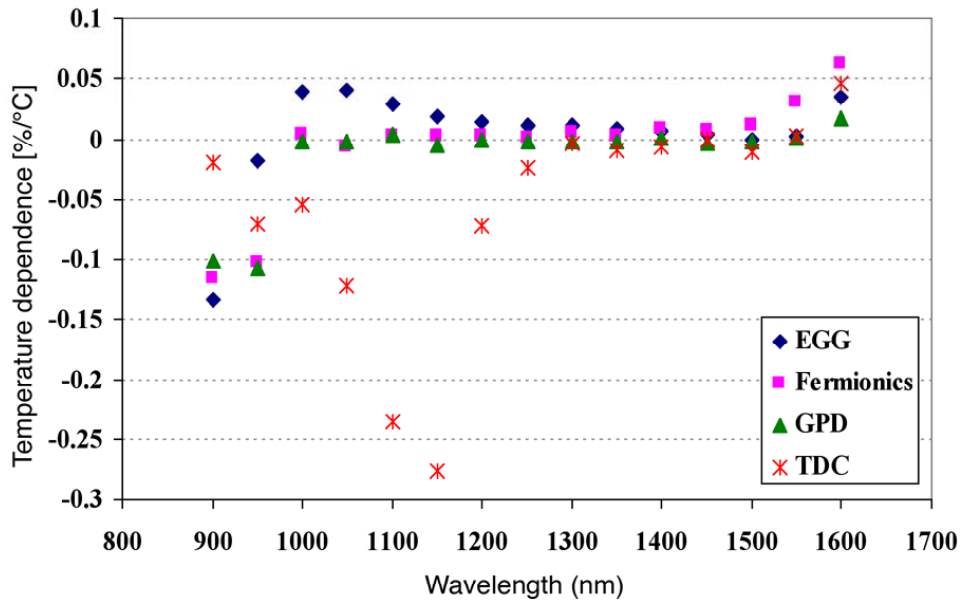


Figure 3.4. Average temperature dependence of the responsivity of the InGaAs transfer detectors over the range from 20 °C to 30 °C.

#### 4. Tabulated Results from Participating Laboratories

In this Section, reported results from the participating Laboratories including the results of the pilot laboratory are tabulated. For each Laboratory, the base of the radiometric scale, the source of the radiant flux, the instrument bandpass, the beam size and geometry, and the incident power are reported in a header section. Next, measurement dates are given, along with thermistor readings at the time of the measurement (in kΩ as well as calculated temperatures). Finally, results from each Laboratory are tabulated according to the detector measured. In each Table, the wavelength, the responsivity and the relative combined standard uncertainty are reported for each of the three measurements, as required by the protocol. Then the average responsivity and the average uncertainty are reported. The values in these tables are the original results reported by the participants and not corrected for temperature differences.

#### 4.1 BNM-INM

**Base of the radiometric scale:** Cryogenic radiometer

**Source:** Quartz halogen lamp

**Bandpass:** 10 nm

**Beam Size:** 3 mm

**Beam Geometry:**

**Incident Power:** 10  $\mu$ W to 20  $\mu$ W

#### Laboratory Results:

Table 4.1.1. BNM-INM laboratory results for photodiode IGA001 (NIST04).

Measurement dates: Not reported.

Thermistor (k $\Omega$ ): 11.23 11.34 11.35

Temperature ( $^{\circ}$ C) 22.492 22.274 22.254

W L [nm]	$s_1$ [A/W]	$u(s_1)$ [%]	$s_2$ [A/W]	$u(s_2)$ [%]	$s_3$ [A/W]	$u(s_3)$ [%]	$s_{avg}$ [A/W]	$u_{avg}$ [%]
900	0.3258	0.3	0.3276	0.31	0.3257	0.3	0.3264	0.30
950	0.5762	0.29	0.5797	0.31	0.5766	0.3	0.5775	0.30
1000	0.6883	0.3	0.6914	0.3	0.6883	0.28	0.6893	0.29
1050	0.7178	0.34	0.722	0.3	0.7185	0.28	0.7194	0.31
1100	0.7861	0.3	0.7887	0.3	0.7856	0.28	0.7868	0.29
1150	0.8377	0.28	0.8405	0.3	0.8371	0.28	0.8384	0.29
1200	0.877	0.29	0.8787	0.3	0.8753	0.28	0.8770	0.29
1250	0.9279	0.28	0.9295	0.3	0.9268	0.28	0.9281	0.29
1300	0.9611	0.34	0.9655	0.29	0.9622	0.28	0.9629	0.30
1350	0.986	0.29	0.9884	0.29	0.9856	0.28	0.9867	0.29
1400	1.02	0.29	1.0194	0.3	1.0156	0.28	1.0183	0.29
1450	1.0588	0.3	1.0571	0.29	1.0548	0.28	1.0569	0.29
1500	1.0877	0.3	1.0883	0.31	1.0852	0.3	1.0871	0.30
1550	1.0887	0.3	1.0886	0.31	1.086	0.28	1.0878	0.30
1600	1.063	0.31	1.0604	0.3	1.0598	0.28	1.0611	0.30

Table 4.1.2. BNM-INM laboratory results for photodiode IGA002 (NIST08).

Measurement dates: Not reported.

Thermistor (k $\Omega$ ): 11.47 11.5 11.53Temperature ( $^{\circ}$ C): 21.917 21.859 21.801

WL [nm]	$s_1$ [A/W]	$u(s_1)$ [%]	$s_2$ [A/W]	$u(s_2)$ [%]	$s_3$ [A/W]	$u(s_3)$ [%]	$S_{avg}$ [A/W]	$u_{avg}$ [%]
900	0.2779	0.21	0.2811	0.29	0.2794	0.28	0.2795	0.26
950	0.6301	0.21	0.6309	0.25	0.6299	0.26	0.6303	0.24
1000	0.7011	0.19	0.7065	0.27	0.7039	0.25	0.7038	0.24
1050	0.7603	0.19	0.7626	0.25	0.7619	0.25	0.7616	0.23
1100	0.791	0.19	0.7952	0.25	0.7931	0.25	0.7931	0.23
1150	0.8404	0.19	0.8445	0.26	0.843	0.25	0.8426	0.23
1200	0.8667	0.19	0.8701	0.25	0.8695	0.25	0.8688	0.23
1250	0.9012	0.19	0.9076	0.25	0.9065	0.25	0.9051	0.23
1300	0.946	0.2	0.95	0.25	0.9492	0.25	0.9484	0.23
1350	0.9669	0.19	0.9693	0.25	0.9687	0.26	0.9683	0.23
1400	0.9689	0.2	0.9753	0.27	0.9752	0.25	0.9731	0.24
1450	0.9941	0.19	1.003	0.25	1.0014	0.25	0.9995	0.23
1500	1.0386	0.19	1.0479	0.25	1.0459	0.26	1.0441	0.23
1550	1.0766	0.19	1.0852	0.29	1.0831	0.29	1.0816	0.26
1600	1.0871	0.23	1.092	0.31	1.0896	0.26	1.0896	0.27

Table 4.1.3. BNM-INM laboratory results for photodiode IGA003 (NIST10).

Measurement dates:

Thermistor (k $\Omega$ ): 11.33 11.25 11.25Temperature ( $^{\circ}$ C): 22.131 22.289 22.289

WL [nm]	$s_1$ [A/W]	$u(s_1)$ [%]	$s_2$ [A/W]	$u(s_2)$ [%]	$s_3$ [A/W]	$u(s_3)$ [%]	$S_{avg}$ [A/W]	$u_{avg}$ [%]
900	0.3015	0.21	0.3025	0.32	0.3017	0.36	0.3019	0.30
950	0.4799	0.21	0.4805	0.3	0.4793	0.33	0.4799	0.28
1000	0.5764	0.22	0.576	0.3	0.5756	0.32	0.5760	0.28
1050	0.6324	0.21	0.6323	0.3	0.6327	0.32	0.6325	0.28
1100	0.6681	0.21	0.6678	0.3	0.6672	0.32	0.6677	0.28
1150	0.717	0.21	0.7162	0.3	0.7156	0.32	0.7163	0.28
1200	0.7755	0.21	0.7734	0.3	0.7741	0.32	0.7743	0.28
1250	0.8271	0.21	0.8257	0.3	0.8259	0.32	0.8262	0.28
1300	0.8661	0.21	0.865	0.3	0.865	0.32	0.8654	0.28
1350	0.8984	0.22	0.8966	0.3	0.8978	0.32	0.8976	0.28
1400	0.9277	0.21	0.9242	0.3	0.9278	0.33	0.9266	0.28
1450	0.9627	0.22	0.961	0.3	0.9628	0.33	0.9622	0.28
1500	0.9994	0.22	0.9966	0.3	0.9978	0.32	0.9979	0.28
1550	1.0297	0.21	1.0286	0.3	1.0264	0.32	1.0282	0.28
1600	1.0406	0.2	1.0417	0.3	1.0409	0.33	1.0411	0.28

## 4.2 CSIR

**Base of the radiometric scale:** Room temperature absolute radiometer (electrical substitution radiometer)

**Source:** Quartz-halogen

**Bandpass:** 5 nm

**Beam Size:** 3 mm for absolute points against absolute radiometer and 2 mm for relative measurements against flat response detector.

**Beam Geometry:** Incident beam convergent at detector surface. Half-angle subtended 6.5 degrees.

**Incident Power:**  $s_1 = 3 \mu\text{W}$  to  $21 \mu\text{W}$ ;  $s_2 = 3 \mu\text{W}$  to  $21 \mu\text{W}$ ;  $s_3 = 14 \mu\text{W}$  to  $22 \mu\text{W}$

### Laboratory Results:

Table 4.2.1. CSIR laboratory results for photodiode IGA010 (NIST04).

Measurement dates: 22-Sep-00 25-Sep-00 26-Sep-00  
 Thermistor (k $\Omega$ ): 9.659 9.399 9.483  
 Temperature ( $^{\circ}\text{C}$ ) 25.901 26.517 26.318

WL [nm]	$s_1$ [A/W]	$u(s_1)$ [%]	$s_2$ [A/W]	$u(s_2)$ [%]	$s_3$ [A/W]	$u(s_3)$ [%]	$s_{\text{avg}}$ [A/W]	$u_{\text{avg}}$ [%]
900	-	-	-	-	0.3311	1.3	0.3311	1.3
950	-	-	0.5779	1.3	0.5838	1.3	0.5809	1.3
1000	0.6957	1.3	0.6930	1.3	0.6966	1.3	0.6951	1.3
1050	0.7245	1.0	0.7252	1.0	0.7259	1.0	0.7252	1.0
1100	0.7943	1.0	0.7945	1.0	0.8007	1.0	0.7965	1.0
1150	0.8456	1.0	0.8455	1.0	0.8461	1.0	0.8457	1.0
1200	0.8839	1.0	0.8860	1.0	-	-	0.8850	1.0
1250	0.9360	1.0	0.9406	1.0	-	-	0.9383	1.0
1300	0.9717	1.0	0.9717	1.0	-	-	0.9717	1.0
1350	0.9980	1.0	0.9976	1.0	-	-	0.9978	1.0
1400	1.0333	1.0	1.0368	1.0	-	-	1.0351	1.0
1450	1.0771	1.0	1.0812	1.0	-	-	1.0792	1.0
1500	1.1089	1.0	1.1163	1.0	-	-	1.1126	1.0
1550	1.1155	1.0	1.1223	1.0	-	-	1.1189	1.0
1600	1.0969	1.0	1.1008	1.0	-	-	1.0989	1.0

Table 4.2.2. CSIR laboratory results for photodiode IGA011 (NIST08).

Measurement dates: 22-Sep-00 25-Sep-00 26-Sep-00  
 Thermistor (k $\Omega$ ): 9.7978 9.5863 9.6052  
 Temperature ( $^{\circ}$ C): 25.464 25.961 25.916

WL [nm]	$s_1$ [A/W]	$u(s_1)$ [%]	$s_2$ [A/W]	$u(s_2)$ [%]	$s_3$ [A/W]	$u(s_3)$ [%]	$s_{avg}$ [A/W]	$u_{avg}$ [%]
900	-	-	-	-	0.2808	1.3	0.2808	1.3
950	0.6411	1.3	-	-	0.6396	1.3	0.6404	1.3
1000	0.7125	1.3	0.7036	1.3	0.7057	1.3	0.7073	1.3
1050	0.7688	1.0	0.7617	1.0	0.7677	1.0	0.7661	1.0
1100	0.8014	1.0	0.7946	1.0	0.7998	1.0	0.7986	1.0
1150	0.8514	1.0	0.8460	1.0	0.8539	1.0	0.8504	1.0
1200	0.8762	1.0	0.8745	1.0	0.8826	1.0	0.8778	1.0
1250	0.9151	1.0	0.9125	1.0	-	-	0.9138	1.0
1300	0.9592	1.0	0.9592	1.0	-	-	0.9592	1.0
1350	0.9788	1.0	0.9825	1.0	-	-	0.9807	1.0
1400	0.9864	1.0	0.9889	1.0	-	-	0.9877	1.0
1450	1.0180	1.0	1.0228	1.0	-	-	1.0204	1.0
1500	1.0679	1.0	1.0741	1.0	-	-	1.0710	1.0
1550	1.1126	1.0	1.1192	1.0	-	-	1.1159	1.0
1600	1.1251	1.0	1.1300	1.0	-	-	1.1276	1.0

Table 4.2.3. CSIR laboratory results for photodiode IGA012 (NIST15).

Measurement dates: 25-Sep-00 25-Sep-00 27-Sep-00  
 Thermistor (k $\Omega$ ): 9.7781 9.6572 9.7285  
 Temperature ( $^{\circ}$ C): 25.558 25.841 25.673

WL [nm]	$s_1$ [A/W]	$u(s_1)$ [%]	$s_2$ [A/W]	$u(s_2)$ [%]	$s_3$ [A/W]	$u(s_3)$ [%]	$s_{avg}$ [A/W]	$u_{avg}$ [%]
900	-	-	-	-	0.1091	1.3	0.1091	1.3
950	0.1495	1.3	0.1484	1.3	-	-	0.1490	1.3
1000	0.2297	1.3	0.2270	1.3	0.2272	1.3	0.2280	1.3
1050	0.3062	1.3	0.3030	1.3	0.3049	1.3	0.3047	1.3
1100	0.4201	1.3	0.4168	1.3	0.4189	1.3	0.4186	1.3
1150	0.6258	1.3	0.6220	1.3	0.6268	1.3	0.6249	1.3
1200	0.7858	1.3	0.7850	1.3	0.7857	1.3	0.7855	1.3
1250	0.8363	1.0	0.8346	1.0	-	-	0.8355	1.0
1300	0.8504	1.0	0.8504	1.0	-	-	0.8504	1.0
1350	0.8717	1.0	0.8747	1.0	-	-	0.8732	1.0
1400	0.8963	1.0	0.8996	1.0	-	-	0.8980	1.0
1450	0.9053	1.0	0.9112	1.0	-	-	0.9083	1.0
1500	0.9139	1.0	0.9194	1.0	-	-	0.9167	1.0
1550	0.9368	1.0	0.9453	1.0	-	-	0.9411	1.0
1600	0.9475	1.0	0.9539	1.0	-	-	0.9507	1.0

### 4.3 CSIRO

**Base of the radiometric scale:** Cryogenic radiometer

**Source:** Tungsten halogen lamp operating at 15V

**Bandpass:** 4 nm

**Beam Size:** 1 mm x 3 mm

**Beam Geometry:** Rectangular image of the monochromator exit slit formed on the photodiode surface, where the beam is converging at  $f/8$ .

**Incident Power:** 10  $\mu$ W (approx.)

Details on the derivation of the uncertainty budget are provided in: "The NML units of spectral responsivity 240 - 1650 nm", Frank Wilkinson, CSIRO Technical Memorandum No. 253, 1998. (PM-HAEA-F18/9).

#### Laboratory Results:

Table 4.3.1. CSIRO laboratory results for photodiode IGA007 (NIST06).

Measurement dates: 12-Aug-99 16-Aug-99 18-Aug-99

Thermistor (k $\Omega$ ): 11.645 11.63 11.279

Temperature ( $^{\circ}$ C) 21.608 21.637 22.32

WL [nm]	$s_1$ [A/W]	$u(s_1)$ [%]	$s_2$ [A/W]	$u(s_2)$ [%]	$s_3$ [A/W]	$u(s_3)$ [%]	$S_{avg}$ [A/W]	$u_{avg}$ [%]
900	0.3058	0.24	0.3065	0.24	0.3065	0.24	0.3063	0.24
950	0.5891	0.14	0.5899	0.14	0.5899	0.14	0.5896	0.14
1000	0.6636	0.21	0.6647	0.21	0.6647	0.21	0.6643	0.21
1050	0.7394	0.14	0.7406	0.14	0.7406	0.14	0.7402	0.14
1100	0.7961	0.14	0.7962	0.14	0.7962	0.14	0.7962	0.14
1150	0.845	0.17	0.845	0.17	0.845	0.17	0.8450	0.17
1200	0.9026	0.11	0.9033	0.11	0.9033	0.11	0.9031	0.11
1250	0.9382	0.09	0.9385	0.09	0.9385	0.09	0.9384	0.09
1300	0.982	0.09	0.9833	0.09	0.9833	0.09	0.9829	0.09
1350	1.032	0.12	1.0334	0.12	1.0334	0.12	1.0329	0.12
1400	1.0564	0.15	1.0572	0.15	1.0572	0.15	1.0569	0.15
1450	1.0615	0.13	1.0629	0.13	1.0629	0.13	1.0624	0.13
1500	1.0811	0.15	1.0827	0.15	1.0827	0.15	1.0822	0.15
1550	1.1175	0.16	1.1195	0.16	1.1195	0.16	1.1188	0.16
1600	1.1369	0.11	1.1364	0.11	1.1364	0.11	1.1366	0.11

Note: The third measurement results ( $S_3$ ) of this photodiode were found to be duplication of the 2nd measurement results by an error by the participant. Since the results were submitted this way and approved with no correction after review of Draft A, no corrections were made in the final report. The effect of this error is considered negligible.

Table 4.3.2. CSIRO laboratory results for photodiode IGA008 (NIST14).

Measurement dates: 12-Aug-99 16-Aug-99 18-Aug-99  
 Thermistor (k $\Omega$ ): 11.575 11.86 11.68  
 Temperature ( $^{\circ}$ C) 21.776 21.235 21.575

WL [nm]	$s_1$ [A/W]	$u(s_1)$ [%]	$s_2$ [A/W]	$u(s_2)$ [%]	$s_3$ [A/W]	$u(s_3)$ [%]	$S_{avg}$ [A/W]	$u_{avg}$ [%]
900	0.1182	0.16	0.118	0.16	0.118	0.16	0.1181	0.16
950	0.1713	0.17	0.1711	0.17	0.1708	0.17	0.1711	0.17
1000	0.2422	0.14	0.242	0.14	0.2418	0.14	0.2420	0.14
1050	0.3207	0.12	0.3206	0.12	0.3204	0.12	0.3206	0.12
1100	0.4381	0.13	0.438	0.13	0.4377	0.13	0.4379	0.13
1150	0.6512	0.12	0.6509	0.12	0.651	0.12	0.6510	0.12
1200	0.8019	0.11	0.8018	0.11	0.8024	0.11	0.8020	0.11
1250	0.8449	0.08	0.8442	0.08	0.8445	0.08	0.8445	0.08
1300	0.8639	0.1	0.8643	0.1	0.8652	0.1	0.8645	0.10
1350	0.8765	0.09	0.8764	0.09	0.8771	0.09	0.8767	0.09
1400	0.9044	0.11	0.9038	0.11	0.9046	0.11	0.9043	0.11
1450	0.9189	0.12	0.9184	0.12	0.9196	0.12	0.9190	0.12
1500	0.9132	0.13	0.9138	0.13	0.9148	0.13	0.9139	0.13
1550	0.9231	0.11	0.9233	0.11	0.9234	0.11	0.9233	0.11
1600	0.9309	0.14	0.929	0.14	0.9303	0.14	0.9301	0.14

Table 4.3.3. CSIRO laboratory results for photodiode IGA009 (NIST03).

Measurement dates: 12-Aug-99 16-Aug-99 18-Aug-99  
 Thermistor (k $\Omega$ ): 11.736 11.315 11.24  
 Temperature ( $^{\circ}$ C) 21.416 22.229 22.378

WL [nm]	$s_1$ [A/W]	$u(s_1)$ [%]	$s_2$ [A/W]	$u(s_2)$ [%]	$s_3$ [A/W]	$u(s_3)$ [%]	$S_{avg}$ [A/W]	$u_{avg}$ [%]
900	0.2438	0.22	0.2442	0.22	0.2436	0.22	0.2439	0.22
950	0.5945	0.19	0.5939	0.19	0.5955	0.19	0.5946	0.19
1000	0.6832	0.13	0.6835	0.13	0.6833	0.13	0.6833	0.13
1050	0.7199	0.3	0.7215	0.3	0.7186	0.3	0.7200	0.30
1100	0.7704	0.22	0.7691	0.22	0.771	0.22	0.7702	0.22
1150	0.837	0.14	0.8366	0.14	0.8357	0.14	0.8364	0.14
1200	0.8647	0.1	0.8637	0.1	0.8648	0.1	0.8644	0.10
1250	0.9138	0.11	0.914	0.11	0.9131	0.11	0.9136	0.11
1300	0.9484	0.06	0.9479	0.06	0.9487	0.06	0.9483	0.06
1350	0.9808	0.07	0.981	0.07	0.9812	0.07	0.9810	0.07
1400	1.0093	0.12	1.0085	0.12	1.0099	0.12	1.0092	0.12
1450	1.0245	0.12	1.0234	0.12	1.024	0.12	1.0240	0.12
1500	1.0534	0.1	1.0536	0.1	1.0533	0.1	1.0534	0.10
1550	1.066	0.13	1.0651	0.13	1.0661	0.13	1.0657	0.13
1600	1.0273	0.22	1.0241	0.22	1.0257	0.22	1.0257	0.22

#### 4.4 HUT

**Base of the radiometric scale:** Cryogenic absolute radiometer

**Source:**

**Bandpass:** 2.0 nm

**Beam Size:** 1.0 mm x 1.7 mm

**Beam Geometry:** A full cone angle of 10 degrees was used for the measurements.

**Incident Power:** 2  $\mu\text{W}$  and 10  $\mu\text{W}$

#### Laboratory Results:

Table 4.4.1. HUT laboratory results for photodiode IGA004 (NIST06).

Measurement dates:	4-May-99	6-May-99	8-May-99
Thermistor (k $\Omega$ ):	10.623	11.324	10.418
Temperature ( $^{\circ}\text{C}$ )	23.665	22.231	24.105

WL [nm]	$s_1$ [A/W]	$u(s_1)$ [%]	$s_2$ [A/W]	$u(s_2)$ [%]	$s_3$ [A/W]	$u(s_3)$ [%]	$S_{\text{avg}}$ [A/W]	$u_{\text{avg}}$ [%]
900	0.307	1.5	0.307	1.5	0.307	1.5	0.3070	1.50
950	0.595	1.7	0.596	1.7	0.596	1.7	0.5957	1.70
1000	0.667	1.7	0.668	1.7	0.666	1.7	0.6670	1.70
1050	0.747	1.7	0.746	1.7	0.747	1.7	0.7467	1.70
1100	0.8	1.7	0.799	1.7	0.798	1.7	0.7990	1.70
1150	0.85	1.7	0.849	1.7	0.849	1.7	0.8493	1.70
1200	0.911	1.7	0.911	1.7	0.91	1.7	0.9107	1.70
1250	0.945	1.7	0.944	1.7	0.943	1.7	0.9440	1.70
1300	0.989	1.7	0.989	1.7	0.989	1.7	0.9890	1.70
1350	1.043	1.7	1.043	1.7	1.042	1.7	1.0427	1.70
1400	1.06	1.7	1.061	1.7	1.059	1.7	1.0600	1.70
1450	1.067	1.7	1.067	1.7	1.065	1.7	1.0663	1.70
1500	1.088	1.7	1.088	1.7	1.088	1.7	1.0880	1.70
1550	1.122	1.7	1.122	1.7	1.123	1.7	1.1223	1.70
1600	1.134	1.7	1.134	1.7	1.135	1.7	1.1343	1.70

Table 4.4.2. HUT laboratory results for photodiode IGA005 (NIST10).

Measurement dates: 4-May-99 5-May-99 7-May-99  
 Thermistor (k $\Omega$ ): 10.381 10.279 10.024  
 Temperature ( $^{\circ}$ C): 24.093 24.316 24.885

WL [nm]	$s_1$ [A/W]	$u(s_1)$ [%]	$s_2$ [A/W]	$u(s_2)$ [%]	$s_3$ [A/W]	$u(s_3)$ [%]	$S_{avg}$ [A/W]	$u_{avg}$ [%]
900	0.326	1.6	0.324	1.6	0.324	1.6	0.3247	1.60
950	0.492	1.8	0.491	1.8	0.491	1.8	0.4913	1.80
1000	0.584	1.8	0.584	1.8	0.583	1.8	0.5837	1.80
1050	0.644	1.8	0.643	1.8	0.644	1.8	0.6437	1.80
1100	0.676	1.8	0.675	1.8	0.676	1.8	0.6757	1.80
1150	0.728	1.8	0.727	1.8	0.727	1.8	0.7273	1.80
1200	0.788	1.8	0.787	1.8	0.787	1.8	0.7873	1.80
1250	0.837	1.8	0.836	1.8	0.837	1.8	0.8367	1.80
1300	0.877	1.8	0.876	1.8	0.876	1.8	0.8763	1.80
1350	0.912	1.8	0.912	1.8	0.912	1.8	0.9120	1.80
1400	0.935	1.8	0.934	1.8	0.935	1.8	0.9347	1.80
1450	0.974	1.8	0.973	1.8	0.973	1.8	0.9733	1.80
1500	1.013	1.8	1.012	1.8	1.012	1.8	1.0123	1.80
1550	1.042	1.8	1.04	1.8	1.042	1.8	1.0413	1.80
1600	1.046	1.8	1.045	1.8	1.047	1.8	1.0460	1.80

Table 4.4.3. HUT laboratory results for photodiode IGA006 (NIST15).

Measurement dates: 2-May-99 5-May-99 7-May-99  
 Thermistor (k $\Omega$ ): 11.736 11.315 11.24  
 Temperature ( $^{\circ}$ C): 21.449 22.263 22.412

WL [nm]	$s_1$ [A/W]	$u(s_1)$ [%]	$s_2$ [A/W]	$u(s_2)$ [%]	$s_3$ [A/W]	$u(s_3)$ [%]	$S_{avg}$ [A/W]	$u_{avg}$ [%]
900	0.108	1.6	0.11	1.6	0.109	1.6	0.1090	1.60
950	0.159	1.9	0.161	1.9	0.16	1.9	0.1600	1.90
1000	0.227	1.7	0.229	1.7	0.229	1.7	0.2283	1.70
1050	0.306	1.8	0.309	1.8	0.308	1.8	0.3077	1.80
1100	0.421	1.7	0.423	1.7	0.422	1.7	0.4220	1.70
1150	0.63	1.7	0.632	1.7	0.63	1.7	0.6307	1.70
1200	0.788	1.7	0.79	1.7	0.79	1.7	0.7893	1.70
1250	0.834	1.7	0.836	1.7	0.836	1.7	0.8353	1.70
1300	0.849	1.7	0.85	1.7	0.851	1.7	0.8500	1.70
1350	0.871	1.7	0.874	1.7	0.873	1.7	0.8727	1.70
1400	0.891	1.7	0.892	1.7	0.892	1.7	0.8917	1.70
1450	0.899	1.7	0.898	1.7	0.9	1.7	0.8990	1.70
1500	0.903	1.7	0.905	1.7	0.905	1.7	0.9043	1.70
1550	0.92	1.7	0.924	1.7	0.923	1.7	0.9223	1.70
1600	0.917	1.7	0.92	1.7	0.92	1.7	0.9190	1.70

## 4.5 IFA-CSIC

**Base of the radiometric scale:** Electrically calibrated pyroelectric radiometer

**Source:** Halogen lamp and monochromator

**Bandpass:** 10 nm

**Beam Size:** 3.2 mm

**Beam Geometry:**

**Incident Power:** 18  $\mu\text{W}$  to 67  $\mu\text{W}$

### Laboratory Results:

Table 4.5.1. IFA laboratory results for photodiode IGA007 (NIST04).

Measurement dates: 4-Apr-99      5-Apr-99      6-Apr-99

Thermistor ( $k\Omega$ ): Error in reported results.

WL [nm]	$s_1$ [A/W]	$u(s_1)$ [%]	$s_2$ [A/W]	$u(s_2)$ [%]	$s_3$ [A/W]	$u(s_3)$ [%]	$s_{\text{avg}}$ [A/W]	$u_{\text{avg}}$ [%]
900	0.3358	1.18	0.336	1.48	0.3357	1.18	0.3358	1.28
950	0.5902	1.18	0.5901	1.3	0.5894	1.13	0.5899	1.20
1000	0.7032	1.19	0.7036	1.23	0.702	1.14	0.7029	1.19
1050	0.7342	1.17	0.7353	1.26	0.7335	1.16	0.7343	1.20
1100	0.8034	1.17	0.8042	1.23	0.8029	1.14	0.8035	1.18
1150	0.8548	1.16	0.856	1.23	0.8539	1.14	0.8549	1.18
1200	0.894	1.16	0.8951	1.24	0.8934	1.13	0.8942	1.18
1250	0.9462	1.19	0.9469	1.21	0.9452	1.14	0.9461	1.18
1300	0.9808	1.19	0.9821	1.24	0.9803	1.13	0.9811	1.19
1350	1.0025	1.16	1.0036	1.19	1.0018	1.16	1.0026	1.17
1400	1.0363	1.15	1.0369	1.15	1.0356	1.15	1.0363	1.15
1450	1.0773	1.17	1.0784	1.2	1.0765	1.16	1.0774	1.18
1500	1.1059	1.16	1.1068	1.18	1.1045	1.14	1.1057	1.16
1550	1.1064	1.14	1.1076	1.18	1.1055	1.17	1.1065	1.16
1600	1.0802	1.16	1.0812	1.19	1.0789	1.16	1.0801	1.17

Table 4.5.2. IFA laboratory results for photodiode IGA008 (NIST03).

Measurement dates: 4-Apr-99 5-Apr-99 6-Apr-99  
 Thermistor (k $\Omega$ ): Error in reported results.

WL [nm]	$s_1$ [A/W]	$u(s_1)$ [%]	$s_2$ [A/W]	$u(s_2)$ [%]	$s_3$ [A/W]	$u(s_3)$ [%]	$s_{avg}$ [A/W]	$u_{avg}$ [%]
900	0.2492	1.18	0.2492	1.48	0.2493	1.21	0.2492	1.29
950	0.6009	1.18	0.6017	1.3	0.6008	1.14	0.6011	1.21
1000	0.6932	1.19	0.6938	1.23	0.6932	1.15	0.6934	1.19
1050	0.7315	1.17	0.7315	1.26	0.7306	1.17	0.7312	1.20
1100	0.783	1.17	0.7843	1.23	0.7825	1.15	0.7833	1.18
1150	0.8482	1.16	0.8488	1.23	0.8474	1.15	0.8481	1.18
1200	0.8797	1.16	0.8809	1.24	0.879	1.14	0.8799	1.18
1250	0.9304	1.19	0.9312	1.21	0.93	1.15	0.9305	1.18
1300	0.9654	1.19	0.9675	1.24	0.9654	1.14	0.9661	1.19
1350	0.9973	1.16	0.9986	1.19	0.9969	1.17	0.9976	1.17
1400	1.0262	1.15	1.0275	1.15	1.0258	1.16	1.0265	1.15
1450	1.0415	1.17	1.043	1.2	1.0413	1.16	1.0419	1.18
1500	1.0715	1.16	1.0722	1.18	1.0699	1.14	1.0712	1.16
1550	1.0843	1.14	1.0863	1.18	1.0838	1.18	1.0848	1.17
1600	1.0466	1.16	1.0488	1.19	1.0464	1.17	1.0473	1.17

Table 4.5.3. IFA laboratory results for photodiode IGA009 (NIST11).

Measurement dates: 4-Apr-99 5-Apr-99 6-Apr-99  
 Thermistor (k $\Omega$ ): Error in reported results.

WL [nm]	$s_1$ [A/W]	$u(s_1)$ [%]	$s_2$ [A/W]	$u(s_2)$ [%]	$s_3$ [A/W]	$u(s_3)$ [%]	$s_{avg}$ [A/W]	$u_{avg}$ [%]
900	0.3037	1.18	0.3035	1.48	0.3044	1.19	0.3039	1.28
950	0.4882	1.18	0.4882	1.3	0.4881	1.14	0.4882	1.21
1000	0.5541	1.19	0.556	1.23	0.5548	1.16	0.5550	1.19
1050	0.5955	1.17	0.5981	1.26	0.5969	1.18	0.5968	1.20
1100	0.6458	1.17	0.647	1.23	0.6461	1.15	0.6463	1.18
1150	0.706	1.16	0.7068	1.23	0.7061	1.16	0.7063	1.18
1200	0.7663	1.16	0.767	1.24	0.7665	1.14	0.7666	1.18
1250	0.818	1.19	0.8186	1.21	0.8177	1.15	0.8181	1.18
1300	0.8584	1.19	0.8602	1.24	0.8592	1.14	0.8593	1.19
1350	0.8931	1.16	0.8952	1.19	0.8941	1.18	0.8941	1.18
1400	0.9212	1.15	0.9234	1.15	0.9231	1.16	0.9226	1.15
1450	0.954	1.17	0.9557	1.2	0.9558	1.17	0.9552	1.18
1500	0.9867	1.16	0.9881	1.18	0.9863	1.14	0.9870	1.16
1550	1.0191	1.14	1.0199	1.18	1.0194	1.18	1.0195	1.17
1600	1.0417	1.16	1.0421	1.19	1.0423	1.17	1.0420	1.17

## 4.6 KRISS

**Base of the radiometric scale:** Spectrally flat pyroelectric detector calibrated with cryogenic radiometer.

**Source:** Tungsten halogen lamp and double monochromator

**Bandpass:** 6 nm

**Beam Size:** 2 mm diameter

**Beam Geometry:** Circular

**Incident Power:** 9  $\mu\text{W}$  to 25  $\mu\text{W}$

### Laboratory Results:

Table 4.6.1. KRISS laboratory results for photodiode IGA004 (NIST17).

Measurement dates: 20-Nov-00 21-Nov-00 22-Nov-00

Thermistor (k $\Omega$ ): 10.391 10.216 10.382

Temperature ( $^{\circ}\text{C}$ ) 23.78 24.169 23.8

WL [nm]	$s_1$ [A/W]	$u(s_1)$ [%]	$s_2$ [A/W]	$u(s_2)$ [%]	$s_3$ [A/W]	$u(s_3)$ [%]	$s_{\text{avg}}$ [A/W]	$u_{\text{avg}}$ [%]
900	0.3107	0.4	0.3112	0.4	0.311	0.4	0.3110	0.40
950	0.6127	0.4	0.612	0.4	0.6127	0.4	0.6125	0.40
1000	0.6788	0.4	0.6791	0.4	0.6784	0.4	0.6788	0.40
1050	0.7536	0.5	0.753	0.5	0.7526	0.5	0.7531	0.50
1100	0.7867	0.5	0.7869	0.5	0.7865	0.5	0.7867	0.50
1150	0.8623	0.5	0.8625	0.5	0.8627	0.5	0.8625	0.50
1200	0.9048	0.5	0.9056	0.5	0.9038	0.5	0.9047	0.50
1250	0.9422	0.5	0.9407	0.5	0.9404	0.5	0.9411	0.50
1300	0.9912	0.5	0.9915	0.5	0.9901	0.5	0.9909	0.50
1350	1.0223	0.5	1.0222	0.5	1.0209	0.5	1.0218	0.50
1400	1.0387	0.5	1.0402	0.5	1.0381	0.5	1.0390	0.50
1450	1.069	0.5	1.0683	0.5	1.0664	0.5	1.0679	0.50
1500	1.1100	0.5	1.1102	0.5	1.1095	0.5	1.1099	0.50
1550	1.1366	0.5	1.1354	0.5	1.1352	0.5	1.1357	0.50
1600	1.1300	0.5	1.1297	0.5	1.1281	0.5	1.1293	0.50

Table 4.6.2. KRISS laboratory results for photodiode IGA005 (NIST10).

Measurement dates: 20-Nov-00 21-Nov-00 22-Nov-00  
 Thermistor (k $\Omega$ ): 10.247 10.048 10.205  
 Temperature ( $^{\circ}$ C): 24.387 24.831 24.48

WL [nm]	$s_1$ [A/W]	$u(s_1)$ [%]	$s_2$ [A/W]	$u(s_2)$ [%]	$s_3$ [A/W]	$u(s_3)$ [%]	$S_{avg}$ [A/W]	$u_{avg}$ [%]
900	0.3134	0.4	0.3144	0.4	0.3137	0.4	0.3138	0.40
950	0.4885	0.4	0.4876	0.4	0.4881	0.4	0.4881	0.40
1000	0.5855	0.4	0.5866	0.4	0.5856	0.4	0.5859	0.40
1050	0.6388	0.5	0.6393	0.5	0.6398	0.5	0.6393	0.50
1100	0.6756	0.5	0.6763	0.5	0.6758	0.5	0.6759	0.50
1150	0.7246	0.5	0.7252	0.5	0.7258	0.5	0.7252	0.50
1200	0.7842	0.5	0.7853	0.5	0.7851	0.5	0.7849	0.50
1250	0.8356	0.5	0.8361	0.5	0.8371	0.5	0.8363	0.50
1300	0.8761	0.5	0.8765	0.5	0.8766	0.5	0.8764	0.50
1350	0.9054	0.5	0.906	0.5	0.9068	0.5	0.9061	0.50
1400	0.9335	0.5	0.9349	0.5	0.9356	0.5	0.9347	0.50
1450	0.9693	0.5	0.9743	0.5	0.9738	0.5	0.9725	0.50
1500	1.0123	0.5	1.0125	0.5	1.0132	0.5	1.0127	0.50
1550	1.0404	0.5	1.0382	0.5	1.042	0.5	1.0402	0.50
1600	1.0532	0.5	1.0543	0.5	1.0548	0.5	1.0541	0.50

Table 4.6.3. KRISS laboratory results for photodiode IGA006 (NIST13).

Measurement dates: 20-Nov-00 21-Nov-00 22-Nov-00  
 Thermistor (k $\Omega$ ): 10.821 10.625 10.767  
 Temperature ( $^{\circ}$ C): 23.28 23.692 23.393

WL [nm]	$s_1$ [A/W]	$u(s_1)$ [%]	$s_2$ [A/W]	$u(s_2)$ [%]	$s_3$ [A/W]	$u(s_3)$ [%]	$S_{avg}$ [A/W]	$u_{avg}$ [%]
900	0.1248	0.4	0.1252	0.4	0.125	0.4	0.1250	0.40
950	0.1808	0.4	0.1805	0.4	0.1805	0.4	0.1806	0.40
1000	0.2546	0.4	0.2542	0.4	0.2529	0.4	0.2539	0.40
1050	0.3341	0.5	0.3337	0.5	0.3324	0.5	0.3334	0.50
1100	0.4610	0.5	0.4598	0.5	0.4588	0.5	0.4599	0.50
1150	0.6796	0.5	0.6807	0.5	0.6796	0.5	0.6800	0.50
1200	0.8036	0.5	0.8034	0.5	0.8015	0.5	0.8028	0.50
1250	0.8444	0.5	0.8436	0.5	0.8442	0.5	0.8441	0.50
1300	0.8558	0.5	0.8571	0.5	0.8567	0.5	0.8565	0.50
1350	0.8793	0.5	0.8799	0.5	0.8784	0.5	0.8792	0.50
1400	0.9003	0.5	0.9	0.5	0.9009	0.5	0.9004	0.50
1450	0.9094	0.5	0.9077	0.5	0.9055	0.5	0.9075	0.50
1500	0.9162	0.5	0.9143	0.5	0.9141	0.5	0.9149	0.50
1550	0.9351	0.5	0.9337	0.5	0.9342	0.5	0.9343	0.50
1600	0.9395	0.6	0.9378	0.6	0.9379	0.6	0.9384	0.50

## 4.7 NIM

**Base of the radiometric scale:** cryogenic radiometer and pyroelectric power meter

**Source:** 250 W quartz halogen lamp

**Bandpass:** 6 nm

**Beam Size:** 3 mm

**Beam Geometry:** f/3.9

**Incident Power:** 7.8  $\mu\text{W}$  to 80  $\mu\text{W}$

### Laboratory Results:

Table 4.7.1. NIM laboratory results for photodiode IGA007 (NIST04).

Measurement dates: 26-Apr-00 29-Apr-00 30-Apr-00  
 Thermistor (k $\Omega$ ): 9.57 8.97 9.2  
 Temperature ( $^{\circ}\text{C}$ ) 26.112 27.533 26.988

WL [nm]	$s_1$ [A/W]	$u(s_1)$ [%]	$s_2$ [A/W]	$u(s_2)$ [%]	$s_3$ [A/W]	$u(s_3)$ [%]	$s_{\text{avg}}$ [A/W]	$u_{\text{avg}}$ [%]
900	0.3430	0.64	0.3391	0.64	0.3409	0.64	0.3410	0.64
950	0.5943	0.48	0.5890	0.48	0.5897	0.48	0.5910	0.48
1000	0.7050	0.46	0.6996	0.46	0.7046	0.46	0.7031	0.46
1050	0.7299	0.40	0.7270	0.40	0.7298	0.40	0.7289	0.40
1100	0.7968	0.47	0.7905	0.47	0.7967	0.47	0.7947	0.47
1150	0.8432	0.40	0.8411	0.40	0.8441	0.40	0.8428	0.40
1200	0.8806	0.46	0.8744	0.46	0.8812	0.46	0.8787	0.46
1250	0.9314	0.43	0.9257	0.43	0.9305	0.43	0.9292	0.43
1300	0.9646	0.43	0.9597	0.43	0.9656	0.43	0.9633	0.43
1350	0.9852	0.43	0.9797	0.43	0.9855	0.43	0.9835	0.43
1400	1.0192	0.42	1.0141	0.42	1.0189	0.42	1.0174	0.42
1450	1.0565	0.46	1.0498	0.46	1.0591	0.46	1.0551	0.46
1500	1.0842	0.50	1.0775	0.50	1.0894	0.50	1.0837	0.50
1550	1.0815	0.52	1.0777	0.52	1.0860	0.52	1.0817	0.52
1600	1.0517	0.57	1.0490	0.57	1.0606	0.57	1.0538	0.57

Table 4.7.2. NIM laboratory results for photodiode IGA008 (NIST11).

Measurement dates: 26-Apr-00 29-Apr-00 30-Apr-00  
 Thermistor (k $\Omega$ ): 9.94 9.35 9.33  
 Temperature ( $^{\circ}$ C) 25.191 26.576 26.624

WL [nm]	$s_1$ [A/W]	$u(s_1)$ [%]	$s_2$ [A/W]	$u(s_2)$ [%]	$s_3$ [A/W]	$u(s_3)$ [%]	$S_{avg}$ [A/W]	$u_{avg}$ [%]
900	0.2866	0.75	0.2924	0.75	0.2907	0.75	0.2899	0.75
950	0.4866	0.39	0.4866	0.39	0.4868	0.39	0.4867	0.39
1000	0.5496	0.44	0.5537	0.44	0.5511	0.44	0.5515	0.44
1050	0.5877	0.45	0.5922	0.45	0.5888	0.45	0.5896	0.45
1100	0.6352	0.45	0.6390	0.45	0.6341	0.45	0.6361	0.45
1150	0.6941	0.39	0.6958	0.39	0.6938	0.39	0.6946	0.39
1200	0.7500	0.44	0.7543	0.44	0.7491	0.44	0.7511	0.44
1250	0.7993	0.40	0.8023	0.40	0.7994	0.40	0.8003	0.40
1300	0.8390	0.43	0.8434	0.43	0.8379	0.43	0.8401	0.43
1350	0.8722	0.41	0.8756	0.41	0.8717	0.41	0.8732	0.41
1400	0.9009	0.39	0.9029	0.39	0.9002	0.39	0.9013	0.39
1450	0.9311	0.46	0.9353	0.46	0.9272	0.46	0.9312	0.46
1500	0.9636	0.49	0.9689	0.49	0.9586	0.49	0.9637	0.49
1550	0.9926	0.53	0.9962	0.53	0.9875	0.53	0.9921	0.53
1600	1.0104	0.59	1.0191	0.59	1.0066	0.59	1.0120	0.59

Table 4.7.3. NIM laboratory results for photodiode IGA009 (NIST09).

Measurement dates: 26-Apr-00 29-Apr-00 30-Apr-00  
 Thermistor (k $\Omega$ ): 9.49 8.91 9.07  
 Temperature ( $^{\circ}$ C) 26.164 27.545 27.164

WL [nm]	$s_1$ [A/W]	$u(s_1)$ [%]	$s_2$ [A/W]	$u(s_2)$ [%]	$s_3$ [A/W]	$u(s_3)$ [%]	$S_{avg}$ [A/W]	$u_{avg}$ [%]
900	0.2919	0.75	0.2977	0.75	0.2995	0.75	0.2964	0.75
950	0.4988	0.49	0.4949	0.49	0.4942	0.49	0.4960	0.49
1000	0.5964	0.43	0.5925	0.43	0.5954	0.43	0.5948	0.43
1050	0.6536	0.41	0.6503	0.41	0.6517	0.41	0.6519	0.41
1100	0.6863	0.44	0.6819	0.44	0.686	0.44	0.6847	0.44
1150	0.7346	0.42	0.7303	0.42	0.7327	0.42	0.7325	0.42
1200	0.7903	0.42	0.786	0.42	0.7905	0.42	0.7889	0.42
1250	0.8438	0.41	0.8393	0.41	0.8425	0.41	0.8419	0.41
1300	0.8829	0.41	0.8788	0.41	0.8828	0.41	0.8815	0.41
1350	0.9136	0.39	0.911	0.39	0.9118	0.39	0.9121	0.39
1400	0.9423	0.40	0.9394	0.40	0.9428	0.40	0.9415	0.40
1450	0.9762	0.51	0.9707	0.51	0.9821	0.51	0.9763	0.51
1500	1.0129	0.51	1.0085	0.51	1.0201	0.51	1.0138	0.51
1550	1.0414	0.57	1.039	0.57	1.0504	0.57	1.0436	0.57
1600	1.0530	0.65	1.0524	0.65	1.0668	0.65	1.0574	0.65

## 4.8 NMi-VSL

### Base of the radiometric scale:

**Source:** 100 W quartz tungsten halogen lamp

**Bandpass:** 9 nm

**Beam Size:** 4 mm in diameter

**Beam Geometry:**  $f/8$

**Incident Power:** 32  $\mu\text{W}$  to 98 $\mu\text{W}$

### Laboratory Results:

Table 4.8.1. NMi-VSL laboratory results for photodiode IGA013 (NIST16).

Measurement dates: 15-Aug-00 24-Aug-00 25-Aug-00

Thermistor (k $\Omega$ ): 11.476 11.412 11.147

Temperature ( $^{\circ}\text{C}$ ): 21.273 21.399 21.929

WL [nm]	$s_1$ [A/W]	$u(s_1)$ [%]	$s_2$ [A/W]	$u(s_2)$ [%]	$s_3$ [A/W]	$u(s_3)$ [%]	$s_{\text{avg}}$ [A/W]	$u_{\text{avg}}$ [%]
900	0.3279	0.57	0.3274	0.57	0.3271	0.57	0.3275	0.57
950	0.6347	0.48	0.6346	0.48	0.6337	0.48	0.6343	0.48
1000	0.7251	0.46	0.7241	0.46	0.7234	0.46	0.7242	0.46
1050	0.7860	0.36	0.7857	0.36	0.7848	0.36	0.7855	0.36
1100	0.8268	0.23	0.8259	0.24	0.8253	0.24	0.8260	0.24
1150	0.9026	0.22	0.9019	0.22	0.9012	0.22	0.9019	0.22
1200	0.9355	0.21	0.9353	0.21	0.9346	0.21	0.9351	0.21
1250	0.9710	0.17	0.9705	0.18	0.97	0.17	0.9705	0.17
1300	1.0159	0.15	1.0155	0.15	1.0149	0.15	1.0154	0.15
1350	1.0399	0.15	1.04	0.16	1.0394	0.16	1.0398	0.16
1400	1.0546	0.17	1.0546	0.17	1.0541	0.17	1.0544	0.17
1450	1.0819	0.15	1.0815	0.15	1.0812	0.15	1.0815	0.15
1500	1.1165	0.15	1.1161	0.16	1.1159	0.15	1.1162	0.15
1550	1.1330	0.37	1.1332	0.37	1.1328	0.37	1.1330	0.37
1600	1.1180	0.73	1.1193	0.73	1.1175	0.73	1.1183	0.73

Table 4.8.2. NMI-VSL laboratory results for photodiode IGA014 (NIST02).

Measurement dates: 15-Aug-00 24-Aug-00 25-Aug-00  
 Thermistor (k $\Omega$ ): 12.135 12.074 11.894  
 Temperature ( $^{\circ}$ C): 20.742 20.854 21.188

WL [nm]	$s_1$ [A/W]	$u(s_1)$ [%]	$s_2$ [A/W]	$u(s_2)$ [%]	$s_3$ [A/W]	$u(s_3)$ [%]	$S_{avg}$ [A/W]	$u_{avg}$ [%]
900	0.2533	0.66	0.2530	0.65	0.2529	0.65	0.2531	0.65
950	0.5809	0.49	0.5802	0.49	0.5806	0.49	0.5806	0.49
1000	0.6562	0.48	0.6557	0.47	0.6549	0.47	0.6556	0.47
1050	0.7412	0.48	0.7406	0.47	0.7394	0.46	0.7404	0.47
1100	0.7737	0.46	0.7726	0.45	0.7737	0.45	0.7733	0.45
1150	0.8330	0.39	0.8328	0.38	0.8314	0.38	0.8324	0.38
1200	0.8683	0.33	0.8676	0.31	0.8682	0.31	0.8680	0.32
1250	0.9215	0.29	0.9213	0.27	0.9206	0.27	0.9211	0.28
1300	0.9468	0.26	0.9465	0.24	0.9463	0.24	0.9465	0.25
1350	0.9875	0.27	0.9874	0.25	0.9871	0.24	0.9873	0.25
1400	1.0053	0.27	1.0053	0.25	1.0049	0.25	1.0052	0.26
1450	1.0340	0.28	1.0338	0.26	1.0341	0.25	1.0340	0.26
1500	1.0593	0.29	1.0594	0.27	1.0588	0.27	1.0592	0.28
1550	1.0472	0.43	1.0473	0.41	1.0462	0.41	1.0469	0.42
1600	1.0313	0.74	1.0291	0.73	1.0304	0.73	1.0303	0.73

Table 4.8.3. NMI-VSL laboratory results for photodiode IGA015 (NIST05).

Measurement dates: 15-Aug-00 24-Aug-00 25-Aug-00  
 Thermistor (k $\Omega$ ): 11.26 11.288 11.193  
 Temperature ( $^{\circ}$ C): 22.293 22.238 22.427

WL [nm]	$s_1$ [A/W]	$u(s_1)$ [%]	$s_2$ [A/W]	$u(s_2)$ [%]	$s_3$ [A/W]	$u(s_3)$ [%]	$S_{avg}$ [A/W]	$u_{avg}$ [%]
900	0.3229	0.55	0.3232	0.55	0.3230	0.55	0.3230	0.55
950	0.6071	0.46	0.6076	0.46	0.6073	0.46	0.6073	0.46
1000	0.7135	0.43	0.7124	0.43	0.7120	0.43	0.7126	0.43
1050	0.7545	0.35	0.7551	0.35	0.7547	0.35	0.7548	0.35
1100	0.8271	0.24	0.8265	0.24	0.8263	0.24	0.8266	0.24
1150	0.8588	0.22	0.8584	0.22	0.8583	0.22	0.8585	0.22
1200	0.9124	0.21	0.9124	0.21	0.9123	0.21	0.9124	0.21
1250	0.9492	0.19	0.9486	0.18	0.9485	0.19	0.9488	0.19
1300	0.9779	0.17	0.9779	0.17	0.9778	0.18	0.9779	0.17
1350	1.0214	0.18	1.0217	0.17	1.0217	0.18	1.0216	0.18
1400	1.0540	0.18	1.0533	0.18	1.0534	0.18	1.0536	0.18
1450	1.0595	0.17	1.0583	0.17	1.0585	0.18	1.0588	0.17
1500	1.0626	0.18	1.0623	0.18	1.0624	0.19	1.0624	0.18
1550	1.0826	0.37	1.0835	0.37	1.0834	0.37	1.0832	0.37
1600	1.1072	0.72	1.1087	0.71	1.1078	0.72	1.1079	0.72

## 4.9 NPL

**Base of the radiometric scale:** Cryogenic radiometer

**Source:** Tungsten strip lamp

**Bandpass:** 6 nm

**Beam Size:** 3.0 mm in diameter

**Beam Geometry:**  $f/7$  converging

**Incident Power:** 1  $\mu\text{W}$  to 5  $\mu\text{W}$

### Laboratory Results:

Table 4.9.1. NPL laboratory results for photodiode IGA001 (NIST07).

Measurement dates: 4-Mar-99      9-Mar-99      10-Mar-99  
 Thermistor (k $\Omega$ ): 11.793    11.821    11.692  
 Temperature ( $^{\circ}\text{C}$ ) 21.258    21.206    21.449

WL [nm]	$s_1$ [A/W]	$u(s_1)$ [%]	$s_2$ [A/W]	$u(s_2)$ [%]	$s_3$ [A/W]	$u(s_3)$ [%]	$S_{\text{avg}}$ [A/W]	$u_{\text{avg}}$ [%]
900	0.3260	0.21	0.3255	0.22	0.3253	0.22	0.3256	0.22
950	0.6245	0.15	0.6237	0.16	0.6237	0.17	0.6240	0.16
1000	0.6723	0.14	0.6721	0.15	0.6715	0.16	0.6720	0.15
1050	0.7535	0.15	0.7528	0.16	0.753	0.16	0.7531	0.16
1100	0.7844	0.15	0.7836	0.16	0.7838	0.17	0.7839	0.16
1150	0.8398	0.15	0.8398	0.16	0.8393	0.16	0.8396	0.16
1200	0.8845	0.15	0.8838	0.16	0.8841	0.17	0.8841	0.16
1250	0.9171	0.15	0.9169	0.16	0.9169	0.17	0.9170	0.16
1300	0.9630	0.13	0.9629	0.14	0.9627	0.15	0.9629	0.14
1350	0.9975	0.15	0.9967	0.16	0.997	0.17	0.9971	0.16
1400	1.0093	0.16	1.0083	0.16	1.0088	0.17	1.0088	0.16
1450	1.0239	0.22	1.0236	0.2	1.0235	0.21	1.0237	0.21
1500	1.0562	0.17	1.0566	0.18	1.0561	0.19	1.0563	0.18
1550	1.0890	0.17	1.0891	0.18	1.0888	0.18	1.0890	0.18
1600	1.0873	0.21	1.0861	0.21	1.0869	0.22	1.0868	0.21

Table 4.9.2. NPL laboratory results for photodiode IGA002 (NIST08).

Measurement dates: 4-Mar-99 9-Mar-99 11-Mar-99  
 Thermistor (k $\Omega$ ): 11.98 11.986 12.005  
 Temperature ( $^{\circ}$ C): 20.95 20.939 20.904

WL [nm]	$s_1$ [A/W]	$u(s_1)$ [%]	$s_2$ [A/W]	$u(s_2)$ [%]	$s_3$ [A/W]	$u(s_3)$ [%]	$S_{avg}$ [A/W]	$u_{avg}$ [%]
900	0.2859	0.24	0.2856	0.24	0.2860	0.24	0.2858	0.24
950	0.6444	0.16	0.6427	0.15	0.6439	0.15	0.6437	0.15
1000	0.7110	0.15	0.7107	0.14	0.7108	0.14	0.7108	0.14
1050	0.7702	0.15	0.7685	0.15	0.7696	0.15	0.7694	0.15
1100	0.8015	0.15	0.8005	0.15	0.8012	0.15	0.8011	0.15
1150	0.8509	0.15	0.8496	0.15	0.8501	0.15	0.8502	0.15
1200	0.8775	0.15	0.876	0.15	0.8769	0.15	0.8768	0.15
1250	0.9136	0.15	0.9131	0.15	0.9135	0.15	0.9134	0.15
1300	0.9579	0.13	0.9569	0.13	0.9572	0.14	0.9573	0.13
1350	0.9779	0.15	0.9761	0.15	0.9766	0.15	0.9769	0.15
1400	0.9814	0.16	0.9801	0.16	0.9805	0.16	0.9807	0.16
1450	1.0093	0.22	1.0091	0.2	1.0091	0.2	1.0092	0.21
1500	1.0554	0.17	1.0557	0.17	1.0553	0.17	1.0555	0.17
1550	1.0945	0.17	1.094	0.17	1.0938	0.17	1.0941	0.17
1600	1.0979	0.21	1.0962	0.2	1.0964	0.2	1.0968	0.20

Table 4.9.3. NPL laboratory results for photodiode IGA003 (NIST14).

Measurement dates: 8-Mar-99 10-Mar-99 11-Mar-99  
 Thermistor (k $\Omega$ ): 12.31 12.354 12.282  
 Temperature ( $^{\circ}$ C): 20.409 20.33 20.459

WL [nm]	$s_1$ [A/W]	$u(s_1)$ [%]	$s_2$ [A/W]	$u(s_2)$ [%]	$s_3$ [A/W]	$u(s_3)$ [%]	$S_{avg}$ [A/W]	$u_{avg}$ [%]
900	0.1193	0.21	0.1190	0.21	0.1192	0.21	0.1192	0.21
950	0.1726	0.17	0.1726	0.17	0.1727	0.17	0.1726	0.17
1000	0.2432	0.22	0.2430	0.22	0.2430	0.22	0.2431	0.22
1050	0.3222	0.18	0.3222	0.18	0.3223	0.18	0.3222	0.18
1100	0.4411	0.16	0.4408	0.16	0.4409	0.16	0.4409	0.16
1150	0.6553	0.16	0.6548	0.16	0.6547	0.16	0.6549	0.16
1200	0.8058	0.19	0.8051	0.19	0.8058	0.19	0.8056	0.19
1250	0.8496	0.16	0.8490	0.16	0.8496	0.16	0.8494	0.16
1300	0.8694	0.13	0.8686	0.14	0.8690	0.13	0.8690	0.13
1350	0.8813	0.15	0.8809	0.15	0.8814	0.15	0.8812	0.15
1400	0.9072	0.16	0.9069	0.16	0.9073	0.16	0.9071	0.16
1450	0.9226	0.2	0.9220	0.2	0.9221	0.2	0.9222	0.20
1500	0.9189	0.17	0.9185	0.17	0.9185	0.17	0.9186	0.17
1550	0.929	0.17	0.9290	0.17	0.9291	0.17	0.9290	0.17
1600	0.9342	0.2	0.9341	0.2	0.9341	0.2	0.9341	0.20

#### 4.10 NRC

**Base of the radiometric scale:** Cryogenic radiometer

**Source:** 100W tungsten halogen lamp

**Bandpass:** 5 nm

**Beam Size:** 3 mm X 1.5 mm

**Beam Geometry:** The angular divergence of the radiation is about  $\pm 2.6^\circ$  ( $f/11$ ).

**Incident Power:** 9  $\mu\text{W}$  to 22  $\mu\text{W}$

#### Laboratory Results:

Table 4.10.1. NRC laboratory results for photodiode IGA001 (NIST16).

Measurement dates: 15-Feb-00 16-Feb-00 17-Feb-00

Thermistor (k $\Omega$ ): 11.235 11.140 11.312

Temperature ( $^\circ\text{C}$ ) 21.752 21.943 21.597

WL [nm]	$s_1$ [A/W]	$u(s_1)$ [%]	$s_2$ [A/W]	$u(s_2)$ [%]	$s_3$ [A/W]	$u(s_3)$ [%]	$s_{\text{avg}}$ [A/W]	$u_{\text{avg}}$ [%]
900	0.3279	0.19	0.3273	0.19	0.3279	0.19	0.3277	0.19
950	0.6340	0.12	0.6339	0.12	0.6346	0.12	0.6342	0.12
1000	0.7211	0.07	0.7219	0.07	0.7217	0.07	0.7216	0.07
1050	0.7842	0.06	0.7848	0.06	0.7846	0.06	0.7845	0.06
1100	0.8234	0.06	0.8236	0.06	0.8237	0.06	0.8236	0.06
1150	0.8999	0.06	0.9002	0.06	0.9003	0.06	0.9001	0.06
1200	0.9330	0.06	0.9333	0.06	0.9335	0.06	0.9333	0.06
1250	0.9681	0.06	0.9683	0.06	0.9688	0.06	0.9684	0.06
1300	1.0129	0.06	1.0131	0.06	1.0135	0.06	1.0132	0.06
1350	1.0386	0.08	1.0380	0.08	1.0383	0.08	1.0383	0.08
1400	1.0526	0.09	1.0513	0.09	1.0521	0.09	1.0520	0.09
1450	1.0794	0.06	1.0790	0.06	1.0790	0.06	1.0791	0.06
1500	1.1143	0.07	1.1139	0.07	1.1140	0.07	1.1141	0.07
1550	1.1329	0.09	1.1327	0.09	1.1326	0.09	1.1327	0.09
1600	1.1187	0.15	1.1186	0.15	1.1185	0.15	1.1186	0.15

Table 4.10.2. NRC laboratory results for photodiode IGA002 (NIST14).

Measurement dates: 15-Feb-00 16-Feb-00 17-Feb-00  
 Thermistor (k $\Omega$ ): 11.735 11.734 11.784  
 Temperature ( $^{\circ}$ C): 21.47 21.472 21.377

WL [nm]	$s_1$ [A/W]	$u(s_1)$ [%]	$s_2$ [A/W]	$u(s_2)$ [%]	$s_3$ [A/W]	$u(s_3)$ [%]	$S_{avg}$ [A/W]	$u_{avg}$ [%]
900	0.1198	0.19	0.1196	0.19	0.1198	0.19	0.1197	0.19
950	0.1720	0.14	0.1719	0.14	0.1722	0.14	0.1720	0.14
1000	0.2429	0.08	0.2432	0.08	0.2432	0.08	0.2431	0.08
1050	0.3215	0.07	0.3215	0.07	0.3216	0.07	0.3215	0.07
1100	0.4391	0.09	0.439	0.09	0.4393	0.09	0.4391	0.09
1150	0.6522	0.09	0.6524	0.09	0.6527	0.09	0.6524	0.09
1200	0.8034	0.06	0.8035	0.06	0.8040	0.06	0.8036	0.06
1250	0.8474	0.06	0.8475	0.06	0.8480	0.06	0.8476	0.06
1300	0.8672	0.06	0.8674	0.06	0.8680	0.06	0.8675	0.06
1350	0.8796	0.08	0.8788	0.08	0.8792	0.08	0.8792	0.08
1400	0.9057	0.09	0.9043	0.09	0.9051	0.09	0.9050	0.09
1450	0.9219	0.06	0.9217	0.06	0.9218	0.06	0.9218	0.06
1500	0.9177	0.06	0.9174	0.06	0.9177	0.06	0.9176	0.06
1550	0.9276	0.06	0.9271	0.06	0.9272	0.06	0.9273	0.06
1600	0.9358	0.06	0.9354	0.06	0.9355	0.06	0.9356	0.06

Table 4.10.3. NRC laboratory results for photodiode IGA003 (NIST08).

Measurement dates: 15-Feb-00 16-Feb-00 17-Feb-00  
 Thermistor (k $\Omega$ ): 11.298 11.526 11.399  
 Temperature ( $^{\circ}$ C): 22.254 21.808 22.055

WL [nm]	$s_1$ [A/W]	$u(s_1)$ [%]	$s_2$ [A/W]	$u(s_2)$ [%]	$s_3$ [A/W]	$u(s_3)$ [%]	$S_{avg}$ [A/W]	$u_{avg}$ [%]
900	0.2876	0.23	0.2871	0.23	0.2876	0.23	0.2874	0.23
950	0.6398	0.12	0.6403	0.12	0.6406	0.12	0.6402	0.12
1000	0.7104	0.07	0.711	0.07	0.7111	0.07	0.7108	0.07
1050	0.7686	0.06	0.7692	0.06	0.769	0.06	0.7689	0.06
1100	0.7995	0.06	0.7997	0.06	0.7999	0.06	0.7997	0.06
1150	0.8489	0.06	0.849	0.06	0.8494	0.06	0.8491	0.06
1200	0.8747	0.06	0.8748	0.06	0.8753	0.06	0.8749	0.06
1250	0.9118	0.06	0.9116	0.06	0.9125	0.06	0.9120	0.06
1300	0.9553	0.06	0.9553	0.06	0.9559	0.06	0.9555	0.06
1350	0.9746	0.08	0.9741	0.08	0.9742	0.08	0.9743	0.08
1400	0.9787	0.09	0.9773	0.09	0.978	0.09	0.9780	0.09
1450	1.0082	0.06	1.0073	0.06	1.0078	0.06	1.0078	0.06
1500	1.0542	0.06	1.053	0.06	1.0538	0.06	1.0537	0.06
1550	1.0925	0.06	1.0918	0.06	1.0921	0.06	1.0921	0.06
1600	1.0981	0.07	1.0981	0.07	1.0978	0.07	1.0980	0.07

#### 4.11 OMH

**Base of the radiometric scale:** PQE detector in the visible, nonselective pyroelectric trap detector in the IR.

**Source:** 1000 W tungsten halogen lamp

**Bandpass:** 4.1 nm to 4.3 nm

**Beam Size:** 2 mm diameter

**Beam Geometry:**  $f/8$  to  $f/11$

**Incident Power:** 1  $\mu$ W

#### Laboratory Results:

Table 4.11.1. OMH laboratory results for photodiode IGA004 (NIST07).

Measurement dates: 12-Aug-99    6-Sep-99    11-Sep-99

Thermistor (k $\Omega$ ):    11.5    11.6    11.4

Temperature ( $^{\circ}$ C)    21.817    21.625    22.012

WL [nm]	$s_1$ [A/W]	$u(s_1)$ [%]	$s_2$ [A/W]	$u(s_2)$ [%]	$s_3$ [A/W]	$u(s_3)$ [%]	$s_{avg}$ [A/W]	$u_{avg}$ [%]
900	0.3247	1.17	0.3244	1.16	0.3258	1.06	0.3250	1.13
950	0.6163	1.35	0.6153	1.36	0.6194	1.14	0.6170	1.28
1000	0.669	1.26	0.6678	1.2	0.6724	1.08	0.6697	1.18
1050	0.7565	1.71	0.7545	1.69	0.7592	1.57	0.7567	1.66
1100	0.7891	1.59	0.788	1.6	0.7909	1.53	0.7893	1.57
1150	0.8428	1.68	0.8408	1.67	0.8456	1.57	0.8431	1.64
1200	0.8869	1.71	0.8846	1.68	0.8901	1.58	0.8872	1.66
1250	0.917	1.72	0.9146	1.7	0.9203	1.6	0.9173	1.67
1300	0.9648	1.75	0.962	1.72	0.9685	1.62	0.9651	1.70
1350	0.9985	1.73	0.9957	1.71	1.0022	1.62	0.9988	1.69
1400	1.0158	1.63	1.0137	1.61	1.0186	1.58	1.0160	1.61
1450	1.0296	1.74	1.0267	1.72	1.0335	1.59	1.0299	1.68
1500	1.059	1.72	1.0563	1.71	1.0629	1.58	1.0594	1.67
1550	1.0571	2.59	1.0554	2.6	1.0601	2.53	1.0575	2.57
1600	1.0589	3.12	1.0531	3.11	1.0674	2.69	1.0598	2.97

Table 4.11.2. OMH laboratory results for photodiode IGA005 (NIST11).

Measurement dates: 13-Aug-99 7-Sep-99 12-Sep-99  
 Thermistor (k $\Omega$ ): 11.7 11.8 11.8  
 Temperature ( $^{\circ}$ C) 21.522 21.333 21.333

WL [nm]	$s_1$ [A/W]	$u(s_1)$ [%]	$s_2$ [A/W]	$u(s_2)$ [%]	$s_3$ [A/W]	$u(s_3)$ [%]	$S_{avg}$ [A/W]	$u_{avg}$ [%]
900	0.2921	1.27	0.2915	1.28	0.2931	1.09	0.2922	1.21
950	0.4806	1.32	0.4801	1.42	0.482	1.27	0.4809	1.34
1000	0.5475	1.3	0.5461	1.29	0.5494	1.12	0.5477	1.24
1050	0.5931	1.72	0.5897	1.72	0.5948	1.59	0.5925	1.68
1100	0.6428	1.67	0.6401	1.77	0.6444	1.56	0.6424	1.67
1150	0.7025	1.75	0.6996	1.93	0.7046	1.62	0.7022	1.77
1200	0.7611	1.77	0.7582	2	0.7638	1.64	0.7610	1.80
1250	0.8088	1.71	0.805	1.76	0.8115	1.57	0.8084	1.68
1300	0.8523	1.76	0.8477	1.79	0.8554	1.6	0.8518	1.72
1350	0.8865	1.74	0.8816	1.75	0.8896	1.6	0.8859	1.70
1400	0.9176	1.7	0.9131	1.73	0.9205	1.59	0.9171	1.67
1450	0.9513	1.75	0.946	1.81	0.9545	1.59	0.9506	1.72
1500	0.9823	1.74	0.9767	1.79	0.985	1.58	0.9813	1.70
1550	0.9789	2.82	0.9745	2.99	0.9833	2.64	0.9789	2.82
1600	1.0082	3.06	1.0013	3.28	1.0144	2.72	1.0080	3.02

Table 4.11.3. OMH laboratory results for photodiode IGA006 (NIST15).

Measurement dates: 8-Sep-99 9-Sep-99 14-Sep-99  
 Thermistor (k $\Omega$ ): 11.5 11.4 11.5  
 Temperature ( $^{\circ}$ C) 21.901 22.096 21.901

WL [nm]	$s_1$ [A/W]	$u(s_1)$ [%]	$s_2$ [A/W]	$u(s_2)$ [%]	$s_3$ [A/W]	$u(s_3)$ [%]	$S_{avg}$ [A/W]	$u_{avg}$ [%]
900	0.1094	1.89	0.1089	1.94	0.1088	2.05	0.1090	1.96
950	0.1585	1.53	0.1577	1.54	0.1575	1.66	0.1579	1.58
1000	0.2294	1.61	0.2286	1.8	0.2282	1.93	0.2287	1.78
1050	0.3093	1.84	0.3077	2	0.3063	2.25	0.3078	2.03
1100	0.4286	1.71	0.4267	1.86	0.4253	2.09	0.4269	1.89
1150	0.6405	1.73	0.6372	1.96	0.6342	2.25	0.6373	1.98
1200	0.7973	1.65	0.7942	1.81	0.79	1.9	0.7938	1.79
1250	0.8424	1.71	0.8393	1.78	0.8349	1.71	0.8389	1.73
1300	0.8595	1.72	0.8563	1.8	0.851	1.69	0.8556	1.74
1350	0.8779	1.77	0.8745	1.83	0.8695	1.7	0.8740	1.77
1400	0.9053	1.69	0.9028	1.7	0.8988	1.59	0.9023	1.66
1450	0.9139	1.69	0.911	1.77	0.9051	1.69	0.9100	1.72
1500	0.9137	1.67	0.9111	1.75	0.9053	1.67	0.9100	1.70
1550	0.9028	2.63	0.9002	2.7	0.8966	2.71	0.8999	2.68
1600	0.9111	2.86	0.9048	3.23	0.8961	3.27	0.9040	3.12

## 4.12 PTB

**Base of the radiometric scale:** Laser-based cryogenic radiometer

**Source:** quartz tungsten halogen lamp

**Bandpass:** WL < 1400 nm: 6.4 nm; WL ≥ 1400 nm: 12.9 nm

**Beam Size:** 1.3 mm diameter at half maximum, 2.3 mm diameter at half maximum

**Beam Geometry:** Circular Gaussian like profile, beam divergence: horizontal full angle = 10°, vertical full angle = 4°, circular flat top profile, beam divergence: horizontal full angle = 2°, vertical full angle = 2°.

**Incident Power:** 3 μW to 13 μW, 5 μW to 22 μW, 1 μW to 4 μW

### Laboratory Results:

Table 4.12.1. PTB laboratory results for photodiode IGA007 (NIST18).

Measurement dates:	28-Aug-00	10-Oct-00	18-Oct-00
Thermistor (kΩ):	9.966	9.88	10.039
Temperature (°C)	24.997	25.18	24.843

WL [nm]	$s_1$ [A/W]	$u(s_1)$ [%]	$s_2$ [A/W]	$u(s_2)$ [%]	$s_3$ [A/W]	$u(s_3)$ [%]	$s_{avg}$ [A/W]	$u_{avg}$ [%]
900	0.3117	0.23	0.3119	0.23	0.3113	0.23	0.3116	0.23
950	0.631	0.17	0.6322	0.17	0.6313	0.17	0.6315	0.17
1000	0.7052	0.14	0.7049	0.14	0.705	0.14	0.7050	0.14
1050	0.7837	0.16	0.7843	0.16	0.7839	0.16	0.7840	0.16
1100	0.8339	0.13	0.8338	0.13	0.834	0.13	0.8339	0.13
1150	0.8778	0.14	0.8783	0.14	0.8781	0.14	0.8781	0.14
1200	0.9319	0.13	0.9322	0.13	0.9322	0.13	0.9321	0.13
1250	0.9601	0.12	0.9604	0.12	0.9606	0.12	0.9604	0.12
1300	0.9984	0.12	0.9989	0.12	0.9989	0.12	0.9987	0.12
1350	1.0398	0.12	1.0403	0.12	1.0403	0.12	1.0401	0.12
1400	1.0559	0.12	1.0562	0.12	1.0564	0.12	1.0562	0.12
1450	1.057	0.12	1.0574	0.12	1.0579	0.12	1.0574	0.12
1500	1.0777	0.11	1.0784	0.11	1.0785	0.11	1.0782	0.11
1550	1.1158	0.11	1.1167	0.11	1.1166	0.11	1.1164	0.11
1600	1.1395	0.11	1.1404	0.11	1.1405	0.11	1.1401	0.11

Table 4.12.2. PTB laboratory results for photodiode IGA008 (NIST11).

Measurement dates: 28-Aug-00 10-Oct-00 18-Oct-00  
 Thermistor (k $\Omega$ ): 10.099 9.972 10.163  
 Temperature ( $^{\circ}$ C) 24.831 25.118 24.687

WL [nm]	$s_1$ [A/W]	$u(s_1)$ [%]	$s_2$ [A/W]	$u(s_2)$ [%]	$s_3$ [A/W]	$u(s_3)$ [%]	$S_{avg}$ [A/W]	$u_{avg}$ [%]
900	0.29	0.27	0.2934	0.27	0.2816	0.27	0.2883	0.27
950	0.48	0.1	0.481	0.1	0.4795	0.1	0.4802	0.10
1000	0.5472	0.13	0.5471	0.13	0.5473	0.13	0.5472	0.13
1050	0.5876	0.13	0.588	0.13	0.5877	0.13	0.5878	0.13
1100	0.6369	0.12	0.6369	0.12	0.6371	0.12	0.6370	0.12
1150	0.6966	0.11	0.6969	0.11	0.6967	0.11	0.6967	0.11
1200	0.7565	0.11	0.7566	0.11	0.7565	0.11	0.7565	0.11
1250	0.8068	0.11	0.8069	0.11	0.8069	0.11	0.8069	0.11
1300	0.8475	0.11	0.8476	0.11	0.8477	0.11	0.8476	0.11
1350	0.8821	0.11	0.8822	0.11	0.8822	0.11	0.8822	0.11
1400	0.9097	0.11	0.9098	0.11	0.9098	0.11	0.9098	0.11
1450	0.9402	0.11	0.9399	0.11	0.9403	0.11	0.9401	0.11
1500	0.9735	0.11	0.9735	0.11	0.9736	0.11	0.9735	0.11
1550	1.0063	0.11	1.0067	0.11	1.0062	0.11	1.0064	0.11
1600	1.0285	0.11	1.0288	0.11	1.0281	0.11	1.0285	0.11

Table 4.12.3. PTB laboratory results for photodiode IGA009 (NIST01).

Measurement dates: 28-Aug-00 10-Oct-00 18-Oct-00  
 Thermistor (k $\Omega$ ): 10.492 10.279 10.553  
 Temperature ( $^{\circ}$ C) 24.015 24.48 23.884

WL [nm]	$s_1$ [A/W]	$u(s_1)$ [%]	$s_2$ [A/W]	$u(s_2)$ [%]	$s_3$ [A/W]	$u(s_3)$ [%]	$S_{avg}$ [A/W]	$u_{avg}$ [%]
900	0.2495	0.13	0.2494	0.13	0.2492	0.13	0.2494	0.13
950	0.6003	0.13	0.6003	0.13	0.5976	0.13	0.5994	0.13
1000	0.6846	0.13	0.6842	0.13	0.6821	0.13	0.6836	0.13
1050	0.7141	0.15	0.7147	0.15	0.7154	0.15	0.7147	0.15
1100	0.7772	0.15	0.7768	0.15	0.7773	0.15	0.7771	0.15
1150	0.8327	0.13	0.8329	0.13	0.8321	0.13	0.8326	0.13
1200	0.871	0.12	0.871	0.12	0.8712	0.12	0.8711	0.12
1250	0.9153	0.12	0.9153	0.12	0.915	0.12	0.9152	0.12
1300	0.9536	0.11	0.9535	0.11	0.9534	0.11	0.9535	0.11
1350	0.9827	0.11	0.9827	0.11	0.9825	0.11	0.9826	0.11
1400	1.0123	0.11	1.0122	0.11	1.0117	0.11	1.0121	0.11
1450	1.0232	0.11	1.0228	0.11	1.0239	0.11	1.0233	0.11
1500	1.0529	0.11	1.0526	0.11	1.0525	0.11	1.0527	0.11
1550	1.0716	0.12	1.0716	0.12	1.0703	0.12	1.0712	0.12
1600	1.0363	0.12	1.0364	0.12	1.0367	0.12	1.0365	0.12

### 4.13 SMU

**Base of the radiometric scale:** Absolute pyroelectric radiometer with electrical calibration model Rs-3964 and trap silicon photodiode detector QED-200

**Source:** 100 W halogen lamp with the monochromator DMT 300

**Bandpass:** 6 nm SHBW

**Beam Size:** 3 mm diameter,

**Beam Geometry:** divergent, 7° full angle

**Incident Power:** 10  $\mu$ W to 40  $\mu$ W

#### Laboratory Results:

Table 4.13.1. SMU laboratory results for photodiode IGA004 (NIST07).

Measurement dates: 21-Feb-00 22-Feb-00 23-Feb-00

Thermistor (k $\Omega$ ): 11.238 11.285 11.026

Temperature ( $^{\circ}$ C) 22.331 22.238 22.757

WL [nm]	$s_1$ [A/W]	$u(s_1)$ [%]	$s_2$ [A/W]	$u(s_2)$ [%]	$s_3$ [A/W]	$u(s_3)$ [%]	$s_{avg}$ [A/W]	$u_{avg}$ [%]
900	0.3239	0.32	0.3237	0.32	0.324	0.32	0.3239	0.32
950	0.6238	0.24	0.6232	0.24	0.6241	0.24	0.6237	0.24
1000	0.6735	0.2	0.6735	0.2	0.6736	0.2	0.6735	0.20
1050	0.7546	0.19	0.7545	0.19	0.7542	0.19	0.7544	0.19
1100	0.7845	0.19	0.7849	0.19	0.7846	0.19	0.7847	0.19
1150	0.8407	0.19	0.8404	0.19	0.8415	0.19	0.8409	0.19
1200	0.8853	0.19	0.8851	0.19	0.8851	0.19	0.8852	0.19
1250	0.9175	0.19	0.9177	0.19	0.9171	0.19	0.9174	0.19
1300	0.9638	0.19	0.9639	0.19	0.9632	0.19	0.9636	0.19
1350	0.9966	0.2	0.9974	0.2	0.9978	0.2	0.9973	0.20
1400	1.0091	0.22	1.0091	0.22	1.0104	0.22	1.0095	0.22
1450	1.0241	0.2	1.0246	0.2	1.0253	0.2	1.0247	0.20
1500	1.0561	0.2	1.0558	0.2	1.0555	0.2	1.0558	0.20
1550	1.0883	0.2	1.0887	0.2	1.0886	0.2	1.0885	0.20
1600	1.0873	0.22	1.09	0.22	1.0882	0.22	1.0885	0.22

Table 4.13.2. SMU laboratory results for photodiode IGA005 (NIST02).

Measurement dates: 21-Feb-00 22-Feb-00 23-Feb-00  
 Thermistor (k $\Omega$ ): 12.435 12.035 12.315  
 Temperature ( $^{\circ}$ C): 20.202 20.926 20.416

WL [nm]	$s_1$ [A/W]	$u(s_1)$ [%]	$s_2$ [A/W]	$u(s_2)$ [%]	$s_3$ [A/W]	$u(s_3)$ [%]	$S_{avg}$ [A/W]	$u_{avg}$ [%]
900	0.2523	0.38	0.2515	0.38	0.2517	0.38	0.2518	0.38
950	0.5823	0.25	0.5817	0.25	0.5822	0.25	0.5821	0.25
1000	0.6553	0.2	0.6551	0.2	0.6548	0.2	0.6551	0.20
1050	0.7415	0.19	0.7412	0.19	0.7414	0.19	0.7414	0.19
1100	0.774	0.19	0.7734	0.19	0.7734	0.19	0.7736	0.19
1150	0.834	0.19	0.8337	0.19	0.8336	0.19	0.8338	0.19
1200	0.8712	0.19	0.8699	0.19	0.8697	0.19	0.8703	0.19
1250	0.9224	0.19	0.9213	0.19	0.9217	0.19	0.9218	0.19
1300	0.948	0.19	0.9477	0.19	0.9476	0.19	0.9478	0.19
1350	0.9884	0.22	0.988	0.22	0.9876	0.22	0.9880	0.22
1400	1.0055	0.2	1.0051	0.2	1.0062	0.2	1.0056	0.20
1450	1.0366	0.2	1.0348	0.2	1.036	0.2	1.0358	0.20
1500	1.0599	0.2	1.0598	0.2	1.0576	0.2	1.0591	0.20
1550	1.0467	0.2	1.0472	0.2	1.0455	0.2	1.0465	0.20
1600	1.0286	0.22	1.0302	0.22	1.029	0.22	1.0293	0.22

Table 4.13.3. SMU laboratory results for photodiode IGA006 (NIST10).

Measurement dates: 21-Feb-00 22-Feb-00 23-Feb-00  
 Thermistor (k $\Omega$ ): 11.736 11.315 11.24  
 Temperature ( $^{\circ}$ C): 21.348 22.16 22.309

WL [nm]	$s_1$ [A/W]	$u(s_1)$ [%]	$s_2$ [A/W]	$u(s_2)$ [%]	$s_3$ [A/W]	$u(s_3)$ [%]	$S_{avg}$ [A/W]	$u_{avg}$ [%]
900	0.3193	0.26	0.3183	0.26	0.3187	0.26	0.3188	0.26
950	0.4896	0.24	0.4895	0.24	0.4896	0.24	0.4896	0.24
1000	0.5842	0.2	0.5839	0.2	0.5847	0.2	0.5843	0.20
1050	0.6397	0.19	0.6392	0.19	0.64	0.19	0.6396	0.19
1100	0.6749	0.19	0.6742	0.19	0.6746	0.19	0.6746	0.19
1150	0.7242	0.19	0.7237	0.19	0.7246	0.19	0.7242	0.19
1200	0.783	0.19	0.7827	0.19	0.7832	0.19	0.7830	0.19
1250	0.8338	0.19	0.8335	0.19	0.8345	0.19	0.8339	0.19
1300	0.8732	0.19	0.8727	0.19	0.8739	0.19	0.8733	0.19
1350	0.9044	0.2	0.904	0.2	0.9047	0.2	0.9044	0.20
1400	0.9321	0.22	0.9315	0.22	0.9332	0.22	0.9323	0.22
1450	0.9712	0.2	0.9701	0.2	0.972	0.2	0.9711	0.20
1500	1.0078	0.2	1.0061	0.2	1.0077	0.2	1.0072	0.20
1550	1.0391	0.2	1.0365	0.2	1.038	0.2	1.0379	0.20
1600	1.0458	0.22	1.0456	0.22	1.0481	0.22	1.0465	0.22

**4.14 VNIIOFI****Base of the radiometric scale:** MAR-1 absolute radiometer**Source:** tungsten ribbon lamp TRU type**Bandpass:** 2 nm**Beam Size:** 2 mm x 3 mm**Beam Geometry:**  $f/3$ **Incident Power:** 1  $\mu$ W to 10  $\mu$  W**Laboratory Results:**

Table 4.14.1. VNIIOFI laboratory results for photodiode IGA001 (NIST07).

Measurement dates: 20-Jul-00 15-Aug-00 25-Aug-00

Thermistor (k $\Omega$ ): 10.52 10.42 11.09Temperature ( $^{\circ}$ C) 23.811 24.027 22.627

WL [nm]	$s_1$ [A/W]	$u(s_1)$ [%]	$s_2$ [A/W]	$u(s_2)$ [%]	$s_3$ [A/W]	$u(s_3)$ [%]	$S_{avg}$ [A/W]	$u_{avg}$ [%]
900	0.3261	0.64	0.3255	0.53	0.3231	0.75	0.3249	0.64
950	0.6138	0.5	0.6126	0.53	0.6146	0.52	0.6137	0.52
1000	0.6679	0.51	0.6666	0.52	0.6679	0.51	0.6675	0.51
1050	0.7473	0.64	0.7459	0.54	0.7398	0.78	0.7443	0.65
1100	0.7748	0.53	0.7733	0.51	0.7727	0.52	0.7736	0.52
1150	0.8282	0.54	0.8266	0.5	0.8246	0.55	0.8265	0.53
1200	0.8664	0.52	0.8647	0.51	0.8648	0.51	0.8653	0.51
1250	0.8962	0.5	0.8944	0.54	0.8981	0.55	0.8962	0.53
1300	0.9401	0.51	0.9383	0.51	0.9396	0.5	0.9393	0.51
1350	0.9694	0.52	0.9675	0.53	0.9691	0.51	0.9687	0.52
1400	0.9939	0.52	0.992	0.53	0.994	0.52	0.9933	0.52
1450	0.9898	0.52	0.9879	0.59	0.9945	0.63	0.9907	0.58
1500	1.0169	0.56	1.015	0.65	1.0253	0.79	1.0191	0.67
1550	1.0432	0.54	1.0412	0.65	1.0506	0.74	1.0450	0.64
1600	1.037	0.56	1.035	0.66	1.045	0.78	1.0390	0.67

Table 4.14.2. VNIIOFI laboratory results for photodiode IGA002 (NIST14).

Measurement dates: 26-Jul-00 17-Aug-00 28-Aug-00  
 Thermistor (k $\Omega$ ): 11.09 11.13 11.78  
 Temperature ( $^{\circ}$ C) 22.733 22.652 21.385

WL [nm]	$s_1$ [A/W]	$u(s_1)$ [%]	$s_2$ [A/W]	$u(s_2)$ [%]	$s_3$ [A/W]	$u(s_3)$ [%]	$S_{avg}$ [A/W]	$u_{avg}$ [%]
900	0.1195	0.54	0.1195	0.54	0.1189	0.61	0.1193	0.56
950	0.1691	0.52	0.1690	0.53	0.1698	0.58	0.1693	0.54
1000	0.2397	0.54	0.2396	0.51	0.2401	0.52	0.2398	0.52
1050	0.3179	0.6	0.3177	0.58	0.3149	0.78	0.3168	0.65
1100	0.4322	0.52	0.4320	0.51	0.4308	0.54	0.4317	0.52
1150	0.6401	0.52	0.6399	0.51	0.6384	0.54	0.6395	0.52
1200	0.7893	0.5	0.7890	0.5	0.7891	0.5	0.7891	0.50
1250	0.8302	0.53	0.8298	0.54	0.8342	0.61	0.8314	0.56
1300	0.8485	0.51	0.8481	0.52	0.8508	0.54	0.8491	0.52
1350	0.8570	0.52	0.8567	0.53	0.8597	0.56	0.8578	0.54
1400	0.8949	0.52	0.8945	0.53	0.8971	0.54	0.8955	0.53
1450	0.8936	0.54	0.8933	0.56	0.8991	0.66	0.8953	0.59
1500	0.8860	0.59	0.8856	0.61	0.8937	0.79	0.8884	0.66
1550	0.8924	0.57	0.8920	0.59	0.8994	0.74	0.8946	0.63
1600	0.8957	0.57	0.8953	0.6	0.9025	0.73	0.8978	0.63

Table 4.14.3. VNIIOFI laboratory results for photodiode IGA003 (NIST09).

Measurement dates: 18-Jul-00 01-Aug-00 24-Aug-00  
 Thermistor (k $\Omega$ ): 10.45 10.45 11.83  
 Temperature ( $^{\circ}$ C) 23.978 23.978 21.205

WL [nm]	$s_1$ [A/W]	$u(s_1)$ [%]	$s_2$ [A/W]	$u(s_2)$ [%]	$s_3$ [A/W]	$u(s_3)$ [%]	$S_{avg}$ [A/W]	$u_{avg}$ [%]
900	0.2831	0.57	0.2831	0.58	0.2807	0.76	0.2823	0.64
950	0.4832	0.5	0.4833	0.5	0.4828	0.51	0.4831	0.50
1000	0.5812	0.54	0.5812	0.54	0.5778	0.64	0.5801	0.57
1050	0.6411	0.57	0.6411	0.58	0.6360	0.74	0.6394	0.63
1100	0.6748	0.57	0.6749	0.58	0.6693	0.78	0.6730	0.64
1150	0.7202	0.56	0.7203	0.56	0.7149	0.71	0.7185	0.61
1200	0.7755	0.55	0.7755	0.55	0.7700	0.69	0.7737	0.60
1250	0.8252	0.51	0.8253	0.51	0.8232	0.53	0.8246	0.52
1300	0.8635	0.54	0.8636	0.54	0.8586	0.64	0.8619	0.57
1350	0.8924	0.54	0.8925	0.55	0.8875	0.63	0.8908	0.57
1400	0.9319	0.53	0.9320	0.53	0.9282	0.58	0.9307	0.55
1450	0.9520	0.51	0.9521	0.51	0.9511	0.52	0.9517	0.51
1500	0.9841	0.52	0.9842	0.52	0.9857	0.53	0.9847	0.52
1550	1.0109	0.51	1.0110	0.51	1.0116	0.51	1.0112	0.51
1600	1.0206	0.52	1.0207	0.52	1.0209	0.25	1.0207	0.43

#### **4.15 NIST (Pilot lab)**

**Base of the radiometric scale:** cryogenic radiometer

**Source:** 100 W quartz tungsten halogen lamp

**Bandpass:** 4 nm

**Beam Size:** 1.1 mm in diameter

**Beam Geometry:** *f/9*

**Incident Power:** 0.1  $\mu\text{W}$  to 0.6  $\mu\text{W}$

#### **Results**

Table 4.15.1. NIST results for detectors measured by BNM-INM.

WL [nm]	IGA001 (NIST04)			IGA002 (NIST08)			IGA003 (NIST10)		
	Average responsivity [A/W]	Difference = (Post-Pre) /Pre [%]	$u_{\text{stability}}$ [%]	Average responsivity [A/W]	Difference = (Post-Pre) /Pre [%]	$u_{\text{stability}}$ [%]	Average responsivity [A/W]	Difference = (Post-Pre) /Pre [%]	$u_{\text{stability}}$ [%]
900	0.3300	-0.003	0.00	0.2846	0.097	0.03	0.2899	-0.341	0.10
950	0.5825	0.115	0.03	0.6394	0.406	0.12	0.4867	0.235	0.07
1000	0.6922	0.129	0.04	0.7099	0.404	0.12	0.5827	0.211	0.06
1050	0.7244	0.010	0.00	0.7708	0.255	0.07	0.6414	0.098	0.03
1100	0.7922	-0.002	0.00	0.8005	0.256	0.07	0.6757	0.105	0.03
1150	0.8430	-0.016	0.00	0.8506	0.203	0.06	0.7255	0.069	0.02
1200	0.8794	0.376	0.11	0.8741	0.592	0.17	0.7823	0.437	0.13
1250	0.9321	-0.011	0.00	0.9125	0.196	0.06	0.8357	0.082	0.02
1300	0.9670	-0.130	0.04	0.9562	0.058	0.02	0.8746	-0.066	0.02
1350	0.9905	-0.004	0.00	0.9763	0.198	0.06	0.9082	0.050	0.01
1400	1.0260	-0.102	0.03	0.9834	0.018	0.01	0.9394	-0.002	0.00
1450	1.0676	0.051	0.01	1.0121	0.205	0.06	0.9774	0.073	0.02
1500	1.1006	-0.072	0.02	1.0622	0.070	0.02	1.0185	-0.005	0.00
1550	1.0962	0.016	0.00	1.0976	0.128	0.04	1.0451	-0.059	0.02
1600	1.0684	-0.033	0.01	1.1030	-0.037	0.01	1.0566	0.058	0.02

Table 4.15.2. NIST results for detectors measured by CSIR.

WL [nm]	IGA010 (NIST04)			IGA011 (NIST08)			IGA012 (NIST15)		
	Average responsivity [A/W]	Difference = (Post-Pre) /Pre [%]	$u_{\text{stability}}$ [%]	Average responsivity [A/W]	Difference = (Post-Pre) /Pre [%]	$u_{\text{stability}}$ [%]	Average responsivity [A/W]	Difference = (Post-Pre) /Pre [%]	$u_{\text{stability}}$ [%]
900	0.3301	0.137	0.04	0.2843	0.381	0.11	0.1094	-0.015	0.00
950	0.5836	0.065	0.02	0.6403	0.245	0.07	0.1597	-0.079	0.02
1000	0.6919	-0.034	0.01	0.7090	0.075	0.02	0.2284	-0.132	0.04
1050	0.7246	-0.076	0.02	0.7699	0.040	0.01	0.3069	-0.114	0.03
1100	0.7926	-0.115	0.03	0.7998	0.030	0.01	0.4226	-0.146	0.04
1150	0.8441	-0.126	0.04	0.8500	0.065	0.02	0.6308	-0.170	0.05
1200	0.8814	-0.145	0.04	0.8748	0.079	0.02	0.7877	0.013	0.00
1250	0.9333	-0.116	0.03	0.9121	0.074	0.02	0.8370	0.007	0.00
1300	0.9686	-0.121	0.03	0.9562	0.073	0.02	0.8517	0.041	0.01
1350	0.9922	-0.076	0.02	0.9766	0.062	0.02	0.8722	0.051	0.01
1400	1.0259	-0.126	0.04	0.9817	0.112	0.03	0.8975	0.034	0.01
1450	1.0686	-0.071	0.02	1.0117	0.078	0.02	0.9066	0.117	0.03
1500	1.1014	-0.009	0.00	1.0617	0.063	0.02	0.9129	0.077	0.02
1550	1.0953	-0.039	0.01	1.0951	0.123	0.04	0.9270	0.191	0.06
1600	1.0684	-0.129	0.04	1.1023	0.120	0.03	0.9312	0.002	0.00

Table 4.15.3. NIST results for detectors measured by CSIRO.

WL [nm]	IGA007 (NIST06)			IGA008 (NIST14)			IGA009 (NIST03)		
	Average responsivity [A/W]	Difference = (Post-Pre) /Pre [%]	$u_{\text{stability}}$ [%]	Average responsivity [A/W]	Difference = (Post- Pre) /Pre [%]	$u_{\text{stability}}$ [%]	Average responsivity [A/W]	Difference = (Post- Pre) /Pre [%]	$u_{\text{stability}}$ [%]
900	0.3079	-0.141	0.04	0.1192	0.025	0.01	0.2448	0.034	0.01
950	0.5909	-0.035	0.01	0.1717	0.150	0.04	0.5950	0.147	0.04
1000	0.6670	0.011	0.00	0.2422	0.151	0.04	0.6844	0.062	0.02
1050	0.7442	-0.120	0.03	0.3214	-0.042	0.01	0.7224	-0.027	0.01
1100	0.7995	-0.130	0.04	0.4370	-0.105	0.03	0.7698	-0.068	0.02
1150	0.8479	-0.156	0.04	0.6480	-0.234	0.07	0.8375	-0.069	0.02
1200	0.9067	0.254	0.07	0.8019	0.415	0.12	0.8644	0.311	0.09
1250	0.9448	-0.127	0.04	0.8480	0.066	0.02	0.9170	-0.071	0.02
1300	0.9890	-0.263	0.08	0.8680	-0.011	0.00	0.9519	-0.208	0.06
1350	1.0407	-0.089	0.03	0.8806	0.105	0.03	0.9850	-0.077	0.02
1400	1.0675	-0.232	0.07	0.9103	-0.063	0.02	1.0157	-0.217	0.06
1450	1.0739	-0.067	0.02	0.9263	0.115	0.03	1.0318	-0.061	0.02
1500	1.0972	-0.103	0.03	0.9251	0.034	0.01	1.0662	-0.156	0.04
1550	1.1299	-0.046	0.01	0.9319	0.133	0.04	1.0746	-0.096	0.03
1600	1.1489	-0.090	0.03	0.9402	0.066	0.02	1.0350	-0.159	0.05

Table 4.15.4. NIST results for detectors measured by HUT.

WL [nm]	IGA004 (NIST06)			IGA005 (NIST10)			IGA006 (NIST15)		
	Average responsivity [A/W]	Difference = (Post-Pre) /Pre [%]	$u_{\text{stability}}$ [%]	Average responsivity [A/W]	Difference = (Post- Pre) /Pre [%]	$u_{\text{stability}}$ [%]	Average responsivity [A/W]	Difference = (Post- Pre) /Pre [%]	$u_{\text{stability}}$ [%]
900	0.3082	-0.069	0.02	0.2904	0.008	0.00	0.1095	0.045	0.01
950	0.5920	-0.316	0.09	0.4867	-0.238	0.07	0.1596	-0.192	0.06
1000	0.6671	-0.028	0.01	0.5823	-0.089	0.03	0.2288	-0.087	0.03
1050	0.7447	-0.011	0.00	0.6411	-0.025	0.01	0.3073	-0.047	0.01
1100	0.8002	-0.054	0.02	0.6755	-0.038	0.01	0.4229	-0.057	0.02
1150	0.8488	-0.055	0.02	0.7253	-0.019	0.01	0.6313	-0.042	0.01
1200	0.9074	-0.399	0.12	0.7821	-0.382	0.11	0.7868	-0.347	0.10
1250	0.9458	-0.074	0.02	0.8358	-0.100	0.03	0.8370	-0.044	0.01
1300	0.9904	-0.018	0.01	0.8751	-0.059	0.02	0.8513	-0.006	0.00
1350	1.0418	-0.123	0.04	0.9087	-0.159	0.05	0.8714	-0.098	0.03
1400	1.0683	0.077	0.02	0.9393	0.025	0.01	0.8986	0.129	0.04
1450	1.0745	-0.052	0.02	0.9777	-0.132	0.04	0.9066	-0.072	0.02
1500	1.0980	-0.045	0.01	1.0187	-0.035	0.01	0.9128	0.057	0.02
1550	1.1297	0.070	0.02	1.0451	0.054	0.02	0.9280	0.115	0.03
1600	1.1494	0.010	0.00	1.0568	-0.098	0.03	0.9306	-0.032	0.01

Table 4.15.5. NIST results for detectors measured by IFA.

WL [nm]	IGA007 (NIST04)			IGA008 (NIST03)			IGA009 (NIST11)		
	Average responsivity [A/W]	Difference = (Post-Pre) /Pre [%]	$u_{\text{stability}}$ [%]	Average responsivity [A/W]	Difference = (Post- Pre) /Pre [%]	$u_{\text{stability}}$ [%]	Average responsivity [A/W]	Difference = (Post- Pre) /Pre [%]	$u_{\text{stability}}$ [%]
900	0.3302	-0.168	0.05	0.2448	-0.075	0.02	0.2811	-0.067	0.02
950	0.5831	-0.315	0.09	0.5955	-0.326	0.09	0.4807	-0.284	0.08
1000	0.6919	-0.067	0.02	0.6844	-0.060	0.02	0.5455	-0.094	0.03
1050	0.7245	-0.047	0.01	0.7225	-0.004	0.00	0.5884	-0.027	0.01
1100	0.7923	-0.033	0.01	0.7702	-0.038	0.01	0.6361	-0.040	0.01
1150	0.8434	-0.072	0.02	0.8379	-0.038	0.01	0.6966	-0.045	0.01
1200	0.8796	-0.415	0.12	0.8647	-0.382	0.11	0.7540	-0.413	0.12
1250	0.9326	-0.095	0.03	0.9177	-0.064	0.02	0.8060	-0.099	0.03
1300	0.9678	-0.040	0.01	0.9530	-0.022	0.01	0.8475	-0.067	0.02
1350	0.9912	-0.140	0.04	0.9860	-0.119	0.03	0.8835	-0.151	0.04
1400	1.0263	0.047	0.01	1.0164	0.074	0.02	0.9134	0.040	0.01
1450	1.0680	-0.119	0.03	1.0325	-0.068	0.02	0.9465	-0.138	0.04
1500	1.1012	-0.042	0.01	1.0671	-0.003	0.00	0.9831	-0.055	0.02
1550	1.0959	0.049	0.01	1.0750	0.010	0.00	1.0105	-0.002	0.00
1600	1.0683	0.049	0.01	1.0357	0.022	0.01	1.0326	0.018	0.01

Table 4.15.6. NIST results for detectors measured by KRIS.

WL [nm]	IGA004 (NIST17)			IGA005 (NIST10)			IGA006 (NIST13)		
	Average responsivity [A/W]	Difference = (Post-Pre) /Pre [%]	$u_{\text{stability}}$ [%]	Average responsivity [A/W]	Difference = (Post- Pre) /Pre [%]	$u_{\text{stability}}$ [%]	Average responsivity [A/W]	Difference = (Post- Pre) /Pre [%]	$u_{\text{stability}}$ [%]
900	0.3101	-0.217	0.06	0.2897	0.670	0.19	0.1253	0.064	0.02
950	0.6130	-0.204	0.06	0.4870	0.025	0.01	0.1816	-0.087	0.03
1000	0.6777	-0.195	0.06	0.5813	-0.063	0.02	0.2534	-0.095	0.03
1050	0.7551	-0.227	0.07	0.6402	-0.019	0.01	0.3351	-0.125	0.04
1100	0.7875	-0.207	0.06	0.6748	-0.005	0.00	0.4603	-0.090	0.03
1150	0.8643	-0.201	0.06	0.7243	0.000	0.00	0.6798	-0.047	0.01
1200	0.9053	-0.198	0.06	0.7822	-0.034	0.01	0.8031	-0.032	0.01
1250	0.9431	-0.224	0.06	0.8346	-0.016	0.00	0.8456	0.004	0.00
1300	0.9926	-0.164	0.05	0.8739	-0.004	0.00	0.8566	0.014	0.00
1350	1.0269	-0.160	0.05	0.9077	-0.009	0.00	0.8848	-0.010	0.00
1400	1.0457	-0.159	0.05	0.9371	-0.062	0.02	0.9062	-0.093	0.03
1450	1.0745	-0.137	0.04	0.9763	0.063	0.02	0.9105	0.072	0.02
1500	1.1188	-0.109	0.03	1.0166	0.011	0.00	0.9214	-0.014	0.00
1550	1.1417	-0.131	0.04	1.0418	0.014	0.00	0.9402	-0.053	0.02
1600	1.1329	0.012	0.00	1.0550	-0.122	0.04	0.9447	0.061	0.02

Table 4.15.7. NIST results for detectors measured by NIM.

WL [nm]	IGA007 (NIST04).			IGA008 (NIST11).			IGA009 (NIST09)		
	Average responsivity [A/W]	Difference = (Post-Pre) /Pre [%]	$u_{\text{stability}}$ [%]	Average responsivity [A/W]	Difference = (Post- Pre) /Pre [%]	$u_{\text{stability}}$ [%]	Average responsivity [A/W]	Difference = (Post- Pre) /Pre [%]	$u_{\text{stability}}$ [%]
900	0.3299	-0.021	0.01	0.2805	-0.319	0.09	0.2845	-0.321	0.09
950	0.5831	0.111	0.03	0.4814	-0.049	0.01	0.4868	-0.073	0.02
1000	0.6923	-0.083	0.02	0.5462	-0.313	0.09	0.5827	-0.118	0.03
1050	0.7246	0.065	0.02	0.5890	-0.193	0.06	0.6457	-0.110	0.03
1100	0.7926	0.114	0.03	0.6366	-0.177	0.05	0.6806	-0.072	0.02
1150	0.8438	0.202	0.06	0.6967	-0.124	0.04	0.7296	-0.088	0.03
1200	0.8815	0.112	0.03	0.7553	-0.210	0.06	0.7883	-0.103	0.03
1250	0.9329	0.190	0.05	0.8059	-0.116	0.03	0.8425	-0.067	0.02
1300	0.9678	0.296	0.09	0.8471	-0.017	0.00	0.8826	-0.011	0.00
1350	0.9915	0.214	0.06	0.8833	-0.023	0.01	0.9169	-0.034	0.01
1400	1.0260	0.106	0.03	0.9125	-0.103	0.03	0.9466	-0.141	0.04
1450	1.0684	0.102	0.03	0.9459	-0.111	0.03	0.9856	-0.127	0.04
1500	1.1008	0.118	0.03	0.9822	-0.130	0.04	1.0272	-0.152	0.04
1550	1.0959	-0.071	0.02	1.0097	-0.306	0.09	1.0551	-0.151	0.04
1600	1.0686	0.083	0.02	1.0320	-0.125	0.04	1.0713	-0.067	0.02

Table 4.15.8. NIST results for detectors measured by NMI-VSL.

WL [nm]	IGA013 (NIST16).			IGA014 (NIST02)			IGA015 (NIST05)		
	Average responsivity [A/W]	Difference = (Post-Pre) /Pre [%]	$u_{\text{stability}}$ [%]	Average responsivity [A/W]	Difference = (Post- Pre) /Pre [%]	$u_{\text{stability}}$ [%]	Average responsivity [A/W]	Difference = (Post- Pre) /Pre [%]	$u_{\text{stability}}$ [%]
900	0.3238	0.016	0.00	0.2513	-0.159	0.05	0.3205	-0.005	0.00
950	0.6337	0.133	0.04	0.5786	-0.015	0.00	0.6056	-0.048	0.01
1000	0.7187	-0.040	0.01	0.6512	-0.004	0.00	0.7083	0.022	0.01
1050	0.7850	0.048	0.01	0.7414	0.015	0.00	0.7534	0.025	0.01
1100	0.8234	-0.008	0.00	0.7714	-0.073	0.02	0.8252	0.015	0.00
1150	0.9014	0.009	0.00	0.8330	0.009	0.00	0.8571	0.046	0.01
1200	0.9334	-0.011	0.00	0.8673	0.000	0.00	0.9101	-0.015	0.00
1250	0.9690	-0.024	0.01	0.9210	0.001	0.00	0.9474	0.017	0.00
1300	1.0143	0.030	0.01	0.9461	0.007	0.00	0.9763	0.025	0.01
1350	1.0413	0.002	0.00	0.9899	-0.011	0.00	1.0224	0.034	0.01
1400	1.0568	0.056	0.02	1.0084	0.042	0.01	1.0560	0.002	0.00
1450	1.0843	0.052	0.02	1.0390	0.057	0.02	1.0617	0.028	0.01
1500	1.1236	-0.032	0.01	1.0670	0.017	0.00	1.0684	0.079	0.02
1550	1.1367	-0.024	0.01	1.0483	0.075	0.02	1.0835	0.059	0.02
1600	1.1230	-0.074	0.02	1.0352	-0.141	0.04	1.1093	0.150	0.04

Table 4.15.9. NIST results for detectors measured by NPL.

WL [nm]	IGA001 (NIST07)			IGA002 (NIST08)			IGA003 (NIST14).		
	Average responsivity [A/W]	Difference = (Post-Pre) /Pre [%]	$u_{\text{stability}}$ [%]	Average responsivity [A/W]	Difference = (Post- Pre) /Pre [%]	$u_{\text{stability}}$ [%]	Average responsivity [A/W]	Difference = (Post- Pre) /Pre [%]	$u_{\text{stability}}$ [%]
900	0.3225	0.007	0.00	0.2846	-0.108	0.03	0.1191	0.137	0.04
950	0.6207	-0.207	0.06	0.6392	-0.332	0.10	0.1718	-0.225	0.07
1000	0.6698	0.012	0.00	0.7089	-0.118	0.03	0.2421	-0.075	0.02
1050	0.7536	0.047	0.01	0.7701	-0.072	0.02	0.3215	-0.054	0.02
1100	0.7826	0.005	0.00	0.7998	-0.064	0.02	0.4375	-0.136	0.04
1150	0.8394	-0.009	0.00	0.8501	-0.073	0.02	0.6495	-0.217	0.06
1200	0.8811	-0.348	0.10	0.8734	-0.433	0.13	0.8016	-0.355	0.10
1250	0.9157	-0.031	0.01	0.9121	-0.098	0.03	0.8479	-0.035	0.01
1300	0.9616	0.003	0.00	0.9562	-0.058	0.02	0.8680	0.012	0.00
1350	0.9971	-0.092	0.03	0.9763	-0.185	0.05	0.8805	-0.077	0.02
1400	1.0121	0.120	0.03	0.9832	0.041	0.01	0.9101	0.111	0.03
1450	1.0271	-0.034	0.01	1.0118	-0.147	0.04	0.9259	-0.044	0.01
1500	1.0635	0.023	0.01	1.0621	-0.060	0.02	0.9248	0.013	0.00
1550	1.0921	0.088	0.03	1.0969	0.000	0.00	0.9311	0.040	0.01
1600	1.0931	0.162	0.05	1.1031	0.015	0.00	0.9395	0.085	0.02

Table 4.15.10. NIST results for detectors measured by NRC.

WL [nm]	IGA001 (NIST16).			IGA002 (NIST14).			IGA003 (NIST08).		
	Average responsivity [A/W]	Difference = (Post-Pre) /Pre [%]	$u_{\text{stability}}$ [%]	Average responsivity [A/W]	Difference = (Post- Pre) /Pre [%]	$u_{\text{stability}}$ [%]	Average responsivity [A/W]	Difference = (Post- Pre) /Pre [%]	$u_{\text{stability}}$ [%]
900	0.3242	-0.256	0.07	0.1191	-0.286	0.08	0.2842	-0.336	0.10
950	0.6339	-0.213	0.06	0.1719	0.007	0.00	0.6401	-0.184	0.05
1000	0.7193	-0.146	0.04	0.2421	-0.266	0.08	0.7100	-0.377	0.11
1050	0.7855	-0.157	0.05	0.3211	-0.164	0.05	0.7707	-0.266	0.08
1100	0.8235	-0.035	0.01	0.4366	-0.041	0.01	0.8006	-0.235	0.07
1150	0.9013	0.012	0.00	0.6475	0.092	0.03	0.8506	-0.212	0.06
1200	0.9335	-0.008	0.00	0.8028	-0.183	0.05	0.8755	-0.258	0.07
1250	0.9689	0.045	0.01	0.8478	-0.113	0.03	0.9126	-0.179	0.05
1300	1.0136	0.108	0.03	0.8679	-0.004	0.00	0.9562	-0.065	0.02
1350	1.0408	0.086	0.02	0.8807	-0.083	0.02	0.9768	-0.098	0.03
1400	1.0566	-0.016	0.00	0.9092	-0.164	0.05	0.9823	-0.242	0.07
1450	1.0837	0.045	0.01	0.9260	-0.172	0.05	1.0122	-0.176	0.05
1500	1.1230	0.130	0.04	0.9250	-0.048	0.01	1.0619	-0.112	0.03
1550	1.1365	0.047	0.01	0.9312	-0.267	0.08	1.0963	-0.352	0.10
1600	1.1227	0.124	0.04	0.9397	-0.157	0.05	1.1022	-0.103	0.03

Table 4.15.11. NIST results for detectors measured by OMH.

WL [nm]	IGA004 (NIST07)			IGA005 (NIST11)			IGA006 (NIST15)		
	Average responsivity [A/W]	Difference = (Post-Pre) /Pre [%]	$u_{\text{stability}}$ [%]	Average responsivity [A/W]	Difference = (Post-Pre) /Pre [%]	$u_{\text{stability}}$ [%]	Average responsivity [A/W]	Difference = (Post-Pre) /Pre [%]	$u_{\text{stability}}$ [%]
900	0.3225	-0.004	0.00	0.2810	-0.014	0.00	0.1096	0.230	0.07
950	0.6206	0.178	0.05	0.4807	0.320	0.09	0.1596	0.222	0.06
1000	0.6706	0.244	0.07	0.5461	0.330	0.10	0.2289	0.174	0.05
1050	0.7542	0.123	0.04	0.5890	0.208	0.06	0.3073	0.046	0.01
1100	0.7832	0.161	0.05	0.6366	0.185	0.05	0.4227	-0.060	0.02
1150	0.8399	0.128	0.04	0.6968	0.093	0.03	0.6304	-0.242	0.07
1200	0.8819	0.538	0.16	0.7543	0.496	0.14	0.7872	0.442	0.13
1250	0.9162	0.135	0.04	0.8060	0.094	0.03	0.8372	0.100	0.03
1300	0.9617	0.017	0.01	0.8472	-0.009	0.00	0.8515	0.042	0.01
1350	0.9974	0.154	0.04	0.8832	0.066	0.02	0.8716	0.152	0.04
1400	1.0129	0.030	0.01	0.9133	-0.060	0.02	0.8992	-0.009	0.00
1450	1.0278	0.158	0.05	0.9461	0.069	0.02	0.9070	0.155	0.04
1500	1.0641	0.079	0.02	0.9828	0.004	0.00	0.9133	0.057	0.02
1550	1.0932	0.116	0.03	1.0109	0.082	0.02	0.9289	0.076	0.02
1600	1.0937	-0.052	0.01	1.0327	0.000	0.00	0.9311	0.148	0.04

Table 4.15.12. NIST results for detectors measured by PTB.

WL [nm]	IGA007 (NIST18)			IGA008 (NIST11)			IGA009 (NIST01)		
	Average responsivity [A/W]	Difference = (Post-Pre) /Pre [%]	$u_{\text{stability}}$ [%]	Average responsivity [A/W]	Difference = (Post-Pre) /Pre [%]	$u_{\text{stability}}$ [%]	Average responsivity [A/W]	Difference = (Post-Pre) /Pre [%]	$u_{\text{stability}}$ [%]
900	0.3121	-0.059	0.02	0.2806	0.373	0.11	0.2498	0.138	0.04
950	0.6347	-0.176	0.05	0.4813	0.005	0.00	0.6033	0.189	0.05
1000	0.7032	0.060	0.02	0.5454	0.025	0.01	0.6823	-0.017	0.00
1050	0.7855	0.050	0.01	0.5884	-0.028	0.01	0.7148	-0.029	0.01
1100	0.8332	0.091	0.03	0.6360	-0.027	0.01	0.7761	-0.033	0.01
1150	0.8777	0.095	0.03	0.6962	-0.015	0.00	0.8318	-0.006	0.00
1200	0.9299	0.124	0.04	0.7545	-0.023	0.01	0.8689	-0.002	0.00
1250	0.9592	0.089	0.03	0.8055	0.017	0.01	0.9136	-0.019	0.01
1300	0.9980	0.103	0.03	0.8470	0.001	0.00	0.9532	-0.014	0.00
1350	1.0416	0.151	0.04	0.8833	0.008	0.00	0.9835	-0.011	0.00
1400	1.0588	0.159	0.05	0.9118	-0.048	0.01	1.0146	-0.058	0.02
1450	1.0633	0.091	0.03	0.9454	-0.010	0.00	1.0288	0.022	0.01
1500	1.0870	0.161	0.05	0.9817	0.025	0.01	1.0615	0.065	0.02
1550	1.1179	0.052	0.02	1.0084	0.051	0.01	1.0734	0.026	0.01
1600	1.1408	0.158	0.05	1.0312	-0.033	0.01	1.0387	-0.113	0.03

Table 4.15.13. NIST results for detectors measured by SMU.

WL [nm]	IGA004 (NIST07)			IGA005 (NIST02)			IGA006 (NIST10)		
	Average responsivity [A/W]	Difference = (Post-Pre) /Pre [%]	$u_{\text{stability}}$ [%]	Average responsivity [A/W]	Difference = (Post- Pre) /Pre [%]	$u_{\text{stability}}$ [%]	Average responsivity [A/W]	Difference = (Post- Pre) /Pre [%]	$u_{\text{stability}}$ [%]
900	0.3223	0.174	0.05	0.2512	0.192	0.06	0.2891	0.225	0.06
950	0.6210	0.052	0.01	0.5782	0.148	0.04	0.4871	0.066	0.02
1000	0.6703	0.336	0.10	0.6511	0.015	0.00	0.5824	0.307	0.09
1050	0.7538	0.223	0.06	0.7413	0.002	0.00	0.6410	0.223	0.06
1100	0.7831	0.205	0.06	0.7712	0.125	0.04	0.6755	0.184	0.05
1150	0.8397	0.178	0.05	0.8326	0.089	0.03	0.7250	0.199	0.06
1200	0.8832	0.255	0.07	0.8672	0.025	0.01	0.7832	0.216	0.06
1250	0.9160	0.172	0.05	0.9206	0.099	0.03	0.8353	0.166	0.05
1300	0.9615	0.059	0.02	0.9454	0.153	0.04	0.8741	0.046	0.01
1350	0.9976	0.104	0.03	0.9893	0.127	0.04	0.9081	0.079	0.02
1400	1.0117	0.271	0.08	1.0080	0.027	0.01	0.9384	0.221	0.06
1450	1.0277	0.171	0.05	1.0385	0.038	0.01	0.9768	0.182	0.05
1500	1.0636	0.174	0.05	1.0664	0.100	0.03	1.0175	0.187	0.05
1550	1.0920	0.339	0.10	1.0478	0.007	0.00	1.0433	0.293	0.08
1600	1.0928	0.100	0.03	1.0351	0.159	0.05	1.0563	0.122	0.04

Table 4.15.14. NIST results for detectors measured by VNIIOFI.

WL [nm]	IGA001 (NIST07)			IGA002 (NIST14)			IGA003 (NIST09)		
	Average responsivity [A/W]	Difference = (Post-Pre) /Pre [%]	$u_{\text{stability}}$ [%]	Average responsivity [A/W]	Difference = (Post- Pre) /Pre [%]	$u_{\text{stability}}$ [%]	Average responsivity [A/W]	Difference = (Post- Pre) /Pre [%]	$u_{\text{stability}}$ [%]
900	0.3225	0.298	0.09	0.1189	0.050	0.01	0.2856	1.084	0.31
950	0.6213	0.157	0.05	0.1718	-0.138	0.04	0.4868	0.075	0.02
1000	0.6697	0.159	0.05	0.2417	-0.051	0.01	0.5821	-0.065	0.02
1050	0.7537	0.200	0.06	0.3209	0.034	0.01	0.6451	-0.066	0.02
1100	0.7831	0.212	0.06	0.4367	0.077	0.02	0.6802	-0.052	0.01
1150	0.8400	0.262	0.08	0.6481	0.089	0.03	0.7292	-0.017	0.01
1200	0.8830	0.218	0.06	0.8022	0.027	0.01	0.7878	-0.035	0.01
1250	0.9164	0.249	0.07	0.8475	0.039	0.01	0.8422	0.002	0.00
1300	0.9622	0.205	0.06	0.8681	0.044	0.01	0.8826	0.000	0.00
1350	0.9980	0.182	0.05	0.8807	0.091	0.03	0.9167	-0.007	0.00
1400	1.0114	0.222	0.06	0.9088	0.061	0.02	0.9459	-0.003	0.00
1450	1.0275	0.135	0.04	0.9256	0.082	0.02	0.9854	0.076	0.02
1500	1.0633	0.124	0.04	0.9251	0.075	0.02	1.0269	0.100	0.03
1550	1.0908	0.120	0.03	0.9300	0.011	0.00	1.0546	0.062	0.02
1600	1.0925	0.036	0.01	0.9392	0.050	0.01	1.0708	-0.024	0.01

## **5. Examination and Correction of the Data**

### **5.1 Temperature correction to the transfer detector responsivities**

After circulation of Draft A-1, due to relatively large differences in laboratory temperatures of participants, the K2.a Working Group decided to apply temperature corrections for all results based on the thermistor readings for Draft A-2. The average temperature-dependence of the responsivities of detectors from each of the four different vendors (Fig. 3.4) was used to correct the measurements by participating laboratories and the measurements at NIST after a round of measurements. The responsivities of the detectors were corrected for recorded temperature differences from the measurements at NIST prior to a measurement round. The thermistor values recorded during each set of measurements were converted to temperatures; Table 5.1 lists the temperatures for each transfer detector measured at NIST before and after measurements at the participating laboratory, as well as the temperatures recorded by each laboratory.

One laboratory, IFA, had an error in their thermistor measurements; no temperature data were available for those measurements. One measurement at NIST, the measurement of detector NIST01 following measurements by the PTB, was considerably lower than all other NIST temperature measurements. This data point was treated as an outlier and no temperature correction was made to the post NIST measurements of the detector. There was an error in the temperature of NIST measurement of detector NIST13 before being measured by KRISS. The post-measurement temperature was used to correct the KRISS measurements.

Table 5.1. Detector measurement temperatures (°C).

Laboratory	Detector	Laboratory Measurement					Vendor	
		NIST Pre	1	2	3	NIST Post		
<b>BNM-INM</b>	NIST04	24.09	22.49	22.27	22.25	24.88	GPD	
	NIST08	24.16	21.92	21.86	21.80	24.40	EGG	
	NIST10	23.60	22.13	22.29	22.29	24.51	EGG	
<b>CSIR</b>	NIST04	25.21	25.90	26.52	26.32	24.01	GPD	
	NIST08	25.15	25.46	25.96	25.92	23.29	EGG	
	NIST15	23.28	25.56	25.84	25.67	23.57	TDC	
<b>CSIRO</b>	NIST06	24.32	21.61	21.64	22.32	24.75	GPD	
	NIST14	23.34	21.78	21.24	21.58	24.70	TDC	
	NIST03	23.77	21.42	22.23	22.38	23.42	Fermionics	
<b>HUT</b>	NIST06	23.01	23.67	22.23	24.11	24.32	GPD	
	NIST10	23.34	24.09	24.32	24.89	23.60	EGG	
	NIST15	22.99	21.45	22.26	22.41	23.29	TDC	
<b>IFA</b>	NIST04	23.50				24.09	GPD	
	NIST03	23.17				23.77	Fermionics	
	NIST11	22.66				23.48	EGG	
<b>KRISS</b>	NIST17	22.59	23.78	24.17	23.80	23.06	GPD	
	NIST10	25.07	24.39	24.83	24.48	23.68	EGG	
	NIST13	xxx	23.28	23.69	23.39	22.92	TDC	
<b>NIM</b>	NIST04	24.88	26.11	27.53	26.99	25.21	GPD	
	NIST11	24.57	25.19	26.58	26.62	24.58	EGG	
	NIST09	25.33	26.16	27.55	27.16	25.42	EGG	
<b>NMi-VSL</b>	NIST16	24.71	21.27	21.40	21.93	23.49	GPD	
	NIST02	23.21	20.74	20.85	21.19	23.10	Fermionics	
	NIST05	23.16	22.29	22.24	22.43	24.13	GPD	
<b>NPL</b>	NIST07	23.43	21.26	21.21	21.45	24.32	GPD	
	NIST08	23.41	20.95	20.94	20.90	24.16	EGG	
	NIST14	22.54	20.41	20.33	20.46	23.34	TDC	
<b>NRC</b>	NIST16	24.20	21.75	21.94	21.60	24.71	GPD	
	NIST14	24.70	21.47	21.47	21.38	24.13	TDC	
	NIST08	24.40	22.25	21.81	22.06	25.15	EGG	
(Continued)	<b>OMH</b>	NIST07	24.32	21.82	21.63	22.01	24.75	GPD
NIST11		23.48	21.52	21.33	21.33	24.57	EGG	
NIST15		23.29	21.90	22.10	21.90	24.63	TDC	
<b>PTB</b>	NIST18	23.30	25.00	25.18	24.84	24.01	GPD	
	NIST11	24.58	24.83	25.12	24.69	23.77	EGG	
	NIST01	24.03	24.02	24.48	23.88	21.70	Fermionics	
<b>SMU</b>	NIST07	24.75	22.33	22.24	22.76	25.42	GPD	
	NIST02	23.03	20.20	20.93	20.42	23.21	Fermionics	
	NIST10	24.51	21.35	22.16	22.31	25.07	EGG	
<b>VNIOFI</b>	NIST07	25.42	23.81	24.03	22.63	24.06	GPD	
	NIST14	24.13	22.73	22.65	21.39	23.37	TDC	
	NIST09	25.42	23.98	23.98	21.21	23.20	EGG	

## 5.2 Repeatability of the measurements at NIST

An average of the standard deviations of the mean of the three measurements of all the transfer detectors measured at NIST was used as the repeatability of the NIST measurements. The results are summarized in Table 5.2. The last column shows the corresponding values for a total of six measurements for each photodiode including before and after transportation.

Table 5.2. Repeatability of NIST measurements of the transfer detectors.

Wavelength [nm]	Std. dev. of the mean of 3 measurements, 1 photodiode [%]	Std. dev. of the mean of 6 measurements (pre, post) 1 photodiode $u_r(s_{\text{NIST}})$ [%]
900	0.07	0.05
950	0.09	0.06
1000	0.08	0.06
1050	0.05	0.03
1100	0.06	0.05
1150	0.05	0.04
1200	0.11	0.08
1250	0.06	0.04
1300	0.05	0.03
1350	0.04	0.03
1400	0.08	0.06
1450	0.06	0.04
1500	0.05	0.03
1550	0.09	0.06
1600	0.04	0.03

## 5.3 Stability of the transfer detectors

Differences in the transfer detectors' responsivities measured at NIST Before (pre) and After (post) participants' measurements in each round were taken into account as an uncertainty component in the Laboratory  $i$  to NIST ratio values. The difference was converted to a standard uncertainty by assuming a rectangular probability distribution:

$$u_{\text{stability}}(\bar{s}_{ij}^{\text{NIST}}) = \frac{1}{2\sqrt{3}} \times \frac{|s_{ij}^{\text{NIST}}(\text{pre}) - s_{ij}^{\text{NIST}}(\text{post})|}{s_{ij}^{\text{NIST}}(\text{pre})}. \quad (5.1)$$

$\bar{s}_{ij}^{\text{NIST}}$  is the average of NIST-measured responsivity, before and after the transfer, of the photodiode  $j$  measured by laboratory  $i$  during the comparison (see eq. 6.3). Figure 5.1 (a, b, c, d) shows the uncertainty due to the transfer detector stability for each round of measurements.

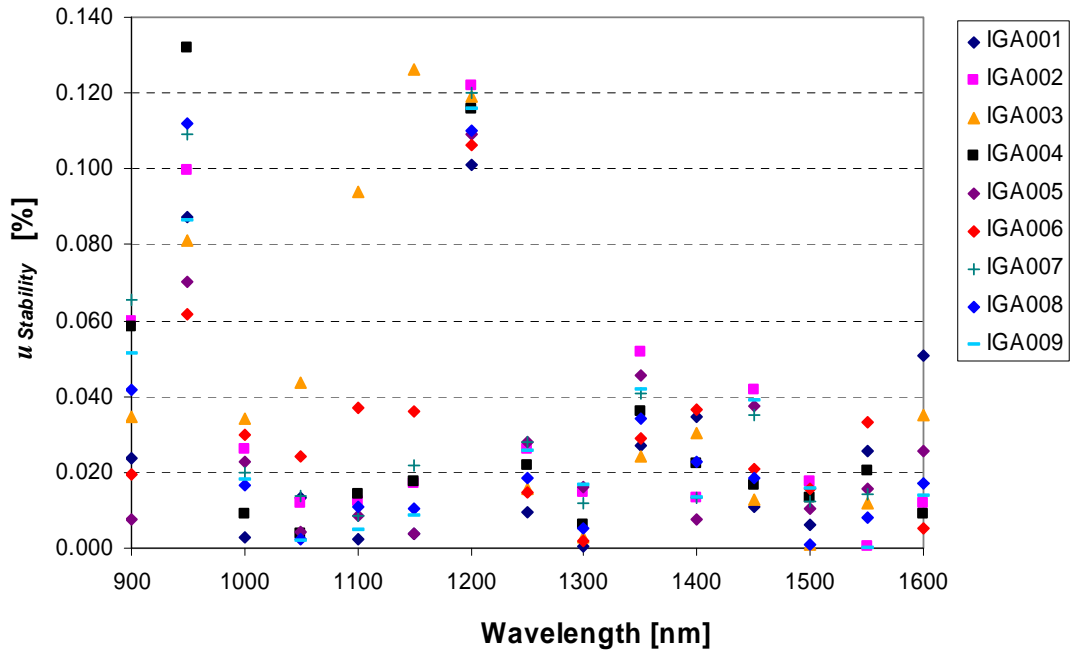


Figure 5.1(a) Round 1 transfer detector stability.

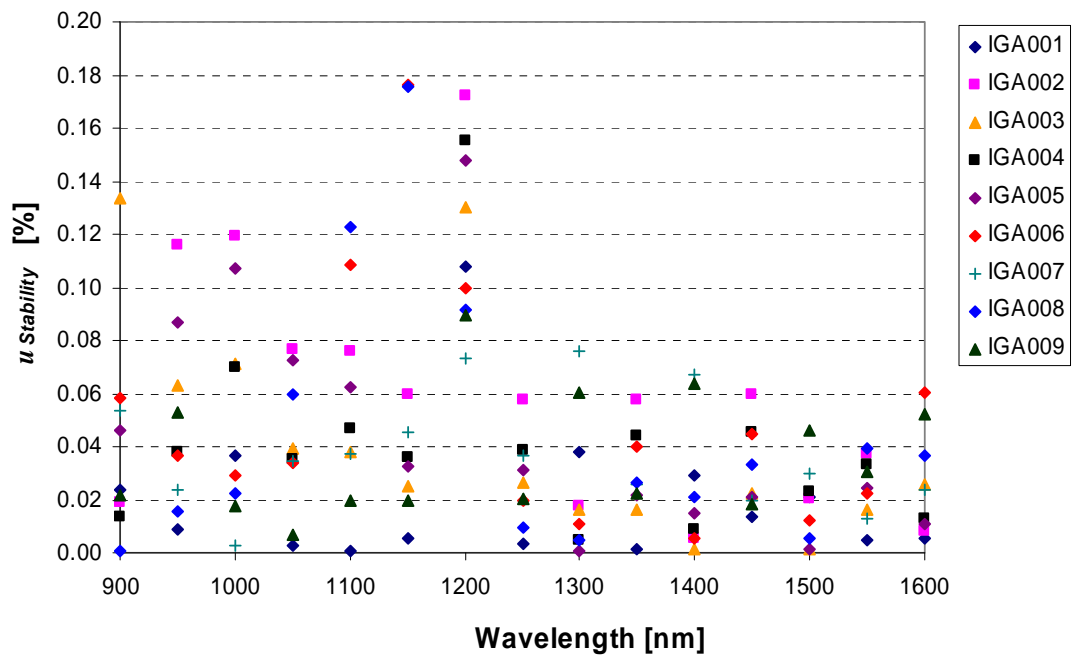


Figure 5.1(b) Round 2 transfer detector stability.

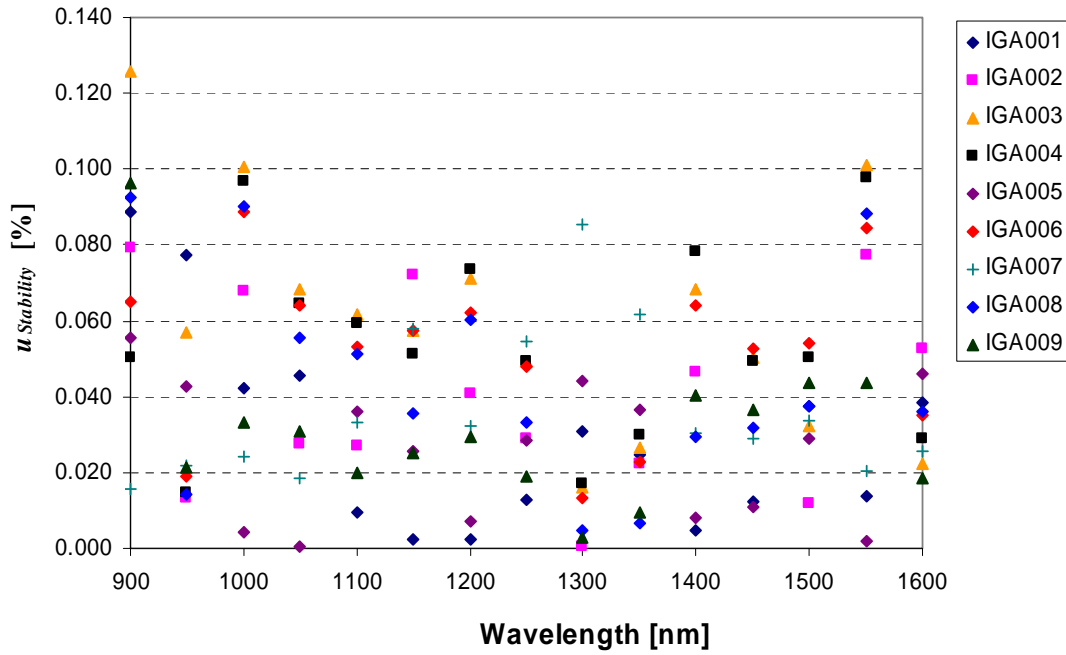


Figure 5.1(c) Round 3 transfer detector stability.

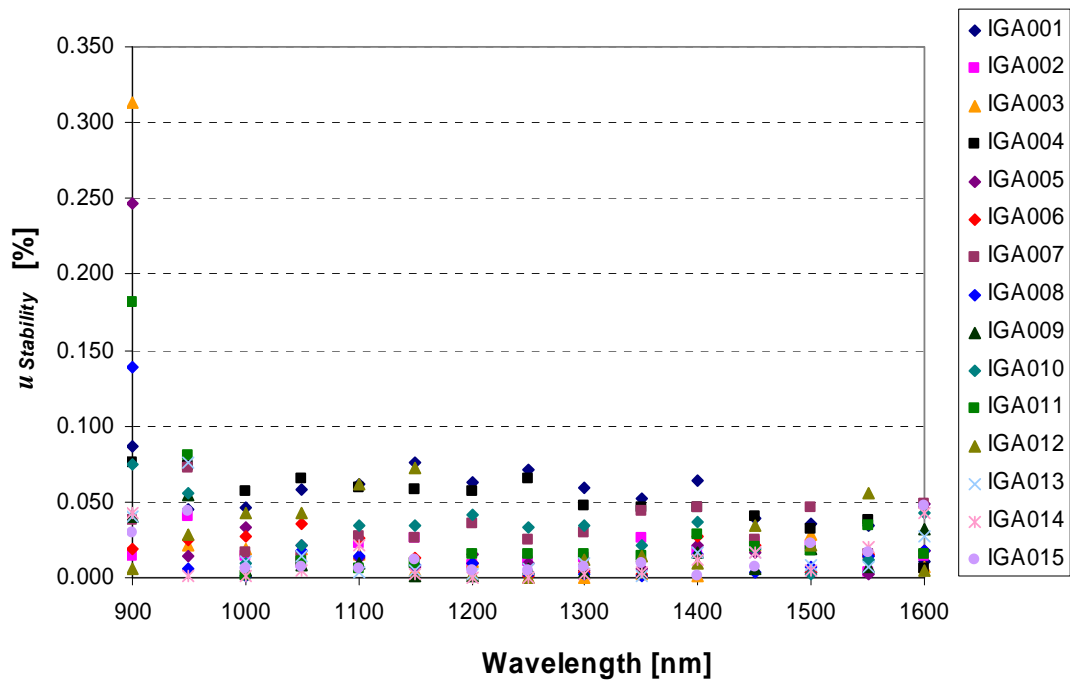


Figure 5.1(d) Round 4 transfer detector stability.

#### 5.4 Instability and anomalous behavior of transfer detectors

The responsivities of most of the photodiodes remained stable within the measurement reproducibility over the course of the comparison. Fig. 5.2 (a, b, c, d) shows example results of the long-term stability of the transfer detectors. Note that the data shown in the figure were not corrected for temperature. Notable effects of temperature are clearly seen around 950 nm. The optical characteristics of two transfer detectors changed significantly enough prior to the Fourth Round of measurements to warrant their removal from the Comparison. NIST03 had stability problems, as shown in Fig. 5.3, and NIST06 had a 'hole' in the responsivity, shown in Fig. 5.4. Neither photodiode participated in Rounds 3 and 4 of the Comparison.

Laboratory results separated by vendor and plotted as a difference from NIST results are shown in Fig. 5.5. The variance in measurements of EGG photodiodes at 900 nm was significantly larger than the variance in measurements of the photodiodes purchased from other vendors at 900 nm and was significantly larger than the variance in measurements of any photodiodes at other wavelengths. Following distribution of Draft A (Jan. 2003) and discussions of the results with members of the Key Comparison Working Group, it was decided that measurements of EGG photodiodes at 900 nm would be removed from the Key Comparison data set.

The difference in the measurement of the TDC photodiode by Laboratory #2 (CSIR) at 950 nm was considered anomalous and this measurement was not included in the analysis.

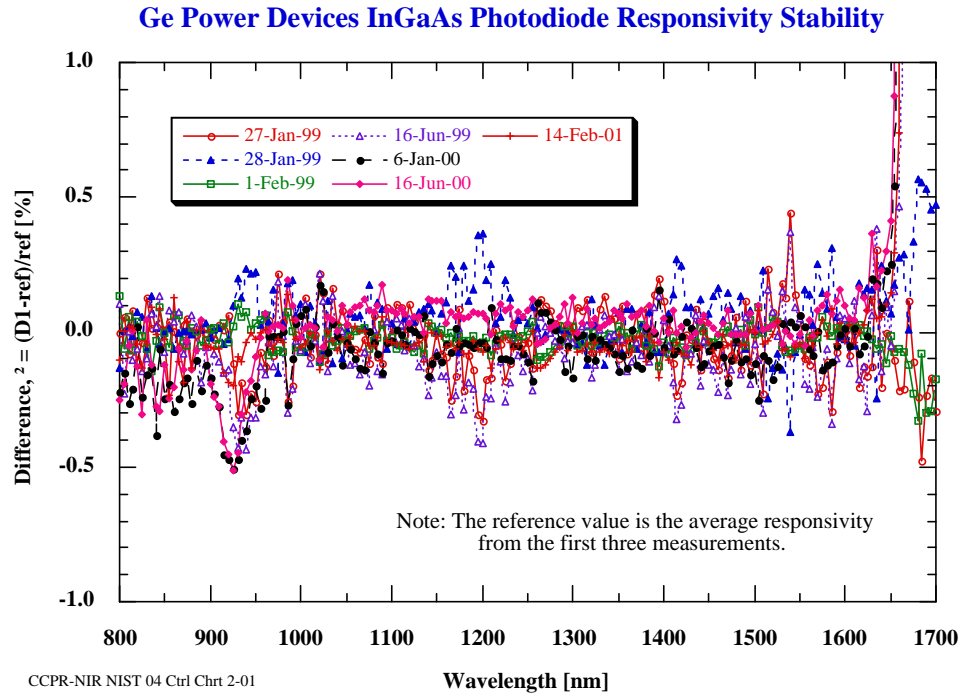


Figure 5.2 (a). Stability of photodiodes over the course of the measurement comparison. Example results for Ge Power Devices photodiodes are shown.

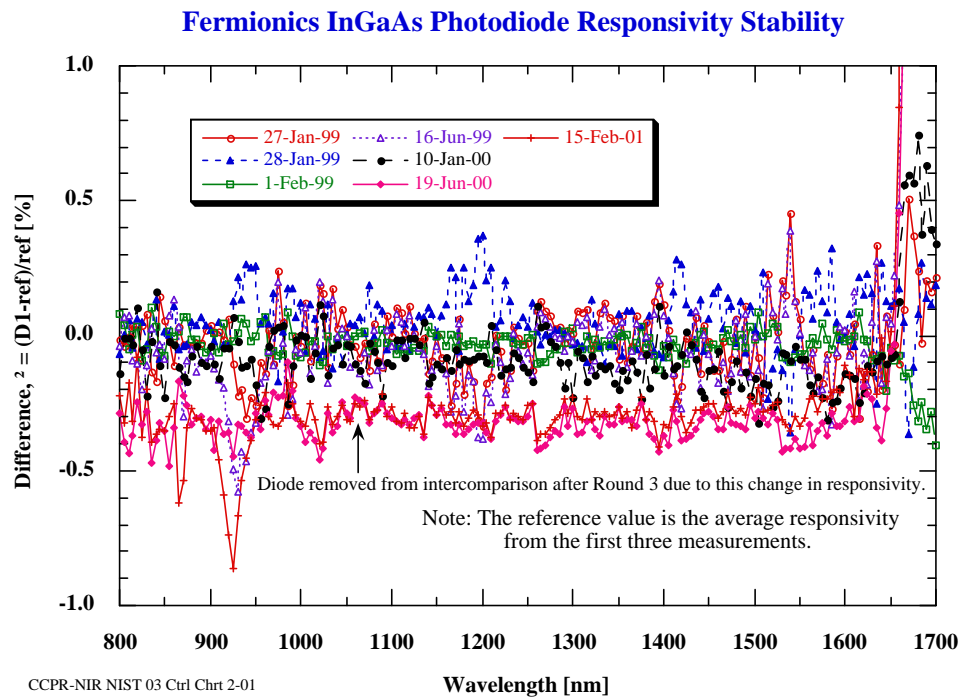


Figure 5.2 (b). Stability of photodiodes over the course of the measurement comparison. Example results for Fermionics photodiodes are shown.

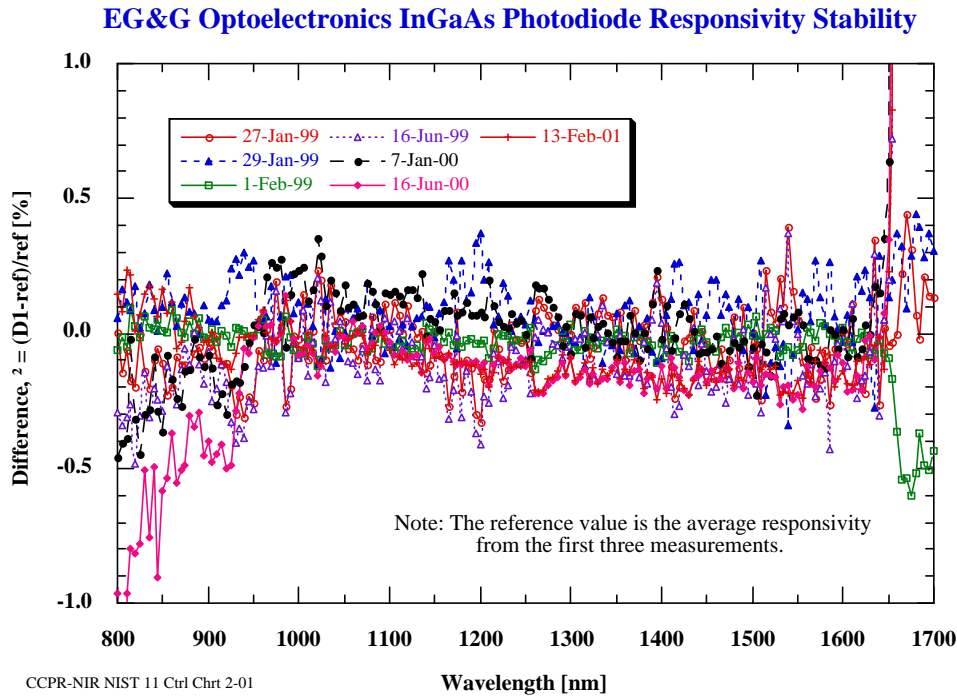


Figure 5.2 (c). Stability of photodiodes over the course of the measurement comparison. Example results for EGG Optoelectronics photodiodes are shown.

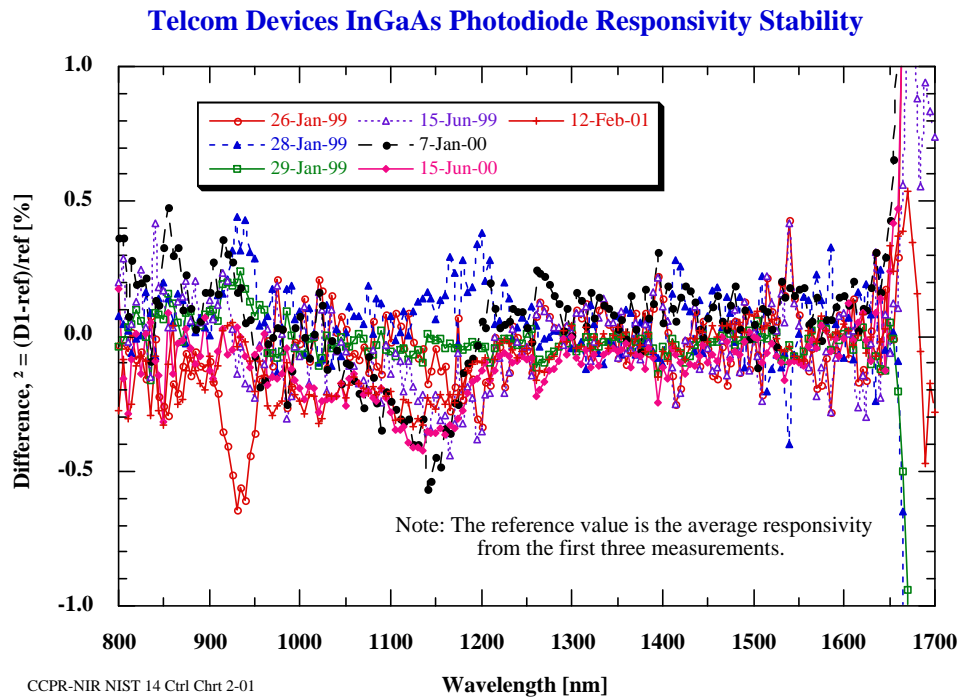


Figure 5.2 (d). Stability of photodiodes over the course of the measurement comparison. Example results for Telcom Devices photodiodes are shown.

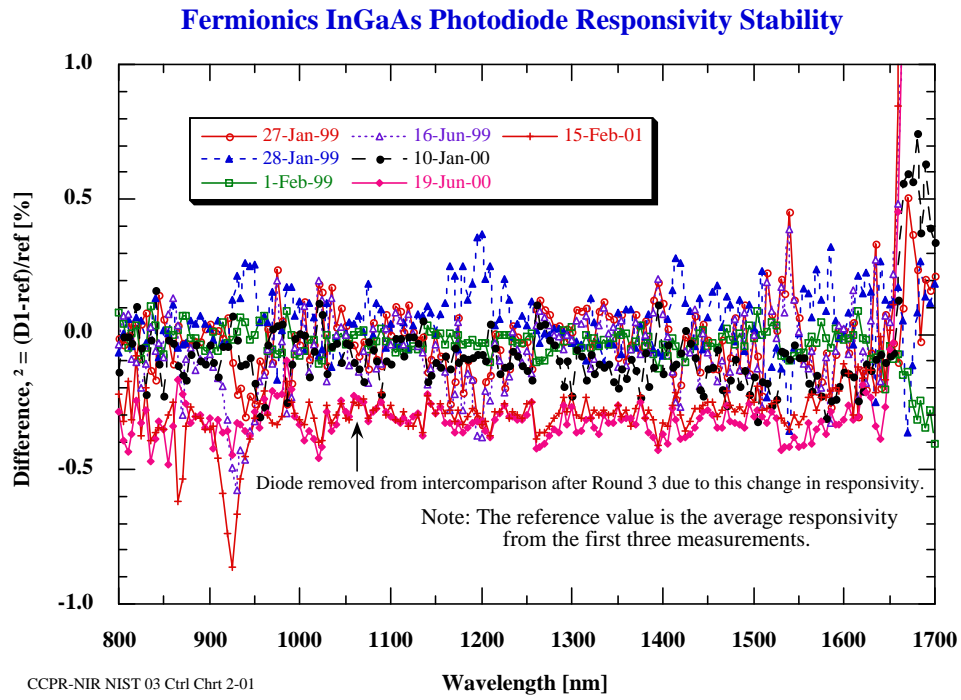


Figure 5.3. Change in the responsivity of NIST03 after Round 3.

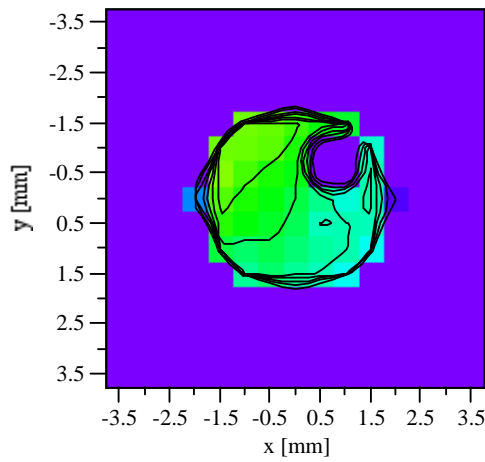


Figure 5.4. Spectral responsivity uniformity of NIST06 measured after Round 3.

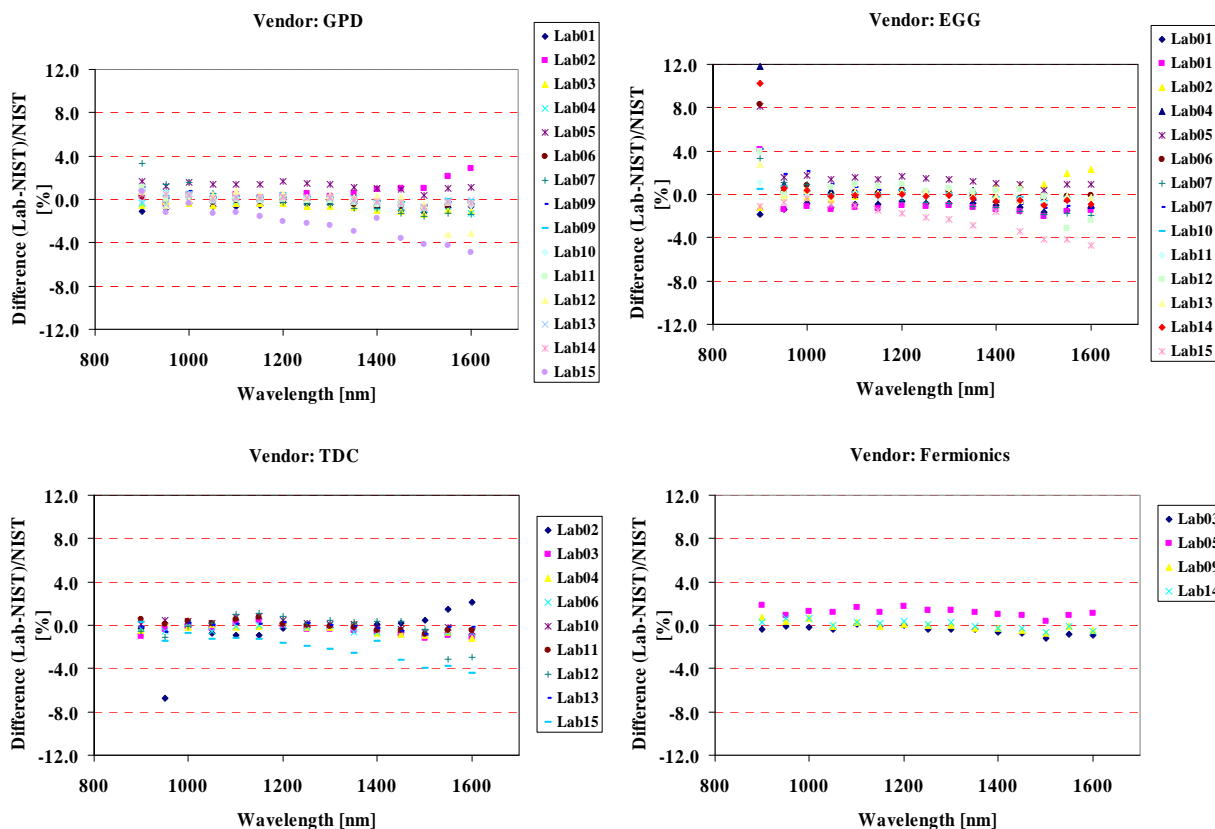


Figure 5.5. Laboratory results, plotted as difference from NIST, separated by vendor.

### 5.5 Uncertainties associated with Laboratory-NIST transfer

The uncertainty in transfer measurements by the Pilot lab consisted of the following components.

#### 5.5.1 Repeatability of NIST measurement

The NIST measurement repeatability data presented in Table 5.2 were taken from the repeated measurements of each transfer detector on different dates with re-mounting photodiodes, thus include the repeatability of wavelength scale and the alignment repeatability associated with spatial nonuniformity of the transfer detectors used in this comparison.

#### 5.5.2 Long-term stability of the comparison scale

The comparison scale was the NIST scale maintained at the time of this intercomparison. The scale was maintained by a group of working standard detectors (Larason 1998), which were not recalibrated during the comparison. Table 5.3 shows the uncertainty contribution from the longterm stability (reproducibility) of the comparison scale estimated from the data in reference (Larason 2008). This longterm stability uncertainty includes longterm shifts in the NIST instrument characteristics as well as drifts of working standard detectors. The correlated components in the scale realization at NIST are cancelled out in the transfer measurements.

Table 5.3. Uncertainty contribution  $u_{\text{long}}(s_{\text{NIST}})$  from the long-term stability of the comparison scale.

Wavelength [nm]	$u_{\text{long}}(s_{\text{NIST}})$ [%]
900	0.04
950	0.04
1000	0.02
1050	0.02
1100	0.02
1150	0.02
1200	0.02
1250	0.02
1300	0.02
1350	0.02
1400	0.03
1450	0.03
1500	0.04
1550	0.04
1600	0.04

### 5.5.3 Wavelength scale uncertainty

The wavelength scale uncertainty of the NIST SCF, evaluated as the residuals after correction, is typically within 0.1 nm as shown in Fig. 5.6 (blue triangle marks with dashed line). Considering small long-term shifts between calibrations, 0.1 nm (rectangular distribution) is assumed for the entire 900 nm to 1600 nm region. The repeatability of the wavelength scale is much smaller as indicated by the standard deviation curve (orange square box marks).

Errors in transfer occur if there are significant random variations or differences in relative spectral responsivity curve between the working standard detectors and photodiodes measured. The NIST working standard detectors are of the Ge Power Device type. The spectral responsivity curves of Ge Power Devices, Fermionics, and EG&G are similar, but there are significant variations in the curves around 900 and 950 nm. The variations of the sensitivity coefficients among these photodiodes used in the comparison were analyzed as one group. The spectral responsivity curves of Telcom Device photodiodes were significantly different from the Ge Power Device, and thus this type of photodiodes was analyzed separately. Figs. 5.7 (a) and (b) show typical relative sensitivity coefficient at each wavelength. The variations and differences from NIST working standard detectors in relative sensitivity coefficient among all photodiodes in the two groups were analyzed. Table 5.4 shows the summary of results for the transfer uncertainty contributions, denoted  $u_{w,p}^T$ , for the two groups of photodiode measured. Subscript  $p$  in  $u_{w,p}^T$  indicates the group of photodiodes.

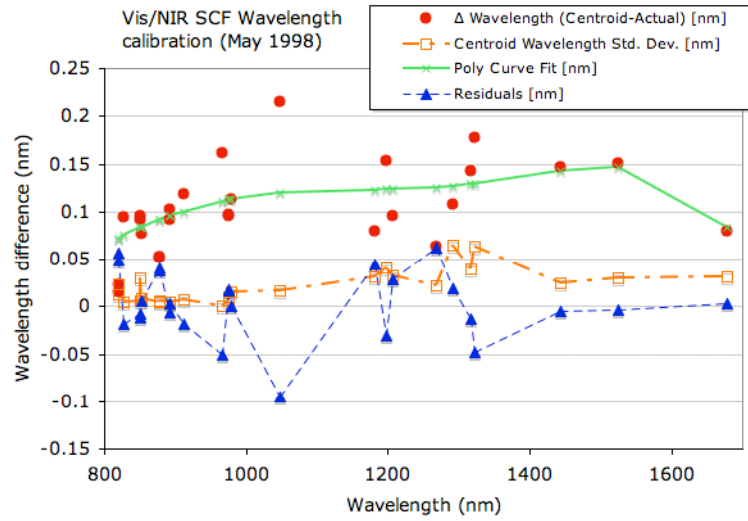


Figure 5.6. An example of the wavelength scale calibration results for the NIST SCF in the near IR region.

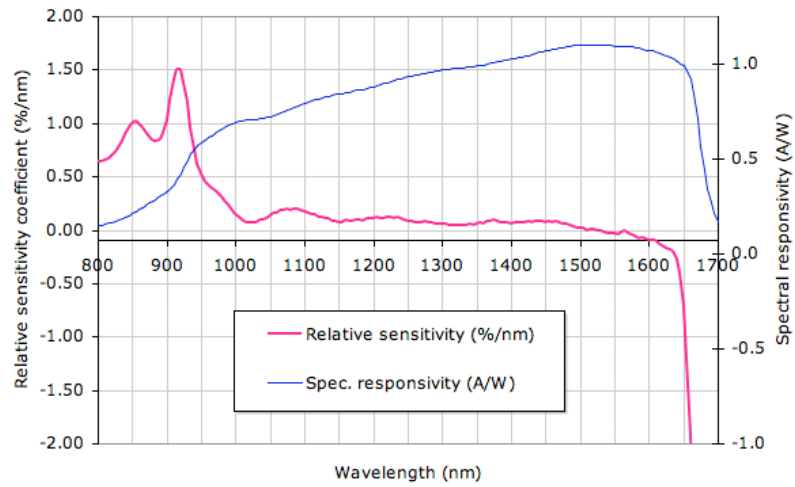


Figure 5.7 (a) Relative sensitivity coefficient for one of NIST working standard detectors (GPD).

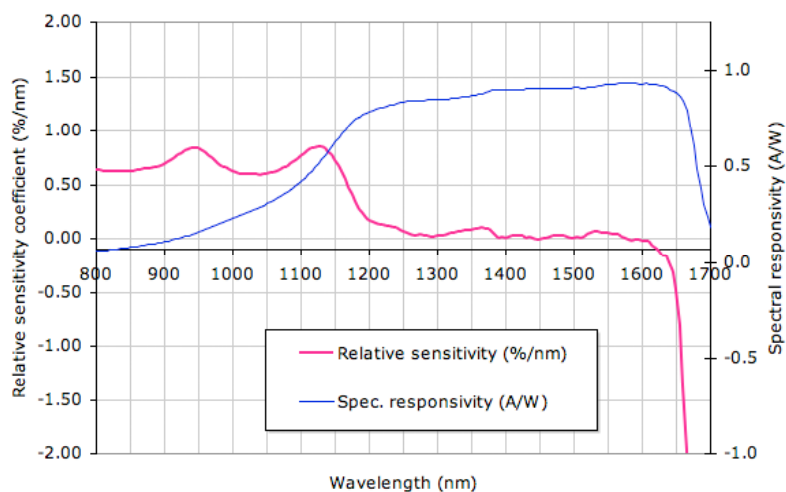


Figure 5.7 (b) Relative sensitivity coefficient for one of the Telcom Devices photodiodes.

Table 5.4 Transfer uncertainty contribution  $u_{w,p}^T$  associated with the wavelength scale uncertainty of NIST SCF.

	Transfer uncertainty contribution (%) for GPD, EG&G, Fermionics	Transfer uncertainty contribution (%) for Telcom
900	0.02	0.02
950	0.02	0.02
1000	0.00	0.03
1050	0.00	0.03
1100	0.00	0.03
1150	0.00	0.04
1200	0.00	0.00
1250	0.00	0.00
1300	0.00	0.00
1350	0.00	0.00
1400	0.00	0.00
1450	0.00	0.00
1500	0.00	0.00
1550	0.00	0.00

### 5.5.4 Bandwidth effect

The bandwidth of the monochromator also affects in transfer measurement if there are significant differences in relative spectral responsivity curve between the working standard detectors and photodiodes measured in the NIST SCF. Figure 5.8 (a) and (b) shows the bandpass errors for two different types of photodiode calculated as the measured value minus the corrected value (Ohno 2005). Even though such data are shown, bandpass error correction was not applied for the NIST measurements in this comparison, thus this factor is evaluated as an uncertainty component. The uncertainty contribution in transfer measurement was analyzed from the

differences in bandpass error between the NIST working standard detectors and various transfer photodiodes used in the comparison. The estimated errors were converted to standard uncertainty using a rectangular distribution. Table 5.5 summarizes the results for the uncertainty contribution in the transfer measurement associated with the effect of bandpass, denoted  $u_{bp,p}^T$ , for the two groups of photodiode.

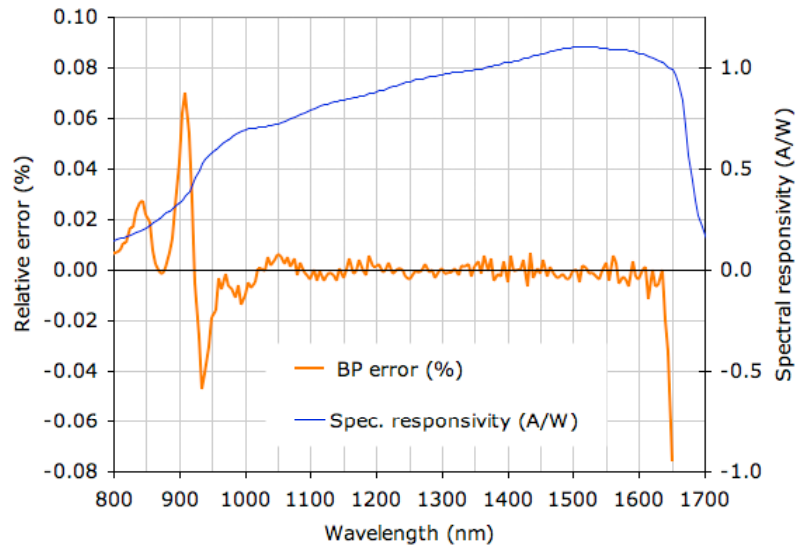


Figure 5.8 (a) Relative errors due to bandwidth (4 nm) of the NIST SCF for a typical GPD photodiode.

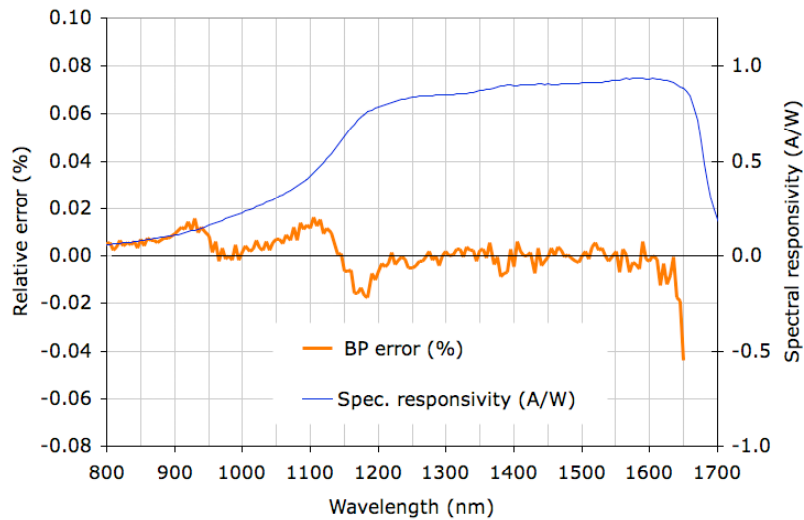


Figure 5.8 (b) Relative errors due to bandwidth (4 nm) of the NIST SCF for one of TDC photodiodes.

Table 5.5 Transfer uncertainty contribution  $u_{bp,p}^T$  associated with the effect of bandpass of NIST SCF.

	GPD, EG&G, Fermionics Transfer uncertainty contribution (%)	TDC Transfer uncertainty contribution (%)
900	0.02	0.02
950	0.01	0.02
1000	0.00	0.01
1050	0.00	0.00
1100	0.00	0.01
1150	0.00	0.00
1200	0.00	0.00
1250	0.00	0.00
1300	0.00	0.00
1350	0.00	0.00
1400	0.00	0.00
1450	0.00	0.00
1500	0.00	0.00
1550	0.00	0.00

### 5.5.5 Beam size

The difference in beam size used by the pilot lab and by the participants also affects the results of the comparison due to the spatial nonuniformity of photodiode responsivity. The spatial nonuniformity of all the transfer photodiode were measured at three wavelengths at least once at the beginning of the comparison (section 3.3). Based on these data, the differences in the results for each photodiode in different beam sizes were analyzed. In this calculation, the beam profile is assumed to be Gaussian, and the function is fit so that most of the beam power is contained within the circle of reported diameter and the center of the beam is placed at the center of the photodiode's sensitive area. The difference in measured responsivity was obtained as the weighted average of the responsivity uniformity data (normalized at the center) weighted by the Gaussian beam distribution.

Table 5.6 shows the results. Corrections were not made to the comparison results based on these data, thus these were considered as a part of transfer uncertainty. Based on these data and reported beam size used at each participant laboratory, the relative difference for each photodiode for each laboratory was estimated. For beam sizes other than 2 mm and 3 mm, a parabolic interpolation was used (with the errors at 1 mm beam size to be zero). The results were converted to standard uncertainties, called  $u_{bs,ij}^T$ , and summarized in Table 5.7. Since it would be too complicated to deal with this uncertainty at each wavelength for each photodiode, the average of 1250 nm and 1600 nm was used for all wavelengths for simplicity. The 900 nm data was not used because many of the data at this wavelength were not used (highlighted gray), and this wavelength tends to have large nonuniformity but data of neighboring wavelengths may not necessarily be similar. An example of a problematic spatial nonuniformity of a photodiode is shown in Fig. 5.9. Fortunately this photodiode was sent only to one laboratory, who used 2 mm beam size.

Table 5.6 Relative difference (%) in measured responsivity for different beam sizes compared to the 1 mm diameter beam used at NIST.

Detector NIST #	2 mm beam size			3 mm beam size		
	900 nm	1250 nm	1600 nm	900 nm	1250 nm	1600 nm
01 Fermionics	-0.04	0.00	0.07	-0.18	-0.05	0.07
02 Fermionics	-0.06	-0.02	0.01	-0.18	-0.11	-0.05
03 Fermionics	-0.04	-0.02	0.01	-0.16	-0.08	-0.02
04 GPD	0.03	-0.02	0.08	-0.02	-0.07	0.09
06 GPD	-0.05	-0.09	-0.02	-0.15	-0.18	-0.04
07 GPD	0.00	-0.01	-0.03	-0.06	-0.06	-0.03
08 EG&G	-0.20	0.00	0.00	-0.48	-0.06	-0.03
09 EG&G	-0.11	-0.05	-0.08	-0.20	-0.12	-0.15
10 EG&G	-0.11	0.00	-0.01	-0.32	-0.13	-0.11
11 EG&G	-0.06	-0.02	-0.03	-0.09	-0.07	-0.10
12 Telcom	0.00	-0.01	0.00	-0.05	-0.05	-0.04
13 Telcom	-0.02	-0.07	-0.19	-0.15	-0.20	-0.44
14 Telcom	-0.05	-0.01	-0.01	-0.14	-0.05	-0.02
15 Telcom	-0.23	-0.02	-0.11	-0.55	-0.09	-0.27
16 GPD	0.06	-0.01	0.00	0.03	-0.07	-0.04
17 GPD	-0.08	-0.07	-0.01	-0.14	-0.15	-0.05
18 GPD	-0.15	-0.02	0.00	-0.60	-0.23	-0.12

\* 900 nm data of gray highlighted diodes were not used in the comparison analysis.

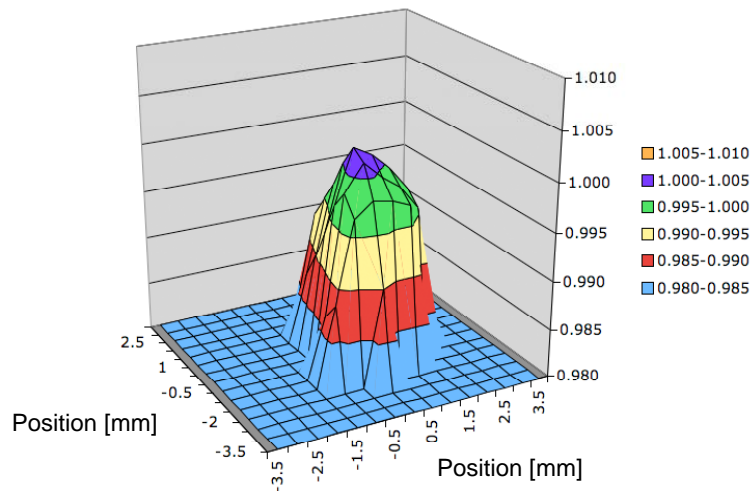


Figure 5.9 Responsivity spatial nonuniformity of NIST#13 at 1600 nm.

Table 5.7 Transfer uncertainty contribution  $u_{bs,ij}^T$  (%) associated with the differences in beam size used by the participants and the spatial nonuniformity of transfer photodiodes.

NMI	Beam size	Detector NIST #		900 nm	1250 nm	1600 nm	$u_{bs,ij}^T$ *1
BNM-INM	3 mm	04	GPD	0.01	0.04	0.05	0.05
		08	EG&G	0.28	0.04	0.02	0.03
		10	EG&G	0.18	0.08	0.07	0.07
CSIR	2 mm	04	GPD	0.02	0.01	0.04	0.03
		08	EG&G	0.11	0.00	0.00	0.00
		15	Telcom	0.13	0.01	0.06	0.04
CSIRO	1 x 3 mm	06	GPD	0.03	0.05	0.01	0.03
		14	Telcom	0.03	0.00	0.01	0.01
		03	Fermionics	0.02	0.01	0.00	0.01
HUT	1 x 1.7 mm	06	GPD	0.01	0.03	0.00	0.01
		10	EG&G	0.02	0.01	0.00	0.01
		15	Telcom	0.05	0.00	0.03	0.01
IFA	3.2 mm	04	GPD	0.03	0.05	0.05	0.05
		03	Fermionics	0.11	0.06	0.02	0.04
		11	EG&G	0.05	0.05	0.06	0.06
KRISS	2 mm	17	GPD	0.05	0.04	0.01	0.02
		10	EG&G	0.07	0.00	0.01	0.00
		13	Telcom	0.01	0.04	0.11	0.07
NIM	3 mm	04	GPD	0.01	0.04	0.05	0.05
		11	EG&G	0.05	0.04	0.06	0.05
		09	EG&G	0.11	0.07	0.08	0.08
NMI-VSL	4 mm	16	GPD	0.05	0.10	0.06	0.08
		02	Fermionics	0.22	0.15	0.10	0.13
		05	GPD	0.10	0.08	0.02	0.05
NPL	3 mm	07	GPD	0.04	0.04	0.02	0.03
		08	EG&G	0.28	0.04	0.02	0.03
		14	Telcom	0.08	0.03	0.01	0.02
NRC	3 x 1.5 mm	16	GPD	0.03	0.01	0.01	0.01
		14	Telcom	0.05	0.01	0.01	0.01
		08	EG&G	0.17	0.01	0.01	0.01
OMH	2 mm	07	GPD	0.00	0.01	0.01	0.01
		11	EG&G	0.03	0.01	0.02	0.01
		15	Telcom	0.13	0.01	0.06	0.04
PTB	1.3 mm HM*1	18	GPD	0.15	0.04	0.01	0.02
		11	EG&G	0.04	0.02	0.03	0.02
		01	Fermionics	0.04	0.00	0.04	0.02
	2.3 nm HM*2	18	GPD	0.34	0.13	0.07	0.10
		11	EG&G	0.05	0.04	0.06	0.05
		01	Fermionics	0.10	0.03	0.04	0.04
SMU	3 mm	07	GPD	0.04	0.04	0.02	0.03
		02	Fermionics	0.10	0.06	0.03	0.05
		10	EG&G	0.18	0.08	0.07	0.07
VNIIOFI	2 x 3 mm	07	GPD	0.02	0.03	0.02	0.02
		14	Telcom	0.07	0.02	0.01	0.02
		09	EG&G	0.10	0.06	0.08	0.07

\*1 Average of 1250 nm and 1600 nm. \*2 1400 nm and lower, \*3 higher than 1400 nm

### 5.5.6 *Alignment of detector*

Due to the significant spatial nonuniformity of the photodiode responsivity, alignment offsets can cause significant variations in results. The repeatability of NIST measurements due to repeatability of alignment is included in the NIST repeatability data in Table 5.2 because these repeated measurements at NIST included re-alignment of the photodiodes. The uncertainty contributions from alignment were evaluated from the spatial nonuniformity data of transfer photodiodes, which showed similar degree of uncertainty contributions from alignment accuracy and used only as verification.

### 5.5.7 *Summary of transfer uncertainties associated with photodiode characteristics*

The transfer uncertainties due to the wavelength scale uncertainty, bandpass, and differences in beam size are dependent on the characteristics of each particular photodiode. The effect of beam size also depends on the instruments used by the participants. These components are to be included in the uncertainty analysis for the laboratory – NIST difference for each photodiode. The tables below summarize these uncertainty contributions for each transfer photodiode measured by each laboratory.  $u_{c,ij}^T$  is the combined standard uncertainties of these components.

Table 5.8.1 BNM-INM additional transfer uncertainty contributions.

Wavelength [nm]	NIST04 (GPD)				NIST08 (EG&G)				NIST10 (EG&G)			
	$u_{w,p}^T$	$u_{bp,p}^T$	$u_{bs,ij}^T$	$u_{c,ij}^T$	$u_{w,p}^T$	$u_{bp,p}^T$	$u_{bs,ij}^T$	$u_{c,ij}^T$	$u_{w,p}^T$	$u_{bp,p}^T$	$u_{bs,ij}^T$	$u_{c,ij}^T$
900	0.02	0.02	0.05	0.05	0.02	0.02	0.03	0.04	0.02	0.02	0.07	0.08
950	0.02	0.01	0.05	0.05	0.02	0.01	0.03	0.03	0.02	0.01	0.07	0.07
1000	0.00	0.00	0.05	0.05	0.00	0.00	0.03	0.03	0.00	0.00	0.07	0.07
1050	0.00	0.00	0.05	0.05	0.00	0.00	0.03	0.03	0.00	0.00	0.07	0.07
1100	0.00	0.00	0.05	0.05	0.00	0.00	0.03	0.03	0.00	0.00	0.07	0.07
1150	0.00	0.00	0.05	0.05	0.00	0.00	0.03	0.03	0.00	0.00	0.07	0.07
1200	0.00	0.00	0.05	0.05	0.00	0.00	0.03	0.03	0.00	0.00	0.07	0.07
1250	0.00	0.00	0.05	0.05	0.00	0.00	0.03	0.03	0.00	0.00	0.07	0.07
1300	0.00	0.00	0.05	0.05	0.00	0.00	0.03	0.03	0.00	0.00	0.07	0.07
1350	0.00	0.00	0.05	0.05	0.00	0.00	0.03	0.03	0.00	0.00	0.07	0.07
1400	0.00	0.00	0.05	0.05	0.00	0.00	0.03	0.03	0.00	0.00	0.07	0.07
1450	0.00	0.00	0.05	0.05	0.00	0.00	0.03	0.03	0.00	0.00	0.07	0.07
1500	0.00	0.00	0.05	0.05	0.00	0.00	0.03	0.03	0.00	0.00	0.07	0.07
1550	0.00	0.00	0.05	0.05	0.00	0.00	0.03	0.03	0.00	0.00	0.07	0.07
1600	0.00	0.00	0.05	0.05	0.00	0.00	0.03	0.03	0.00	0.00	0.07	0.07

Table 5.8.2 CSIR additional transfer uncertainty contributions.

Wavelength [nm]	NIST04 (GPD)				NIST08 (EG&G)				NIST15 (TDC)			
	$u_{w,p}^T$	$u_{bp,p}^T$	$u_{bs,ij}^T$	$u_{c,ij}^T$	$u_{w,p}^T$	$u_{bp,p}^T$	$u_{bs,ij}^T$	$u_{c,ij}^T$	$u_{w,p}^T$	$u_{bp,p}^T$	$u_{bs,ij}^T$	$u_{c,ij}^T$
900	0.02	0.02	0.03	0.04	0.02	0.02	0.00	0.02	0.02	0.02	0.04	0.05
950	0.02	0.01	0.03	0.03	0.02	0.01	0.00	0.02	0.02	0.02	0.04	0.04
1000	0.00	0.00	0.03	0.03	0.00	0.00	0.00	0.01	0.03	0.01	0.04	0.05
1050	0.00	0.00	0.03	0.03	0.00	0.00	0.00	0.00	0.03	0.00	0.04	0.05
1100	0.00	0.00	0.03	0.03	0.00	0.00	0.00	0.00	0.03	0.01	0.04	0.05
1150	0.00	0.00	0.03	0.03	0.00	0.00	0.00	0.00	0.04	0.00	0.04	0.05
1200	0.00	0.00	0.03	0.03	0.00	0.00	0.00	0.00	0.00	0.00	0.04	0.04
1250	0.00	0.00	0.03	0.03	0.00	0.00	0.00	0.00	0.00	0.00	0.04	0.04
1300	0.00	0.00	0.03	0.03	0.00	0.00	0.00	0.00	0.00	0.00	0.04	0.04
1350	0.00	0.00	0.03	0.03	0.00	0.00	0.00	0.00	0.00	0.00	0.04	0.04
1400	0.00	0.00	0.03	0.03	0.00	0.00	0.00	0.00	0.00	0.00	0.04	0.04
1450	0.00	0.00	0.03	0.03	0.00	0.00	0.00	0.00	0.00	0.00	0.04	0.04
1500	0.00	0.00	0.03	0.03	0.00	0.00	0.00	0.00	0.00	0.00	0.04	0.04
1550	0.00	0.00	0.03	0.03	0.00	0.00	0.00	0.00	0.00	0.00	0.04	0.04
1600	0.00	0.00	0.03	0.03	0.00	0.00	0.00	0.00	0.00	0.00	0.04	0.04

Table 5.8.3 CSIRO additional transfer uncertainty contributions.

Wavelength [nm]	NIST06 (GPD)				NIST14 (TDC)				NIST03 (Fermionics)			
	$u_{w,p}^T$	$u_{bp,p}^T$	$u_{bs,ij}^T$	$u_{c,ij}^T$	$u_{w,p}^T$	$u_{bp,p}^T$	$u_{bs,ij}^T$	$u_{c,ij}^T$	$u_{w,p}^T$	$u_{bp,p}^T$	$u_{bs,ij}^T$	$u_{c,ij}^T$
900	0.02	0.02	0.03	0.04	0.02	0.02	0.01	0.03	0.02	0.02	0.01	0.03
950	0.02	0.01	0.03	0.04	0.02	0.02	0.01	0.02	0.02	0.01	0.01	0.02
1000	0.00	0.00	0.03	0.03	0.03	0.01	0.01	0.03	0.00	0.00	0.01	0.01
1050	0.00	0.00	0.03	0.03	0.03	0.00	0.01	0.03	0.00	0.00	0.01	0.01
1100	0.00	0.00	0.03	0.03	0.03	0.01	0.01	0.04	0.00	0.00	0.01	0.01
1150	0.00	0.00	0.03	0.03	0.04	0.00	0.01	0.04	0.00	0.00	0.01	0.01
1200	0.00	0.00	0.03	0.03	0.00	0.00	0.01	0.01	0.00	0.00	0.01	0.01
1250	0.00	0.00	0.03	0.03	0.00	0.00	0.01	0.01	0.00	0.00	0.01	0.01
1300	0.00	0.00	0.03	0.03	0.00	0.00	0.01	0.01	0.00	0.00	0.01	0.01
1350	0.00	0.00	0.03	0.03	0.00	0.00	0.01	0.01	0.00	0.00	0.01	0.01
1400	0.00	0.00	0.03	0.03	0.00	0.00	0.01	0.01	0.00	0.00	0.01	0.01
1450	0.00	0.00	0.03	0.03	0.00	0.00	0.01	0.01	0.00	0.00	0.01	0.01
1500	0.00	0.00	0.03	0.03	0.00	0.00	0.01	0.01	0.00	0.00	0.01	0.01
1550	0.00	0.00	0.03	0.03	0.00	0.00	0.01	0.01	0.00	0.00	0.01	0.01
1600	0.00	0.00	0.03	0.03	0.00	0.00	0.01	0.01	0.00	0.00	0.01	0.01

Table 5.8.4 HUT additional transfer uncertainty contributions.

Wavelength [nm]	NIST06 (GPD)				NIST10 (EG&G)				NIST15 (TDC)			
	$u_{w,p}^T$	$u_{bp,p}^T$	$u_{bs,ij}^T$	$u_{c,ij}^T$	$u_{w,p}^T$	$u_{bp,p}^T$	$u_{bs,ij}^T$	$u_{c,ij}^T$	$u_{w,p}^T$	$u_{bp,p}^T$	$u_{bs,ij}^T$	$u_{c,ij}^T$
900	0.02	0.02	0.01	0.03	0.02	0.02	0.01	0.03	0.02	0.02	0.01	0.03
950	0.02	0.01	0.01	0.02	0.02	0.01	0.01	0.02	0.02	0.02	0.01	0.03
1000	0.00	0.00	0.01	0.02	0.00	0.00	0.01	0.01	0.03	0.01	0.01	0.03
1050	0.00	0.00	0.01	0.02	0.00	0.00	0.01	0.01	0.03	0.00	0.01	0.03
1100	0.00	0.00	0.01	0.02	0.00	0.00	0.01	0.01	0.03	0.01	0.01	0.04
1150	0.00	0.00	0.01	0.02	0.00	0.00	0.01	0.01	0.04	0.00	0.01	0.04
1200	0.00	0.00	0.01	0.01	0.00	0.00	0.01	0.01	0.00	0.00	0.01	0.01
1250	0.00	0.00	0.01	0.01	0.00	0.00	0.01	0.01	0.00	0.00	0.01	0.01
1300	0.00	0.00	0.01	0.01	0.00	0.00	0.01	0.01	0.00	0.00	0.01	0.01
1350	0.00	0.00	0.01	0.01	0.00	0.00	0.01	0.01	0.00	0.00	0.01	0.01
1400	0.00	0.00	0.01	0.01	0.00	0.00	0.01	0.01	0.00	0.00	0.01	0.01
1450	0.00	0.00	0.01	0.02	0.00	0.00	0.01	0.01	0.00	0.00	0.01	0.01
1500	0.00	0.00	0.01	0.02	0.00	0.00	0.01	0.01	0.00	0.00	0.01	0.01
1550	0.00	0.00	0.01	0.02	0.00	0.00	0.01	0.01	0.00	0.00	0.01	0.01
1600	0.00	0.00	0.01	0.02	0.00	0.00	0.01	0.01	0.00	0.00	0.01	0.01

Table 5.8.5 IFA additional transfer uncertainty contributions.

Wavelength [nm]	NIST04 (GPD)				NIST03 (Fermionics)				NIST11 (EG&G)			
	$u_{w,p}^T$	$u_{bp,p}^T$	$u_{bs,ij}^T$	$u_{c,ij}^T$	$u_{w,p}^T$	$u_{bp,p}^T$	$u_{bs,ij}^T$	$u_{c,ij}^T$	$u_{w,p}^T$	$u_{bp,p}^T$	$u_{bs,ij}^T$	$u_{c,ij}^T$
900	0.02	0.02	0.05	0.05	0.02	0.02	0.04	0.04	0.02	0.02	0.06	0.06
950	0.02	0.01	0.05	0.05	0.02	0.01	0.04	0.04	0.02	0.01	0.06	0.06
1000	0.00	0.00	0.05	0.05	0.00	0.00	0.04	0.04	0.00	0.00	0.06	0.06
1050	0.00	0.00	0.05	0.05	0.00	0.00	0.04	0.04	0.00	0.00	0.06	0.06
1100	0.00	0.00	0.05	0.05	0.00	0.00	0.04	0.04	0.00	0.00	0.06	0.06
1150	0.00	0.00	0.05	0.05	0.00	0.00	0.04	0.04	0.00	0.00	0.06	0.06
1200	0.00	0.00	0.05	0.05	0.00	0.00	0.04	0.04	0.00	0.00	0.06	0.06
1250	0.00	0.00	0.05	0.05	0.00	0.00	0.04	0.04	0.00	0.00	0.06	0.06
1300	0.00	0.00	0.05	0.05	0.00	0.00	0.04	0.04	0.00	0.00	0.06	0.06
1350	0.00	0.00	0.05	0.05	0.00	0.00	0.04	0.04	0.00	0.00	0.06	0.06
1400	0.00	0.00	0.05	0.05	0.00	0.00	0.04	0.04	0.00	0.00	0.06	0.06
1450	0.00	0.00	0.05	0.05	0.00	0.00	0.04	0.04	0.00	0.00	0.06	0.06
1500	0.00	0.00	0.05	0.05	0.00	0.00	0.04	0.04	0.00	0.00	0.06	0.06
1550	0.00	0.00	0.05	0.05	0.00	0.00	0.04	0.04	0.00	0.00	0.06	0.06
1600	0.00	0.00	0.05	0.05	0.00	0.00	0.04	0.04	0.00	0.00	0.06	0.06

Table 5.8.6 KRISS additional transfer uncertainty contributions.

Wavelength [nm]	NIST17 (GPD)				NIST10 (EG&G)				NIST13 (TDC)			
	$u_{w,p}^T$	$u_{bp,p}^T$	$u_{bs,ij}^T$	$u_{c,ij}^T$	$u_{w,p}^T$	$u_{bp,p}^T$	$u_{bs,ij}^T$	$u_{c,ij}^T$	$u_{w,p}^T$	$u_{bp,p}^T$	$u_{bs,ij}^T$	$u_{c,ij}^T$
900	0.02	0.02	0.02	0.03	0.02	0.02	0.00	0.02	0.02	0.02	0.07	0.08
950	0.02	0.01	0.02	0.03	0.02	0.01	0.00	0.02	0.02	0.02	0.07	0.08
1000	0.00	0.00	0.02	0.02	0.00	0.00	0.00	0.01	0.03	0.01	0.07	0.08
1050	0.00	0.00	0.02	0.02	0.00	0.00	0.00	0.00	0.03	0.00	0.07	0.08
1100	0.00	0.00	0.02	0.02	0.00	0.00	0.00	0.00	0.03	0.01	0.07	0.08
1150	0.00	0.00	0.02	0.02	0.00	0.00	0.00	0.00	0.04	0.00	0.07	0.08
1200	0.00	0.00	0.02	0.02	0.00	0.00	0.00	0.00	0.00	0.00	0.07	0.07
1250	0.00	0.00	0.02	0.02	0.00	0.00	0.00	0.00	0.00	0.00	0.07	0.07
1300	0.00	0.00	0.02	0.02	0.00	0.00	0.00	0.00	0.00	0.00	0.07	0.07
1350	0.00	0.00	0.02	0.02	0.00	0.00	0.00	0.00	0.00	0.00	0.07	0.07
1400	0.00	0.00	0.02	0.02	0.00	0.00	0.00	0.00	0.00	0.00	0.07	0.07
1450	0.00	0.00	0.02	0.02	0.00	0.00	0.00	0.00	0.00	0.00	0.07	0.07
1500	0.00	0.00	0.02	0.02	0.00	0.00	0.00	0.00	0.00	0.00	0.07	0.07
1550	0.00	0.00	0.02	0.02	0.00	0.00	0.00	0.00	0.00	0.00	0.07	0.07
1600	0.00	0.00	0.02	0.02	0.00	0.00	0.00	0.00	0.00	0.00	0.07	0.07

Table 5.8.7 NIM additional transfer uncertainty contributions.

Wavelength [nm]	NIST04 (GPD)				NIST11 (EG&G)				NIST09 (EG&G)			
	$u_{w,p}^T$	$u_{bp,p}^T$	$u_{bs,ij}^T$	$u_{c,ij}^T$	$u_{w,p}^T$	$u_{bp,p}^T$	$u_{bs,ij}^T$	$u_{c,ij}^T$	$u_{w,p}^T$	$u_{bp,p}^T$	$u_{bs,ij}^T$	$u_{c,ij}^T$
900	0.02	0.02	0.05	0.05	0.02	0.02	0.05	0.05	0.02	0.02	0.08	0.08
950	0.02	0.01	0.05	0.05	0.02	0.01	0.05	0.05	0.02	0.01	0.08	0.08
1000	0.00	0.00	0.05	0.05	0.00	0.00	0.05	0.05	0.00	0.00	0.08	0.08
1050	0.00	0.00	0.05	0.05	0.00	0.00	0.05	0.05	0.00	0.00	0.08	0.08
1100	0.00	0.00	0.05	0.05	0.00	0.00	0.05	0.05	0.00	0.00	0.08	0.08
1150	0.00	0.00	0.05	0.05	0.00	0.00	0.05	0.05	0.00	0.00	0.08	0.08
1200	0.00	0.00	0.05	0.05	0.00	0.00	0.05	0.05	0.00	0.00	0.08	0.08
1250	0.00	0.00	0.05	0.05	0.00	0.00	0.05	0.05	0.00	0.00	0.08	0.08
1300	0.00	0.00	0.05	0.05	0.00	0.00	0.05	0.05	0.00	0.00	0.08	0.08
1350	0.00	0.00	0.05	0.05	0.00	0.00	0.05	0.05	0.00	0.00	0.08	0.08
1400	0.00	0.00	0.05	0.05	0.00	0.00	0.05	0.05	0.00	0.00	0.08	0.08
1450	0.00	0.00	0.05	0.05	0.00	0.00	0.05	0.05	0.00	0.00	0.08	0.08
1500	0.00	0.00	0.05	0.05	0.00	0.00	0.05	0.05	0.00	0.00	0.08	0.08
1550	0.00	0.00	0.05	0.05	0.00	0.00	0.05	0.05	0.00	0.00	0.08	0.08
1600	0.00	0.00	0.05	0.05	0.00	0.00	0.05	0.05	0.00	0.00	0.08	0.08

Table 5.8.8 NMI-VSL additional transfer uncertainty contributions.

Wavelength [nm]	NIST16 (GPD)				NIST02 (Fermionics)				NIST05 (GPD)			
	$u_{w,p}^T$	$u_{bp,p}^T$	$u_{bs,ij}^T$	$u_{c,ij}^T$	$u_{w,p}^T$	$u_{bp,p}^T$	$u_{bs,ij}^T$	$u_{c,ij}^T$	$u_{w,p}^T$	$u_{bp,p}^T$	$u_{bs,ij}^T$	$u_{c,ij}^T$
900	0.02	0.02	0.08	0.08	0.02	0.02	0.13	0.13	0.02	0.02	0.05	0.06
950	0.02	0.01	0.08	0.08	0.02	0.01	0.13	0.13	0.02	0.01	0.05	0.06
1000	0.00	0.00	0.08	0.08	0.00	0.00	0.13	0.13	0.00	0.00	0.05	0.05
1050	0.00	0.00	0.08	0.08	0.00	0.00	0.13	0.13	0.00	0.00	0.05	0.05
1100	0.00	0.00	0.08	0.08	0.00	0.00	0.13	0.13	0.00	0.00	0.05	0.05
1150	0.00	0.00	0.08	0.08	0.00	0.00	0.13	0.13	0.00	0.00	0.05	0.05
1200	0.00	0.00	0.08	0.08	0.00	0.00	0.13	0.13	0.00	0.00	0.05	0.05
1250	0.00	0.00	0.08	0.08	0.00	0.00	0.13	0.13	0.00	0.00	0.05	0.05
1300	0.00	0.00	0.08	0.08	0.00	0.00	0.13	0.13	0.00	0.00	0.05	0.05
1350	0.00	0.00	0.08	0.08	0.00	0.00	0.13	0.13	0.00	0.00	0.05	0.05
1400	0.00	0.00	0.08	0.08	0.00	0.00	0.13	0.13	0.00	0.00	0.05	0.05
1450	0.00	0.00	0.08	0.08	0.00	0.00	0.13	0.13	0.00	0.00	0.05	0.05
1500	0.00	0.00	0.08	0.08	0.00	0.00	0.13	0.13	0.00	0.00	0.05	0.05
1550	0.00	0.00	0.08	0.08	0.00	0.00	0.13	0.13	0.00	0.00	0.05	0.05
1600	0.00	0.00	0.08	0.08	0.00	0.00	0.13	0.13	0.00	0.00	0.05	0.05

Table 5.8.9 NPL additional transfer uncertainty contributions.

Wavelength [nm]	NIST07 (GPD)				NIST08 (EG&G)				NIST14 (TDC)			
	$u_{w,p}^T$	$u_{bp,p}^T$	$u_{bs,ij}^T$	$u_{c,ij}^T$	$u_{w,p}^T$	$u_{bp,p}^T$	$u_{bs,ij}^T$	$u_{c,ij}^T$	$u_{w,p}^T$	$u_{bp,p}^T$	$u_{bs,ij}^T$	$u_{c,ij}^T$
900	0.02	0.02	0.03	0.04	0.02	0.02	0.03	0.04	0.02	0.02	0.02	0.04
950	0.02	0.01	0.03	0.03	0.02	0.01	0.03	0.03	0.02	0.02	0.02	0.03
1000	0.00	0.00	0.03	0.03	0.00	0.00	0.03	0.03	0.03	0.01	0.02	0.04
1050	0.00	0.00	0.03	0.03	0.00	0.00	0.03	0.03	0.03	0.00	0.02	0.03
1100	0.00	0.00	0.03	0.03	0.00	0.00	0.03	0.03	0.03	0.01	0.02	0.04
1150	0.00	0.00	0.03	0.03	0.00	0.00	0.03	0.03	0.04	0.00	0.02	0.04
1200	0.00	0.00	0.03	0.03	0.00	0.00	0.03	0.03	0.00	0.00	0.02	0.02
1250	0.00	0.00	0.03	0.03	0.00	0.00	0.03	0.03	0.00	0.00	0.02	0.02
1300	0.00	0.00	0.03	0.03	0.00	0.00	0.03	0.03	0.00	0.00	0.02	0.02
1350	0.00	0.00	0.03	0.03	0.00	0.00	0.03	0.03	0.00	0.00	0.02	0.02
1400	0.00	0.00	0.03	0.03	0.00	0.00	0.03	0.03	0.00	0.00	0.02	0.02
1450	0.00	0.00	0.03	0.03	0.00	0.00	0.03	0.03	0.00	0.00	0.02	0.02
1500	0.00	0.00	0.03	0.03	0.00	0.00	0.03	0.03	0.00	0.00	0.02	0.02
1550	0.00	0.00	0.03	0.03	0.00	0.00	0.03	0.03	0.00	0.00	0.02	0.02
1600	0.00	0.00	0.03	0.03	0.00	0.00	0.03	0.03	0.00	0.00	0.02	0.02

Table 5.8.10 NRC additional transfer uncertainty contributions.

Wavelength [nm]	NIST16 (GPD)				NIST14 (TDC)				NIST08 (EG&G)			
	$u_{w,p}^T$	$u_{bp,p}^T$	$u_{bs,ij}^T$	$u_{c,ij}^T$	$u_{w,p}^T$	$u_{bp,p}^T$	$u_{bs,ij}^T$	$u_{c,ij}^T$	$u_{w,p}^T$	$u_{bp,p}^T$	$u_{bs,ij}^T$	$u_{c,ij}^T$
900	0.02	0.02	0.01	0.03	0.02	0.02	0.01	0.03	0.02	0.02	0.01	0.03
950	0.02	0.01	0.01	0.02	0.02	0.02	0.01	0.03	0.02	0.01	0.01	0.02
1000	0.00	0.00	0.01	0.01	0.03	0.01	0.01	0.03	0.00	0.00	0.01	0.01
1050	0.00	0.00	0.01	0.01	0.03	0.00	0.01	0.03	0.00	0.00	0.01	0.01
1100	0.00	0.00	0.01	0.01	0.03	0.01	0.01	0.04	0.00	0.00	0.01	0.01
1150	0.00	0.00	0.01	0.01	0.04	0.00	0.01	0.04	0.00	0.00	0.01	0.01
1200	0.00	0.00	0.01	0.01	0.00	0.00	0.01	0.01	0.00	0.00	0.01	0.01
1250	0.00	0.00	0.01	0.01	0.00	0.00	0.01	0.01	0.00	0.00	0.01	0.01
1300	0.00	0.00	0.01	0.01	0.00	0.00	0.01	0.01	0.00	0.00	0.01	0.01
1350	0.00	0.00	0.01	0.01	0.00	0.00	0.01	0.01	0.00	0.00	0.01	0.01
1400	0.00	0.00	0.01	0.01	0.00	0.00	0.01	0.01	0.00	0.00	0.01	0.01
1450	0.00	0.00	0.01	0.01	0.00	0.00	0.01	0.01	0.00	0.00	0.01	0.01
1500	0.00	0.00	0.01	0.01	0.00	0.00	0.01	0.01	0.00	0.00	0.01	0.01
1550	0.00	0.00	0.01	0.01	0.00	0.00	0.01	0.01	0.00	0.00	0.01	0.01
1600	0.00	0.00	0.01	0.01	0.00	0.00	0.01	0.01	0.00	0.00	0.01	0.01

Table 5.8.11 OMH additional transfer uncertainty contributions.

Wavelength [nm]	NIST07 (GPD)				NIST11 (EG&G)				NIST15 (TDC)			
	$u_{w,p}^T$	$u_{bp,p}^T$	$u_{bs,ij}^T$	$u_{c,ij}^T$	$u_{w,p}^T$	$u_{bp,p}^T$	$u_{bs,ij}^T$	$u_{c,ij}^T$	$u_{w,p}^T$	$u_{bp,p}^T$	$u_{bs,ij}^T$	$u_{c,ij}^T$
900	0.02	0.02	0.01	0.03	0.02	0.02	0.01	0.03	0.02	0.02	0.04	0.05
950	0.02	0.01	0.01	0.02	0.02	0.01	0.01	0.02	0.02	0.02	0.04	0.04
1000	0.00	0.00	0.01	0.01	0.00	0.00	0.01	0.02	0.03	0.01	0.04	0.05
1050	0.00	0.00	0.01	0.01	0.00	0.00	0.01	0.01	0.03	0.00	0.04	0.05
1100	0.00	0.00	0.01	0.01	0.00	0.00	0.01	0.01	0.03	0.01	0.04	0.05
1150	0.00	0.00	0.01	0.01	0.00	0.00	0.01	0.01	0.04	0.00	0.04	0.05
1200	0.00	0.00	0.01	0.01	0.00	0.00	0.01	0.01	0.00	0.00	0.04	0.04
1250	0.00	0.00	0.01	0.01	0.00	0.00	0.01	0.01	0.00	0.00	0.04	0.04
1300	0.00	0.00	0.01	0.01	0.00	0.00	0.01	0.01	0.00	0.00	0.04	0.04
1350	0.00	0.00	0.01	0.01	0.00	0.00	0.01	0.01	0.00	0.00	0.04	0.04
1400	0.00	0.00	0.01	0.01	0.00	0.00	0.01	0.01	0.00	0.00	0.04	0.04
1450	0.00	0.00	0.01	0.01	0.00	0.00	0.01	0.01	0.00	0.00	0.04	0.04
1500	0.00	0.00	0.01	0.01	0.00	0.00	0.01	0.01	0.00	0.00	0.04	0.04
1550	0.00	0.00	0.01	0.01	0.00	0.00	0.01	0.01	0.00	0.00	0.04	0.04
1600	0.00	0.00	0.01	0.01	0.00	0.00	0.01	0.01	0.00	0.00	0.04	0.04

Table 5.8.12 PTB additional transfer uncertainty contributions.

Wavelength [nm]	NIST18 (GPD)				NIST11 (EG&G)				NIST01 (Fermionics)			
	$u_{w,p}^T$	$u_{bp,p}^T$	$u_{bs,ij}^T$	$u_{c,ij}^T$	$u_{w,p}^T$	$u_{bp,p}^T$	$u_{bs,ij}^T$	$u_{c,ij}^T$	$u_{w,p}^T$	$u_{bp,p}^T$	$u_{bs,ij}^T$	$u_{c,ij}^T$
900	0.02	0.02	0.02	0.03	0.02	0.02	0.02	0.03	0.02	0.02	0.02	0.03
950	0.02	0.01	0.02	0.03	0.02	0.01	0.02	0.03	0.02	0.01	0.02	0.03
1000	0.00	0.00	0.02	0.03	0.00	0.00	0.02	0.02	0.00	0.00	0.02	0.02
1050	0.00	0.00	0.02	0.02	0.00	0.00	0.02	0.02	0.00	0.00	0.02	0.02
1100	0.00	0.00	0.02	0.02	0.00	0.00	0.02	0.02	0.00	0.00	0.02	0.02
1150	0.00	0.00	0.02	0.02	0.00	0.00	0.02	0.02	0.00	0.00	0.02	0.02
1200	0.00	0.00	0.02	0.02	0.00	0.00	0.02	0.02	0.00	0.00	0.02	0.02
1250	0.00	0.00	0.02	0.02	0.00	0.00	0.02	0.02	0.00	0.00	0.02	0.02
1300	0.00	0.00	0.02	0.02	0.00	0.00	0.02	0.02	0.00	0.00	0.02	0.02
1350	0.00	0.00	0.02	0.02	0.00	0.00	0.02	0.02	0.00	0.00	0.02	0.02
1400	0.00	0.00	0.02	0.02	0.00	0.00	0.02	0.02	0.00	0.00	0.02	0.02
1450	0.00	0.00	0.02	0.02	0.00	0.00	0.02	0.02	0.00	0.00	0.02	0.02
1500	0.00	0.00	0.02	0.02	0.00	0.00	0.02	0.02	0.00	0.00	0.02	0.02
1550	0.00	0.00	0.02	0.02	0.00	0.00	0.02	0.02	0.00	0.00	0.02	0.02
1600	0.00	0.00	0.02	0.02	0.00	0.00	0.02	0.02	0.00	0.00	0.02	0.02

Table 5.8.13 SMU additional transfer uncertainty contributions.

Wavelength [nm]	NIST07 (GPD)				NIST02 (Fermionics)				NIST10 (EG&G)			
	$u_{w,p}^T$	$u_{bp,p}^T$	$u_{bs,ij}^T$	$u_{c,ij}^T$	$u_{w,p}^T$	$u_{bp,p}^T$	$u_{bs,ij}^T$	$u_{c,ij}^T$	$u_{w,p}^T$	$u_{bp,p}^T$	$u_{bs,ij}^T$	$u_{c,ij}^T$
900	0.02	0.02	0.03	0.04	0.02	0.02	0.05	0.05	0.02	0.02	0.07	0.08
950	0.02	0.01	0.03	0.03	0.02	0.01	0.05	0.05	0.02	0.01	0.07	0.07
1000	0.00	0.00	0.03	0.03	0.00	0.00	0.05	0.05	0.00	0.00	0.07	0.07
1050	0.00	0.00	0.03	0.03	0.00	0.00	0.05	0.05	0.00	0.00	0.07	0.07
1100	0.00	0.00	0.03	0.03	0.00	0.00	0.05	0.05	0.00	0.00	0.07	0.07
1150	0.00	0.00	0.03	0.03	0.00	0.00	0.05	0.05	0.00	0.00	0.07	0.07
1200	0.00	0.00	0.03	0.03	0.00	0.00	0.05	0.05	0.00	0.00	0.07	0.07
1250	0.00	0.00	0.03	0.03	0.00	0.00	0.05	0.05	0.00	0.00	0.07	0.07
1300	0.00	0.00	0.03	0.03	0.00	0.00	0.05	0.05	0.00	0.00	0.07	0.07
1350	0.00	0.00	0.03	0.03	0.00	0.00	0.05	0.05	0.00	0.00	0.07	0.07
1400	0.00	0.00	0.03	0.03	0.00	0.00	0.05	0.05	0.00	0.00	0.07	0.07
1450	0.00	0.00	0.03	0.03	0.00	0.00	0.05	0.05	0.00	0.00	0.07	0.07
1500	0.00	0.00	0.03	0.03	0.00	0.00	0.05	0.05	0.00	0.00	0.07	0.07
1550	0.00	0.00	0.03	0.03	0.00	0.00	0.05	0.05	0.00	0.00	0.07	0.07
1600	0.00	0.00	0.03	0.03	0.00	0.00	0.05	0.05	0.00	0.00	0.07	0.07

Table 5.8.14 VNIIOFI additional transfer uncertainty contributions.

Wavelength [nm]	NIST07 (GPD)				NIST14 (TDC)				NIST09 (EG&G)			
	$u_{w,p}^T$	$u_{bp,p}^T$	$u_{bs,ij}^T$	$u_{c,ij}^T$	$u_{w,p}^T$	$u_{bp,p}^T$	$u_{bs,ij}^T$	$u_{c,ij}^T$	$u_{w,p}^T$	$u_{bp,p}^T$	$u_{bs,ij}^T$	$u_{c,ij}^T$
900	0.02	0.02	0.02	0.03	0.02	0.02	0.02	0.03	0.02	0.02	0.07	0.07
950	0.02	0.01	0.02	0.03	0.02	0.02	0.02	0.03	0.02	0.01	0.07	0.07
1000	0.00	0.00	0.02	0.02	0.03	0.01	0.02	0.03	0.00	0.00	0.07	0.07
1050	0.00	0.00	0.02	0.02	0.03	0.00	0.02	0.03	0.00	0.00	0.07	0.07
1100	0.00	0.00	0.02	0.02	0.03	0.01	0.02	0.04	0.00	0.00	0.07	0.07
1150	0.00	0.00	0.02	0.02	0.04	0.00	0.02	0.04	0.00	0.00	0.07	0.07
1200	0.00	0.00	0.02	0.02	0.00	0.00	0.02	0.02	0.00	0.00	0.07	0.07
1250	0.00	0.00	0.02	0.02	0.00	0.00	0.02	0.02	0.00	0.00	0.07	0.07
1300	0.00	0.00	0.02	0.02	0.00	0.00	0.02	0.02	0.00	0.00	0.07	0.07
1350	0.00	0.00	0.02	0.02	0.00	0.00	0.02	0.02	0.00	0.00	0.07	0.07
1400	0.00	0.00	0.02	0.02	0.00	0.00	0.02	0.02	0.00	0.00	0.07	0.07
1450	0.00	0.00	0.02	0.02	0.00	0.00	0.02	0.02	0.00	0.00	0.07	0.07
1500	0.00	0.00	0.02	0.02	0.00	0.00	0.02	0.02	0.00	0.00	0.07	0.07
1550	0.00	0.00	0.02	0.02	0.00	0.00	0.02	0.02	0.00	0.00	0.07	0.07
1600	0.00	0.00	0.02	0.02	0.00	0.00	0.02	0.02	0.00	0.00	0.07	0.07

## 6. Data Analysis

The data analysis of this comparison basically follows the Guidelines for CCPR Comparison Report Preparation (CCPR 2006), while different intermediate steps (used in Draft A-1 and accepted by the participants) are used. In the analysis of the data set, we first calculate the mean relative difference, called  $\bar{\Delta}_i$ , between each participant  $i$  and the Pilot Laboratory (NIST), weighted by the transfer uncertainty of the measurements of each photodiode. Weighted mean is used in this intermediate step so that results from detectors that experienced larger changes during comparison were less weighted. We then calculate the Key Comparison Reference Value (KCRV) of the relative difference, and calculate individual laboratories results, including results from the Pilot Laboratory, with respect to the KCRV. The KCRV is calculated as a weighted mean with cut-off following the CCPR Guidelines.

### 6.1 Analysis method

The calculation steps are detailed below. The following notations are used.

laboratory  $i$  ( $i=0$  to 14, where  $i=0$  is the pilot lab.)

photodiode  $j$  ( $j=1$  to 3 for each participant)

repeat of measurement  $n$  ( $n=1$  to 3) for each photodiode

$s_{ij,n}$  : spectral responsivity measured by a participant

$s_{ij,n}^{\text{NIST}}$  (pre,post): spectral responsivity measured by the pilot lab (before and after transportation).

1. Calculate the relative difference  $\Delta_{ij}$  for each laboratory  $i$  ( $=1$  to 14) for each photodiode  $j$  compared to NIST measurement:

$$\Delta_{ij} = \left( \bar{s}_{ij} / \bar{s}_{ij}^{\text{NIST}} - 1 \right). \quad (6.1)$$

where  $\bar{s}_{ij}$  is the average of the three measurements of detector  $j$  at laboratory  $i$ :

$$\bar{s}_{ij} = \frac{1}{3} \sum_{n=1}^3 (s_{ij,n}), \quad (6.2)$$

and  $\bar{s}_{ij}^{\text{NIST}}$  is the average of the measurements at NIST of detector  $j$  measured by laboratory  $i$  before (pre) and after (post) each round of the comparison:

$$\bar{s}_{ij}^{\text{NIST}} = \frac{1}{2} \cdot \left[ \frac{1}{3} \sum_{n=1}^3 s_{ij,n}^{\text{NIST}} (\text{pre}) + \frac{1}{3} \sum_{n=1}^3 s_{ij,n}^{\text{NIST}} (\text{post}) \right]. \quad (6.3)$$

2. Calculate the relative transfer uncertainty of  $\Delta_{ij}$ , calculated as a combination of the repeatability of the laboratory's three measurements, the NIST repeatability, the detector stability measured by NIST, and additional transfer uncertainty components  $u_{c,ij}^{\text{T}}$ :

$$u_{\text{r}}^2(\Delta_{ij}) = u_{\text{r}}^2(\bar{s}_{ij}) + u_{\text{r}}^2(s_{\text{NIST}}) + u_{\text{stability}}^2(s_{ij}^{\text{NIST}}) + (u_{c,ij}^{\text{T}})^2, \quad (6.4)$$

where  $u_{\text{r}}(\bar{s}_{ij})$  is the standard deviation of the mean of the three reported measurements of detector  $j$  at laboratory  $i$ :

$$u_{\text{r}}^2(\bar{s}_{ij}) = \frac{1}{(n-1) \cdot n} \sum_{k=1}^n (s_{ij}^k - \bar{s}_{ij})^2 \quad ; n = 3, \quad (6.5)$$

$u_r(s_{\text{NIST}})$  is the relative NIST measurement repeatability uncertainty given in Table 5.2 and  $u_{\text{stability}}(s_{ij}^{\text{NIST}})$  is calculated according to Eq. 5.1, and  $u_{c,ij}^T$  are the additional transfer uncertainty component combined as listed in Tables 5.8.1 to 5.8.14.

3. For each laboratory  $i$ , calculate the weighted mean (call it  $\bar{\Delta}_i$ ) of its three  $\Delta_{ij}$  ( $j=1$  to 3) using the relative transfer uncertainty derived in Step 2:

$$\bar{\Delta}_i = \sum_{j=1}^3 w_{ij} \cdot \Delta_{ij} \quad (6.6)$$

where

$$w_{ij} = \frac{u_t(\Delta_{ij})^{-2}}{\sum_{j=1}^3 u_t(\Delta_{ij})^{-2}} \quad (6.7)$$

For NIST,  $\Delta_0 = 0$ .

4. Calculate the transfer uncertainty of  $\bar{\Delta}_i$ , call it  $u_t(\bar{\Delta}_i)$ :

$$u_t(\bar{\Delta}_i) = \sqrt{\frac{1}{\sum_{j=1}^3 \left( \frac{1}{u_t^2(\Delta_{ij})} \right)}} \quad (6.8)$$

This transfer uncertainty includes the repeatability of the detectors in the participant's measurement as indicated by eq. (6.4). The propagated transfer uncertainty excluding this component, denoted  $u_{t,\text{corr}}(\bar{\Delta}_i)$ , is given by

$$u_{t,\text{corr}}^2(\bar{\Delta}_i) = \sum_{j=1}^3 w_{ij}^2 \cdot \left\{ u_r^2(s_{\text{NIST}}) + u_{\text{stability}}^2(\bar{s}_{ij}^{\text{NIST}}) + (u_{c,ij}^T)^2 \right\} \quad (6.9)$$

Note that  $u_{c,ij}^T$  is partially correlated among the three photodiodes measured by each participant, but it is treated as uncorrelated here since the degree of correlation is unknown and it should be taken as approximation. For NIST,

$$u_{t,\text{corr}}^2(\bar{\Delta}_0) = \left[ u_r^2(s_{\text{NIST}}) + \text{average} \left\{ u_{\text{stability}}^2(\bar{s}_{ij}^{\text{NIST}}) \right\} + \text{average} \left\{ u_{c,ij}^T \right\}^2 \right] / 3 \quad (6.10)$$

is used. Averages are for all diodes measured by all participants.

5. Apply a cut-off value for the reported uncertainties  $u_i$  of each laboratory.

$$\begin{aligned} u_{\text{adjusted},i} &= u_i \quad \text{when } u_i \geq u_{\text{cut-off}} \\ u_{\text{adjusted},i} &= u_{\text{cut-off}} \quad \text{when } u_i < u_{\text{cut-off}} \end{aligned} \quad (6.11)$$

where  $u_{\text{cut-off}}$  is the cut-off value for the reported uncertainty (discussed in Section 7.2), and

$$u_i = \text{average} \left\{ u_{\text{rel}}(s_{ij,n}) \right\} \quad (6.12)$$

6. Calculate the combined standard uncertainty  $u_c(\bar{\Delta}_i)$  (cut-off not applied) and the adjusted combined standard uncertainty  $u_{c,\text{adj}}(\bar{\Delta}_i)$  (cut-off applied) for each laboratory  $i$  as

$$u_c^2(\bar{\Delta}_i) = u_i^2 + u_{t,\text{corr}}^2(\bar{\Delta}_i) + u_{\text{long}}^2(s_{\text{NIST}}) \quad (6.13)$$

$$u_{c,\text{adj}}^2(\bar{\Delta}_i) = u_{\text{adjusted},i}^2 + u_{t,\text{corr}}^2(\bar{\Delta}_i) + u_{\text{long}}^2(s_{\text{NIST}}) \quad (6.14)$$

$u_{\text{long}}(s_{\text{NIST}})$  is the uncertainty contribution from the longterm stability of the comparison scale as listed in Table 5.3. Note that  $u_{t,\text{corr}}(\bar{\Delta}_i)$  (eq. 6.9) rather than  $u_i(\bar{\Delta}_i)$  (eq. 6.8) is used above because the reported uncertainty  $u_i$  already includes the uncertainty contribution from the repeatability of measurements at participants, and this component should not be duplicated.

7. Calculate the KCRV,  $\bar{\Delta}_{\text{KCRV}}$ , as a weighted mean of  $\bar{\Delta}_i$  for all participating laboratories, using the adjusted uncertainties in eq. (6.14).

$$\bar{\Delta}_{\text{KCRV}} = \sum_{i=0}^{14} w_i \cdot \bar{\Delta}_i \quad (6.15)$$

where

$$w_i = \frac{u_{c,\text{adj}}^{-2}(\bar{\Delta}_i)}{\sum_{i=0}^{14} u_{c,\text{adj}}^{-2}(\bar{\Delta}_i)} \quad (6.16)$$

8. Calculate the propagated uncertainty of  $\bar{\Delta}_{\text{KCRV}}$ , call it  $u(\bar{\Delta}_{\text{KCRV}})$ , for weighted mean with cut-off,

$$u(\bar{\Delta}_{\text{KCRV}}) = \sqrt{\frac{\sum_{i=0}^N u_c^2(\bar{\Delta}_i)}{\sum_{i=0}^N u_{c,\text{adj}}^4(\bar{\Delta}_i)} \bigg/ \sum_{i=0}^N u_{c,\text{adj}}^{-2}(\bar{\Delta}_i)} \quad (6.17)$$

9. The difference  $d_i$  from KCRV for each participant  $i$  is given by

$$d_i = \bar{\Delta}_i - \bar{\Delta}_{\text{KCRV}} \quad (6.18)$$

and the uncertainty in the difference  $d_i$  is given by

$$u(d_i) = \sqrt{u_c^2(\bar{\Delta}_i) + u^2(\bar{\Delta}_{\text{KCRV}}) - 2 \left( \frac{u_c^2(\bar{\Delta}_i)}{u_{c,\text{adj}}^2(\bar{\Delta}_i)} \bigg/ \sum_{j=0}^N u_{c,\text{adj}}^{-2}(\bar{\Delta}_j) \right)} \quad (6.19)$$

$$u(d_i) = \sqrt{u_c^2(\bar{\Delta}_i) + u^2(\bar{\Delta}_{\text{KCRV}})} \text{ for CSIR and KRISS.} \quad (6.20)$$

Note that eq. (6.19) takes into account the partial correlation between  $\bar{\Delta}_i$  and  $\bar{\Delta}_{\text{KCRV}}$ .

10. The unilateral Degree of Equivalence (DoE) of laboratory  $i$  is given by

$$D_i = d_i \quad (6.21)$$

$$U_i = k \cdot u(d_i) \quad ; k=2 \text{ (coverage factor)} \quad (6.22)$$

11. The bilateral DoE between laboratory  $i$  and laboratory  $m$  is given by

$$D_{i,m} = d_i - d_m \quad (6.23)$$

$$U_{i,m} = k \cdot \sqrt{u_c^2(\bar{\Delta}_i) + u_c^2(\bar{\Delta}_m)} \quad ; (k=2) \quad (6.24)$$

## 7. Results of the Comparison

### 7.1 Intermediate calculation results

To determine the KCRV at each wavelength, the temperature-corrected, measured values from each laboratory are first analyzed with respect to the values of the pilot laboratory (NIST) using Eqs. (6.1) to (6.9). The results are summarized in Tables 7.1 to 7.14. The four columns for each photodiode sample show the results of calculation for  $\Delta_{ij}$  by eq. (6.1),  $u_r(\bar{s}_{ij})$  by eq. (6.5),  $u_{\text{stability}}(\bar{s}_{ij}^{\text{NIST}})$  by eq. (5.1), and  $u_t(\Delta_{ij})$  by eq. (6.4).  $u_{\text{stability}}(\bar{s}_{ij}^{\text{NIST}})$  is labeled as simply  $u_{\text{stability}}$  and their values are different from those in Tables 4.15.1 to 4.15.14 because the results in Tables 7.1 to 7.14 are corrected for temperature variations.

The last two columns of the table show the laboratory's mean difference  $\bar{\Delta}_i$  by eq. (6.6), the transfer uncertainty  $u_t(\bar{\Delta}_i)$  by eq. (6.8), and  $u_{t,\text{corr}}(\bar{\Delta}_i)$  calculated by eq. (6.9).

Table 7.1. BNM-INM intermediate calculation results (values in %).

WL [nm]	NIST04 $\Delta_{i,1}$	$u_r(\bar{s}_{i,1})$	$u_{\text{stability}}$	$u_t(\Delta_{i,1})$	NIST08 $\Delta_{i,2}$	$u_r(\bar{s}_{i,2})$	$u_{\text{stability}}$	$u_t(\Delta_{i,2})$	NIST10 $\Delta_{i,3}$	$u_r(\bar{s}_{i,3})$	$u_{\text{stability}}$	$u_t(\Delta_{i,3})$	$\bar{\Delta}_i$	$u_t(\bar{\Delta}_i)$	$u_{t,\text{corr}}(\bar{\Delta}_i)$
900	-1.313	0.186	0.022	0.201	-2.118	0.332	0.037	0.340	3.888	0.098	0.063	0.147	-1.313	0.201	0.074
950	-1.084	0.186	0.058	0.205	-1.466	0.048	0.119	0.143	-1.423	0.066	0.072	0.116	-1.382	0.083	0.078
1000	-0.411	0.152	0.038	0.166	-0.769	0.222	0.114	0.256	-1.075	0.039	0.051	0.086	-0.922	0.073	0.078
1050	-0.681	0.178	0.003	0.181	-1.093	0.091	0.071	0.121	-1.318	0.016	0.018	0.042	-1.266	0.039	0.069
1100	-0.671	0.123	0.002	0.131	-0.860	0.152	0.072	0.174	-1.137	0.040	0.023	0.065	-1.027	0.055	0.065
1150	-0.553	0.126	0.003	0.132	-0.894	0.141	0.057	0.157	-1.236	0.057	0.015	0.071	-1.058	0.058	0.057
1200	-0.270	0.112	0.109	0.175	-0.578	0.121	0.170	0.223	-0.993	0.082	0.122	0.167	-0.633	0.106	0.094
1250	-0.434	0.085	0.003	0.094	-0.785	0.216	0.056	0.227	-1.117	0.052	0.021	0.070	-0.871	0.054	0.056
1300	-0.420	0.138	0.037	0.147	-0.786	0.129	0.016	0.134	-1.030	0.042	0.022	0.059	-0.922	0.051	0.061
1350	-0.389	0.090	0.001	0.094	-0.805	0.074	0.057	0.098	-1.159	0.058	0.012	0.066	-0.881	0.048	0.045
1400	-0.746	0.134	0.029	0.150	-1.029	0.219	0.005	0.227	-1.360	0.126	0.002	0.139	-1.067	0.093	0.053
1450	-1.011	0.110	0.016	0.118	-1.232	0.275	0.059	0.284	-1.548	0.062	0.020	0.076	-1.381	0.063	0.059
1500	-1.229	0.088	0.020	0.096	-1.698	0.271	0.020	0.274	-2.015	0.080	0.001	0.087	-1.662	0.063	0.048
1550	-0.769	0.081	0.004	0.101	-1.445	0.239	0.037	0.249	-1.607	0.094	0.018	0.114	-1.165	0.072	0.055
1600	-0.650	0.092	0.013	0.098	-1.131	0.133	0.013	0.137	-1.407	0.032	0.007	0.044	-1.266	0.039	0.060

Table 7.2. CSIR intermediate calculation results (values in %).

WL [nm]	NIST04 $\Delta_{i,1}$	$u_r(\bar{s}_{i,1})$	$u_{\text{stability}}$	$u_t(\Delta_{i,1})$	NIST08 $\Delta_{i,2}$	$u_r(\bar{s}_{i,2})$	$u_{\text{stability}}$	$u_t(\Delta_{i,2})$	NIST15 $\Delta_{i,3}$	$u_r(\bar{s}_{i,3})$	$u_{\text{stability}}$	$u_t(\Delta_{i,3})$	$\bar{\Delta}_i$	$u_t(\bar{\Delta}_i)$	$u_{t,\text{corr}}(\bar{\Delta}_i)$
900	0.471		0.004	0.061	-1.008		0.038	0.066	-0.194		0.003	0.067	0.167	0.045	0.045
950	-0.285	0.406	0.019	0.411	0.035	0.092	0.061	0.127	<b>-6.559</b>	0.293	0.017	0.301	0.007	0.122	0.082
1000	0.465	0.155	0.011	0.166	-0.297	0.386	0.042	0.392	-0.081	0.377	0.034	0.383	0.290	0.142	0.050
1050	0.087	0.056	0.023	0.069	-0.555	0.292	0.033	0.296	-0.428	0.295	0.023	0.298	0.030	0.066	0.045
1100	0.487	0.264	0.032	0.269	-0.196	0.260	0.024	0.265	-0.426	0.211	0.022	0.217	-0.104	0.143	0.039
1150	0.202	0.022	0.038	0.058	0.027	0.275	0.029	0.279	-0.319	0.216	0.026	0.221	0.162	0.055	0.055
1200	0.408	0.097	0.042	0.132	0.322	0.280	0.031	0.293	-0.122	0.026	0.010	0.083	0.045	0.068	0.064
1250	0.543	0.201	0.034	0.207	0.168	0.118	0.027	0.128	-0.127	0.080	0.004	0.090	0.035	0.070	0.037
1300	0.322	0.000	0.036	0.050	0.298	0.002	0.027	0.044	-0.139	0.000	0.012	0.037	0.110	0.025	0.031
1350	0.564	0.016	0.022	0.040	0.400	0.153	0.022	0.157	0.140	0.141	0.015	0.145	0.526	0.038	0.041
1400	0.890	0.138	0.036	0.155	0.595	0.102	0.036	0.123	0.066	0.151	0.010	0.163	0.542	0.083	0.043
1450	0.994	0.156	0.022	0.163	0.854	0.191	0.024	0.197	0.178	0.265	0.034	0.270	0.803	0.114	0.033
1500	1.018	0.272	0.003	0.274	0.879	0.236	0.018	0.239	0.442	0.246	0.023	0.250	0.768	0.146	0.027
1550	2.151	0.248	0.011	0.256	1.897	0.241	0.037	0.251	1.512	0.369	0.055	0.378	1.928	0.162	0.044
1600	2.823	0.141	0.031	0.147	2.239	0.170	0.053	0.181	1.990	0.270	0.003	0.271	2.500	0.105	0.034

Table 7.3. CSIRO intermediate calculation results (values in %).

WL [nm]	NIST06 $\Delta_{i,1}$	$u_r(\bar{s}_{i,1})$	$u_{\text{stability}}$	$u_t(\Delta_{i,1})$	NIST14 $\Delta_{i,2}$	$u_r(\bar{s}_{i,2})$	$u_{\text{stability}}$	$u_t(\Delta_{i,2})$	NIST03 $\Delta_{i,3}$	$u_r(\bar{s}_{i,3})$	$u_{\text{stability}}$	$u_t(\Delta_{i,3})$	$\bar{\Delta}_i$	$u_t(\bar{\Delta}_i)$	$u_{t,\text{corr}}(\bar{\Delta}_i)$
900	-0.785	0.091	0.028	0.114	-1.027	0.059	0.015	0.082	-0.547	0.082	0.002	0.098	-0.818	0.055	0.035
950	-0.504	0.091	0.003	0.089	-0.564	0.088	0.071	0.130	-0.221	0.092	0.032	0.116	-0.437	0.062	0.047
1000	-0.409	0.091	0.003	0.080	-0.221	0.051	0.065	0.101	-0.150	0.012	0.018	0.061	-0.241	0.044	0.040
1050	-0.539	0.091	0.034	0.073	-0.559	0.036	0.036	0.061	-0.348	0.116	0.008	0.122	-0.525	0.044	0.036
1100	-0.400	0.091	0.038	0.060	-0.363	0.048	0.062	0.091	0.054	0.073	0.019	0.088	-0.281	0.043	0.042
1150	-0.357	0.091	0.044	0.059	-0.223	0.057	0.041	0.080	-0.124	0.046	0.020	0.063	-0.243	0.038	0.035
1200	-0.406	0.091	0.073	0.110	-0.160	0.029	0.148	0.170	0.003	0.041	0.090	0.126	-0.215	0.075	0.073
1250	-0.684	0.091	0.037	0.056	-0.467	0.028	0.028	0.057	-0.368	0.030	0.020	0.055	-0.505	0.032	0.031
1300	-0.626	0.091	0.076	0.094	-0.415	0.044	0.002	0.057	-0.367	0.025	0.059	0.073	-0.439	0.040	0.032
1350	-0.748	0.091	0.026	0.060	-0.469	0.025	0.034	0.052	-0.406	0.011	0.022	0.039	-0.496	0.028	0.025
1400	-0.991	0.091	0.067	0.093	-0.678	0.028	0.015	0.067	-0.625	0.040	0.062	0.095	-0.745	0.047	0.045
1450	-1.079	0.091	0.019	0.063	-0.789	0.038	0.034	0.065	-0.749	0.033	0.017	0.055	-0.861	0.035	0.029
1500	-1.374	0.091	0.029	0.067	-1.231	0.051	0.014	0.063	-1.180	0.009	0.044	0.056	-1.251	0.035	0.029
1550	-0.974	0.091	0.013	0.086	-0.919	0.010	0.038	0.073	-0.775	0.033	0.025	0.074	-0.882	0.044	0.041
1600	-1.031	0.091	0.028	0.044	-0.963	0.053	0.001	0.061	-0.801	0.105	0.040	0.116	-0.989	0.034	0.032

Table 7.4. HUT intermediate calculation results (values in %).

WL [nm]	NIST06 $\Delta_{i,1}$	$u_r(\bar{s}_{i,1})$	$u_{\text{stability}}$	$u_t(\Delta_{i,1})$	NIST10 $\Delta_{i,2}$	$u_r(\bar{s}_{i,2})$	$u_{\text{stability}}$	$u_t(\Delta_{i,2})$	NIST15 $\Delta_{i,3}$	$u_r(\bar{s}_{i,3})$	$u_{\text{stability}}$	$u_t(\Delta_{i,3})$	$\bar{\Delta}_i$	$u_t(\bar{\Delta}_i)$	$u_{t,\text{corr}}(\bar{\Delta}_i)$
900	-0.415	0.057	0.018	0.082	11.955	0.184	0.012	0.193	-0.469	0.534	0.015	0.538	-0.416	0.081	0.058
950	0.592	0.070	0.051	0.107	0.977	0.065	0.067	0.113	0.167	0.378	0.049	0.386	0.750	0.076	0.061
1000	-0.013	0.085	0.007	0.103	0.198	0.066	0.029	0.092	-0.256	0.308	0.020	0.314	0.088	0.067	0.043
1050	0.267	0.045	0.003	0.057	0.355	0.050	0.010	0.062	-0.011	0.319	0.003	0.321	0.302	0.042	0.026
1100	-0.147	0.073	0.017	0.088	-0.002	0.048	0.013	0.068	-0.473	0.197	0.004	0.202	-0.083	0.052	0.033
1150	0.061	0.040	0.014	0.057	0.261	0.049	0.007	0.063	-0.410	0.157	0.012	0.162	0.116	0.041	0.028
1200	0.362	0.036	0.115	0.143	0.656	0.045	0.111	0.143	0.245	0.106	0.094	0.162	0.435	0.086	0.078
1250	-0.189	0.061	0.021	0.076	0.095	0.039	0.030	0.064	-0.222	0.087	0.011	0.097	-0.063	0.044	0.030
1300	-0.142	0.001	0.005	0.035	0.130	0.040	0.018	0.056	-0.162	0.069	0.001	0.077	-0.077	0.028	0.026
1350	0.085	0.031	0.035	0.056	0.352	0.002	0.046	0.055	0.139	0.104	0.027	0.111	0.211	0.037	0.033
1400	-0.781	0.055	0.022	0.084	-0.504	0.035	0.007	0.070	-0.781	0.039	0.038	0.081	-0.667	0.045	0.038
1450	-0.765	0.061	0.013	0.074	-0.446	0.035	0.038	0.066	-0.836	0.064	0.021	0.079	-0.656	0.042	0.030
1500	-0.911	0.001	0.012	0.036	-0.623	0.033	0.010	0.048	-0.939	0.077	0.017	0.086	-0.821	0.027	0.026
1550	-0.653	0.029	0.020	0.071	-0.365	0.064	0.015	0.090	-0.610	0.130	0.033	0.147	-0.551	0.052	0.043
1600	-1.303	0.024	0.003	0.039	-1.056	0.050	0.031	0.066	-1.193	0.095	0.013	0.101	-1.235	0.032	0.025

Table 7.5. IFA intermediate calculation results (values in %).

WL [nm]	NIST04 $\Delta_{i,1}$	$u_r(\bar{s}_{i,1})$	$u_{\text{stability}}$	$u_t(\Delta_{i,1})$	NIST03 $\Delta_{i,2}$	$u_r(\bar{s}_{i,2})$	$u_{\text{stability}}$	$u_t(\Delta_{i,2})$	NIST13 $\Delta_{i,3}$	$u_r(\bar{s}_{i,3})$	$u_{\text{stability}}$	$u_t(\Delta_{i,3})$	$\bar{\Delta}_i$	$u_t(\bar{\Delta}_i)$	$u_{t,\text{corr}}(\bar{\Delta}_i)$
900	1.849	0.033	0.031	0.085	2.027	0.010	0.001	0.067	8.415	0.078	0.012	0.111	1.960	0.052	0.051
950	1.341	0.057	0.073	0.112	1.138	0.049	0.076	0.111	1.601	0.009	0.078	0.100	1.376	0.062	0.065
1000	1.592	0.069	0.019	0.091	1.311	0.029	0.018	0.066	1.647	0.103	0.036	0.123	1.446	0.049	0.047
1050	1.362	0.071	0.013	0.080	1.211	0.042	0.000	0.054	1.333	0.130	0.017	0.135	1.266	0.043	0.036
1100	1.409	0.047	0.010	0.066	1.695	0.068	0.011	0.083	1.536	0.057	0.018	0.076	1.525	0.043	0.040
1150	1.376	0.071	0.020	0.083	1.213	0.048	0.011	0.062	1.347	0.036	0.017	0.056	1.305	0.037	0.039
1200	1.664	0.056	0.120	0.153	1.749	0.063	0.111	0.149	1.643	0.028	0.123	0.148	1.685	0.087	0.086
1250	1.452	0.052	0.027	0.072	1.401	0.038	0.019	0.059	1.469	0.032	0.031	0.061	1.439	0.036	0.040
1300	1.375	0.055	0.011	0.066	1.367	0.073	0.007	0.081	1.358	0.061	0.022	0.074	1.368	0.042	0.036
1350	1.154	0.052	0.040	0.072	1.174	0.051	0.035	0.069	1.183	0.068	0.045	0.087	1.169	0.043	0.039
1400	0.972	0.036	0.013	0.071	0.977	0.050	0.020	0.080	0.991	0.076	0.010	0.097	0.978	0.047	0.046
1450	0.887	0.051	0.034	0.073	0.903	0.052	0.021	0.069	0.912	0.062	0.041	0.084	0.900	0.043	0.040
1500	0.415	0.061	0.012	0.070	0.367	0.063	0.003	0.071	0.404	0.055	0.016	0.067	0.396	0.040	0.035
1550	0.969	0.055	0.014	0.083	0.853	0.070	0.002	0.093	0.884	0.023	0.001	0.065	0.902	0.045	0.049
1600	1.079	0.061	0.011	0.068	0.999	0.074	0.004	0.080	0.838	0.022	0.003	0.037	0.908	0.030	0.044

Table 7.6. KRIS intermediate calculation results (values in %).

WL [nm]	NIST17 $\Delta_{i,1}$	$u_r(\bar{s}_{i,1})$	$u_{\text{stability}}$	$u_t(\Delta_{i,1})$	NIST10 $\Delta_{i,2}$	$u_r(\bar{s}_{i,2})$	$u_{\text{stability}}$	$u_t(\Delta_{i,2})$	NIST13 $\Delta_{i,3}$	$u_r(\bar{s}_{i,3})$	$u_{\text{stability}}$	$u_t(\Delta_{i,3})$	$\bar{\Delta}_i$	$u_t(\bar{\Delta}_i)$	$u_{t,\text{corr}}(\bar{\Delta}_i)$
900	0.389	0.058	0.049	0.096	8.355	0.112	0.139	0.187	-0.255	0.095	0.018	0.133	0.169	0.078	0.060
950	0.026	0.025	0.044	0.081	0.230	0.051	0.000	0.081	-0.501	0.050	0.025	0.084	-0.071	0.047	0.049
1000	0.159	0.030	0.056	0.085	0.785	0.055	0.003	0.079	0.213	0.202	0.027	0.212	0.476	0.056	0.047
1050	-0.265	0.039	0.065	0.083	-0.149	0.044	0.011	0.057	-0.453	0.155	0.036	0.163	-0.207	0.045	0.033
1100	-0.104	0.014	0.060	0.077	0.155	0.027	0.010	0.054	0.024	0.132	0.026	0.142	0.066	0.042	0.038
1150	-0.199	0.013	0.057	0.070	0.119	0.047	0.007	0.061	0.180	0.087	0.014	0.096	0.019	0.042	0.036
1200	-0.062	0.058	0.057	0.113	0.341	0.042	0.004	0.089	0.011	0.085	0.009	0.116	0.140	0.060	0.054
1250	-0.215	0.059	0.064	0.096	0.199	0.053	0.000	0.067	-0.174	0.026	0.001	0.048	-0.070	0.036	0.050
1300	-0.170	0.043	0.047	0.073	0.290	0.017	0.003	0.039	-0.005	0.045	0.004	0.057	0.137	0.029	0.031
1350	-0.494	0.044	0.046	0.070	-0.182	0.045	0.000	0.054	-0.626	0.050	0.003	0.058	-0.411	0.034	0.033
1400	-0.644	0.060	0.046	0.096	-0.258	0.066	0.015	0.090	-0.638	0.029	0.027	0.072	-0.530	0.048	0.052
1450	-0.613	0.073	0.039	0.092	-0.390	0.163	0.020	0.169	-0.331	0.124	0.021	0.132	-0.499	0.069	0.042
1500	-0.792	0.019	0.031	0.050	-0.387	0.027	0.003	0.043	-0.703	0.072	0.004	0.080	-0.582	0.030	0.028
1550	-0.527	0.039	0.038	0.082	-0.153	0.106	0.005	0.123	-0.629	0.044	0.015	0.077	-0.507	0.051	0.053
1600	-0.335	0.052	0.001	0.060	-0.088	0.043	0.021	0.057	-0.689	0.063	0.018	0.072	-0.324	0.036	0.028

Table 7.7. NIM intermediate calculation results (values in %).

WL [nm]	NIST04 $\Delta_{i,1}$	$u_r(\bar{s}_{i,1})$	$u_{\text{stability}}$	$u_t(\Delta_{i,1})$	NIST11 $\Delta_{i,2}$	$u_r(\bar{s}_{i,2})$	$u_{\text{stability}}$	$u_t(\Delta_{i,2})$	NIST09 $\Delta_{i,3}$	$u_r(\bar{s}_{i,3})$	$u_{\text{stability}}$	$u_t(\Delta_{i,3})$	$\bar{\Delta}_i$	$u_t(\bar{\Delta}_i)$	$u_{t,\text{corr}}(\bar{\Delta}_i)$
900	3.541	0.289	0.004	0.297	3.544	0.650	0.092	0.661	4.392	0.819	0.089	0.829	3.541	0.297	0.071
950	1.553	0.237	0.042	0.249	1.120	0.018	0.014	0.067	1.917	0.285	0.021	0.293	1.185	0.063	0.074
1000	1.560	0.247	0.024	0.255	0.901	0.202	0.090	0.229	2.020	0.213	0.035	0.224	1.498	0.136	0.060
1050	0.588	0.129	0.019	0.135	0.031	0.218	0.056	0.228	0.894	0.163	0.033	0.170	0.586	0.096	0.044
1100	0.256	0.267	0.033	0.272	-0.123	0.232	0.051	0.242	0.558	0.218	0.021	0.224	0.248	0.141	0.050
1150	-0.105	0.108	0.059	0.129	-0.331	0.088	0.036	0.102	0.377	0.176	0.026	0.182	-0.143	0.073	0.048
1200	-0.312	0.246	0.033	0.261	-0.582	0.211	0.061	0.233	0.052	0.188	0.030	0.206	-0.249	0.133	0.064
1250	-0.396	0.191	0.055	0.203	-0.715	0.123	0.033	0.134	-0.087	0.164	0.020	0.170	-0.458	0.093	0.047
1300	-0.457	0.191	0.086	0.212	-0.846	0.198	0.005	0.201	-0.145	0.157	0.003	0.161	-0.429	0.108	0.050
1350	-0.811	0.193	0.062	0.205	-1.164	0.136	0.007	0.140	-0.531	0.087	0.010	0.093	-0.735	0.072	0.053
1400	-0.842	0.164	0.030	0.177	-1.239	0.090	0.030	0.112	-0.551	0.113	0.041	0.134	-0.935	0.077	0.055
1450	-1.238	0.261	0.030	0.266	-1.564	0.249	0.032	0.254	-0.949	0.337	0.037	0.342	-1.305	0.162	0.043
1500	-1.554	0.316	0.034	0.320	-1.882	0.307	0.038	0.311	-1.298	0.335	0.044	0.339	-1.594	0.186	0.044
1550	-1.300	0.222	0.021	0.231	-1.752	0.254	0.088	0.276	-1.097	0.334	0.044	0.343	-1.404	0.157	0.058
1600	-1.419	0.333	0.022	0.336	-1.986	0.365	0.036	0.368	-1.348	0.442	0.020	0.444	-1.599	0.216	0.039

Table 7.8. NMI-VSL intermediate calculation results (values in %).

WL [nm]	NIST16 $\Delta_{i,1}$	$u_r(\bar{s}_{i,1})$	$u_{\text{stability}}$	$u_t(\Delta_{i,1})$	NIST02 $\Delta_{i,2}$	$u_r(\bar{s}_{i,2})$	$u_{\text{stability}}$	$u_t(\Delta_{i,2})$	NIST05 $\Delta_{i,3}$	$u_r(\bar{s}_{i,3})$	$u_{\text{stability}}$	$u_t(\Delta_{i,3})$	$\bar{\Delta}_i$	$u_t(\bar{\Delta}_i)$	$u_{t,\text{corr}}(\bar{\Delta}_i)$
900	0.879	0.054	0.031	0.115	0.452	0.035	0.050	0.152	0.660	0.025	0.027	0.084	0.689	0.062	0.058
950	-0.175	0.029	0.000	0.069	0.105	0.035	0.008	0.073	0.142	0.022	0.016	0.069	0.022	0.040	0.064
1000	0.765	0.068	0.012	0.089	0.690	0.058	0.001	0.082	0.603	0.063	0.007	0.085	0.684	0.049	0.065
1050	0.056	0.046	0.013	0.059	-0.149	0.071	0.004	0.079	0.178	0.023	0.008	0.042	0.091	0.031	0.048
1100	0.331	0.054	0.001	0.070	0.255	0.047	0.021	0.069	0.183	0.029	0.003	0.054	0.243	0.036	0.056
1150	0.042	0.044	0.001	0.058	-0.068	0.061	0.003	0.072	0.155	0.018	0.015	0.045	0.078	0.032	0.050
1200	0.182	0.029	0.004	0.083	0.090	0.025	0.000	0.082	0.249	0.004	0.004	0.078	0.176	0.047	0.069
1250	0.151	0.029	0.007	0.051	0.013	0.030	0.000	0.051	0.143	0.023	0.005	0.047	0.104	0.029	0.057
1300	0.104	0.028	0.008	0.046	0.054	0.016	0.002	0.038	0.162	0.003	0.008	0.036	0.110	0.023	0.057
1350	-0.149	0.018	0.000	0.035	-0.258	0.012	0.003	0.032	-0.083	0.010	0.010	0.033	-0.165	0.019	0.057
1400	-0.224	0.016	0.016	0.064	-0.301	0.014	0.012	0.063	-0.227	0.021	0.001	0.063	-0.251	0.036	0.064
1450	-0.263	0.018	0.014	0.046	-0.464	0.008	0.017	0.044	-0.282	0.035	0.009	0.054	-0.345	0.028	0.064
1500	-0.664	0.016	0.010	0.038	-0.713	0.019	0.005	0.039	-0.558	0.008	0.023	0.042	-0.649	0.023	0.059
1550	-0.320	0.010	0.007	0.062	-0.065	0.037	0.023	0.075	-0.030	0.026	0.017	0.069	-0.155	0.039	0.062
1600	-0.375	0.050	0.015	0.060	-0.340	0.064	0.039	0.080	-0.100	0.040	0.039	0.063	-0.266	0.038	0.054

Table 7.9. NPL intermediate calculation results (values in %).

WL [nm]	NIST07 $\Delta_{i,1}$	$u_r(\bar{s}_{i,1})$	$u_{\text{stability}}$	$u_t(\Delta_{i,1})$	NIST08 $\Delta_{i,2}$	$u_r(\bar{s}_{i,2})$	$u_{\text{stability}}$	$u_t(\Delta_{i,2})$	NIST14 $\Delta_{i,3}$	$u_r(\bar{s}_{i,3})$	$u_{\text{stability}}$	$u_t(\Delta_{i,3})$	$\bar{\Delta}_i$	$u_t(\bar{\Delta}_i)$	$u_{t,\text{corr}}(\bar{\Delta}_i)$
900	0.690	0.053	0.028	0.086	0.049	0.039	0.002	0.072	-0.002	0.068	0.044	0.100	0.399	0.065	0.050
950	0.246	0.040	0.032	0.081	0.655	0.081	0.092	0.138	0.309	0.024	0.049	0.083	0.334	0.054	0.052
1000	0.324	0.033	0.004	0.066	0.383	0.013	0.042	0.072	0.250	0.033	0.009	0.066	0.316	0.039	0.040
1050	-0.065	0.026	0.014	0.046	0.038	0.064	0.029	0.079	-0.092	0.015	0.012	0.039	-0.066	0.028	0.031
1100	0.184	0.032	0.000	0.056	0.237	0.038	0.025	0.064	0.181	0.026	0.015	0.055	0.197	0.033	0.034
1150	0.014	0.017	0.001	0.042	0.066	0.043	0.025	0.063	0.134	0.028	0.001	0.048	0.066	0.028	0.031
1200	0.338	0.022	0.100	0.129	0.429	0.048	0.128	0.158	0.308	0.031	0.086	0.120	0.347	0.077	0.076
1250	0.135	0.009	0.009	0.043	0.179	0.018	0.031	0.054	0.118	0.026	0.005	0.049	0.141	0.028	0.030
1300	0.125	0.008	0.001	0.036	0.149	0.030	0.019	0.050	0.107	0.027	0.005	0.044	0.125	0.024	0.027
1350	-0.006	0.023	0.026	0.046	0.083	0.056	0.055	0.084	0.063	0.018	0.020	0.040	0.039	0.028	0.029
1400	-0.329	0.029	0.035	0.075	-0.231	0.039	0.010	0.072	-0.341	0.015	0.034	0.070	-0.300	0.042	0.041
1450	-0.347	0.011	0.009	0.042	-0.244	0.006	0.043	0.059	-0.399	0.021	0.013	0.047	-0.342	0.028	0.031
1500	-0.683	0.016	0.007	0.038	-0.625	0.011	0.017	0.039	-0.698	0.015	0.006	0.037	-0.670	0.022	0.026
1550	-0.288	0.006	0.025	0.067	-0.246	0.018	0.001	0.064	-0.211	0.003	0.011	0.062	-0.246	0.037	0.040
1600	-0.534	0.034	0.042	0.062	-0.468	0.049	0.003	0.057	-0.454	0.005	0.014	0.034	-0.471	0.026	0.028

Table 7.10. NRC intermediate calculation results (values in %).

WL [nm]	NIST16 $\Delta_{i,1}$	$u_r(\bar{s}_{i,1})$	$u_{\text{stability}}$	$u_t(\Delta_{i,1})$	NIST14 $\Delta_{i,2}$	$u_r(\bar{s}_{i,2})$	$u_{\text{stability}}$	$u_t(\Delta_{i,2})$	NIST08 $\Delta_{i,3}$	$u_r(\bar{s}_{i,3})$	$u_{\text{stability}}$	$u_t(\Delta_{i,3})$	$\bar{\Delta}_i$	$u_t(\bar{\Delta}_i)$	$u_{t,\text{corr}}(\bar{\Delta}_i)$
900	0.812	0.055	0.059	0.097	0.480	0.066	0.086	0.122	0.752	0.075	0.068	0.115	0.683	0.076	0.063
950	-0.259	0.025	0.046	0.082	-0.112	0.053	0.010	0.083	-0.030	0.036	0.049	0.087	-0.138	0.048	0.045
1000	0.305	0.035	0.042	0.079	0.249	0.038	0.086	0.110	0.219	0.037	0.117	0.136	0.274	0.058	0.054
1050	-0.119	0.022	0.045	0.061	-0.215	0.011	0.067	0.076	-0.122	0.027	0.086	0.096	-0.149	0.043	0.042
1100	0.014	0.009	0.011	0.048	-0.135	0.009	0.051	0.069	-0.038	0.016	0.074	0.088	-0.035	0.036	0.037
1150	-0.144	0.014	0.004	0.041	-0.076	0.016	0.019	0.046	-0.125	0.017	0.065	0.077	-0.115	0.028	0.031
1200	-0.029	0.018	0.002	0.080	-0.115	0.022	0.065	0.104	-0.028	0.018	0.078	0.112	-0.053	0.055	0.054
1250	-0.057	0.022	0.013	0.048	-0.088	0.023	0.037	0.060	-0.037	0.028	0.054	0.073	-0.063	0.033	0.031
1300	-0.054	0.018	0.031	0.050	-0.059	0.028	0.002	0.045	-0.043	0.021	0.021	0.046	-0.052	0.027	0.024
1350	-0.244	0.017	0.025	0.042	-0.198	0.025	0.025	0.047	-0.237	0.013	0.030	0.044	-0.228	0.026	0.024
1400	-0.433	0.035	0.005	0.069	-0.483	0.043	0.049	0.088	-0.423	0.042	0.071	0.102	-0.446	0.048	0.043
1450	-0.437	0.013	0.014	0.044	-0.454	0.008	0.050	0.064	-0.431	0.027	0.052	0.071	-0.440	0.032	0.032
1500	-0.802	0.011	0.038	0.052	-0.833	0.009	0.016	0.038	-0.778	0.032	0.032	0.057	-0.812	0.027	0.026
1550	-0.333	0.007	0.013	0.063	-0.417	0.017	0.077	0.100	-0.374	0.019	0.102	0.121	-0.360	0.049	0.049
1600	-0.318	0.005	0.033	0.045	-0.311	0.013	0.038	0.050	-0.284	0.013	0.037	0.050	-0.305	0.028	0.028

Table 7.11. OMH intermediate calculation results (values in %).

WL [nm]	NIST07 $\Delta_{i,1}$	$u_r(\bar{s}_{i,1})$	$u_{\text{stability}}$	$u_t(\Delta_{i,1})$	NIST11 $\Delta_{i,2}$	$u_r(\bar{s}_{i,2})$	$u_{\text{stability}}$	$u_t(\Delta_{i,2})$	NIST15 $\Delta_{i,3}$	$u_r(\bar{s}_{i,3})$	$u_{\text{stability}}$	$u_t(\Delta_{i,3})$	$\bar{\Delta}_i$	$u_t(\bar{\Delta}_i)$	$u_{t,\text{corr}}(\bar{\Delta}_i)$
900	0.468	0.144	0.012	0.154	3.629	0.161	0.038	0.175	-0.574	0.148	0.074	0.179	0.024	0.117	0.053
950	-0.873	0.210	0.065	0.229	-0.012	0.120	0.098	0.168	-1.225	0.187	0.091	0.217	-0.567	0.115	0.069
1000	-0.137	0.206	0.071	0.225	0.382	0.172	0.083	0.200	-0.173	0.155	0.071	0.180	0.020	0.115	0.059
1050	0.332	0.178	0.036	0.185	0.710	0.255	0.047	0.262	-0.079	0.282	0.060	0.290	0.344	0.134	0.036
1100	0.788	0.108	0.046	0.126	0.993	0.196	0.045	0.206	0.518	0.220	0.074	0.236	0.788	0.098	0.046
1150	0.365	0.165	0.037	0.174	0.829	0.204	0.021	0.208	0.529	0.285	0.037	0.290	0.551	0.121	0.034
1200	0.592	0.178	0.156	0.249	0.933	0.214	0.139	0.267	0.702	0.269	0.156	0.320	0.739	0.158	0.100
1250	0.118	0.180	0.039	0.189	0.326	0.231	0.024	0.236	0.149	0.259	0.038	0.265	0.187	0.129	0.034
1300	0.342	0.196	0.005	0.200	0.567	0.264	0.006	0.267	0.472	0.290	0.014	0.292	0.434	0.140	0.024
1350	0.136	0.189	0.045	0.196	0.330	0.264	0.017	0.266	0.252	0.280	0.048	0.286	0.215	0.138	0.033
1400	0.312	0.139	0.009	0.151	0.434	0.233	0.020	0.241	0.335	0.212	0.000	0.220	0.343	0.111	0.040
1450	0.198	0.193	0.046	0.203	0.484	0.262	0.019	0.266	0.335	0.286	0.045	0.293	0.310	0.141	0.037
1500	-0.443	0.182	0.023	0.187	-0.153	0.251	0.001	0.253	-0.378	0.272	0.021	0.275	-0.349	0.132	0.027
1550	-3.266	0.130	0.033	0.147	-3.154	0.258	0.023	0.266	-3.120	0.198	0.021	0.209	-3.206	0.110	0.046
1600	-3.053	0.390	0.017	0.391	-2.302	0.374	0.011	0.376	-2.822	0.480	0.025	0.482	-2.701	0.236	0.023

Table 7.12. PTB intermediate calculation results (values in %).

WL [nm]	NIST18 $\Delta_{i,1}$	$u_r(\bar{s}_{i,1})$	$u_{\text{stability}}$	$u_t(\Delta_{i,1})$	NIST11 $\Delta_{i,2}$	$u_r(\bar{s}_{i,2})$	$u_{\text{stability}}$	$u_t(\Delta_{i,2})$	NIST01 $\Delta_{i,3}$	$u_r(\bar{s}_{i,3})$	$u_{\text{stability}}$	$u_t(\Delta_{i,3})$	$\bar{\Delta}_i$	$u_t(\bar{\Delta}_i)$	$u_{t,\text{corr}}(\bar{\Delta}_i)$
900	-0.022	0.066	0.004	0.089	2.846	1.232	0.076	1.235	-0.157	0.048	0.040	0.086	-0.092	0.062	0.047
950	-0.356	0.065	0.029	0.095	-0.221	0.094	0.003	0.113	-0.641	0.163	0.055	0.183	-0.347	0.068	0.047
1000	0.269	0.012	0.018	0.061	0.302	0.015	0.016	0.061	0.194	0.113	0.005	0.127	0.276	0.041	0.041
1050	-0.190	0.023	0.015	0.044	-0.130	0.016	0.001	0.038	-0.013	0.052	0.008	0.063	-0.132	0.026	0.026
1100	0.081	0.007	0.025	0.053	0.140	0.013	0.001	0.048	0.134	0.020	0.009	0.051	0.120	0.029	0.031
1150	0.053	0.017	0.029	0.051	0.064	0.011	0.000	0.040	0.091	0.029	0.002	0.048	0.069	0.026	0.028
1200	0.237	0.011	0.036	0.087	0.264	0.003	0.003	0.078	0.251	0.008	0.001	0.079	0.252	0.047	0.048
1250	0.126	0.015	0.026	0.051	0.156	0.004	0.008	0.042	0.175	0.011	0.005	0.043	0.155	0.026	0.029
1300	0.072	0.017	0.030	0.049	0.058	0.007	0.003	0.036	0.033	0.006	0.004	0.036	0.051	0.022	0.026
1350	-0.141	0.016	0.044	0.055	-0.132	0.004	0.004	0.030	-0.091	0.007	0.003	0.031	-0.115	0.020	0.024
1400	-0.245	0.014	0.046	0.077	-0.233	0.004	0.012	0.061	-0.253	0.018	0.017	0.064	-0.243	0.038	0.040
1450	-0.542	0.024	0.027	0.054	-0.555	0.013	0.002	0.042	-0.531	0.033	0.006	0.052	-0.545	0.028	0.029
1500	-0.806	0.023	0.047	0.062	-0.830	0.003	0.007	0.035	-0.831	0.012	0.019	0.040	-0.827	0.024	0.028
1550	-0.136	0.026	0.015	0.068	-0.204	0.015	0.015	0.065	-0.208	0.037	0.008	0.072	-0.182	0.039	0.039
1600	-0.079	0.028	0.042	0.059	-0.288	0.016	0.001	0.034	-0.219	0.020	0.032	0.048	-0.232	0.025	0.027

Table 7.13. SMU intermediate calculation results (values in %).

WL [nm]	NIST07 $\Delta_{i,1}$	$u_r(\bar{s}_{i,1})$	$u_{\text{stability}}$	$u_t(\Delta_{i,1})$	NIST02 $\Delta_{i,2}$	$u_r(\bar{s}_{i,2})$	$u_{\text{stability}}$	$u_t(\Delta_{i,2})$	NIST10 $\Delta_{i,3}$	$u_r(\bar{s}_{i,3})$	$u_{\text{stability}}$	$u_t(\Delta_{i,3})$	$\bar{\Delta}_i$	$u_t(\bar{\Delta}_i)$	$u_{t,\text{NIST}}(\bar{\Delta}_i)$
900	0.230	0.042	0.031	0.080	-0.065	0.075	0.061	0.120	9.855	0.061	0.043	0.116	0.139	0.066	0.055
950	0.149	0.058	0.006	0.086	0.391	0.010	0.048	0.080	0.463	0.007	0.016	0.065	0.360	0.044	0.055
1000	0.475	0.005	0.097	0.112	0.615	0.022	0.004	0.061	0.434	0.038	0.095	0.117	0.557	0.049	0.056
1050	0.076	0.016	0.064	0.074	-0.012	0.010	0.001	0.036	-0.095	0.038	0.071	0.088	-0.008	0.030	0.044
1100	0.214	0.016	0.060	0.077	0.317	0.026	0.036	0.064	-0.051	0.037	0.058	0.082	0.189	0.042	0.048
1150	0.128	0.040	0.050	0.075	0.146	0.015	0.026	0.048	-0.067	0.036	0.060	0.080	0.098	0.036	0.045
1200	0.221	0.007	0.073	0.108	0.361	0.054	0.007	0.095	0.017	0.019	0.065	0.103	0.208	0.059	0.062
1250	0.152	0.019	0.049	0.067	0.136	0.035	0.029	0.061	-0.137	0.034	0.050	0.073	0.066	0.038	0.044
1300	0.213	0.022	0.017	0.045	0.266	0.013	0.044	0.058	-0.061	0.039	0.015	0.055	0.146	0.030	0.037
1350	-0.041	0.036	0.030	0.055	-0.132	0.023	0.037	0.053	-0.391	0.022	0.024	0.044	-0.217	0.029	0.042
1400	-0.211	0.043	0.078	0.107	-0.220	0.033	0.008	0.069	-0.633	0.053	0.065	0.103	-0.317	0.050	0.054
1450	-0.308	0.035	0.049	0.072	-0.238	0.053	0.011	0.067	-0.578	0.057	0.053	0.087	-0.344	0.043	0.042
1500	-0.736	0.016	0.050	0.062	-0.657	0.070	0.028	0.083	-1.013	0.055	0.054	0.084	-0.787	0.043	0.043
1550	-0.317	0.011	0.098	0.116	-0.054	0.045	0.000	0.076	-0.508	0.073	0.085	0.128	-0.208	0.057	0.057
1600	-0.353	0.074	0.032	0.086	-0.405	0.033	0.043	0.062	-0.825	0.071	0.041	0.087	-0.496	0.044	0.043

Table 7.14. VNIIOFI intermediate calculation results (values in %).

WL [nm]	NIST07 $\Delta_{i,1}$	$u_r(\bar{s}_{i,1})$	$u_{\text{stability}}$	$u_t(\Delta_{i,1})$	NIST14 $\Delta_{i,2}$	$u_r(\bar{s}_{i,2})$	$u_{\text{stability}}$	$u_t(\Delta_{i,2})$	NIST09 $\Delta_{i,3}$	$u_r(\bar{s}_{i,3})$	$u_{\text{stability}}$	$u_t(\Delta_{i,3})$	$\bar{\Delta}_i$	$u_t(\bar{\Delta}_i)$	$u_{t,\text{corr}}(\bar{\Delta}_i)$
900	0.635	0.326	0.046	0.334	0.277	0.177	0.010	0.186	-1.316	0.407	0.226	0.473	0.362	0.163	0.048
950	-1.363	0.057	0.003	0.085	-1.552	0.115	0.055	0.142	-0.783	0.046	0.010	0.078	-1.121	0.053	0.053
1000	-0.341	0.064	0.045	0.097	-0.851	0.038	0.027	0.074	-0.311	0.160	0.006	0.170	-0.626	0.055	0.048
1050	-1.250	0.310	0.057	0.317	-1.427	0.355	0.017	0.357	-0.833	0.232	0.007	0.235	-1.079	0.167	0.044
1100	-1.205	0.081	0.063	0.112	-1.504	0.200	0.029	0.207	-1.019	0.247	0.003	0.251	-1.239	0.092	0.057
1150	-1.620	0.130	0.074	0.154	-1.742	0.203	0.035	0.210	-1.445	0.233	0.007	0.237	-1.616	0.110	0.050
1200	-2.008	0.064	0.062	0.119	-1.736	0.036	0.008	0.086	-1.776	0.223	0.001	0.236	-1.826	0.067	0.059
1250	-2.198	0.116	0.071	0.142	-1.932	0.158	0.006	0.163	-2.078	0.074	0.008	0.085	-2.080	0.067	0.052
1300	-2.381	0.057	0.058	0.089	-2.190	0.099	0.012	0.105	-2.330	0.181	0.007	0.184	-2.305	0.064	0.041
1350	-2.943	0.060	0.052	0.085	-2.617	0.106	0.024	0.113	-2.817	0.178	0.003	0.180	-2.824	0.064	0.039
1400	-1.791	0.066	0.064	0.109	-1.470	0.086	0.016	0.106	-1.601	0.130	0.004	0.143	-1.620	0.067	0.047
1450	-3.586	0.194	0.037	0.201	-3.268	0.210	0.023	0.215	-3.406	0.029	0.024	0.055	-3.410	0.052	0.072
1500	-4.163	0.310	0.035	0.314	-3.985	0.291	0.019	0.294	-4.113	0.054	0.029	0.070	-4.109	0.067	0.073
1550	-4.199	0.274	0.035	0.283	-3.809	0.271	0.003	0.278	-4.119	0.024	0.020	0.069	-4.106	0.065	0.083
1600	-4.876	0.301	0.017	0.303	-4.345	0.282	0.024	0.284	-4.633	0.040	0.015	0.053	-4.630	0.051	0.071

## 7.2 Determination of the Key Comparison Reference Values

The KCRV is derived at each wavelength from the results summarized in Section 7.1 according to the procedures described in Section 6 (Eqs. 6.15 to 6.24). It is based on the weighted mean, with individual weights limited by the adoption of a cut-off value for the reported uncertainties of each laboratory. The following measurements were excluded from the calculation of the KCRV:

1. Measurements by CSIR because they were incomplete and did not conform to the protocol.
2. Measurements by KRISS because KRISS was unable to provide details on their uncertainty budget, as requested of all laboratories following the Working Group discussion of Draft A results in June, 2004.

The combined uncertainty  $u_c(\bar{A}_i)$  (Eq. 6.13) for each laboratory with no cutoff value applied are listed in Table 7.15. The corresponding weights are listed in Table 7.16 and shown in Fig. 7.1. Note that with no cutoff value applied, the KCRV would be dominated by one laboratory, NRC, with weights ranging from 0.16 to 0.48, depending on the wavelength. In Draft A-1 (Jan. 2003), the uncertainty cut-off value of 0.25 % was selected for all wavelengths. This limited the weight assigned to each laboratory to be less than 0.15, also for all wavelengths. In this final report, following the recommendation of the Working Group that resulted from their meeting in June 2004, the cut-off value  $u_{\text{cut-off}}$  is determined to be the average uncertainty of all uncertainties less than the median uncertainty:

$$u_{\text{cut-off}} \equiv \text{Average}\{u_i\} \text{ for } u_i \leq \text{Median}\{u_i\}. \quad (7.1)$$

The cut-off uncertainties are given in Table 7.17. The combined uncertainties applying the cut-off,  $u_{c, \text{adj}}(\bar{A}_i)$  (Eq. 6.14), are listed in Table 7.18 and the resultant weights used in the calculation of the KCRVs (Eq. 6.16) in Table 7.19 and Fig. 7.2. Note that in this case no laboratory has a weight larger than 0.17, and four laboratories have almost equal weight at each wavelength.

Using the laboratory weights in Table 7.19, the weighed mean difference  $\bar{A}_{\text{KCRV}}$  of the laboratory differences  $\bar{A}_i$  from the pilot is calculated according to Eq. 6.15. The uncertainty of KCRV,  $u(\bar{A}_{\text{KCRV}})$ , is calculated using Eq. 6.17.  $\bar{A}_{\text{KCRV}}$  is the KCRV, and the difference  $\bar{A}_i - \bar{A}_{\text{KCRV}}$  (eq. 6.18) is the relative laboratory difference from the KCRV.

## 7.3 Birge Ratio

The Birge ratio is the ratio of the external consistency to the internal consistency, with the internal and external consistencies defined as:

$$u_{\text{int}}^2 = 1 / \sum_{i=1}^N u_i^{-2} \quad (7.2)$$

$$u_{\text{ext}}^2 = \frac{\sum_{i=1}^N \frac{(x_i - x_w)^2}{u^2(x_i)}}{(N-1) \sum_{i=1}^N \frac{1}{u^2(x_i)}}, \quad (7.3)$$

where  $x_i$  is measurement  $i$  and  $x_w$  is the weighted mean of the measurement [Taylor 1969]. The Birge ratio  $R_B$  is defined as:

$$R_B = \frac{u_{\text{ext}}}{u_{\text{int}}}. \quad (7.4)$$

The consistency check fails if the Birge ratio is significantly greater than one. The Birge ratios with and without cut-off are given in Table 7.20. The data of CSIR and KRIS are excluded in the calculation as they are excluded from the calculation of KCRV. The Birge ratio is found to be significantly greater than 1 (1.4 or larger) for all wavelengths, which indicates that the uncertainties reported by participants, on the average, were underestimated.

#### 7.4 Summarized laboratory results with respect to the KCRV

Table 7.21 summarizes  $\bar{\Delta}_{\text{KCRV}}$  and its uncertainty  $u(\bar{\Delta}_{\text{KCRV}})$  for each wavelength. Each laboratory's relative percent difference  $d_i = \bar{\Delta}_i - \bar{\Delta}_{\text{KCRV}}$  (eq. 6.18) is listed in Table 7.22. This corresponds to the unilateral Degree of Equivalence (DoE)  $D_i$  of each laboratory at each wavelength. The uncertainties  $u(d_i)$  in the relative difference  $d_i$ , calculated by eqs. 6.19 and 6.20, are given in Table 7.23. Multiplying the values by 2 in Table 7.23 gives  $U(D_i)$ , the expanded uncertainty ( $k=2$ ) in the unilateral DoE, which are listed in Table 7.24. The results are shown for each wavelength in Fig. 7.3 (a) – (o), plotting each laboratory's relative difference  $d_i$ . Error bars corresponds to the values of  $U(D_i)$ , thus the expanded uncertainties ( $k=2$ ) of the relative difference  $d_i$  given by eq. (6.22), which includes the laboratory's reported uncertainty, transfer uncertainty in the comparison, and the uncertainty of KCRV. For reference, Table 7.25 lists the laboratories' reported uncertainties (average of the measurements reported in Section 4). In Fig. 7.4 (a) – (o), the results are summarized for each laboratory; laboratories are given in Table 7.26. In these figures, the expanded uncertainty ( $k=2$ ) in the KCRV is plotted as well.

The tables of the unilateral and bilateral DoE of all combinations of laboratories are presented in Appendix A.

Table 7.15. Combined uncertainty  $u_c(\bar{A}_i)$  for each laboratory (no cut-off applied) [%].

WL [nm]	BNM	CSIR	CSIRO	HUT	IFA	KRISS	NIM	NIST	NMi-VSL	NPL	NRC	OMH	PTB	SMU	VNIIOFI
900	0.30	1.30	0.21	1.57	0.65	0.41	0.72	0.21	0.60	0.23	0.22	1.40	0.22	0.33	0.62
950	0.29	1.30	0.18	1.80	0.61	0.41	0.46	0.67	0.48	0.18	0.14	1.39	0.15	0.25	0.53
1000	0.28	1.30	0.17	1.73	0.60	0.40	0.45	0.47	0.46	0.18	0.09	1.39	0.14	0.21	0.54
1050	0.28	1.10	0.19	1.77	0.60	0.50	0.42	0.44	0.40	0.16	0.08	1.77	0.15	0.20	0.65
1100	0.27	1.10	0.17	1.73	0.59	0.50	0.45	0.25	0.32	0.16	0.08	1.67	0.14	0.20	0.57
1150	0.27	1.10	0.15	1.73	0.59	0.50	0.41	0.41	0.28	0.16	0.07	1.76	0.13	0.20	0.56
1200	0.28	1.10	0.13	1.74	0.60	0.50	0.44	0.76	0.26	0.18	0.08	1.72	0.13	0.20	0.54
1250	0.27	1.00	0.10	1.73	0.59	0.50	0.42	0.46	0.22	0.16	0.07	1.69	0.12	0.20	0.54
1300	0.28	1.00	0.09	1.73	0.60	0.50	0.43	0.43	0.20	0.14	0.06	1.72	0.12	0.19	0.54
1350	0.27	1.00	0.10	1.73	0.59	0.50	0.41	0.44	0.20	0.16	0.09	1.72	0.12	0.21	0.55
1400	0.28	1.00	0.14	1.73	0.58	0.50	0.41	0.62	0.21	0.17	0.10	1.64	0.12	0.22	0.54
1450	0.28	1.00	0.13	1.73	0.59	0.50	0.48	0.45	0.21	0.21	0.08	1.70	0.12	0.21	0.57
1500	0.28	1.00	0.14	1.73	0.58	0.50	0.50	0.50	0.22	0.18	0.08	1.68	0.12	0.21	0.62
1550	0.28	1.00	0.15	1.73	0.59	0.50	0.54	0.54	0.39	0.18	0.09	2.64	0.13	0.21	0.60
1600	0.29	1.00	0.17	1.73	0.59	0.54	0.61	0.64	0.73	0.21	0.11	3.02	0.12	0.23	0.58

Table 7.16. Corresponding weights  $w_i$  used in the calculation of the KCRV if no cut-off value is applied.

WL [nm]	BNM	CSIR	CSIRO	HUT	IFA	KRISS	NIM	NIST	NMi-VSL	NPL	NRC	OMH	PTB	SMU	VNIIOFI
900	0.081	0.000	0.160	0.003	0.017	0.000	0.014	0.168	0.021	0.137	0.155	0.004	0.152	0.068	0.019
950	0.059	0.000	0.154	0.002	0.013	0.000	0.023	0.011	0.021	0.158	0.239	0.003	0.224	0.076	0.018
1000	0.043	0.000	0.125	0.001	0.010	0.000	0.017	0.015	0.016	0.109	0.398	0.002	0.173	0.079	0.012
1050	0.038	0.000	0.082	0.001	0.008	0.000	0.017	0.015	0.019	0.111	0.488	0.001	0.133	0.078	0.007
1100	0.037	0.000	0.096	0.001	0.008	0.000	0.013	0.043	0.028	0.107	0.442	0.001	0.145	0.071	0.009
1150	0.035	0.000	0.117	0.001	0.007	0.000	0.016	0.015	0.033	0.102	0.447	0.001	0.151	0.067	0.008
1200	0.035	0.000	0.162	0.001	0.008	0.000	0.014	0.005	0.042	0.081	0.413	0.001	0.162	0.068	0.009
1250	0.027	0.000	0.199	0.001	0.006	0.000	0.011	0.009	0.041	0.079	0.434	0.001	0.135	0.052	0.007
1300	0.023	0.000	0.214	0.001	0.005	0.000	0.010	0.009	0.045	0.089	0.423	0.001	0.128	0.047	0.006
1350	0.031	0.000	0.241	0.001	0.007	0.000	0.014	0.012	0.056	0.091	0.318	0.001	0.169	0.052	0.008
1400	0.041	0.000	0.164	0.001	0.009	0.000	0.019	0.008	0.068	0.110	0.304	0.001	0.201	0.063	0.011
1450	0.032	0.000	0.146	0.001	0.007	0.000	0.011	0.012	0.058	0.057	0.440	0.001	0.169	0.058	0.008
1500	0.033	0.000	0.138	0.001	0.008	0.000	0.010	0.010	0.055	0.078	0.424	0.001	0.177	0.059	0.007
1550	0.040	0.000	0.155	0.001	0.010	0.000	0.011	0.011	0.021	0.100	0.365	0.000	0.204	0.073	0.009
1600	0.047	0.000	0.142	0.001	0.011	0.000	0.011	0.009	0.007	0.086	0.346	0.000	0.254	0.075	0.011

Table 7.17.  $u_{\text{cut-off}}$  at each wavelength [%].

WL [nm]	Median $u_{\text{rel}}$	$u_{\text{cut-off}}$
900	0.320	0.24
950	0.450	0.22
1000	0.443	0.21
1050	0.393	0.20
1100	0.266	0.18
1150	0.274	0.17
1200	0.265	0.16
1250	0.263	0.16
1300	0.272	0.15
1350	0.267	0.16
1400	0.270	0.17
1450	0.269	0.17
1500	0.272	0.16
1550	0.386	0.19
1600	0.577	0.24

Table 7.18. Combined uncertainty  $u_{\text{c,adj}}(\bar{A}_i)$  of each lab with cut-off applied [%].

WL [nm]	BNM	CSIR	CSIRO	HUT	IFA	KRISS	NIM	NIST	NMi-VSL	NPL	NRC	OMH	PTB	SMU	VNIIOFI
900	0.30	1.30	0.24	1.57	0.65	0.41	0.72	0.24	0.60	0.24	0.25	1.40	0.24	0.33	0.62
950	0.29	1.30	0.23	1.80	0.61	0.41	0.46	0.67	0.48	0.23	0.23	1.39	0.23	0.25	0.53
1000	0.28	1.30	0.21	1.73	0.60	0.40	0.45	0.47	0.46	0.21	0.21	1.39	0.21	0.22	0.54
1050	0.28	1.10	0.21	1.77	0.60	0.50	0.42	0.44	0.40	0.21	0.21	1.77	0.20	0.21	0.65
1100	0.27	1.10	0.18	1.73	0.59	0.50	0.45	0.25	0.32	0.18	0.18	1.67	0.18	0.20	0.57
1150	0.27	1.10	0.18	1.73	0.59	0.50	0.41	0.41	0.28	0.18	0.18	1.76	0.18	0.20	0.56
1200	0.28	1.10	0.18	1.74	0.60	0.50	0.44	0.76	0.26	0.18	0.17	1.72	0.17	0.20	0.54
1250	0.27	1.00	0.16	1.73	0.59	0.50	0.42	0.46	0.22	0.16	0.16	1.69	0.16	0.20	0.54
1300	0.28	1.00	0.15	1.73	0.60	0.50	0.43	0.43	0.20	0.15	0.15	1.72	0.15	0.19	0.54
1350	0.27	1.00	0.16	1.73	0.59	0.50	0.41	0.44	0.20	0.16	0.16	1.72	0.16	0.21	0.55
1400	0.28	1.00	0.18	1.73	0.58	0.50	0.41	0.62	0.21	0.18	0.18	1.64	0.18	0.22	0.54
1450	0.28	1.00	0.17	1.73	0.59	0.50	0.48	0.45	0.21	0.21	0.17	1.70	0.17	0.21	0.57
1500	0.28	1.00	0.17	1.73	0.58	0.50	0.50	0.50	0.22	0.18	0.17	1.68	0.17	0.21	0.62
1550	0.28	1.00	0.20	1.73	0.59	0.50	0.54	0.54	0.39	0.20	0.20	2.64	0.20	0.21	0.60
1600	0.29	1.00	0.24	1.73	0.59	0.54	0.61	0.64	0.73	0.24	0.24	3.02	0.24	0.24	0.58

Table 7.19. Corresponding weights  $w_i$  used in the calculation of the KCRV, with cut-off applied.

WL [nm]	BNM	CSIR	CSIRO	HUT	IFA	KRISS	NIM	NIST	NMi-VSL	NPL	NRC	OMH	PTB	SMU	VNIIOFI
900	0.097	0.000	0.149	0.004	0.021	0.000	0.017	0.147	0.024	0.145	0.142	0.004	0.146	0.081	0.023
950	0.100	0.000	0.155	0.003	0.022	0.000	0.039	0.018	0.035	0.153	0.155	0.004	0.155	0.129	0.030
1000	0.088	0.000	0.155	0.002	0.020	0.000	0.035	0.031	0.033	0.155	0.150	0.004	0.155	0.150	0.024
1050	0.082	0.000	0.154	0.002	0.018	0.000	0.036	0.033	0.041	0.155	0.152	0.002	0.156	0.151	0.016
1100	0.067	0.000	0.153	0.002	0.014	0.000	0.024	0.078	0.050	0.155	0.154	0.002	0.157	0.129	0.016
1150	0.069	0.000	0.159	0.002	0.015	0.000	0.031	0.030	0.065	0.160	0.160	0.002	0.161	0.132	0.016
1200	0.065	0.000	0.158	0.002	0.015	0.000	0.026	0.009	0.079	0.152	0.171	0.002	0.174	0.129	0.018
1250	0.059	0.000	0.167	0.001	0.012	0.000	0.024	0.020	0.087	0.167	0.167	0.001	0.168	0.111	0.015
1300	0.051	0.000	0.167	0.001	0.011	0.000	0.022	0.021	0.099	0.169	0.170	0.001	0.170	0.104	0.014
1350	0.059	0.000	0.166	0.001	0.013	0.000	0.025	0.022	0.104	0.164	0.166	0.001	0.166	0.097	0.015
1400	0.065	0.000	0.161	0.002	0.015	0.000	0.030	0.013	0.108	0.162	0.162	0.002	0.163	0.101	0.017
1450	0.065	0.000	0.170	0.002	0.014	0.000	0.022	0.024	0.116	0.115	0.168	0.002	0.170	0.117	0.016
1500	0.063	0.000	0.167	0.002	0.015	0.000	0.019	0.019	0.105	0.149	0.168	0.002	0.167	0.113	0.013
1550	0.081	0.000	0.162	0.002	0.019	0.000	0.022	0.022	0.043	0.162	0.159	0.001	0.163	0.146	0.018
1600	0.108	0.000	0.155	0.003	0.026	0.000	0.024	0.022	0.017	0.155	0.155	0.001	0.155	0.153	0.026

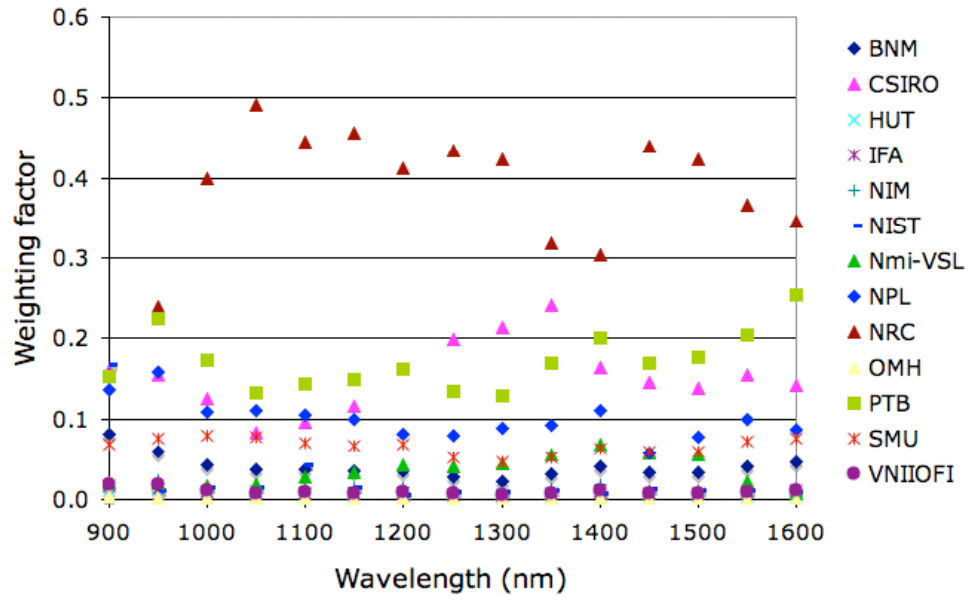


Figure 7.1. Weighting factors with no cut-off value applied to the data.

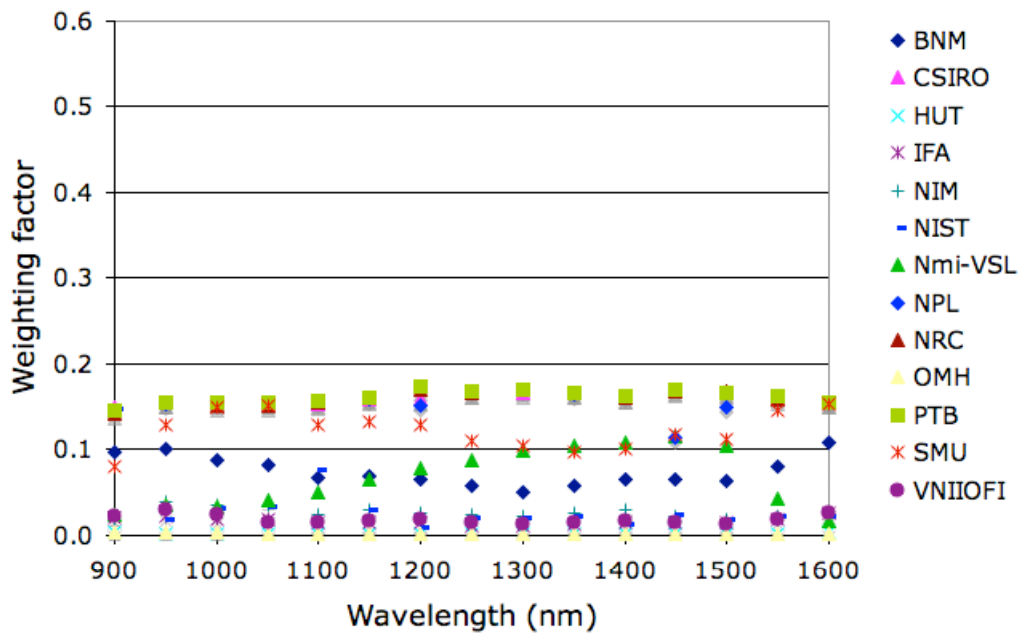


Figure 7.2. Weighting factors with cut-off value applied to the data.

Table 7.20. Birge ratios calculated with and without cutoff (CSIR and KRISS excluded).

Wavelength [nm]	Birge ratio without cut-off	Birge ratio with cut-off
900	2.6	2.5
950	2.1	2.0
1000	1.9	1.8
1050	1.6	1.6
1100	1.6	1.6
1150	1.6	1.6
1200	1.8	1.7
1250	2.1	1.9
1300	2.1	1.9
1350	2.0	1.9
1400	1.5	1.4
1450	2.2	2.1
1500	2.2	2.1
1550	2.4	2.3
1600	2.7	2.4

Table 7.21. The KCRV  $\bar{\Delta}_{\text{KCRV}}$  and its uncertainty  $u(\bar{\Delta}_{\text{KCRV}})$  and  $U(\bar{\Delta}_{\text{KCRV}})$  with  $k=2$ .

Wavelength [nm]	$\bar{\Delta}_{\text{KCRV}}$ [%]	$u(\bar{\Delta}_{\text{KCRV}})$ [%]	$U(\bar{\Delta}_{\text{KCRV}})$ [%]
900	0.03	0.09	0.17
950	-0.14	0.08	0.15
1000	0.19	0.07	0.14
1050	-0.21	0.07	0.14
1100	-0.02	0.06	0.12
1150	-0.10	0.06	0.12
1200	0.04	0.06	0.12
1250	-0.10	0.05	0.11
1300	-0.10	0.05	0.10
1350	-0.27	0.05	0.11
1400	-0.45	0.06	0.12
1450	-0.59	0.06	0.12
1500	-0.92	0.06	0.12
1550	-0.49	0.07	0.13
1600	-0.67	0.07	0.15

Table 7.22. Laboratory differences  $d_i$  [%] from the KCRV, or unilateral Degree of Equivalence  $D_i$  [%].

WL [nm]	BNM	CSIR	CSIRO	HUT	IFA	KRISS	NIM	NIST	NMi-VSL	NPL	NRC	OMH	PTB	SMU	VNIIOFI
900	-1.34	0.14	-0.85	-0.44	1.93	0.14	3.51	-0.03	0.66	0.37	0.65	0.00	-0.12	0.11	0.33
950	-1.24	0.15	-0.30	0.89	1.52	0.07	1.32	0.14	0.16	0.47	0.00	-0.43	-0.21	0.50	-0.98
1000	-1.11	0.10	-0.43	-0.10	1.26	0.29	1.31	-0.19	0.50	0.13	0.09	-0.17	0.09	0.37	-0.81
1050	-1.06	0.24	-0.32	0.51	1.47	0.00	0.79	0.21	0.30	0.14	0.06	0.55	0.08	0.20	-0.87
1100	-1.01	-0.08	-0.26	-0.06	1.55	0.09	0.27	0.02	0.26	0.22	-0.01	0.81	0.14	0.21	-1.22
1150	-0.96	0.26	-0.14	0.22	1.41	0.12	-0.04	0.10	0.18	0.17	-0.01	0.65	0.17	0.20	-1.52
1200	-0.67	0.00	-0.26	0.39	1.64	0.10	-0.29	-0.04	0.14	0.31	-0.09	0.70	0.21	0.17	-1.87
1250	-0.77	0.14	-0.40	0.04	1.54	0.03	-0.35	0.10	0.21	0.24	0.04	0.29	0.26	0.17	-1.98
1300	-0.82	0.21	-0.34	0.02	1.47	0.23	-0.33	0.10	0.21	0.22	0.05	0.53	0.15	0.24	-2.21
1350	-0.61	0.79	-0.23	0.48	1.44	-0.14	-0.47	0.27	0.10	0.31	0.04	0.48	0.15	0.05	-2.56
1400	-0.62	0.99	-0.29	-0.22	1.43	-0.08	-0.48	0.45	0.20	0.15	0.00	0.79	0.21	0.13	-1.17
1450	-0.79	1.39	-0.27	-0.06	1.49	0.09	-0.71	0.59	0.25	0.25	0.15	0.90	0.05	0.25	-2.82
1500	-0.74	1.69	-0.33	0.10	1.32	0.34	-0.67	0.92	0.27	0.25	0.11	0.57	0.10	0.14	-3.19
1550	-0.67	2.42	-0.39	-0.06	1.39	-0.01	-0.91	0.49	0.34	0.25	0.13	-2.71	0.31	0.29	-3.61
1600	-0.60	3.17	-0.32	-0.56	1.58	0.35	-0.93	0.67	0.40	0.20	0.37	-2.03	0.44	0.17	-3.96

Table 7.23. Standard uncertainties  $u(d_i)$  in laboratory difference  $d_i$  [%].

WL	BNM	CSIR	CSIRO	HUT	IFA	KRISS	NIM	NIST	NMi-VSL	NPL	NRC	OMH	PTB	SMU	VNIIOFI
900	0.28	1.30	0.20	1.57	0.64	0.42	0.71	0.20	0.59	0.21	0.20	1.40	0.20	0.31	0.61
950	0.27	1.31	0.17	1.80	0.60	0.41	0.45	0.67	0.47	0.16	0.14	1.39	0.14	0.23	0.51
1000	0.27	1.30	0.15	1.73	0.59	0.41	0.44	0.46	0.45	0.16	0.10	1.39	0.14	0.19	0.53
1050	0.27	1.10	0.17	1.76	0.59	0.51	0.41	0.43	0.39	0.15	0.09	1.77	0.14	0.18	0.64
1100	0.26	1.10	0.15	1.73	0.59	0.51	0.45	0.24	0.31	0.15	0.09	1.67	0.13	0.18	0.56
1150	0.26	1.10	0.14	1.73	0.59	0.51	0.40	0.40	0.27	0.14	0.09	1.75	0.12	0.18	0.55
1200	0.27	1.10	0.12	1.73	0.59	0.51	0.44	0.76	0.24	0.17	0.09	1.72	0.12	0.18	0.53
1250	0.26	1.00	0.10	1.73	0.59	0.51	0.41	0.46	0.21	0.14	0.08	1.69	0.11	0.18	0.53
1300	0.27	1.00	0.09	1.73	0.59	0.50	0.42	0.43	0.19	0.13	0.07	1.71	0.11	0.18	0.53
1350	0.26	1.00	0.10	1.73	0.58	0.50	0.41	0.44	0.19	0.14	0.09	1.72	0.11	0.20	0.54
1400	0.27	1.00	0.13	1.73	0.57	0.51	0.40	0.62	0.20	0.15	0.10	1.64	0.12	0.21	0.53
1450	0.27	1.00	0.12	1.73	0.59	0.51	0.47	0.45	0.19	0.19	0.09	1.70	0.12	0.19	0.56
1500	0.27	1.00	0.13	1.73	0.58	0.51	0.50	0.50	0.20	0.16	0.09	1.68	0.12	0.19	0.62
1550	0.27	1.00	0.14	1.73	0.58	0.51	0.54	0.54	0.38	0.16	0.10	2.64	0.12	0.19	0.60
1600	0.27	1.00	0.16	1.73	0.58	0.54	0.60	0.63	0.72	0.19	0.12	3.02	0.13	0.20	0.57

Table 7.24. Expanded uncertainties  $U(d_i)$  [%] in laboratory difference, or  $U(D_i)$  [%] in DoE, with coverage factor  $k=2$ .

WL [nm]	BNM	CSIR	CSIRO	HUT	IFA	KRISS	NIM	NIST	NMi-VSL	NPL	NRC	OMH	PTB	SMU	VNIIOFI
900	0.56	2.61	0.40	3.13	1.28	0.83	1.42	0.39	1.17	0.43	0.41	2.80	0.41	0.62	1.22
950	0.54	2.61	0.33	3.60	1.20	0.82	0.89	1.33	0.94	0.33	0.28	2.78	0.29	0.46	1.03
1000	0.53	2.61	0.31	3.46	1.18	0.82	0.87	0.93	0.90	0.33	0.21	2.78	0.27	0.37	1.06
1050	0.53	2.21	0.34	3.53	1.19	1.01	0.83	0.86	0.77	0.30	0.19	3.53	0.28	0.35	1.28
1100	0.52	2.21	0.31	3.46	1.17	1.01	0.89	0.48	0.61	0.29	0.18	3.34	0.26	0.36	1.12
1150	0.52	2.21	0.27	3.46	1.17	1.01	0.80	0.81	0.54	0.29	0.17	3.51	0.25	0.36	1.10
1200	0.54	2.21	0.25	3.47	1.18	1.01	0.87	1.52	0.48	0.33	0.18	3.44	0.24	0.37	1.07
1250	0.52	2.00	0.20	3.46	1.18	1.01	0.82	0.91	0.41	0.28	0.15	3.38	0.23	0.36	1.07
1300	0.54	2.00	0.18	3.46	1.18	1.01	0.84	0.85	0.37	0.25	0.15	3.43	0.22	0.36	1.06
1350	0.52	2.00	0.19	3.46	1.17	1.01	0.81	0.87	0.38	0.28	0.18	3.44	0.22	0.40	1.08
1400	0.53	2.01	0.26	3.46	1.15	1.01	0.80	1.23	0.40	0.30	0.21	3.28	0.24	0.42	1.06
1450	0.53	2.01	0.24	3.46	1.17	1.01	0.95	0.89	0.38	0.39	0.17	3.40	0.23	0.38	1.12
1500	0.54	2.01	0.25	3.46	1.15	1.01	0.99	0.99	0.40	0.33	0.17	3.36	0.23	0.39	1.24
1550	0.54	2.01	0.27	3.46	1.16	1.02	1.07	1.07	0.76	0.33	0.20	5.28	0.25	0.38	1.19
1600	0.53	2.01	0.31	3.46	1.16	1.08	1.19	1.27	1.44	0.38	0.23	6.04	0.25	0.41	1.14

Table 7.25. Laboratories' reported uncertainties  $u_i$  [%].

WL [nm]	BNM	CSIR	CSIRO	HUT	IFA	KRISS	NIM	NIST	NMi-VSL	NPL	NRC	OMH	PTB	SMU	VNIIOFI
900	0.29	1.30	0.21	1.57	0.64	0.40	0.71	0.20	0.59	0.22	0.20	1.40	0.21	0.32	0.61
950	0.27	1.30	0.17	1.80	0.60	0.40	0.45	0.67	0.48	0.16	0.13	1.39	0.13	0.24	0.52
1000	0.27	1.30	0.16	1.73	0.59	0.40	0.44	0.47	0.45	0.17	0.07	1.39	0.13	0.20	0.54
1050	0.27	1.10	0.19	1.77	0.60	0.50	0.42	0.44	0.39	0.16	0.06	1.77	0.15	0.19	0.65
1100	0.27	1.10	0.16	1.73	0.59	0.50	0.45	0.25	0.31	0.16	0.07	1.67	0.13	0.19	0.56
1150	0.27	1.10	0.14	1.73	0.59	0.50	0.40	0.41	0.27	0.16	0.07	1.75	0.13	0.19	0.55
1200	0.26	1.10	0.11	1.73	0.59	0.50	0.44	0.76	0.25	0.17	0.06	1.72	0.12	0.19	0.54
1250	0.26	1.00	0.09	1.73	0.59	0.50	0.42	0.46	0.21	0.15	0.06	1.69	0.12	0.19	0.54
1300	0.27	1.00	0.08	1.73	0.59	0.50	0.42	0.43	0.19	0.14	0.06	1.72	0.11	0.19	0.53
1350	0.27	1.00	0.09	1.73	0.59	0.50	0.41	0.44	0.20	0.16	0.08	1.72	0.11	0.21	0.54
1400	0.27	1.00	0.13	1.73	0.58	0.50	0.40	0.62	0.20	0.16	0.09	1.64	0.11	0.21	0.53
1450	0.27	1.00	0.12	1.73	0.59	0.50	0.48	0.45	0.20	0.20	0.06	1.70	0.11	0.20	0.56
1500	0.27	1.00	0.13	1.73	0.58	0.50	0.50	0.50	0.20	0.18	0.06	1.68	0.11	0.20	0.62
1550	0.28	1.00	0.13	1.73	0.58	0.50	0.54	0.54	0.39	0.17	0.07	2.64	0.11	0.20	0.60
1600	0.28	1.00	0.16	1.73	0.59	0.53	0.60	0.64	0.73	0.21	0.09	3.02	0.11	0.22	0.58

Table 7.26. Laboratory name and associated figure label.

Laboratory	Label
BNM-INM	1
CSIR	2
CSIRO	3
HUT	4
IFA	5
KRISS	6
NIM	7
NIST	8
NMi-VSL	9
NPL	10
NRC	11
OMH	12
PTB	13
SMU	14
VNIIOFI	15

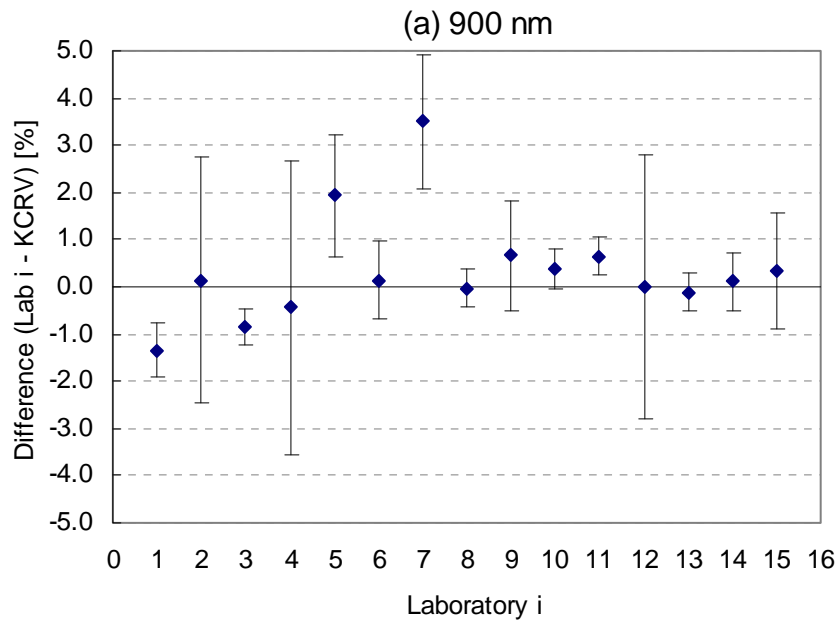


Figure 7.3(a). Laboratory differences from the KCRV at 900 nm. Error bars correspond to uncertainties listed in Table 7.24.

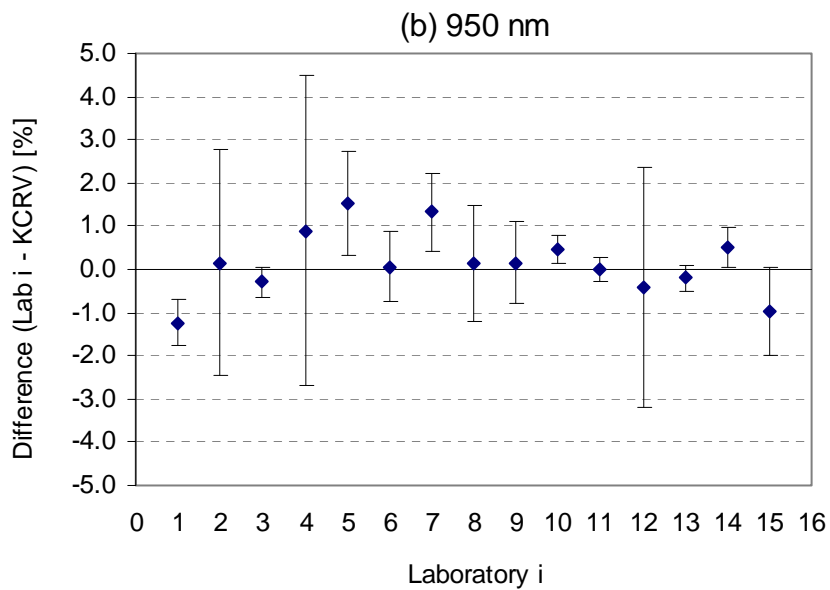


Figure 7.3(b). Laboratory differences from the KCRV at 950 nm. Error bars correspond to uncertainties listed in Table 7.24.

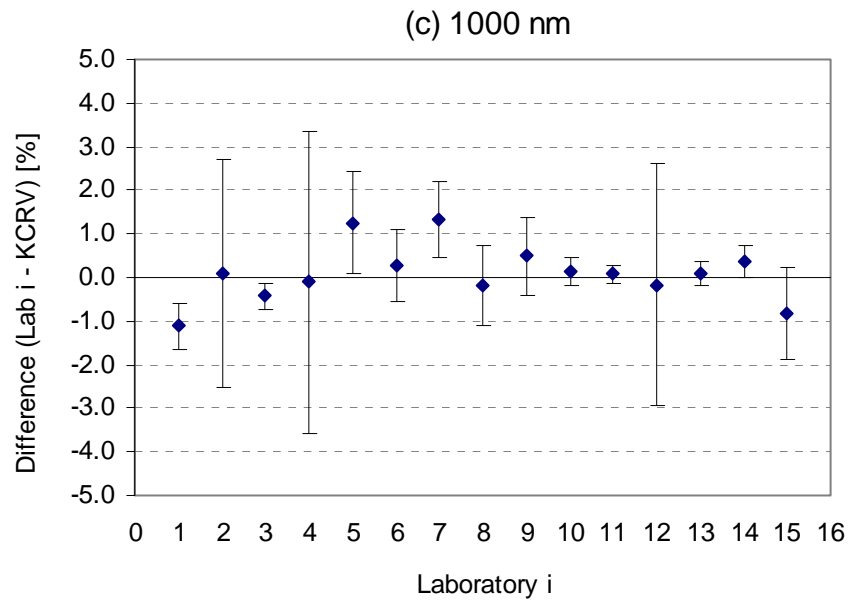


Figure 7.3(c). Laboratory differences from the KCRV at 1000 nm. Error bars correspond to uncertainties listed in Table 7.24.

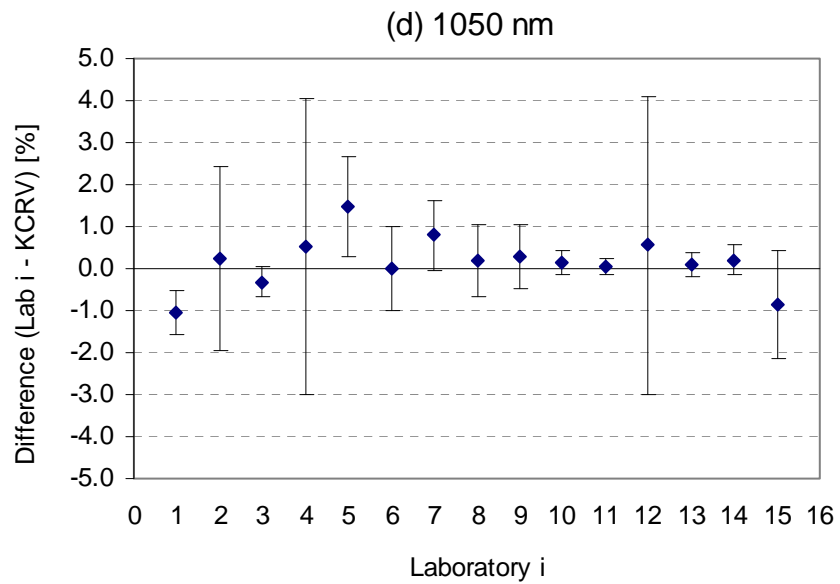


Figure 7.3(d). Laboratory differences from the KCRV at 1050 nm. Error bars correspond to uncertainties listed in Table 7.24.

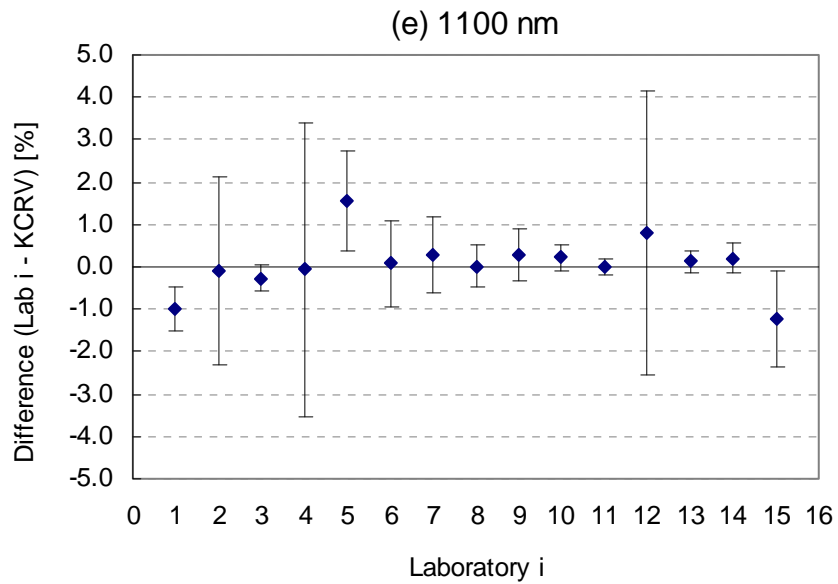


Figure 7.3(e). Laboratory differences from the KCRV at 1100 nm. Error bars correspond to uncertainties listed in Table 7.24.

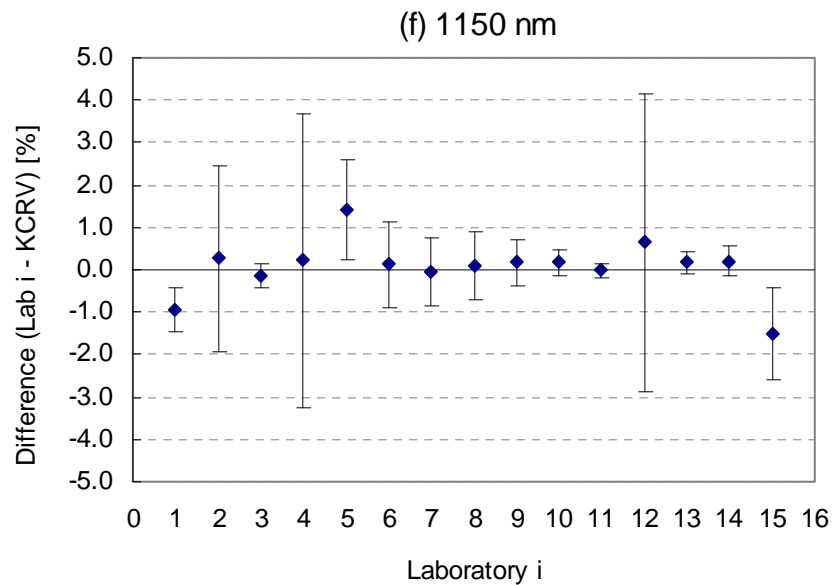


Figure 7.3(f). Laboratory differences from the KCRV at 1150 nm. Error bars correspond to uncertainties listed in Table 7.24.

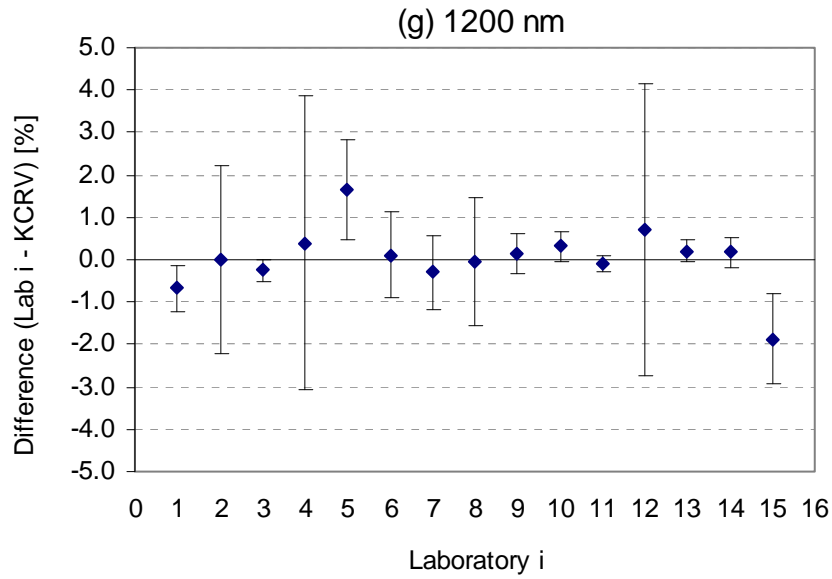


Figure 7.3(g). Laboratory differences from the KCRV at 1200 nm. Error bars correspond to uncertainties listed in Table 7.24.

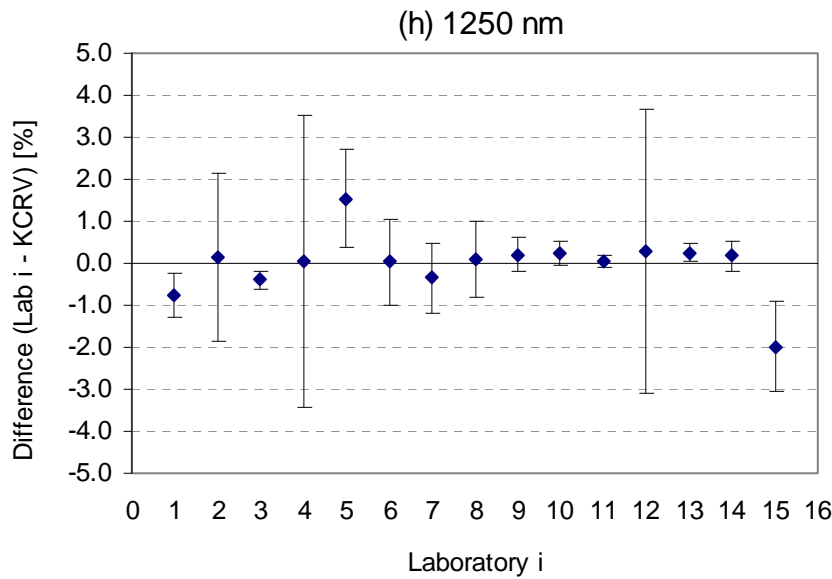


Figure 7.3(h). Laboratory differences from the KCRV at 1250 nm. Error bars correspond to uncertainties listed in Table 7.24.

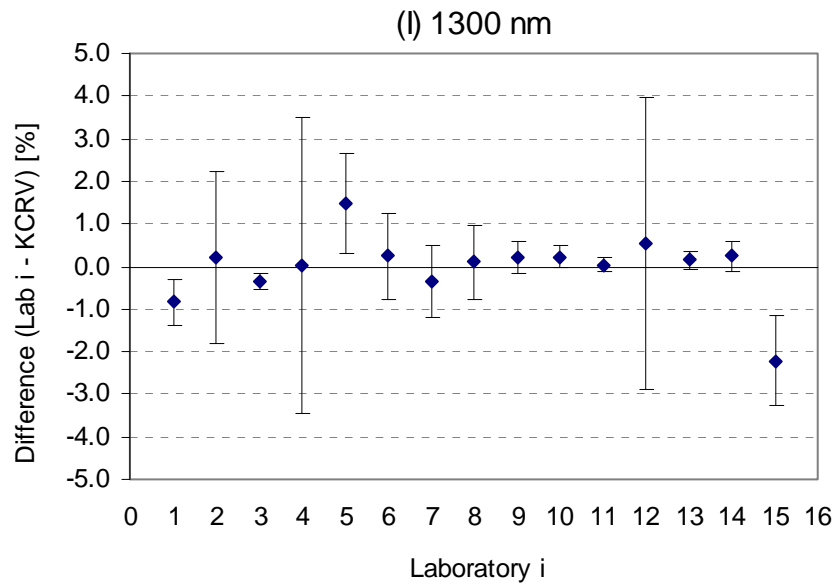


Figure 7.3(i). Laboratory differences from the KCRV at 1300 nm. Error bars correspond to uncertainties listed in Table 7.24.

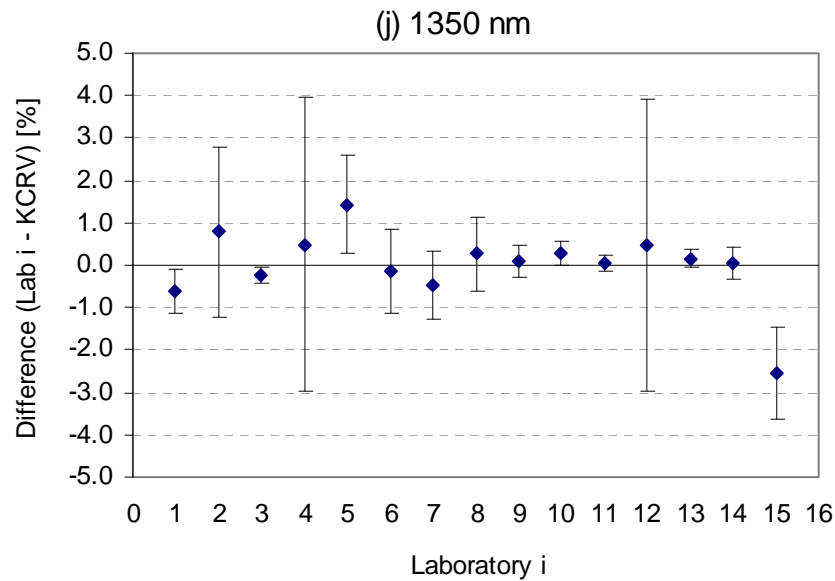


Figure 7.3(j). Laboratory differences from the KCRV at 1350 nm. Error bars correspond to uncertainties listed in Table 7.24.

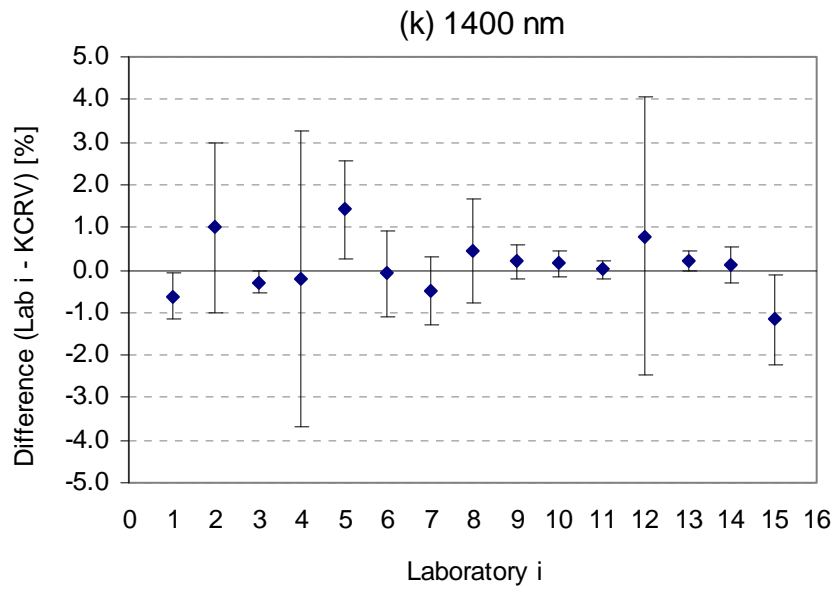


Figure 7.3(k). Laboratory differences from the KCRV at 1400 nm. Error bars correspond to uncertainties listed in Table 7.24.

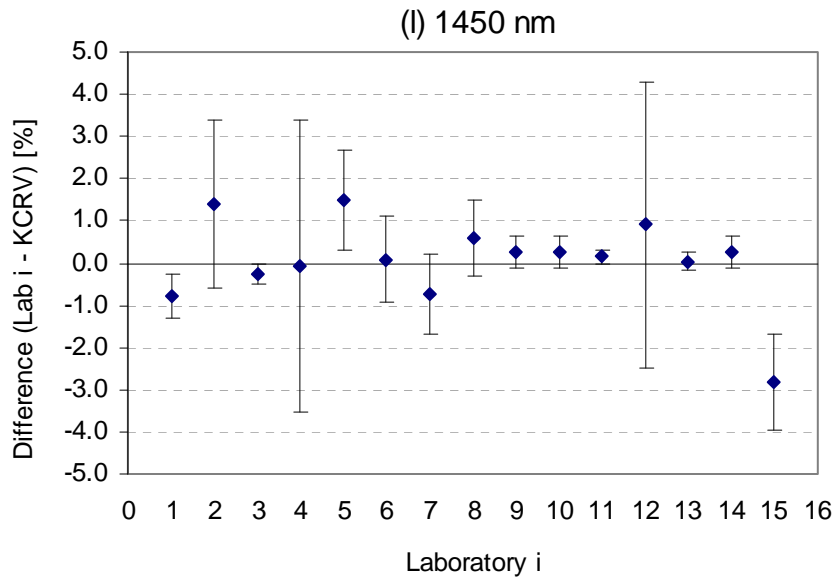


Figure 7.3(l). Laboratory differences from the KCRV at 1450 nm. Error bars correspond to uncertainties listed in Table 7.24.

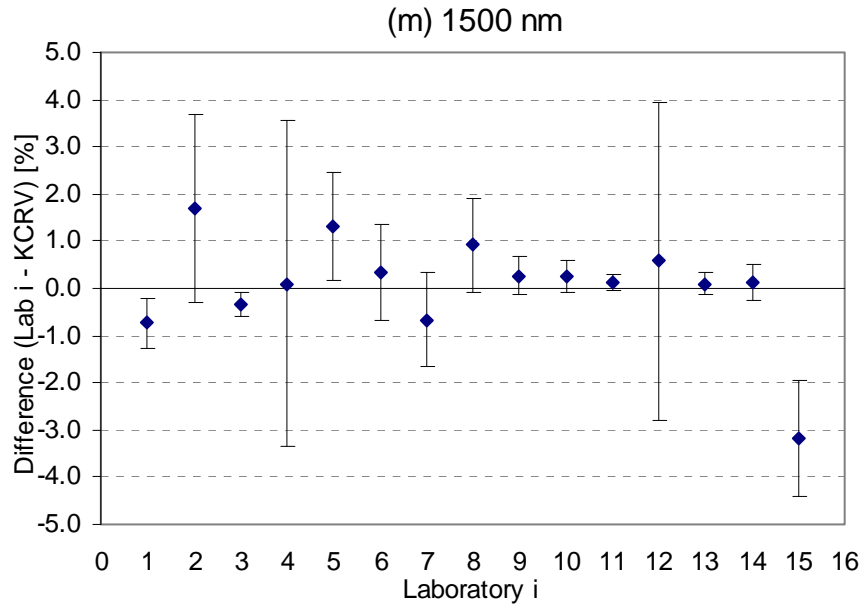


Figure 7.3(m). Laboratory differences from the KCRV at 1500 nm. Error bars correspond to uncertainties listed in Table 7.24.

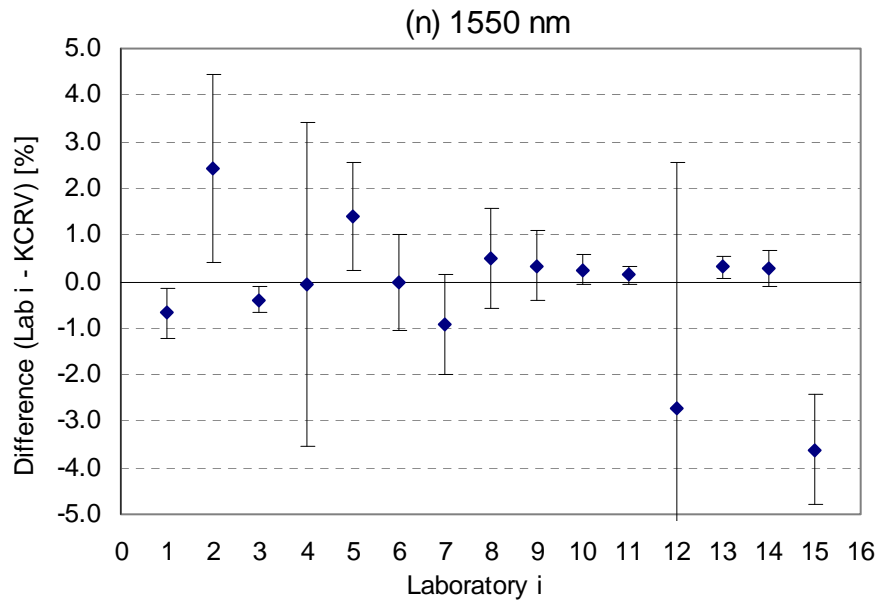


Figure 7.3(n). Laboratory differences from the KCRV at 1550 nm. Error bars correspond to uncertainties listed in Table 7.24.

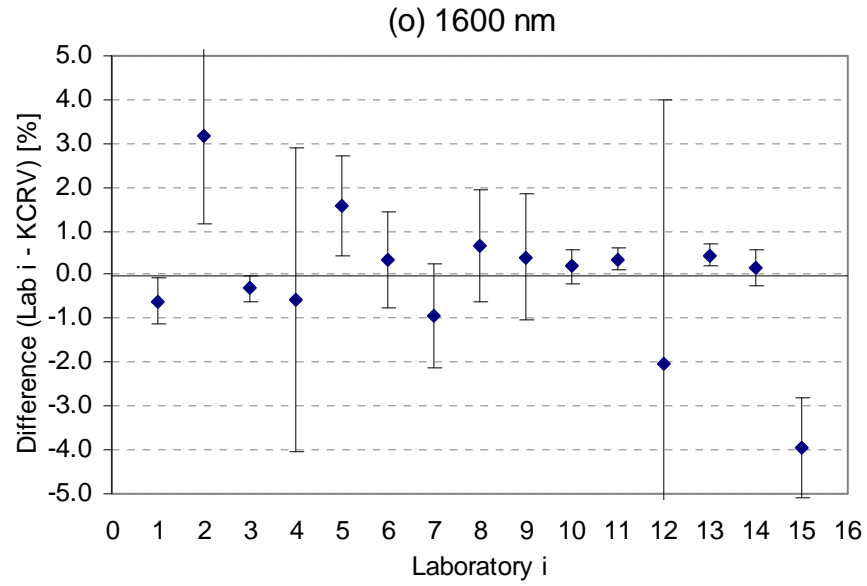


Figure 7.3(o). Laboratory differences from the KCRV at 1600 nm. Error bars correspond to uncertainties listed in Table 7.24.

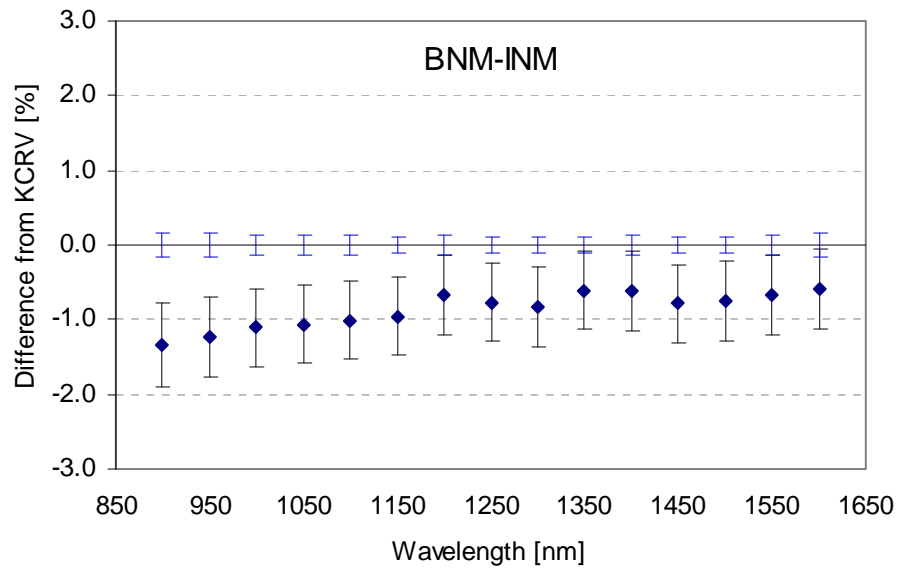


Figure 7.4(a). BNM-INM differences from the KCRV. Error bars correspond to uncertainties listed in Table 7.24; KCRV error bars ( $k=2$ ) from Table 7.21.

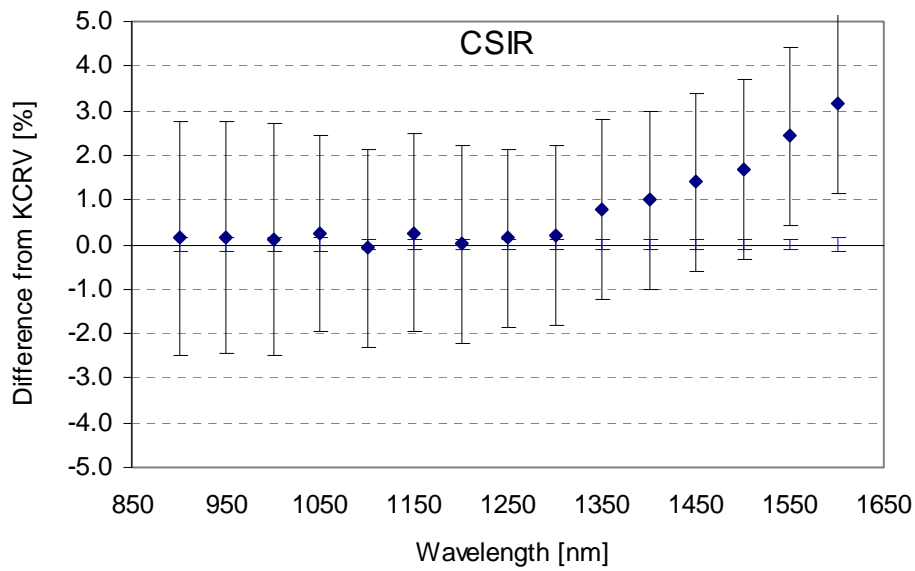


Figure 7.4(b). CSIR differences from the KCRV. Error bars correspond to uncertainties listed in Table 7.24; KCRV error bars ( $k=2$ ) from Table 7.21.

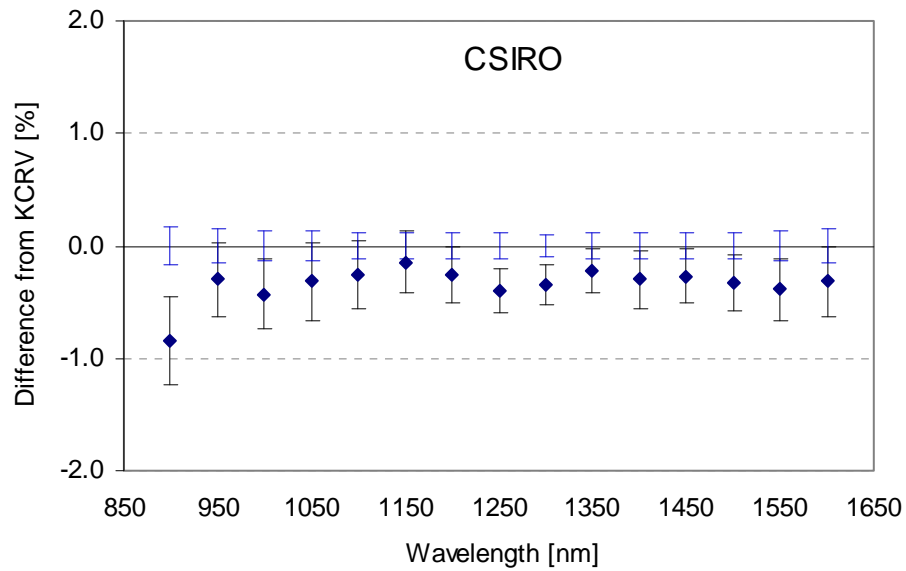


Figure 7.4(c). CSIRO differences from the KCRV. Error bars correspond to uncertainties listed in Table 7.24; KCRV error bars ( $k=2$ ) from Table 7.21.

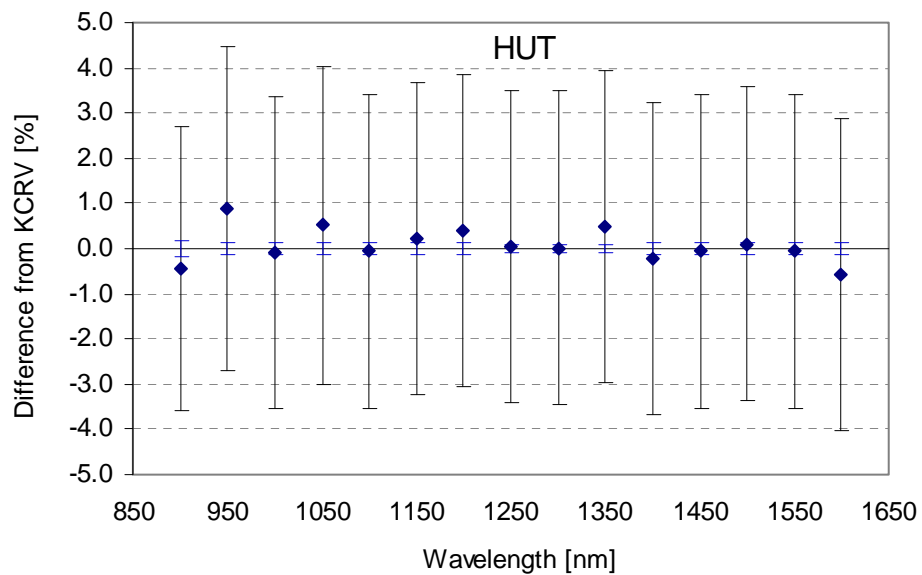


Figure 7.4(d). HUT differences from the KCRV. Error bars correspond to uncertainties listed in Table 7.24; KCRV error bars ( $k=2$ ) from Table 7.21.

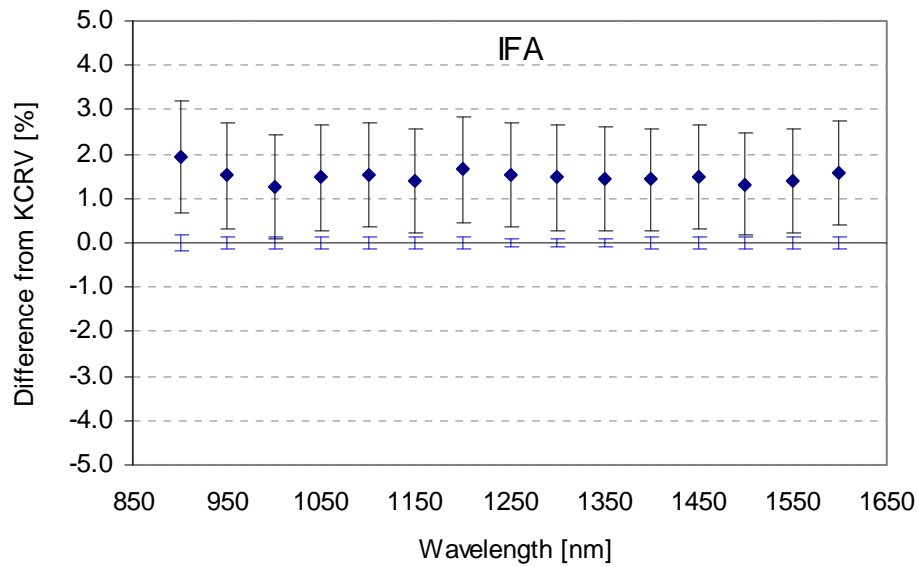


Figure 7.4(e). IFA differences from the KCRV. Error bars correspond to uncertainties from Table 7.24; KCRV error bars ( $k=2$ ) from Table 7.21.

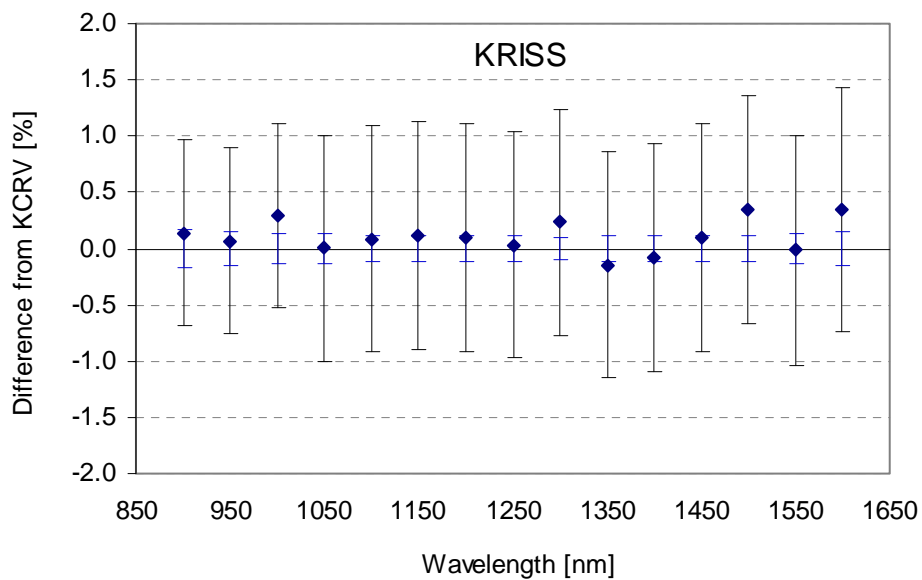


Figure 7.4(f). KRIS differences from the KCRV. Error bars correspond to uncertainties from Table 7.24; KCRV error bars ( $k=2$ ) from Table 7.21.

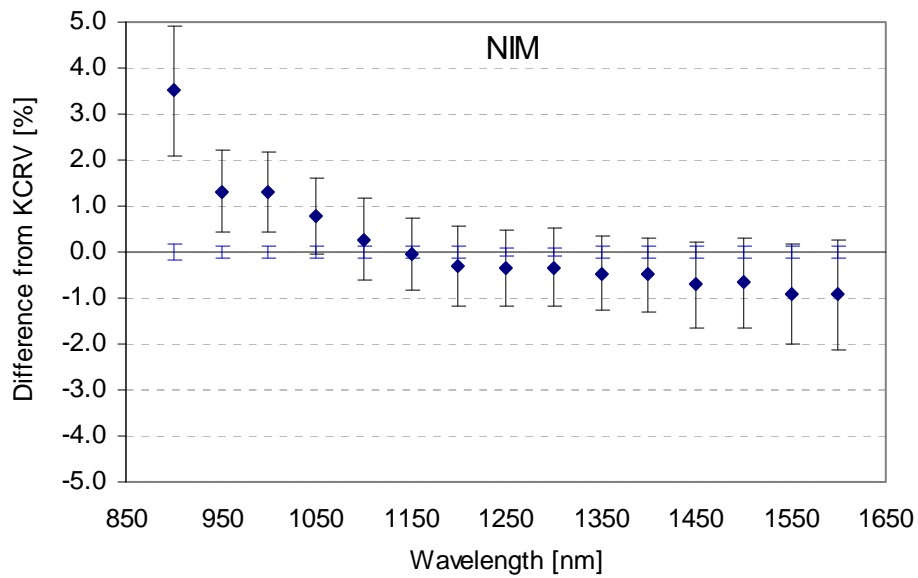


Figure 7.4(g). NIM differences from the KCRV. Error bars correspond to uncertainties from Table 7.24; KCRV error bars ( $k=2$ ) from Table 7.21.

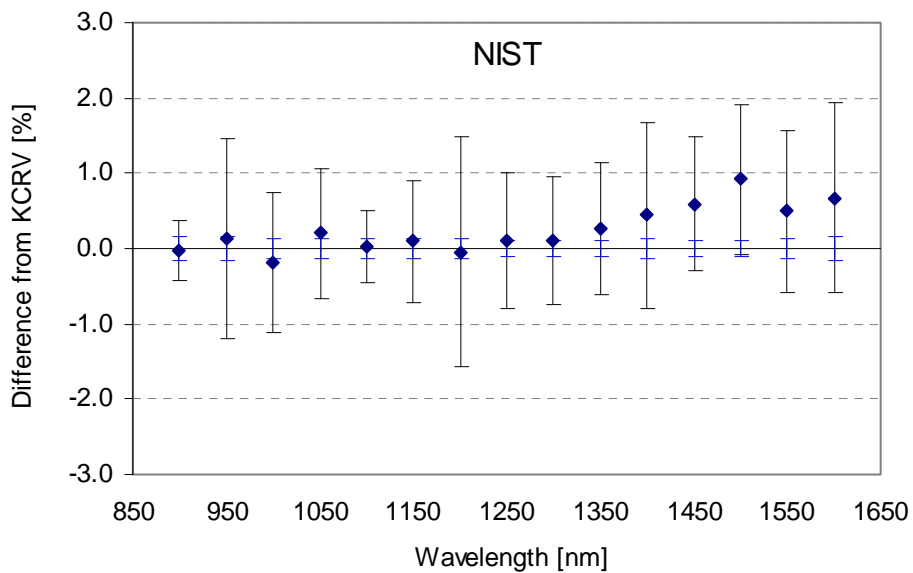


Figure 7.4(h). NIST differences from the KCRV. Error bars correspond to uncertainties listed in Table 7.24; KCRV error bars ( $k=2$ ) from Table 7.21.

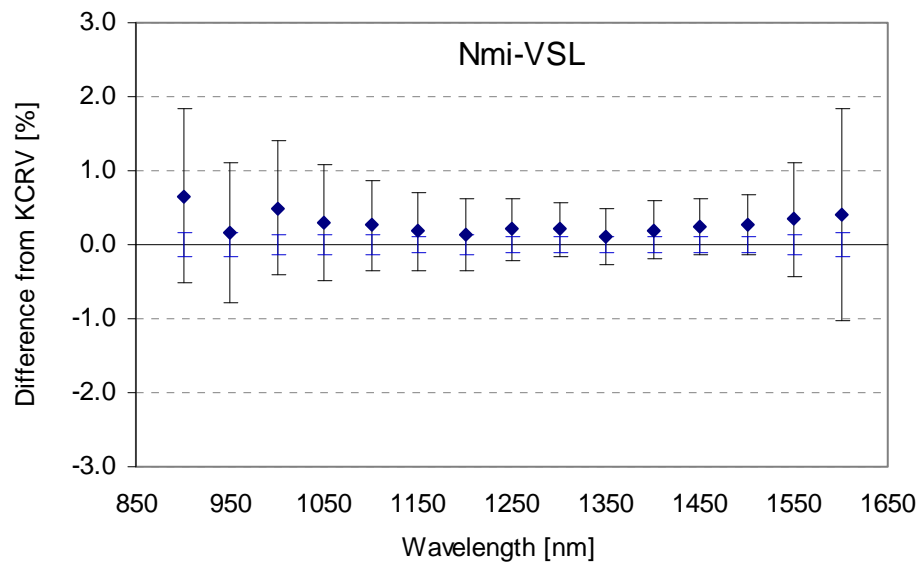


Figure 7.4(i). NMI-VSL differences from the KCRV. Error bars correspond to uncertainties listed in Table 7.24; KCRV error bars ( $k=2$ ) from Table 7.21.

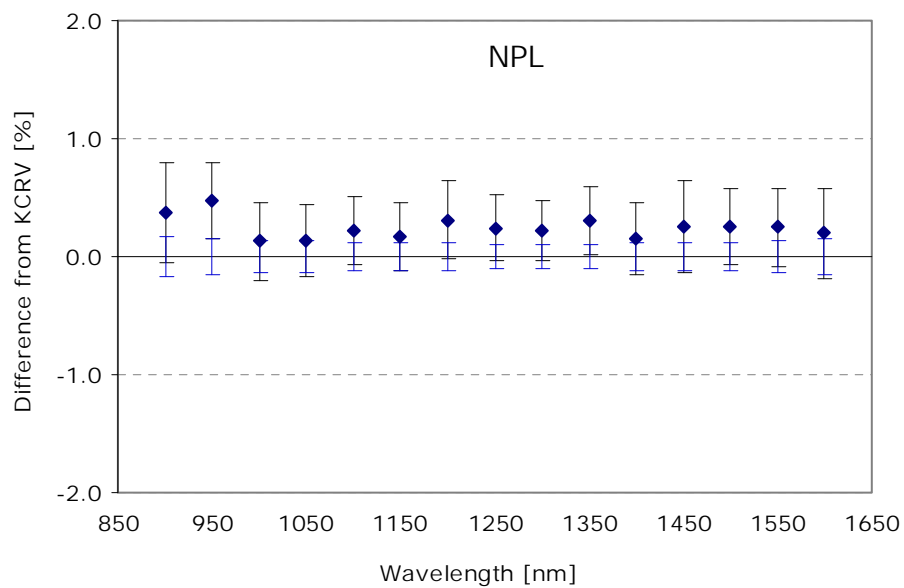


Figure 7.4(j). NPL differences from the KCRV. Error bars correspond to uncertainties listed in Table 7.24; KCRV error bars ( $k=2$ ) from Table 7.21.

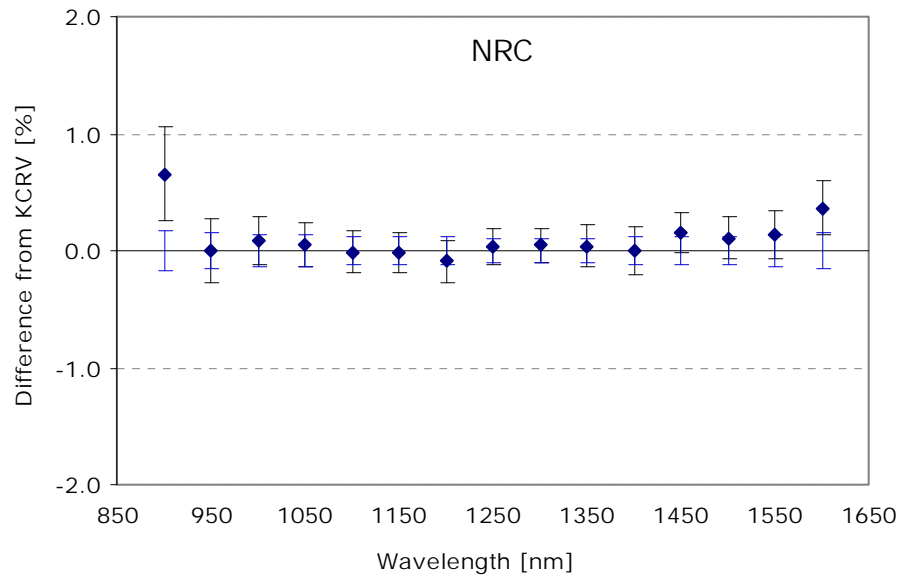


Figure 7.2(k). NRC differences from the KCRV. Error bars correspond to uncertainties listed in Table 7.24; KCRV error bars ( $k=2$ ) from Table 7.21.

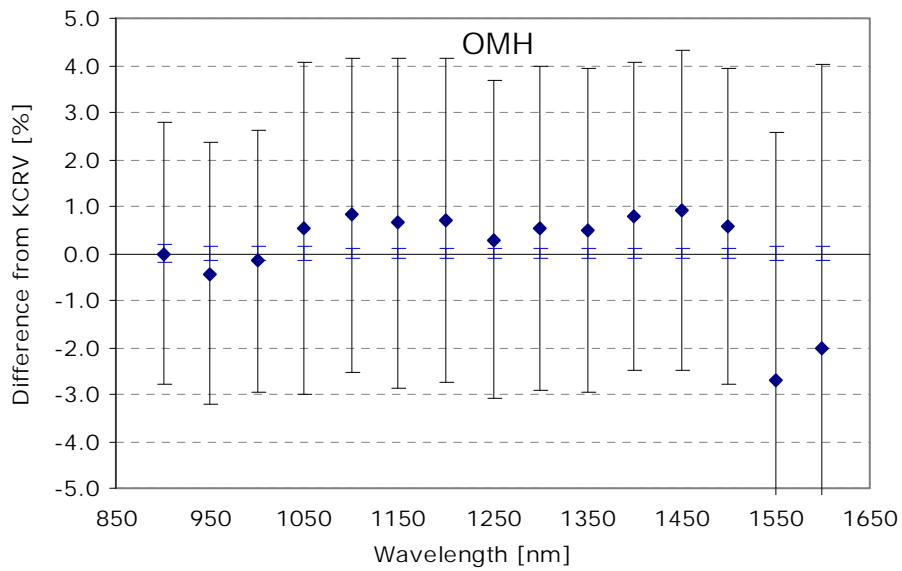


Figure 7.4(l). OMH differences from the KCRV. Error bars correspond to uncertainties listed in Table 7.24; KCRV error bars ( $k=2$ ) from Table 7.21.

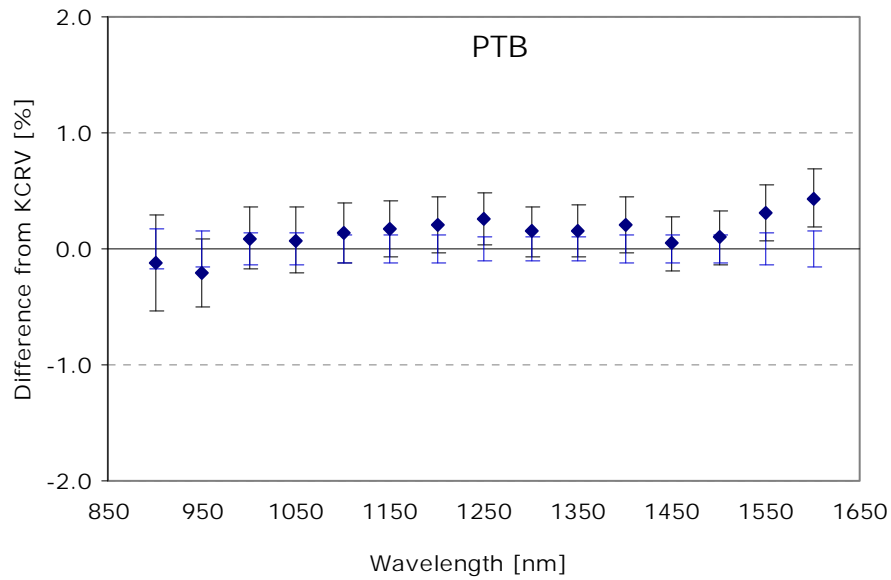


Figure 7.4(m). PTB differences from the KCRV. Error bars correspond to uncertainties listed in Table 7.24; KCRV error bars ( $k=2$ ) from Table 7.21.

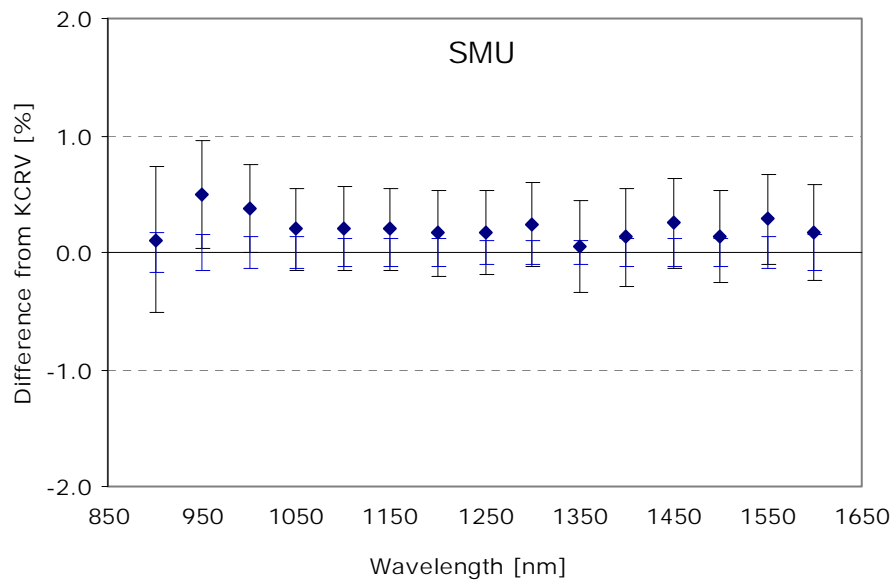


Figure 7.4(n). SMU differences from the KCRV. Error bars correspond to uncertainties listed in Table 7.24; KCRV error bars ( $k=2$ ) from Table 7.21.

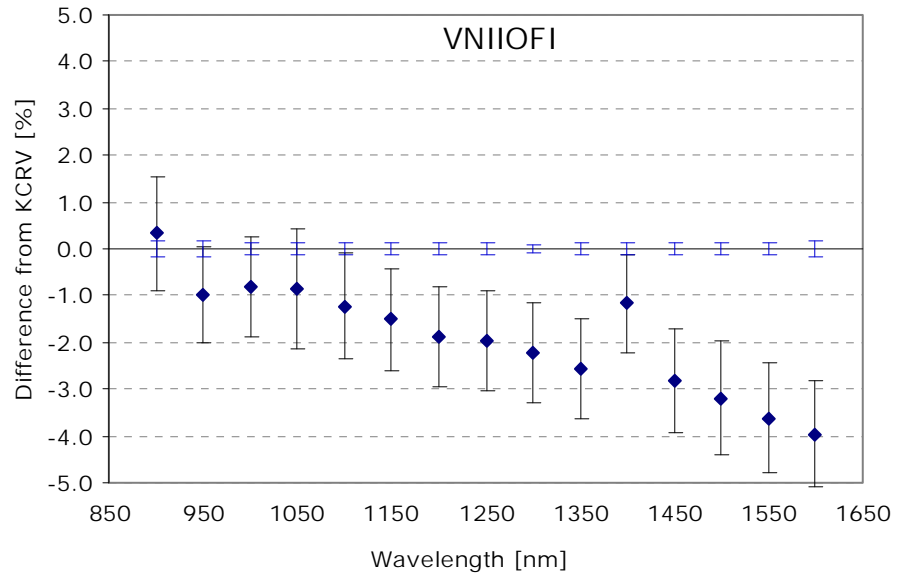


Figure 7.4(o). VNIIOFI differences from the KCRV. Error bars correspond to uncertainties listed in Table 7.24; KCRV error bars ( $k=2$ ) from Table 7.21.

## 8. Discussion of results

To summarize the results, Laboratory differences  $d_i$  [%] from the KCRV listed in Table 7.22 of all participants are presented in Figs. 8.1 and 8.2, and the laboratories' reported uncertainties  $u_i$  [%] listed in Table 7.25 of all participants are presented in Fig. 8.3. From Fig. 8.1, except for two or three laboratories, the results of most of the laboratories agreed within  $\pm 1$  % difference in the entire spectral range, which is considered an expected level of agreement for the near IR range. It should be noted, however, that the uncertainties reported by the participants were generally underestimated as indicated by the Berge ratio (Table 7.20), and also as observed in the plots of some of the participants where the uncertainty bars ( $k=2$ ) are not overlapping with that of KCRV ( $k=2$ ) in a large portion of the spectral range.

It is also observed from Fig. 8.2 that many curves are above the 0 % line, and much fewer curves are below 0 %, which indicates that the KCRV seems to be deviated slightly to the lower direction. This may be caused by one or two laboratories that deviated significantly from the KCRV in lower direction and reported relatively low uncertainties. No results were removed as outliers in this comparison. It would be useful to implement a procedure to exclude outliers in future comparisons. It is also observed from Fig. 8.2 that several laboratories agree within  $\sim 0.3$  % in most of the wavelength range, which is encouraging.

The changes of detector responsivity before and after transportation in this comparison were generally much less than the reported uncertainties of the laboratories (except NRC whose uncertainties were very low), and it can be said that transfer standards served generally well in this comparison. The use of the detectors from four different manufactures was also useful as one type of photodiode showed instability at 900 nm and excluded for that wavelength, but two other photodiodes of other types served for those participants for that wavelength.

As presented in sections 5.3 and 5.5.5, the responsivity spatial uniformity of some of the InGaAs transfer detectors, especially at 900 nm and 1600 nm, were significantly large. Due to this, the differences in beam size caused considerable measurement variations in some cases as reported in Tables 5.6 and 5.7. The 900 nm data of EG&G photodiodes were removed from the analysis due to very large inconsistencies in results (Fig. 5.5), which seems to be caused by other instability factors. The final results (Fig. 7.4 (a) to 7.4 (o)) also showed some anomalous feature at 900 nm for several participants. In the future comparisons of this type, the transfer photodiodes may be selected for better spatial uniformity, and/or the wavelength point of 900 nm (overlapping with K2.b) might be dropped.

The wavelength points of 900 nm, 950 nm, and 1000 nm were overlapped with CCPR K2.b, and the consistency of results between K2.a and K2.b were checked. Measurements for K2.b were performed in 2000, about the same time as K2.a. Figures 8.4 (a), (b), and (c) show relative differences from KCRV of the laboratories that participated in both K2.a and K2.b. From these figures, no correlations between the two comparisons were found.

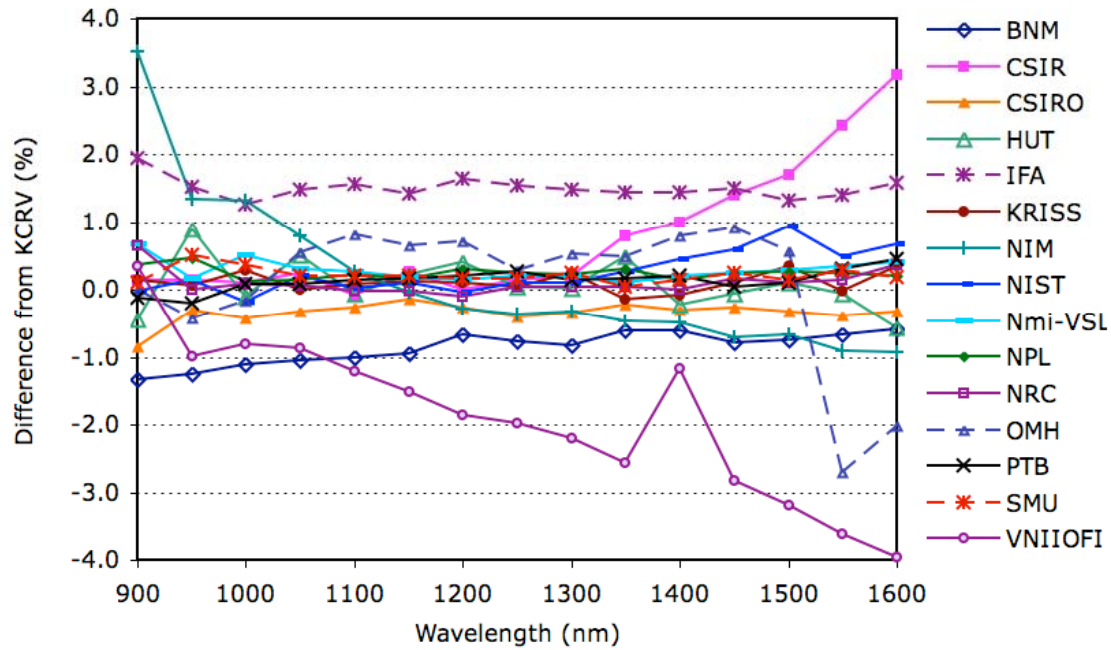


Figure 8.1. Laboratory differences  $d_i$  [%] from the KCRV listed in Table 7.22.

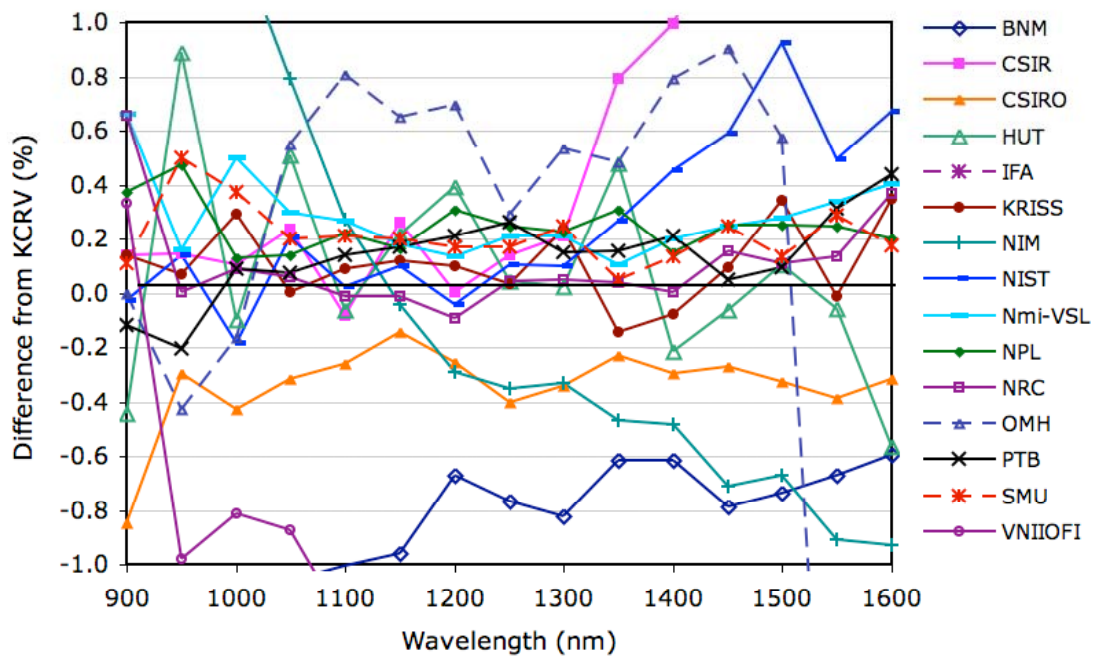


Figure 8.2. Magnification (-1.0 % to 1.0 %) of the Laboratory differences  $d_i$  [%] from the KCRV listed in Table 7.22.

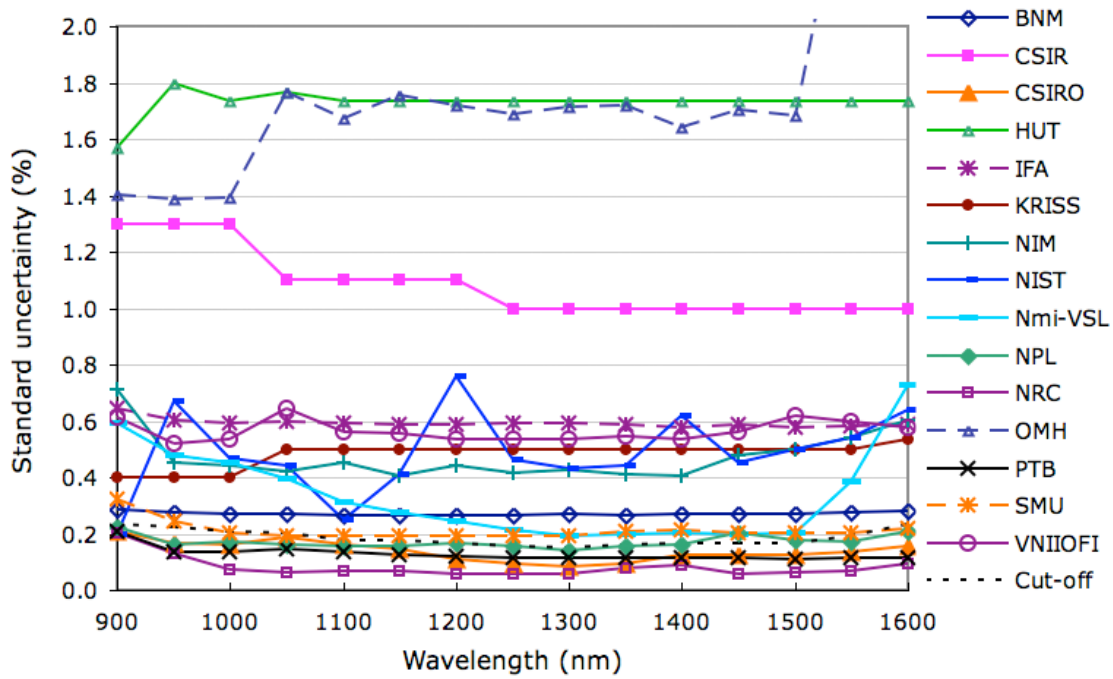


Figure 8.3. Laboratories' reported uncertainties  $u_i$  [%] listed in Table 7.25.

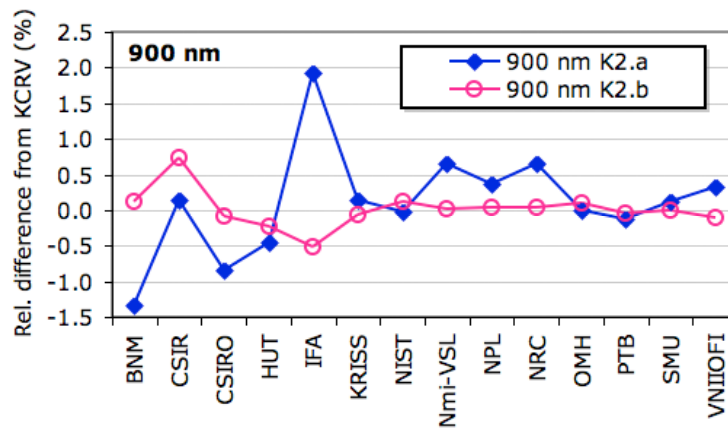


Figure 8.4 (a). Comparison of the results between CCPR K2.a and CCPR K2.b (single photodiodes) at 900 nm.

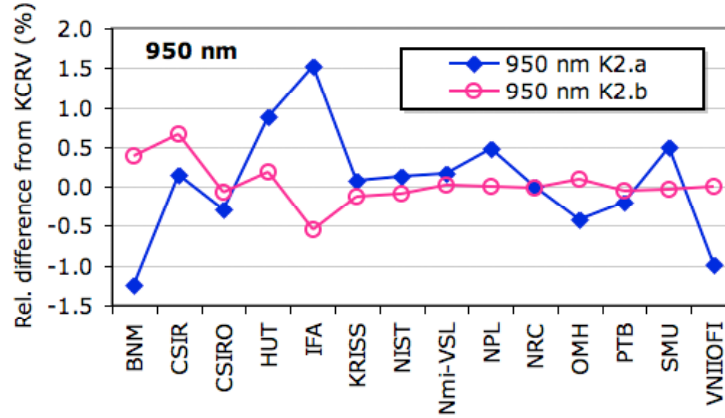


Figure 8.4 (b). Comparison of the results between CCPR K2.a and CCPR K2.b (single photodiodes) at 950 nm.

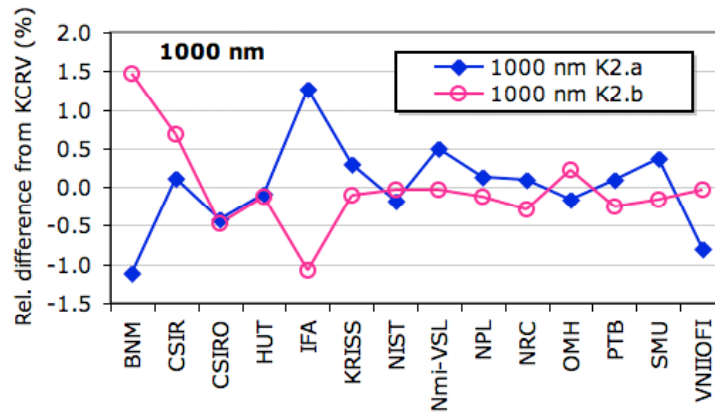


Figure 8.4 (c). Comparison of the results between CCPR K2.a and CCPR K2.b (single photodiodes) at 1000 nm.

## 9. Conclusions

Fifteen laboratories participated in the international intercomparison of spectral responsivity measurements in the near-IR wavelength range of 900 nm to 1600 nm. This was the first international comparison for near-IR region spectral responsivity. The results showed overall good agreement at a level of  $\pm 1\%$ , except a few laboratories that deviated up to 4% at some wavelengths. The deviations were generally constant over the entire spectral range, except that the outlier results tend to deviate larger at longer wavelengths.

The degrees of equivalence which have been calculated from the data are to be used within the framework of the Mutual Recognition Arrangement.

## 10. References

Boivin, L. P., “Properties of sphere radiometers suitable for high-accuracy cryogenic-radiometer-based calibrations in the near-infrared,” *Metrologia* **37**, 273 (2000).

CCPR, “Guidelines for CCPR comparisons report preparation”, March 2006. The document is available at the BIPM website: <http://www.bipm.fr/en/committees/cc/ccpr>.

Fox, N., “Improved near-infrared detectors,” *Metrologia* **30**, 321 (1993).

Larason, T. C., S. S. Bruce and A. C. Parr, *Spectroradiometric detector measurements*, Natl. Inst. Stand. Technol. Spec. Publ. 250-41, U. S. Government Printing Office, Washington, DC, 1998.

Larason, T. C. and Houston, J. M., *Spectroradiometric detector measurements*, Natl. Inst. Stand. Technol. Spec. Publ. 250-41 (2008), U. S. Government Printing Office, Washington, DC, 2008.

Ohno, Y., A Flexible Bandpass Correction Method for Spectrometers, Proc. AIC Colour 05 - 10th Congress of the International Colour Association, May 9-13, 2005, Granada, Spain, pp. 697-700 (2005).

Shaw, P.-S., T. C. Larason, R. Gupta, S. W. Brown, and K. R. Lykke, “Improved near-infrared spectral responsivity scale,” *J. Res. Natl. Inst. Stand. Technol.* **105**, 689 (2000).

Taylor, B. N., W. H. Parker, and D. N. Langenberg, *Rev. Mod. Phys.*, **41**, 3275-3496 (1969).

Yoon, H. W., J. J. Butler, T. C. Larason, and G.P. Eppeldauer, “Linearity of InGaAs photodiodes,” *Metrologia* **40**, S155 (2003).

**Appendix A. Degree of Equivalence Tables**

Table A1. 900 nm Unilateral and Bilateral Degrees of Equivalence (unit: %)

Lab <i>i</i>	Unilateral DoE		Lab <i>m</i>	BNM	CSIR	CSIRO	HUT	IFA	KRISS	NIM	NIST	NMi-VSL	NPL	NRC	OMH	PTB	SMU	VNIIOFI
BNM	$D_i$	-1.3	$D_{i,m}$		-1.5	-0.5	-0.9	-3.3	-1.5	-4.9	-1.3	-2.0	-1.7	-2.0	-1.3	-1.2	-1.5	-1.7
	$U_i$	0.6	$U_{i,m}$		2.7	0.7	3.2	1.4	1.0	1.6	0.7	1.3	0.8	0.7	2.9	0.7	0.9	1.4
CSIR	$D_i$	0.1	$D_{i,m}$	1.5		1.0	0.6	-1.8	0.0	-3.4	0.2	-0.5	-0.2	-0.5	0.1	0.3	0.0	-0.2
	$U_i$	2.6	$U_{i,m}$	2.7		2.6	4.1	2.9	2.7	3.0	2.6	2.9	2.6	2.6	3.8	2.6	2.7	2.9
CSIRO	$D_i$	-0.8	$D_{i,m}$	0.5	-1.0		-0.4	-2.8	-1.0	-4.4	-0.8	-1.5	-1.2	-1.5	-0.8	-0.7	-1.0	-1.2
	$U_i$	0.4	$U_{i,m}$	0.7	2.6		3.2	1.4	0.9	1.5	0.6	1.3	0.6	0.6	2.8	0.6	0.8	1.3
HUT	$D_i$	-0.4	$D_{i,m}$	0.9	-0.6	0.4		-2.4	-0.6	-4.0	-0.4	-1.1	-0.8	-1.1	-0.4	-0.3	-0.6	-0.8
	$U_i$	3.1	$U_{i,m}$	3.2	4.1	3.2		3.4	3.2	3.4	3.2	3.4	3.2	3.2	4.2	3.2	3.2	3.4
IFA	$D_i$	1.9	$D_{i,m}$	3.3	1.8	2.8	2.4		1.8	-1.6	2.0	1.3	1.6	1.3	1.9	2.1	1.8	1.6
	$U_i$	1.3	$U_{i,m}$	1.4	2.9	1.4	3.4		1.5	1.9	1.4	1.8	1.4	1.4	3.1	1.4	1.4	1.8
KRISS	$D_i$	0.1	$D_{i,m}$	1.5	0.0	1.0	0.6	-1.8		-3.4	0.2	-0.5	-0.2	-0.5	0.1	0.3	0.0	-0.2
	$U_i$	0.8	$U_{i,m}$	1.0	2.7	0.9	3.2	1.5		1.6	0.9	1.4	0.9	0.9	2.9	0.9	1.0	1.5
NIM	$D_i$	3.5	$D_{i,m}$	4.9	3.4	4.4	4.0	1.6	3.4		3.5	2.9	3.1	2.9	3.5	3.6	3.4	3.2
	$U_i$	1.4	$U_{i,m}$	1.6	3.0	1.5	3.4	1.9	1.6		1.5	1.9	1.5	1.5	3.2	1.5	1.6	1.9
NIST	$D_i$	0.0	$D_{i,m}$	1.3	-0.2	0.8	0.4	-2.0	-0.2	-3.5		-0.7	-0.4	-0.7	0.0	0.1	-0.1	-0.4
	$U_i$	0.4	$U_{i,m}$	0.7	2.6	0.6	3.2	1.4	0.9	1.5		1.3	0.6	0.6	2.8	0.6	0.8	1.3
NMi-VSL	$D_i$	0.7	$D_{i,m}$	2.0	0.5	1.5	1.1	-1.3	0.5	-2.9	0.7		0.3	0.0	0.7	0.8	0.5	0.3
	$U_i$	1.2	$U_{i,m}$	1.3	2.9	1.3	3.4	1.8	1.4	1.9	1.3		1.3	1.3	3.0	1.3	1.4	1.7
NPL	$D_i$	0.4	$D_{i,m}$	1.7	0.2	1.2	0.8	-1.6	0.2	-3.1	0.4	-0.3		-0.3	0.4	0.5	0.3	0.0
	$U_i$	0.4	$U_{i,m}$	0.8	2.6	0.6	3.2	1.4	0.9	1.5	0.6	1.3		0.6	2.8	0.6	0.8	1.3
NRC	$D_i$	0.7	$D_{i,m}$	2.0	0.5	1.5	1.1	-1.3	0.5	-2.9	0.7	0.0	0.3		0.7	0.8	0.5	0.3
	$U_i$	0.4	$U_{i,m}$	0.7	2.6	0.6	3.2	1.4	0.9	1.5	0.6	1.3	0.6		2.8	0.6	0.8	1.3
OMH	$D_i$	0.0	$D_{i,m}$	1.3	-0.1	0.8	0.4	-1.9	-0.1	-3.5	0.0	-0.7	-0.4	-0.7		0.1	-0.1	-0.3
	$U_i$	2.8	$U_{i,m}$	2.9	3.8	2.8	4.2	3.1	2.9	3.2	2.8	3.0	2.8	2.8		2.8	2.9	3.1
PTB	$D_i$	-0.1	$D_{i,m}$	1.2	-0.3	0.7	0.3	-2.1	-0.3	-3.6	-0.1	-0.8	-0.5	-0.8	-0.1		-0.2	-0.5
	$U_i$	0.4	$U_{i,m}$	0.7	2.6	0.6	3.2	1.4	0.9	1.5	0.6	1.3	0.6	0.6	2.8		0.8	1.3
SMU	$D_i$	0.1	$D_{i,m}$	1.5	0.0	1.0	0.6	-1.8	0.0	-3.4	0.1	-0.5	-0.3	-0.5	0.1	0.2		-0.2
	$U_i$	0.6	$U_{i,m}$	0.9	2.7	0.8	3.2	1.4	1.0	1.6	0.8	1.4	0.8	0.8	2.9	0.8		1.4
VNIIOFI	$D_i$	0.3	$D_{i,m}$	1.7	0.2	1.2	0.8	-1.6	0.2	-3.2	0.4	-0.3	0.0	-0.3	0.3	0.5	0.2	
	$U_i$	1.2	$U_{i,m}$	1.4	2.9	1.3	3.4	1.8	1.5	1.9	1.3	1.7	1.3	1.3	3.1	1.3	1.4	

Table A2. 950 nm Unilateral and Bilateral Degrees of Equivalence (unit: %)

Lab <i>i</i>	Unilateral DoE		Lab <i>m</i>	BNM	CSIR	CSIRO	HUT	IFA	KRISS	NIM	NIST	NMI-VSL	NPL	NRC	OMH	PTB	SMU	VNIIOFI
	$D_i$	$U_i$																
BNM	$D_i$	-1.2	$D_{i,m}$		-1.4	-0.9	-2.1	-2.8	-1.3	-2.6	-1.4	-1.4	-1.7	-1.2	-0.8	-1.0	-1.7	-0.3
	$U_i$	0.5	$U_{i,m}$		2.7	0.7	3.6	1.3	1.0	1.1	1.5	1.1	0.7	0.6	2.8	0.6	0.8	1.2
CSIR	$D_i$	0.1	$D_{i,m}$	1.4		0.4	-0.7	-1.4	0.1	-1.2	0.0	0.0	-0.3	0.1	0.6	0.4	-0.4	1.1
	$U_i$	2.6	$U_{i,m}$	2.7		2.6	4.4	2.9	2.7	2.8	2.9	2.8	2.6	2.6	3.8	2.6	2.7	2.8
CSIRO	$D_i$	-0.3	$D_{i,m}$	0.9	-0.4		-1.2	-1.8	-0.4	-1.6	-0.4	-0.5	-0.8	-0.3	0.1	-0.1	-0.8	0.7
	$U_i$	0.3	$U_{i,m}$	0.7	2.6		3.6	1.3	0.9	1.0	1.4	1.0	0.5	0.5	2.8	0.5	0.6	1.1
HUT	$D_i$	0.9	$D_{i,m}$	2.1	0.7	1.2		-0.6	0.8	-0.4	0.8	0.7	0.4	0.9	1.3	1.1	0.4	1.9
	$U_i$	3.6	$U_{i,m}$	3.6	4.4	3.6		3.8	3.7	3.7	3.8	3.7	3.6	3.6	4.6	3.6	3.6	3.8
IFA	$D_i$	1.5	$D_{i,m}$	2.8	1.4	1.8	0.6		1.4	0.2	1.4	1.4	1.0	1.5	1.9	1.7	1.0	2.5
	$U_i$	1.2	$U_{i,m}$	1.3	2.9	1.3	3.8		1.5	1.5	1.8	1.6	1.3	1.2	3.0	1.3	1.3	1.6
KRISS	$D_i$	0.1	$D_{i,m}$	1.3	-0.1	0.4	-0.8	-1.4		-1.3	-0.1	-0.1	-0.4	0.1	0.5	0.3	-0.4	1.0
	$U_i$	0.8	$U_{i,m}$	1.0	2.7	0.9	3.7	1.5		1.2	1.6	1.3	0.9	0.9	2.9	0.9	1.0	1.3
NIM	$D_i$	1.3	$D_{i,m}$	2.6	1.2	1.6	0.4	-0.2	1.3		1.2	1.2	0.9	1.3	1.8	1.5	0.8	2.3
	$U_i$	0.9	$U_{i,m}$	1.1	2.8	1.0	3.7	1.5	1.2		1.6	1.3	1.0	1.0	2.9	1.0	1.0	1.4
NIST	$D_i$	0.1	$D_{i,m}$	1.4	0.0	0.4	-0.8	-1.4	0.1	-1.2		0.0	-0.3	0.1	0.6	0.3	-0.4	1.1
	$U_i$	1.3	$U_{i,m}$	1.5	2.9	1.4	3.8	1.8	1.6	1.6		1.7	1.4	1.4	3.1	1.4	1.4	1.7
NMI-VSL	$D_i$	0.2	$D_{i,m}$	1.4	0.0	0.5	-0.7	-1.4	0.1	-1.2	0.0		-0.3	0.2	0.6	0.4	-0.3	1.1
	$U_i$	0.9	$U_{i,m}$	1.1	2.8	1.0	3.7	1.6	1.3	1.3	1.7		1.0	1.0	2.9	1.0	1.1	1.4
NPL	$D_i$	0.5	$D_{i,m}$	1.7	0.3	0.8	-0.4	-1.0	0.4	-0.9	0.3	0.3		0.5	0.9	0.7	0.0	1.5
	$U_i$	0.3	$U_{i,m}$	0.7	2.6	0.5	3.6	1.3	0.9	1.0	1.4	1.0		0.5	2.8	0.5	0.6	1.1
NRC	$D_i$	0.0	$D_{i,m}$	1.2	-0.1	0.3	-0.9	-1.5	-0.1	-1.3	-0.1	-0.2	-0.5		0.4	0.2	-0.5	1.0
	$U_i$	0.3	$U_{i,m}$	0.6	2.6	0.5	3.6	1.2	0.9	1.0	1.4	1.0	0.5		2.8	0.4	0.6	1.1
OMH	$D_i$	-0.4	$D_{i,m}$	0.8	-0.6	-0.1	-1.3	-1.9	-0.5	-1.8	-0.6	-0.6	-0.9	-0.4		-0.2	-0.9	0.6
	$U_i$	2.8	$U_{i,m}$	2.8	3.8	2.8	4.6	3.0	2.9	2.9	3.1	2.9	2.8	2.8		2.8	2.8	3.0
PTB	$D_i$	-0.2	$D_{i,m}$	1.0	-0.4	0.1	-1.1	-1.7	-0.3	-1.5	-0.3	-0.4	-0.7	-0.2	0.2		-0.7	0.8
	$U_i$	0.3	$U_{i,m}$	0.6	2.6	0.5	3.6	1.3	0.9	1.0	1.4	1.0	0.5	0.4	2.8		0.6	1.1
SMU	$D_i$	0.5	$D_{i,m}$	1.7	0.4	0.8	-0.4	-1.0	0.4	-0.8	0.4	0.3	0.0	0.5	0.9	0.7		1.5
	$U_i$	0.5	$U_{i,m}$	0.8	2.7	0.6	3.6	1.3	1.0	1.0	1.4	1.1	0.6	0.6	2.8	0.6		1.2
VNIIOFI	$D_i$	-1.0	$D_{i,m}$	0.3	-1.1	-0.7	-1.9	-2.5	-1.0	-2.3	-1.1	-1.1	-1.5	-1.0	-0.6	-0.8	-1.5	
	$U_i$	1.0	$U_{i,m}$	1.2	2.8	1.1	3.8	1.6	1.3	1.4	1.7	1.4	1.1	1.1	3.0	1.1	1.2	

Table A3. 1000 nm Unilateral and Bilateral Degrees of Equivalence (unit: %)

Lab <i>i</i>	Unilateral DoE		Lab <i>m</i>	BNM	CSIR	CSIRO	HUT	IFA	KRISS	NIM	NIST	NMi-VSL	NPL	NRC	OMH	PTB	SMU	VNIOFI
BNM	$D_i$	-1.1	$D_{i,m}$		-1.2	-0.7	-1.0	-2.4	-1.4	-2.4	-0.9	-1.6	-1.2	-1.2	-0.9	-1.2	-1.5	-0.3
	$U_i$	0.5	$U_{i,m}$		2.7	0.7	3.5	1.3	1.0	1.1	1.1	1.1	0.7	0.6	2.8	0.6	0.7	1.2
CSIR	$D_i$	0.1	$D_{i,m}$	1.2		0.5	0.2	-1.2	-0.2	-1.2	0.3	-0.4	0.0	0.0	0.3	0.0	-0.3	0.9
	$U_i$	2.6	$U_{i,m}$	2.7		2.6	4.3	2.9	2.7	2.8	2.8	2.8	2.6	2.6	3.8	2.6	2.6	2.8
CSIRO	$D_i$	-0.4	$D_{i,m}$	0.7	-0.5		-0.3	-1.7	-0.7	-1.7	-0.2	-0.9	-0.6	-0.5	-0.3	-0.5	-0.8	0.4
	$U_i$	0.3	$U_{i,m}$	0.7	2.6		3.5	1.2	0.9	1.0	1.0	1.0	0.5	0.4	2.8	0.4	0.5	1.1
HUT	$D_i$	-0.1	$D_{i,m}$	1.0	-0.2	0.3		-1.4	-0.4	-1.4	0.1	-0.6	-0.2	-0.2	0.1	-0.2	-0.5	0.7
	$U_i$	3.5	$U_{i,m}$	3.5	4.3	3.5		3.7	3.6	3.6	3.6	3.6	3.5	3.5	4.4	3.5	3.5	3.6
IFA	$D_i$	1.3	$D_{i,m}$	2.4	1.2	1.7	1.4		1.0	-0.1	1.4	0.8	1.1	1.2	1.4	1.2	0.9	2.1
	$U_i$	1.2	$U_{i,m}$	1.3	2.9	1.2	3.7		1.4	1.5	1.5	1.5	1.2	1.2	3.0	1.2	1.3	1.6
KRISS	$D_i$	0.3	$D_{i,m}$	1.4	0.2	0.7	0.4	-1.0		-1.0	0.5	-0.2	0.2	0.2	0.5	0.2	-0.1	1.1
	$U_i$	0.8	$U_{i,m}$	1.0	2.7	0.9	3.6	1.4		1.2	1.2	1.2	0.9	0.8	2.9	0.9	0.9	1.3
NIM	$D_i$	1.3	$D_{i,m}$	2.4	1.2	1.7	1.4	0.1	1.0		1.5	0.8	1.2	1.2	1.5	1.2	0.9	2.1
	$U_i$	0.9	$U_{i,m}$	1.1	2.8	1.0	3.6	1.5	1.2		1.3	1.3	1.0	0.9	2.9	0.9	1.0	1.4
NIST	$D_i$	-0.2	$D_{i,m}$	0.9	-0.3	0.2	-0.1	-1.4	-0.5	-1.5		-0.7	-0.3	-0.3	0.0	-0.3	-0.6	0.6
	$U_i$	0.9	$U_{i,m}$	1.1	2.8	1.0	3.6	1.5	1.2	1.3		1.3	1.0	1.0	2.9	1.0	1.0	1.4
NMi-VSL	$D_i$	0.5	$D_{i,m}$	1.6	0.4	0.9	0.6	-0.8	0.2	-0.8	0.7		0.4	0.4	0.7	0.4	0.1	1.3
	$U_i$	0.9	$U_{i,m}$	1.1	2.8	1.0	3.6	1.5	1.2	1.3	1.3		1.0	0.9	2.9	1.0	1.0	1.4
NPL	$D_i$	0.1	$D_{i,m}$	1.2	0.0	0.6	0.2	-1.1	-0.2	-1.2	0.3	-0.4		0.0	0.3	0.0	-0.2	0.9
	$U_i$	0.3	$U_{i,m}$	0.7	2.6	0.5	3.5	1.2	0.9	1.0	1.0	1.0		0.4	2.8	0.5	0.5	1.1
NRC	$D_i$	0.1	$D_{i,m}$	1.2	0.0	0.5	0.2	-1.2	-0.2	-1.2	0.3	-0.4	0.0		0.3	0.0	-0.3	0.9
	$U_i$	0.2	$U_{i,m}$	0.6	2.6	0.4	3.5	1.2	0.8	0.9	1.0	0.9	0.4		2.8	0.3	0.5	1.1
OMH	$D_i$	-0.2	$D_{i,m}$	0.9	-0.3	0.3	-0.1	-1.4	-0.5	-1.5	0.0	-0.7	-0.3	-0.3		-0.3	-0.5	0.6
	$U_i$	2.8	$U_{i,m}$	2.8	3.8	2.8	4.4	3.0	2.9	2.9	2.9	2.9	2.8	2.8		2.8	2.8	3.0
PTB	$D_i$	0.1	$D_{i,m}$	1.2	0.0	0.5	0.2	-1.2	-0.2	-1.2	0.3	-0.4	0.0	0.0	0.3		-0.3	0.9
	$U_i$	0.3	$U_{i,m}$	0.6	2.6	0.4	3.5	1.2	0.9	0.9	1.0	1.0	0.5	0.3	2.8		0.5	1.1
SMU	$D_i$	0.4	$D_{i,m}$	1.5	0.3	0.8	0.5	-0.9	0.1	-0.9	0.6	-0.1	0.2	0.3	0.5	0.3		1.2
	$U_i$	0.4	$U_{i,m}$	0.7	2.6	0.5	3.5	1.3	0.9	1.0	1.0	1.0	0.5	0.5	2.8	0.5		1.2
VNIOFI	$D_i$	-0.8	$D_{i,m}$	0.3	-0.9	-0.4	-0.7	-2.1	-1.1	-2.1	-0.6	-1.3	-0.9	-0.9	-0.6	-0.9	-1.2	
	$U_i$	1.1	$U_{i,m}$	1.2	2.8	1.1	3.6	1.6	1.3	1.4	1.4	1.4	1.1	1.1	3.0	1.1	1.2	

Table A4. 1050 nm Unilateral and Bilateral Degrees of Equivalence (unit: %)

Lab <i>i</i>	Unilateral DoE		Lab <i>m</i>	BNM	CSIR	CSIRO	HUT	IFA	KRISS	NIM	NIST	NMi-VSL	NPL	NRC	OMH	PTB	SMU	VNIOFI
BNM	$D_i$	-1.1	$D_{i,m}$		-1.3	-0.7	-1.6	-2.5	-1.1	-1.9	-1.3	-1.4	-1.2	-1.1	-1.6	-1.1	-1.3	-0.2
	$U_i$	0.5	$U_{i,m}$		2.3	0.7	3.6	1.3	1.2	1.0	1.0	1.0	0.7	0.6	3.6	0.6	0.7	1.4
CSIR	$D_i$	0.2	$D_{i,m}$	1.3		0.6	-0.3	-1.2	0.2	-0.6	0.0	-0.1	0.1	0.2	-0.3	0.2	0.0	1.1
	$U_i$	2.2	$U_{i,m}$	2.3		2.2	4.2	2.5	2.4	2.4	2.4	2.3	2.2	2.2	4.2	2.2	2.2	2.6
CSIRO	$D_i$	-0.3	$D_{i,m}$	0.7	-0.6		-0.8	-1.8	-0.3	-1.1	-0.5	-0.6	-0.5	-0.4	-0.9	-0.4	-0.5	0.6
	$U_i$	0.3	$U_{i,m}$	0.7	2.2		3.6	1.3	1.1	0.9	1.0	0.9	0.5	0.4	3.6	0.5	0.5	1.3
HUT	$D_i$	0.5	$D_{i,m}$	1.6	0.3	0.8		-1.0	0.5	-0.3	0.3	0.2	0.4	0.5	0.0	0.4	0.3	1.4
	$U_i$	3.5	$U_{i,m}$	3.6	4.2	3.6		3.7	3.7	3.6	3.6	3.6	3.5	3.5	5.0	3.5	3.6	3.8
IFA	$D_i$	1.5	$D_{i,m}$	2.5	1.2	1.8	1.0		1.5	0.7	1.3	1.2	1.3	1.4	0.9	1.4	1.3	2.3
	$U_i$	1.2	$U_{i,m}$	1.3	2.5	1.3	3.7		1.6	1.5	1.5	1.4	1.2	1.2	3.7	1.2	1.3	1.8
KRISS	$D_i$	0.0	$D_{i,m}$	1.1	-0.2	0.3	-0.5	-1.5		-0.8	-0.2	-0.3	-0.1	-0.1	-0.6	-0.1	-0.2	0.9
	$U_i$	1.0	$U_{i,m}$	1.2	2.4	1.1	3.7	1.6		1.3	1.3	1.3	1.1	1.0	3.7	1.0	1.1	1.6
NIM	$D_i$	0.8	$D_{i,m}$	1.9	0.6	1.1	0.3	-0.7	0.8		0.6	0.5	0.7	0.7	0.2	0.7	0.6	1.7
	$U_i$	0.8	$U_{i,m}$	1.0	2.4	0.9	3.6	1.5	1.3		1.2	1.2	0.9	0.9	3.6	0.9	0.9	1.5
NIST	$D_i$	0.2	$D_{i,m}$	1.3	0.0	0.5	-0.3	-1.3	0.2	-0.6		-0.1	0.1	0.1	-0.3	0.1	0.0	1.1
	$U_i$	0.9	$U_{i,m}$	1.0	2.4	1.0	3.6	1.5	1.3	1.2		1.2	0.9	0.9	3.6	0.9	1.0	1.6
NMi-VSL	$D_i$	0.3	$D_{i,m}$	1.4	0.1	0.6	-0.2	-1.2	0.3	-0.5	0.1		0.2	0.2	-0.3	0.2	0.1	1.2
	$U_i$	0.8	$U_{i,m}$	1.0	2.3	0.9	3.6	1.4	1.3	1.2	1.2		0.9	0.8	3.6	0.8	0.9	1.5
NPL	$D_i$	0.1	$D_{i,m}$	1.2	-0.1	0.5	-0.4	-1.3	0.1	-0.7	-0.1	-0.2		0.1	-0.4	0.1	-0.1	1.0
	$U_i$	0.3	$U_{i,m}$	0.7	2.2	0.5	3.5	1.2	1.1	0.9	0.9	0.9		0.4	3.6	0.4	0.5	1.3
NRC	$D_i$	0.1	$D_{i,m}$	1.1	-0.2	0.4	-0.5	-1.4	0.1	-0.7	-0.1	-0.2	-0.1		-0.5	0.0	-0.1	0.9
	$U_i$	0.2	$U_{i,m}$	0.6	2.2	0.4	3.5	1.2	1.0	0.9	0.9	0.8	0.4		3.5	0.3	0.4	1.3
OMH	$D_i$	0.6	$D_{i,m}$	1.6	0.3	0.9	0.0	-0.9	0.6	-0.2	0.3	0.3	0.4	0.5		0.5	0.4	1.4
	$U_i$	3.5	$U_{i,m}$	3.6	4.2	3.6	5.0	3.7	3.7	3.6	3.6	3.6	3.6	3.5		3.6	3.6	3.8
PTB	$D_i$	0.1	$D_{i,m}$	1.1	-0.2	0.4	-0.4	-1.4	0.1	-0.7	-0.1	-0.2	-0.1	0.0	-0.5		-0.1	0.9
	$U_i$	0.3	$U_{i,m}$	0.6	2.2	0.5	3.5	1.2	1.0	0.9	0.9	0.8	0.4	0.3	3.6		0.5	1.3
SMU	$D_i$	0.2	$D_{i,m}$	1.3	0.0	0.5	-0.3	-1.3	0.2	-0.6	0.0	-0.1	0.1	0.1	-0.4	0.1		1.1
	$U_i$	0.4	$U_{i,m}$	0.7	2.2	0.5	3.6	1.3	1.1	0.9	1.0	0.9	0.5	0.4	3.6	0.5		1.4
VNIOFI	$D_i$	-0.9	$D_{i,m}$	0.2	-1.1	-0.6	-1.4	-2.3	-0.9	-1.7	-1.1	-1.2	-1.0	-0.9	-1.4	-0.9	-1.1	
	$U_i$	1.3	$U_{i,m}$	1.4	2.6	1.3	3.8	1.8	1.6	1.5	1.6	1.5	1.3	1.3	3.8	1.3	1.4	

Table A5. 1100 nm Unilateral and Bilateral Degrees of Equivalence (unit: %)

Lab <i>i</i>	Unilateral DoE		Lab <i>m</i>	BNM	CSIR	CSIRO	HUT	IFA	KRISS	NIM	NIST	NMi-VSL	NPL	NRC	OMH	PTB	SMU	VNIOFI
BNM	$D_i$	-1.0	$D_{i,m}$		-0.9	-0.7	-0.9	-2.6	-1.1	-1.3	-1.0	-1.3	-1.2	-1.0	-1.8	-1.1	-1.2	0.2
	$U_i$	0.5	$U_{i,m}$		2.3	0.6	3.5	1.3	1.1	1.1	0.7	0.8	0.6	0.6	3.4	0.6	0.7	1.3
CSIR	$D_i$	-0.1	$D_{i,m}$	0.9		0.2	0.0	-1.6	-0.2	-0.4	-0.1	-0.3	-0.3	-0.1	-0.9	-0.2	-0.3	1.1
	$U_i$	2.2	$U_{i,m}$	2.3		2.2	4.1	2.5	2.4	2.4	2.3	2.3	2.2	2.2	4.0	2.2	2.2	2.5
CSIRO	$D_i$	-0.3	$D_{i,m}$	0.7	-0.2		-0.2	-1.8	-0.3	-0.5	-0.3	-0.5	-0.5	-0.2	-1.1	-0.4	-0.5	1.0
	$U_i$	0.3	$U_{i,m}$	0.6	2.2		3.5	1.2	1.1	1.0	0.6	0.7	0.5	0.4	3.4	0.4	0.5	1.2
HUT	$D_i$	-0.1	$D_{i,m}$	0.9	0.0	0.2		-1.6	-0.1	-0.3	-0.1	-0.3	-0.3	0.0	-0.9	-0.2	-0.3	1.2
	$U_i$	3.5	$U_{i,m}$	3.5	4.1	3.5		3.7	3.6	3.6	3.5	3.5	3.5	3.5	4.8	3.5	3.5	3.6
IFA	$D_i$	1.5	$D_{i,m}$	2.6	1.6	1.8	1.6		1.5	1.3	1.5	1.3	1.3	1.6	0.7	1.4	1.3	2.8
	$U_i$	1.2	$U_{i,m}$	1.3	2.5	1.2	3.7		1.6	1.5	1.3	1.3	1.2	1.2	3.5	1.2	1.2	1.6
KRISS	$D_i$	0.1	$D_{i,m}$	1.1	0.2	0.3	0.1	-1.5		-0.2	0.1	-0.2	-0.1	0.1	-0.7	-0.1	-0.1	1.3
	$U_i$	1.0	$U_{i,m}$	1.1	2.4	1.1	3.6	1.6		1.4	1.1	1.2	1.1	1.0	3.5	1.0	1.1	1.5
NIM	$D_i$	0.3	$D_{i,m}$	1.3	0.4	0.5	0.3	-1.3	0.2		0.2	0.0	0.1	0.3	-0.5	0.1	0.1	1.5
	$U_i$	0.9	$U_{i,m}$	1.1	2.4	1.0	3.6	1.5	1.4		1.0	1.1	1.0	0.9	3.5	0.9	1.0	1.4
NIST	$D_i$	0.0	$D_{i,m}$	1.0	0.1	0.3	0.1	-1.5	-0.1	-0.2		-0.2	-0.2	0.0	-0.8	-0.1	-0.2	1.2
	$U_i$	0.5	$U_{i,m}$	0.7	2.3	0.6	3.5	1.3	1.1	1.0		0.8	0.6	0.5	3.4	0.6	0.6	1.2
NMi-VSL	$D_i$	0.3	$D_{i,m}$	1.3	0.3	0.5	0.3	-1.3	0.2	0.0	0.2		0.0	0.3	-0.5	0.1	0.1	1.5
	$U_i$	0.6	$U_{i,m}$	0.8	2.3	0.7	3.5	1.3	1.2	1.1	0.8		0.7	0.7	3.4	0.7	0.7	1.3
NPL	$D_i$	0.2	$D_{i,m}$	1.2	0.3	0.5	0.3	-1.3	0.1	-0.1	0.2	0.0		0.2	-0.6	0.1	0.0	1.4
	$U_i$	0.3	$U_{i,m}$	0.6	2.2	0.5	3.5	1.2	1.1	1.0	0.6	0.7		0.4	3.4	0.4	0.5	1.2
NRC	$D_i$	0.0	$D_{i,m}$	1.0	0.1	0.2	0.0	-1.6	-0.1	-0.3	0.0	-0.3	-0.2		-0.8	-0.2	-0.2	1.2
	$U_i$	0.2	$U_{i,m}$	0.6	2.2	0.4	3.5	1.2	1.0	0.9	0.5	0.7	0.4		3.3	0.3	0.4	1.1
OMH	$D_i$	0.8	$D_{i,m}$	1.8	0.9	1.1	0.9	-0.7	0.7	0.5	0.8	0.5	0.6	0.8		0.7	0.6	2.0
	$U_i$	3.3	$U_{i,m}$	3.4	4.0	3.4	4.8	3.5	3.5	3.5	3.4	3.4	3.4	3.3		3.4	3.4	3.5
PTB	$D_i$	0.1	$D_{i,m}$	1.1	0.2	0.4	0.2	-1.4	0.1	-0.1	0.1	-0.1	-0.1	0.2	-0.7		-0.1	1.4
	$U_i$	0.3	$U_{i,m}$	0.6	2.2	0.4	3.5	1.2	1.0	0.9	0.6	0.7	0.4	0.3	3.4		0.5	1.2
SMU	$D_i$	0.2	$D_{i,m}$	1.2	0.3	0.5	0.3	-1.3	0.1	-0.1	0.2	-0.1	0.0	0.2	-0.6	0.1		1.4
	$U_i$	0.4	$U_{i,m}$	0.7	2.2	0.5	3.5	1.2	1.1	1.0	0.6	0.7	0.5	0.4	3.4	0.5		1.2
VNIOFI	$D_i$	-1.2	$D_{i,m}$	-0.2	-1.1	-1.0	-1.2	-2.8	-1.3	-1.5	-1.2	-1.5	-1.4	-1.2	-2.0	-1.4	-1.4	
	$U_i$	1.1	$U_{i,m}$	1.3	2.5	1.2	3.6	1.6	1.5	1.4	1.2	1.3	1.2	1.1	3.5	1.2	1.2	

Table A6. 1150 nm Unilateral and Bilateral Degrees of Equivalence (unit: %)

Lab <i>i</i>	Unilateral DoE		Lab <i>m</i>	BNM	CSIR	CSIRO	HUT	IFA	KRISS	NIM	NIST	NMi-VSL	NPL	NRC	OMH	PTB	SMU	VNIOFI
BNM	$D_i$	-1.0	$D_{i,m}$		-1.2	-0.8	-1.2	-2.4	-1.1	-0.9	-1.1	-1.1	-1.1	-0.9	-1.6	-1.1	-1.2	0.6
	$U_i$	0.5	$U_{i,m}$		2.3	0.6	3.5	1.3	1.1	1.0	1.0	0.8	0.6	0.6	3.6	0.6	0.7	1.2
CSIR	$D_i$	0.3	$D_{i,m}$	1.2		0.4	0.0	-1.1	0.1	0.3	0.2	0.1	0.1	0.3	-0.4	0.1	0.1	1.8
	$U_i$	2.2	$U_{i,m}$	2.3		2.2	4.1	2.5	2.4	2.3	2.4	2.3	2.2	2.2	4.1	2.2	2.2	2.5
CSIRO	$D_i$	-0.1	$D_{i,m}$	0.8	-0.4		-0.4	-1.5	-0.3	-0.1	-0.2	-0.3	-0.3	-0.1	-0.8	-0.3	-0.3	1.4
	$U_i$	0.3	$U_{i,m}$	0.6	2.2		3.5	1.2	1.0	0.9	0.9	0.6	0.4	0.3	3.5	0.4	0.5	1.2
HUT	$D_i$	0.2	$D_{i,m}$	1.2	0.0	0.4		-1.2	0.1	0.3	0.1	0.0	0.0	0.2	-0.4	0.0	0.0	1.7
	$U_i$	3.5	$U_{i,m}$	3.5	4.1	3.5		3.7	3.6	3.6	3.6	3.5	3.5	3.5	4.9	3.5	3.5	3.6
IFA	$D_i$	1.4	$D_{i,m}$	2.4	1.1	1.5	1.2		1.3	1.4	1.3	1.2	1.2	1.4	0.8	1.2	1.2	2.9
	$U_i$	1.2	$U_{i,m}$	1.3	2.5	1.2	3.7		1.5	1.4	1.4	1.3	1.2	1.2	3.7	1.2	1.2	1.6
KRISS	$D_i$	0.1	$D_{i,m}$	1.1	-0.1	0.3	-0.1	-1.3		0.2	0.0	-0.1	0.0	0.1	-0.5	-0.1	-0.1	1.6
	$U_i$	1.0	$U_{i,m}$	1.1	2.4	1.0	3.6	1.5		1.3	1.3	1.1	1.1	1.0	3.7	1.0	1.1	1.5
NIM	$D_i$	0.0	$D_{i,m}$	0.9	-0.3	0.1	-0.3	-1.4	-0.2		-0.1	-0.2	-0.2	0.0	-0.7	-0.2	-0.2	1.5
	$U_i$	0.8	$U_{i,m}$	1.0	2.3	0.9	3.6	1.4	1.3		1.2	1.0	0.9	0.8	3.6	0.9	0.9	1.4
NIST	$D_i$	0.1	$D_{i,m}$	1.1	-0.2	0.2	-0.1	-1.3	0.0	0.1		-0.1	-0.1	0.1	-0.6	-0.1	-0.1	1.6
	$U_i$	0.8	$U_{i,m}$	1.0	2.4	0.9	3.6	1.4	1.3	1.2		1.0	0.9	0.8	3.6	0.9	0.9	1.4
NMi-VSL	$D_i$	0.2	$D_{i,m}$	1.1	-0.1	0.3	0.0	-1.2	0.1	0.2	0.1		0.0	0.2	-0.5	0.0	0.0	1.7
	$U_i$	0.5	$U_{i,m}$	0.8	2.3	0.6	3.5	1.3	1.1	1.0	1.0		0.6	0.6	3.6	0.6	0.7	1.2
NPL	$D_i$	0.2	$D_{i,m}$	1.1	-0.1	0.3	0.0	-1.2	0.0	0.2	0.1	0.0		0.2	-0.5	0.0	0.0	1.7
	$U_i$	0.3	$U_{i,m}$	0.6	2.2	0.4	3.5	1.2	1.1	0.9	0.9	0.6		0.4	3.5	0.4	0.5	1.2
NRC	$D_i$	0.0	$D_{i,m}$	0.9	-0.3	0.1	-0.2	-1.4	-0.1	0.0	-0.1	-0.2	-0.2		-0.7	-0.2	-0.2	1.5
	$U_i$	0.2	$U_{i,m}$	0.6	2.2	0.3	3.5	1.2	1.0	0.8	0.8	0.6	0.4		3.5	0.3	0.4	1.1
OMH	$D_i$	0.7	$D_{i,m}$	1.6	0.4	0.8	0.4	-0.8	0.5	0.7	0.6	0.5	0.5	0.7		0.5	0.5	2.2
	$U_i$	3.5	$U_{i,m}$	3.6	4.1	3.5	4.9	3.7	3.7	3.6	3.6	3.6	3.5	3.5		3.5	3.5	3.7
PTB	$D_i$	0.2	$D_{i,m}$	1.1	-0.1	0.3	0.0	-1.2	0.1	0.2	0.1	0.0	0.0	0.2	-0.5		0.0	1.7
	$U_i$	0.2	$U_{i,m}$	0.6	2.2	0.4	3.5	1.2	1.0	0.9	0.9	0.6	0.4	0.3	3.5		0.5	1.1
SMU	$D_i$	0.2	$D_{i,m}$	1.2	-0.1	0.3	0.0	-1.2	0.1	0.2	0.1	0.0	0.0	0.2	-0.5	0.0		1.7
	$U_i$	0.4	$U_{i,m}$	0.7	2.2	0.5	3.5	1.2	1.1	0.9	0.9	0.7	0.5	0.4	3.5	0.5		1.2
VNIOFI	$D_i$	-1.5	$D_{i,m}$	-0.6	-1.8	-1.4	-1.7	-2.9	-1.6	-1.5	-1.6	-1.7	-1.7	-1.5	-2.2	-1.7	-1.7	
	$U_i$	1.1	$U_{i,m}$	1.2	2.5	1.2	3.6	1.6	1.5	1.4	1.4	1.2	1.2	1.1	3.7	1.1	1.2	

Table A7. 1200 nm Unilateral and Bilateral Degrees of Equivalence (unit: %)

Lab <i>i</i>	Unilateral DoE		Lab <i>m</i>	BNM	CSIR	CSIRO	HUT	IFA	KRISS	NIM	NIST	NMi-VSL	NPL	NRC	OMH	PTB	SMU	VNIOFI
BNM	$D_i$	-0.7	$D_{i,m}$		-0.7	-0.4	-1.1	-2.3	-0.8	-0.4	-0.6	-0.8	-1.0	-0.6	-1.4	-0.9	-0.8	1.2
	$U_i$	0.5	$U_{i,m}$		2.3	0.6	3.5	1.3	1.2	1.1	1.6	0.8	0.7	0.6	3.5	0.6	0.7	1.2
CSIR	$D_i$	0.0	$D_{i,m}$	0.7		0.3	-0.4	-1.6	-0.1	0.3	0.0	-0.1	-0.3	0.1	-0.7	-0.2	-0.2	1.9
	$U_i$	2.2	$U_{i,m}$	2.3		2.2	4.1	2.5	2.4	2.4	2.7	2.3	2.2	2.2	4.1	2.2	2.2	2.5
CSIRO	$D_i$	-0.3	$D_{i,m}$	0.4	-0.3		-0.7	-1.9	-0.4	0.0	-0.2	-0.4	-0.6	-0.2	-1.0	-0.5	-0.4	1.6
	$U_i$	0.2	$U_{i,m}$	0.6	2.2		3.5	1.2	1.0	0.9	1.5	0.6	0.5	0.3	3.5	0.4	0.5	1.1
HUT	$D_i$	0.4	$D_{i,m}$	1.1	0.4	0.7		-1.3	0.3	0.7	0.4	0.3	0.1	0.5	-0.3	0.2	0.2	2.3
	$U_i$	3.5	$U_{i,m}$	3.5	4.1	3.5		3.7	3.6	3.6	3.8	3.5	3.5	3.5	4.9	3.5	3.5	3.6
IFA	$D_i$	1.6	$D_{i,m}$	2.3	1.6	1.9	1.3		1.5	1.9	1.7	1.5	1.3	1.7	0.9	1.4	1.5	3.5
	$U_i$	1.2	$U_{i,m}$	1.3	2.5	1.2	3.7		1.6	1.5	1.9	1.3	1.2	1.2	3.6	1.2	1.3	1.6
KRISS	$D_i$	0.1	$D_{i,m}$	0.8	0.1	0.4	-0.3	-1.5		0.4	0.1	0.0	-0.2	0.2	-0.6	-0.1	-0.1	2.0
	$U_i$	1.0	$U_{i,m}$	1.2	2.4	1.0	3.6	1.6		1.3	1.8	1.1	1.1	1.0	3.6	1.0	1.1	1.5
NIM	$D_i$	-0.3	$D_{i,m}$	0.4	-0.3	0.0	-0.7	-1.9	-0.4		-0.2	-0.4	-0.6	-0.2	-1.0	-0.5	-0.5	1.6
	$U_i$	0.9	$U_{i,m}$	1.1	2.4	0.9	3.6	1.5	1.3		1.8	1.0	1.0	0.9	3.6	0.9	1.0	1.4
NIST	$D_i$	0.0	$D_{i,m}$	0.6	0.0	0.2	-0.4	-1.7	-0.1	0.2		-0.2	-0.3	0.1	-0.7	-0.3	-0.2	1.8
	$U_i$	1.5	$U_{i,m}$	1.6	2.7	1.5	3.8	1.9	1.8	1.8		1.6	1.6	1.5	3.8	1.5	1.6	1.9
NMi-VSL	$D_i$	0.1	$D_{i,m}$	0.8	0.1	0.4	-0.3	-1.5	0.0	0.4	0.2		-0.2	0.2	-0.6	-0.1	0.0	2.0
	$U_i$	0.5	$U_{i,m}$	0.8	2.3	0.6	3.5	1.3	1.1	1.0	1.6		0.6	0.5	3.5	0.6	0.6	1.2
NPL	$D_i$	0.3	$D_{i,m}$	1.0	0.3	0.6	-0.1	-1.3	0.2	0.6	0.3	0.2		0.4	-0.4	0.1	0.1	2.2
	$U_i$	0.3	$U_{i,m}$	0.7	2.2	0.5	3.5	1.2	1.1	1.0	1.6	0.6		0.4	3.5	0.5	0.5	1.1
NRC	$D_i$	-0.1	$D_{i,m}$	0.6	-0.1	0.2	-0.5	-1.7	-0.2	0.2	-0.1	-0.2	-0.4		-0.8	-0.3	-0.3	1.8
	$U_i$	0.2	$U_{i,m}$	0.6	2.2	0.3	3.5	1.2	1.0	0.9	1.5	0.5	0.4		3.4	0.3	0.4	1.1
OMH	$D_i$	0.7	$D_{i,m}$	1.4	0.7	1.0	0.3	-0.9	0.6	1.0	0.7	0.6	0.4	0.8		0.5	0.5	2.6
	$U_i$	3.4	$U_{i,m}$	3.5	4.1	3.5	4.9	3.6	3.6	3.6	3.8	3.5	3.5	3.4		3.5	3.5	3.6
PTB	$D_i$	0.2	$D_{i,m}$	0.9	0.2	0.5	-0.2	-1.4	0.1	0.5	0.3	0.1	-0.1	0.3	-0.5		0.0	2.1
	$U_i$	0.2	$U_{i,m}$	0.6	2.2	0.4	3.5	1.2	1.0	0.9	1.5	0.6	0.5	0.3	3.5		0.5	1.1
SMU	$D_i$	0.2	$D_{i,m}$	0.8	0.2	0.4	-0.2	-1.5	0.1	0.5	0.2	0.0	-0.1	0.3	-0.5	0.0		2.0
	$U_i$	0.4	$U_{i,m}$	0.7	2.2	0.5	3.5	1.3	1.1	1.0	1.6	0.6	0.5	0.4	3.5	0.5		1.2
VNIOFI	$D_i$	-1.9	$D_{i,m}$	-1.2	-1.9	-1.6	-2.3	-3.5	-2.0	-1.6	-1.8	-2.0	-2.2	-1.8	-2.6	-2.1	-2.0	
	$U_i$	1.1	$U_{i,m}$	1.2	2.5	1.1	3.6	1.6	1.5	1.4	1.9	1.2	1.1	1.1	3.6	1.1	1.2	

Table A8. 1250 nm Unilateral and Bilateral Degrees of Equivalence (unit: %)

Lab <i>i</i>	Unilateral DoE		Lab <i>m</i>	BNM	CSIR	CSIRO	HUT	IFA	KRISS	NIM	NIST	NMi-VSL	NPL	NRC	OMH	PTB	SMU	VNIOFI
BNM	$D_i$	-0.8	$D_{i,m}$		-0.9	-0.4	-0.8	-2.3	-0.8	-0.4	-0.9	-1.0	-1.0	-0.8	-1.1	-1.0	-0.9	1.2
	$U_i$	0.5	$U_{i,m}$		2.1	0.6	3.5	1.3	1.1	1.0	1.1	0.7	0.6	0.6	3.4	0.6	0.7	1.2
CSIR	$D_i$	0.1	$D_{i,m}$	0.9		0.5	0.1	-1.4	0.1	0.5	0.0	-0.1	-0.1	0.1	-0.2	-0.1	0.0	2.1
	$U_i$	2.0	$U_{i,m}$	2.1		2.0	4.0	2.3	2.2	2.2	2.2	2.0	2.0	2.0	3.9	2.0	2.0	2.3
CSIRO	$D_i$	-0.4	$D_{i,m}$	0.4	-0.5		-0.4	-1.9	-0.4	0.0	-0.5	-0.6	-0.6	-0.4	-0.7	-0.7	-0.6	1.6
	$U_i$	0.2	$U_{i,m}$	0.6	2.0		3.5	1.2	1.0	0.9	0.9	0.5	0.4	0.2	3.4	0.3	0.4	1.1
HUT	$D_i$	0.0	$D_{i,m}$	0.8	-0.1	0.4		-1.5	0.0	0.4	-0.1	-0.2	-0.2	0.0	-0.3	-0.2	-0.1	2.0
	$U_i$	3.5	$U_{i,m}$	3.5	4.0	3.5		3.7	3.6	3.6	3.6	3.5	3.5	3.5	4.8	3.5	3.5	3.6
IFA	$D_i$	1.5	$D_{i,m}$	2.3	1.4	1.9	1.5		1.5	1.9	1.4	1.3	1.3	1.5	1.3	1.3	1.4	3.5
	$U_i$	1.2	$U_{i,m}$	1.3	2.3	1.2	3.7		1.6	1.5	1.5	1.3	1.2	1.2	3.6	1.2	1.3	1.6
KRISS	$D_i$	0.0	$D_{i,m}$	0.8	-0.1	0.4	0.0	-1.5		0.4	-0.1	-0.2	-0.2	0.0	-0.3	-0.2	-0.1	2.0
	$U_i$	1.0	$U_{i,m}$	1.1	2.2	1.0	3.6	1.6		1.3	1.4	1.1	1.1	1.0	3.5	1.0	1.1	1.5
NIM	$D_i$	-0.4	$D_{i,m}$	0.4	-0.5	0.0	-0.4	-1.9	-0.4		-0.5	-0.6	-0.6	-0.4	-0.6	-0.6	-0.5	1.6
	$U_i$	0.8	$U_{i,m}$	1.0	2.2	0.9	3.6	1.5	1.3		1.2	0.9	0.9	0.8	3.5	0.9	0.9	1.4
NIST	$D_i$	0.1	$D_{i,m}$	0.9	0.0	0.5	0.1	-1.4	0.1	0.5		-0.1	-0.1	0.1	-0.2	-0.2	-0.1	2.1
	$U_i$	0.9	$U_{i,m}$	1.1	2.2	0.9	3.6	1.5	1.4	1.2		1.0	1.0	0.9	3.5	1.0	1.0	1.4
NMi-VSL	$D_i$	0.2	$D_{i,m}$	1.0	0.1	0.6	0.2	-1.3	0.2	0.6	0.1		0.0	0.2	-0.1	-0.1	0.0	2.2
	$U_i$	0.4	$U_{i,m}$	0.7	2.0	0.5	3.5	1.3	1.1	0.9	1.0		0.5	0.5	3.4	0.5	0.6	1.2
NPL	$D_i$	0.2	$D_{i,m}$	1.0	0.1	0.6	0.2	-1.3	0.2	0.6	0.1	0.0		0.2	0.0	0.0	0.1	2.2
	$U_i$	0.3	$U_{i,m}$	0.6	2.0	0.4	3.5	1.2	1.1	0.9	1.0	0.5		0.3	3.4	0.4	0.5	1.1
NRC	$D_i$	0.0	$D_{i,m}$	0.8	-0.1	0.4	0.0	-1.5	0.0	0.4	-0.1	-0.2	-0.2		-0.3	-0.2	-0.1	2.0
	$U_i$	0.2	$U_{i,m}$	0.6	2.0	0.2	3.5	1.2	1.0	0.8	0.9	0.5	0.3		3.4	0.3	0.4	1.1
OMH	$D_i$	0.3	$D_{i,m}$	1.1	0.2	0.7	0.3	-1.3	0.3	0.6	0.2	0.1	0.0	0.3		0.0	0.1	2.3
	$U_i$	3.4	$U_{i,m}$	3.4	3.9	3.4	4.8	3.6	3.5	3.5	3.5	3.4	3.4	3.4		3.4	3.4	3.5
PTB	$D_i$	0.3	$D_{i,m}$	1.0	0.1	0.7	0.2	-1.3	0.2	0.6	0.2	0.1	0.0	0.2	0.0		0.1	2.2
	$U_i$	0.2	$U_{i,m}$	0.6	2.0	0.3	3.5	1.2	1.0	0.9	1.0	0.5	0.4	0.3	3.4		0.5	1.1
SMU	$D_i$	0.2	$D_{i,m}$	0.9	0.0	0.6	0.1	-1.4	0.1	0.5	0.1	0.0	-0.1	0.1	-0.1	-0.1		2.1
	$U_i$	0.4	$U_{i,m}$	0.7	2.0	0.4	3.5	1.3	1.1	0.9	1.0	0.6	0.5	0.4	3.4	0.5		1.1
VNIOFI	$D_i$	-2.0	$D_{i,m}$	-1.2	-2.1	-1.6	-2.0	-3.5	-2.0	-1.6	-2.1	-2.2	-2.2	-2.0	-2.3	-2.2	-2.1	
	$U_i$	1.1	$U_{i,m}$	1.2	2.3	1.1	3.6	1.6	1.5	1.4	1.4	1.2	1.1	1.1	3.5	1.1	1.1	

Table A9. 1300 nm Unilateral and Bilateral Degrees of Equivalence (unit: %)

Lab <i>i</i>	Unilateral DoE		Lab <i>m</i>	BNM	CSIR	CSIRO	HUT	IFA	KRISS	NIM	NIST	NMi-VSL	NPL	NRC	OMH	PTB	SMU	VNIOFI
BNM	$D_i$	-0.8	$D_{i,m}$		-1.0	-0.5	-0.8	-2.3	-1.1	-0.5	-0.9	-1.0	-1.0	-0.9	-1.4	-1.0	-1.1	1.4
	$U_i$	0.5	$U_{i,m}$		2.1	0.6	3.5	1.3	1.1	1.0	1.0	0.7	0.6	0.6	3.5	0.6	0.7	1.2
CSIR	$D_i$	0.2	$D_{i,m}$	1.0		0.5	0.2	-1.3	0.0	0.5	0.1	0.0	0.0	0.2	-0.3	0.1	0.0	2.4
	$U_i$	2.0	$U_{i,m}$	2.1		2.0	4.0	2.3	2.2	2.2	2.2	2.0	2.0	2.0	4.0	2.0	2.0	2.3
CSIRO	$D_i$	-0.3	$D_{i,m}$	0.5	-0.5		-0.4	-1.8	-0.6	0.0	-0.4	-0.5	-0.6	-0.4	-0.9	-0.5	-0.6	1.9
	$U_i$	0.2	$U_{i,m}$	0.6	2.0		3.5	1.2	1.0	0.9	0.9	0.4	0.3	0.2	3.4	0.3	0.4	1.1
HUT	$D_i$	0.0	$D_{i,m}$	0.8	-0.2	0.4		-1.4	-0.2	0.4	-0.1	-0.2	-0.2	0.0	-0.5	-0.1	-0.2	2.2
	$U_i$	3.5	$U_{i,m}$	3.5	4.0	3.5		3.7	3.6	3.6	3.6	3.5	3.5	3.5	4.9	3.5	3.5	3.6
IFA	$D_i$	1.5	$D_{i,m}$	2.3	1.3	1.8	1.4		1.2	1.8	1.4	1.3	1.2	1.4	0.9	1.3	1.2	3.7
	$U_i$	1.2	$U_{i,m}$	1.3	2.3	1.2	3.7		1.6	1.5	1.5	1.3	1.2	1.2	3.6	1.2	1.3	1.6
KRISS	$D_i$	0.2	$D_{i,m}$	1.1	0.0	0.6	0.2	-1.2		0.6	0.1	0.0	0.0	0.2	-0.3	0.1	0.0	2.4
	$U_i$	1.0	$U_{i,m}$	1.1	2.2	1.0	3.6	1.6		1.3	1.3	1.1	1.0	1.0	3.6	1.0	1.1	1.5
NIM	$D_i$	-0.3	$D_{i,m}$	0.5	-0.5	0.0	-0.4	-1.8	-0.6		-0.4	-0.5	-0.6	-0.4	-0.9	-0.5	-0.6	1.9
	$U_i$	0.8	$U_{i,m}$	1.0	2.2	0.9	3.6	1.5	1.3		1.2	0.9	0.9	0.9	3.5	0.9	0.9	1.4
NIST	$D_i$	0.1	$D_{i,m}$	0.9	-0.1	0.4	0.1	-1.4	-0.1	0.4		-0.1	-0.1	0.1	-0.4	-0.1	-0.1	2.3
	$U_i$	0.9	$U_{i,m}$	1.0	2.2	0.9	3.6	1.5	1.3	1.2		1.0	0.9	0.9	3.5	0.9	0.9	1.4
NMi-VSL	$D_i$	0.2	$D_{i,m}$	1.0	0.0	0.5	0.2	-1.3	0.0	0.5	0.1		0.0	0.2	-0.3	0.1	0.0	2.4
	$U_i$	0.4	$U_{i,m}$	0.7	2.0	0.4	3.5	1.3	1.1	0.9	1.0		0.5	0.4	3.5	0.5	0.6	1.1
NPL	$D_i$	0.2	$D_{i,m}$	1.0	0.0	0.6	0.2	-1.2	0.0	0.6	0.1	0.0		0.2	-0.3	0.1	0.0	2.4
	$U_i$	0.3	$U_{i,m}$	0.6	2.0	0.3	3.5	1.2	1.0	0.9	0.9	0.5		0.3	3.4	0.4	0.5	1.1
NRC	$D_i$	0.0	$D_{i,m}$	0.9	-0.2	0.4	0.0	-1.4	-0.2	0.4	-0.1	-0.2	-0.2		-0.5	-0.1	-0.2	2.3
	$U_i$	0.1	$U_{i,m}$	0.6	2.0	0.2	3.5	1.2	1.0	0.9	0.9	0.4	0.3		3.4	0.3	0.4	1.1
OMH	$D_i$	0.5	$D_{i,m}$	1.4	0.3	0.9	0.5	-0.9	0.3	0.9	0.4	0.3	0.3	0.5		0.4	0.3	2.7
	$U_i$	3.4	$U_{i,m}$	3.5	4.0	3.4	4.9	3.6	3.6	3.5	3.5	3.5	3.4	3.4		3.4	3.5	3.6
PTB	$D_i$	0.1	$D_{i,m}$	1.0	-0.1	0.5	0.1	-1.3	-0.1	0.5	0.1	-0.1	-0.1	0.1	-0.4		-0.1	2.4
	$U_i$	0.2	$U_{i,m}$	0.6	2.0	0.3	3.5	1.2	1.0	0.9	0.9	0.5	0.4	0.3	3.4		0.5	1.1
SMU	$D_i$	0.2	$D_{i,m}$	1.1	0.0	0.6	0.2	-1.2	0.0	0.6	0.1	0.0	0.0	0.2	-0.3	0.1		2.5
	$U_i$	0.4	$U_{i,m}$	0.7	2.0	0.4	3.5	1.3	1.1	0.9	0.9	0.6	0.5	0.4	3.5	0.5		1.1
VNIOFI	$D_i$	-2.2	$D_{i,m}$	-1.4	-2.4	-1.9	-2.2	-3.7	-2.4	-1.9	-2.3	-2.4	-2.4	-2.3	-2.7	-2.4	-2.5	
	$U_i$	1.1	$U_{i,m}$	1.2	2.3	1.1	3.6	1.6	1.5	1.4	1.4	1.1	1.1	1.1	3.6	1.1	1.1	

Table A10. 1350 nm Unilateral and Bilateral Degrees of Equivalence (unit: %)

Lab <i>i</i>	Unilateral DoE		Lab <i>m</i>	BNM	CSIR	CSIRO	HUT	IFA	KRISS	NIM	NIST	NMi-VSL	NPL	NRC	OMH	PTB	SMU	VNIOFI
BNM	$D_i$	-0.6	$D_{i,m}$		-1.4	-0.4	-1.1	-2.1	-0.5	-0.1	-0.9	-0.7	-0.9	-0.7	-1.1	-0.8	-0.7	1.9
	$U_i$	0.5	$U_{i,m}$		2.1	0.6	3.5	1.3	1.1	1.0	1.0	0.7	0.6	0.6	3.5	0.6	0.7	1.2
CSIR	$D_i$	0.8	$D_{i,m}$	1.4		1.0	0.3	-0.6	0.9	1.3	0.5	0.7	0.5	0.8	0.3	0.6	0.7	3.3
	$U_i$	2.0	$U_{i,m}$	2.1		2.0	4.0	2.3	2.2	2.2	2.2	2.0	2.0	2.0	4.0	2.0	2.0	2.3
CSIRO	$D_i$	-0.2	$D_{i,m}$	0.4	-1.0		-0.7	-1.7	-0.1	0.2	-0.5	-0.3	-0.5	-0.3	-0.7	-0.4	-0.3	2.3
	$U_i$	0.2	$U_{i,m}$	0.6	2.0		3.5	1.2	1.0	0.8	0.9	0.5	0.4	0.3	3.4	0.3	0.5	1.1
HUT	$D_i$	0.5	$D_{i,m}$	1.1	-0.3	0.7		-1.0	0.6	0.9	0.2	0.4	0.2	0.4	0.0	0.3	0.4	3.0
	$U_i$	3.5	$U_{i,m}$	3.5	4.0	3.5		3.7	3.6	3.6	3.6	3.5	3.5	3.5	4.9	3.5	3.5	3.6
IFA	$D_i$	1.4	$D_{i,m}$	2.1	0.6	1.7	1.0		1.6	1.9	1.2	1.3	1.1	1.4	1.0	1.3	1.4	4.0
	$U_i$	1.2	$U_{i,m}$	1.3	2.3	1.2	3.7		1.5	1.4	1.5	1.2	1.2	1.2	3.6	1.2	1.2	1.6
KRISS	$D_i$	-0.1	$D_{i,m}$	0.5	-0.9	0.1	-0.6	-1.6		0.3	-0.4	-0.2	-0.4	-0.2	-0.6	-0.3	-0.2	2.4
	$U_i$	1.0	$U_{i,m}$	1.1	2.2	1.0	3.6	1.5		1.3	1.3	1.1	1.1	1.0	3.6	1.0	1.1	1.5
NIM	$D_i$	-0.5	$D_{i,m}$	0.1	-1.3	-0.2	-0.9	-1.9	-0.3		-0.7	-0.6	-0.8	-0.5	-1.0	-0.6	-0.5	2.1
	$U_i$	0.8	$U_{i,m}$	1.0	2.2	0.8	3.6	1.4	1.3		1.2	0.9	0.9	0.8	3.5	0.9	0.9	1.4
NIST	$D_i$	0.3	$D_{i,m}$	0.9	-0.5	0.5	-0.2	-1.2	0.4	0.7		0.2	0.0	0.2	-0.2	0.1	0.2	2.8
	$U_i$	0.9	$U_{i,m}$	1.0	2.2	0.9	3.6	1.5	1.3	1.2		1.0	0.9	0.9	3.6	0.9	1.0	1.4
NMi-VSL	$D_i$	0.1	$D_{i,m}$	0.7	-0.7	0.3	-0.4	-1.3	0.2	0.6	-0.2		-0.2	0.1	-0.4	0.0	0.1	2.7
	$U_i$	0.4	$U_{i,m}$	0.7	2.0	0.5	3.5	1.2	1.1	0.9	1.0		0.5	0.4	3.5	0.5	0.6	1.2
NPL	$D_i$	0.3	$D_{i,m}$	0.9	-0.5	0.5	-0.2	-1.1	0.4	0.8	0.0	0.2		0.3	-0.2	0.2	0.3	2.9
	$U_i$	0.3	$U_{i,m}$	0.6	2.0	0.4	3.5	1.2	1.1	0.9	0.9	0.5		0.4	3.5	0.4	0.5	1.1
NRC	$D_i$	0.0	$D_{i,m}$	0.7	-0.8	0.3	-0.4	-1.4	0.2	0.5	-0.2	-0.1	-0.3		-0.4	-0.1	0.0	2.6
	$U_i$	0.2	$U_{i,m}$	0.6	2.0	0.3	3.5	1.2	1.0	0.8	0.9	0.4	0.4		3.4	0.3	0.5	1.1
OMH	$D_i$	0.5	$D_{i,m}$	1.1	-0.3	0.7	0.0	-1.0	0.6	1.0	0.2	0.4	0.2	0.4		0.3	0.4	3.0
	$U_i$	3.4	$U_{i,m}$	3.5	4.0	3.4	4.9	3.6	3.6	3.5	3.6	3.5	3.5	3.4		3.5	3.5	3.6
PTB	$D_i$	0.2	$D_{i,m}$	0.8	-0.6	0.4	-0.3	-1.3	0.3	0.6	-0.1	0.0	-0.2	0.1	-0.3		0.1	2.7
	$U_i$	0.2	$U_{i,m}$	0.6	2.0	0.3	3.5	1.2	1.0	0.9	0.9	0.5	0.4	0.3	3.5		0.5	1.1
SMU	$D_i$	0.1	$D_{i,m}$	0.7	-0.7	0.3	-0.4	-1.4	0.2	0.5	-0.2	-0.1	-0.3	0.0	-0.4	-0.1		2.6
	$U_i$	0.4	$U_{i,m}$	0.7	2.0	0.5	3.5	1.2	1.1	0.9	1.0	0.6	0.5	0.5	3.5	0.5		1.2
VNIOFI	$D_i$	-2.6	$D_{i,m}$	-1.9	-3.3	-2.3	-3.0	-4.0	-2.4	-2.1	-2.8	-2.7	-2.9	-2.6	-3.0	-2.7	-2.6	
	$U_i$	1.1	$U_{i,m}$	1.2	2.3	1.1	3.6	1.6	1.5	1.4	1.4	1.2	1.1	1.1	3.6	1.1	1.2	

Table A11. 1400 nm Unilateral and Bilateral Degrees of Equivalence (unit: %)

Lab <i>i</i>	Unilateral DoE		Lab <i>m</i>	BNM	CSIR	CSIRO	HUT	IFA	KRISS	NIM	NIST	NMi-VSL	NPL	NRC	OMH	PTB	SMU	VNIOFI
BNM	$D_i$	-0.6	$D_{i,m}$		-1.6	-0.3	-0.4	-2.0	-0.5	-0.1	-1.1	-0.8	-0.8	-0.6	-1.4	-0.8	-0.7	0.6
	$U_i$	0.5	$U_{i,m}$		2.1	0.6	3.5	1.3	1.1	1.0	1.4	0.7	0.6	0.6	3.3	0.6	0.7	1.2
CSIR	$D_i$	1.0	$D_{i,m}$	1.6		1.3	1.2	-0.4	1.1	1.5	0.5	0.8	0.8	1.0	0.2	0.8	0.9	2.2
	$U_i$	2.0	$U_{i,m}$	2.1		2.0	4.0	2.3	2.2	2.2	2.4	2.0	2.0	2.0	3.8	2.0	2.1	2.3
CSIRO	$D_i$	-0.3	$D_{i,m}$	0.3	-1.3		-0.1	-1.7	-0.2	0.2	-0.7	-0.5	-0.4	-0.3	-1.1	-0.5	-0.4	0.9
	$U_i$	0.3	$U_{i,m}$	0.6	2.0		3.5	1.2	1.0	0.9	1.3	0.5	0.4	0.3	3.3	0.4	0.5	1.1
HUT	$D_i$	-0.2	$D_{i,m}$	0.4	-1.2	0.1		-1.6	-0.1	0.3	-0.7	-0.4	-0.4	-0.2	-1.0	-0.4	-0.3	1.0
	$U_i$	3.5	$U_{i,m}$	3.5	4.0	3.5		3.7	3.6	3.6	3.7	3.5	3.5	3.5	4.8	3.5	3.5	3.6
IFA	$D_i$	1.4	$D_{i,m}$	2.0	0.4	1.7	1.6		1.5	1.9	1.0	1.2	1.3	1.4	0.6	1.2	1.3	2.6
	$U_i$	1.1	$U_{i,m}$	1.3	2.3	1.2	3.7		1.5	1.4	1.7	1.2	1.2	1.2	3.5	1.2	1.2	1.6
KRISS	$D_i$	-0.1	$D_{i,m}$	0.5	-1.1	0.2	0.1	-1.5		0.4	-0.5	-0.3	-0.2	-0.1	-0.9	-0.3	-0.2	1.1
	$U_i$	1.0	$U_{i,m}$	1.1	2.2	1.0	3.6	1.5		1.3	1.6	1.1	1.1	1.0	3.4	1.0	1.1	1.5
NIM	$D_i$	-0.5	$D_{i,m}$	0.1	-1.5	-0.2	-0.3	-1.9	-0.4		-0.9	-0.7	-0.6	-0.5	-1.3	-0.7	-0.6	0.7
	$U_i$	0.8	$U_{i,m}$	1.0	2.2	0.9	3.6	1.4	1.3		1.5	0.9	0.9	0.8	3.4	0.9	0.9	1.3
NIST	$D_i$	0.5	$D_{i,m}$	1.1	-0.5	0.7	0.7	-1.0	0.5	0.9		0.3	0.3	0.4	-0.3	0.2	0.3	1.6
	$U_i$	1.2	$U_{i,m}$	1.4	2.4	1.3	3.7	1.7	1.6	1.5		1.3	1.3	1.3	3.5	1.3	1.3	1.6
NMi-VSL	$D_i$	0.2	$D_{i,m}$	0.8	-0.8	0.5	0.4	-1.2	0.3	0.7	-0.3		0.0	0.2	-0.6	0.0	0.1	1.4
	$U_i$	0.4	$U_{i,m}$	0.7	2.0	0.5	3.5	1.2	1.1	0.9	1.3		0.5	0.5	3.3	0.5	0.6	1.2
NPL	$D_i$	0.2	$D_{i,m}$	0.8	-0.8	0.4	0.4	-1.3	0.2	0.6	-0.3	0.0		0.1	-0.6	-0.1	0.0	1.3
	$U_i$	0.3	$U_{i,m}$	0.6	2.0	0.4	3.5	1.2	1.1	0.9	1.3	0.5		0.4	3.3	0.4	0.6	1.1
NRC	$D_i$	0.0	$D_{i,m}$	0.6	-1.0	0.3	0.2	-1.4	0.1	0.5	-0.4	-0.2	-0.1		-0.8	-0.2	-0.1	1.2
	$U_i$	0.2	$U_{i,m}$	0.6	2.0	0.3	3.5	1.2	1.0	0.8	1.3	0.5	0.4		3.3	0.3	0.5	1.1
OMH	$D_i$	0.8	$D_{i,m}$	1.4	-0.2	1.1	1.0	-0.6	0.9	1.3	0.3	0.6	0.6	0.8		0.6	0.7	2.0
	$U_i$	3.3	$U_{i,m}$	3.3	3.8	3.3	4.8	3.5	3.4	3.4	3.5	3.3	3.3	3.3		3.3	3.3	3.5
PTB	$D_i$	0.2	$D_{i,m}$	0.8	-0.8	0.5	0.4	-1.2	0.3	0.7	-0.2	0.0	0.1	0.2	-0.6		0.1	1.4
	$U_i$	0.2	$U_{i,m}$	0.6	2.0	0.4	3.5	1.2	1.0	0.9	1.3	0.5	0.4	0.3	3.3		0.5	1.1
SMU	$D_i$	0.1	$D_{i,m}$	0.7	-0.9	0.4	0.3	-1.3	0.2	0.6	-0.3	-0.1	0.0	0.1	-0.7	-0.1		1.3
	$U_i$	0.4	$U_{i,m}$	0.7	2.1	0.5	3.5	1.2	1.1	0.9	1.3	0.6	0.6	0.5	3.3	0.5		1.2
VNIOFI	$D_i$	-1.2	$D_{i,m}$	-0.6	-2.2	-0.9	-1.0	-2.6	-1.1	-0.7	-1.6	-1.4	-1.3	-1.2	-2.0	-1.4	-1.3	
	$U_i$	1.1	$U_{i,m}$	1.2	2.3	1.1	3.6	1.6	1.5	1.3	1.6	1.2	1.1	1.1	3.5	1.1	1.2	

Table A12. 1450 nm Unilateral and Bilateral Degrees of Equivalence (unit: %)

Lab <i>i</i>	Unilateral DoE		Lab <i>m</i>	BNM	CSIR	CSIRO	HUT	IFA	KRISS	NIM	NIST	NMi-VSL	NPL	NRC	OMH	PTB	SMU	VNIOFI
BNM	$D_i$	-0.8	$D_{i,m}$		-2.2	-0.5	-0.7	-2.3	-0.9	-0.1	-1.4	-1.0	-1.0	-0.9	-1.7	-0.8	-1.0	2.0
	$U_i$	0.5	$U_{i,m}$		2.1	0.6	3.5	1.3	1.1	1.1	1.1	0.7	0.7	0.6	3.5	0.6	0.7	1.3
CSIR	$D_i$	1.4	$D_{i,m}$	2.2		1.7	1.5	-0.1	1.3	2.1	0.8	1.1	1.1	1.2	0.5	1.3	1.1	4.2
	$U_i$	2.0	$U_{i,m}$	2.1		2.0	4.0	2.3	2.2	2.2	2.2	2.0	2.0	2.0	4.0	2.0	2.0	2.3
CSIRO	$D_i$	-0.3	$D_{i,m}$	0.5	-1.7		-0.2	-1.8	-0.4	0.4	-0.9	-0.5	-0.5	-0.4	-1.2	-0.3	-0.5	2.5
	$U_i$	0.2	$U_{i,m}$	0.6	2.0		3.5	1.2	1.0	1.0	0.9	0.5	0.5	0.3	3.4	0.4	0.5	1.2
HUT	$D_i$	-0.1	$D_{i,m}$	0.7	-1.5	0.2		-1.6	-0.2	0.6	-0.7	-0.3	-0.3	-0.2	-1.0	-0.1	-0.3	2.8
	$U_i$	3.5	$U_{i,m}$	3.5	4.0	3.5		3.7	3.6	3.6	3.6	3.5	3.5	3.5	4.9	3.5	3.5	3.6
IFA	$D_i$	1.5	$D_{i,m}$	2.3	0.1	1.8	1.6		1.4	2.2	0.9	1.2	1.2	1.3	0.6	1.4	1.2	4.3
	$U_i$	1.2	$U_{i,m}$	1.3	2.3	1.2	3.7		1.6	1.5	1.5	1.3	1.3	1.2	3.6	1.2	1.3	1.6
KRISS	$D_i$	0.1	$D_{i,m}$	0.9	-1.3	0.4	0.2	-1.4		0.8	-0.5	-0.2	-0.2	-0.1	-0.8	0.0	-0.2	2.9
	$U_i$	1.0	$U_{i,m}$	1.1	2.2	1.0	3.6	1.6		1.4	1.4	1.1	1.1	1.0	3.6	1.0	1.1	1.5
NIM	$D_i$	-0.7	$D_{i,m}$	0.1	-2.1	-0.4	-0.6	-2.2	-0.8		-1.3	-1.0	-1.0	-0.9	-1.6	-0.8	-1.0	2.1
	$U_i$	0.9	$U_{i,m}$	1.1	2.2	1.0	3.6	1.5	1.4		1.3	1.0	1.0	1.0	3.5	1.0	1.0	1.5
NIST	$D_i$	0.6	$D_{i,m}$	1.4	-0.8	0.9	0.7	-0.9	0.5	1.3		0.3	0.3	0.4	-0.3	0.5	0.3	3.4
	$U_i$	0.9	$U_{i,m}$	1.1	2.2	0.9	3.6	1.5	1.4	1.3		1.0	1.0	0.9	3.5	0.9	1.0	1.4
NMi-VSL	$D_i$	0.2	$D_{i,m}$	1.0	-1.1	0.5	0.3	-1.2	0.2	1.0	-0.3		0.0	0.1	-0.7	0.2	0.0	3.1
	$U_i$	0.4	$U_{i,m}$	0.7	2.0	0.5	3.5	1.3	1.1	1.0	1.0		0.6	0.4	3.4	0.5	0.6	1.2
NPL	$D_i$	0.2	$D_{i,m}$	1.0	-1.1	0.5	0.3	-1.2	0.2	1.0	-0.3	0.0		0.1	-0.7	0.2	0.0	3.1
	$U_i$	0.4	$U_{i,m}$	0.7	2.0	0.5	3.5	1.3	1.1	1.0	1.0	0.6		0.4	3.4	0.5	0.6	1.2
NRC	$D_i$	0.2	$D_{i,m}$	0.9	-1.2	0.4	0.2	-1.3	0.1	0.9	-0.4	-0.1	-0.1		-0.8	0.1	-0.1	3.0
	$U_i$	0.2	$U_{i,m}$	0.6	2.0	0.3	3.5	1.2	1.0	1.0	0.9	0.4	0.4		3.4	0.3	0.4	1.1
OMH	$D_i$	0.9	$D_{i,m}$	1.7	-0.5	1.2	1.0	-0.6	0.8	1.6	0.3	0.7	0.7	0.8		0.9	0.7	3.7
	$U_i$	3.4	$U_{i,m}$	3.5	4.0	3.4	4.9	3.6	3.6	3.5	3.5	3.4	3.4	3.4		3.4	3.4	3.6
PTB	$D_i$	0.0	$D_{i,m}$	0.8	-1.3	0.3	0.1	-1.4	0.0	0.8	-0.5	-0.2	-0.2	-0.1	-0.9		-0.2	2.9
	$U_i$	0.2	$U_{i,m}$	0.6	2.0	0.4	3.5	1.2	1.0	1.0	0.9	0.5	0.5	0.3	3.4		0.5	1.2
SMU	$D_i$	0.2	$D_{i,m}$	1.0	-1.1	0.5	0.3	-1.2	0.2	1.0	-0.3	0.0	0.0	0.1	-0.7	0.2		3.1
	$U_i$	0.4	$U_{i,m}$	0.7	2.0	0.5	3.5	1.3	1.1	1.0	1.0	0.6	0.6	0.4	3.4	0.5		1.2
VNIOFI	$D_i$	-2.8	$D_{i,m}$	-2.0	-4.2	-2.5	-2.8	-4.3	-2.9	-2.1	-3.4	-3.1	-3.1	-3.0	-3.7	-2.9	-3.1	
	$U_i$	1.1	$U_{i,m}$	1.3	2.3	1.2	3.6	1.6	1.5	1.5	1.4	1.2	1.2	1.1	3.6	1.2	1.2	

Table A13. 1500 nm Unilateral and Bilateral Degrees of Equivalence (unit: %)

Lab <i>i</i>	Unilateral DoE		Lab <i>m</i>	BNM	CSIR	CSIRO	HUT	IFA	KRISS	NIM	NIST	NMi-VSL	NPL	NRC	OMH	PTB	SMU	VNIOFI
BNM	$D_i$	-0.7	$D_{i,m}$		-2.4	-0.4	-0.8	-2.1	-1.1	-0.1	-1.7	-1.0	-1.0	-0.8	-1.3	-0.8	-0.9	2.4
	$U_i$	0.5	$U_{i,m}$		2.1	0.6	3.5	1.3	1.2	1.2	1.2	0.7	0.7	0.6	3.4	0.6	0.7	1.4
CSIR	$D_i$	1.7	$D_{i,m}$	2.4		2.0	1.6	0.4	1.4	2.4	0.8	1.4	1.4	1.6	1.1	1.6	1.6	4.9
	$U_i$	2.0	$U_{i,m}$	2.1		2.0	4.0	2.3	2.2	2.2	2.2	2.0	2.0	2.0	3.9	2.0	2.0	2.4
CSIRO	$D_i$	-0.3	$D_{i,m}$	0.4	-2.0		-0.4	-1.6	-0.7	0.3	-1.3	-0.6	-0.6	-0.4	-0.9	-0.4	-0.5	2.9
	$U_i$	0.3	$U_{i,m}$	0.6	2.0		3.5	1.2	1.0	1.0	1.0	0.5	0.5	0.3	3.4	0.4	0.5	1.3
HUT	$D_i$	0.1	$D_{i,m}$	0.8	-1.6	0.4		-1.2	-0.2	0.8	-0.8	-0.2	-0.2	0.0	-0.5	0.0	0.0	3.3
	$U_i$	3.5	$U_{i,m}$	3.5	4.0	3.5		3.7	3.6	3.6	3.6	3.5	3.5	3.5	4.8	3.5	3.5	3.7
IFA	$D_i$	1.3	$D_{i,m}$	2.1	-0.4	1.6	1.2		1.0	2.0	0.4	1.0	1.1	1.2	0.7	1.2	1.2	4.5
	$U_i$	1.2	$U_{i,m}$	1.3	2.3	1.2	3.7		1.5	1.5	1.5	1.2	1.2	1.2	3.6	1.2	1.2	1.7
KRISS	$D_i$	0.3	$D_{i,m}$	1.1	-1.4	0.7	0.2	-1.0		1.0	-0.6	0.1	0.1	0.2	-0.2	0.2	0.2	3.5
	$U_i$	1.0	$U_{i,m}$	1.2	2.2	1.0	3.6	1.5		1.4	1.4	1.1	1.1	1.0	3.5	1.0	1.1	1.6
NIM	$D_i$	-0.7	$D_{i,m}$	0.1	-2.4	-0.3	-0.8	-2.0	-1.0		-1.6	-0.9	-0.9	-0.8	-1.2	-0.8	-0.8	2.5
	$U_i$	1.0	$U_{i,m}$	1.2	2.2	1.0	3.6	1.5	1.4		1.4	1.1	1.1	1.0	3.5	1.0	1.1	1.6
NIST	$D_i$	0.9	$D_{i,m}$	1.7	-0.8	1.3	0.8	-0.4	0.6	1.6		0.6	0.7	0.8	0.3	0.8	0.8	4.1
	$U_i$	1.0	$U_{i,m}$	1.2	2.2	1.0	3.6	1.5	1.4	1.4		1.1	1.1	1.0	3.5	1.0	1.1	1.6
NMi-VSL	$D_i$	0.3	$D_{i,m}$	1.0	-1.4	0.6	0.2	-1.0	-0.1	0.9	-0.6		0.0	0.2	-0.3	0.2	0.1	3.5
	$U_i$	0.4	$U_{i,m}$	0.7	2.0	0.5	3.5	1.2	1.1	1.1	1.1		0.6	0.5	3.4	0.5	0.6	1.3
NPL	$D_i$	0.3	$D_{i,m}$	1.0	-1.4	0.6	0.2	-1.1	-0.1	0.9	-0.7	0.0		0.1	-0.3	0.2	0.1	3.4
	$U_i$	0.3	$U_{i,m}$	0.7	2.0	0.5	3.5	1.2	1.1	1.1	1.1	0.6		0.4	3.4	0.4	0.6	1.3
NRC	$D_i$	0.1	$D_{i,m}$	0.8	-1.6	0.4	0.0	-1.2	-0.2	0.8	-0.8	-0.2	-0.1		-0.5	0.0	0.0	3.3
	$U_i$	0.2	$U_{i,m}$	0.6	2.0	0.3	3.5	1.2	1.0	1.0	1.0	0.5	0.4		3.4	0.3	0.4	1.3
OMH	$D_i$	0.6	$D_{i,m}$	1.3	-1.1	0.9	0.5	-0.7	0.2	1.2	-0.3	0.3	0.3	0.5		0.5	0.4	3.8
	$U_i$	3.4	$U_{i,m}$	3.4	3.9	3.4	4.8	3.6	3.5	3.5	3.5	3.4	3.4	3.4		3.4	3.4	3.6
PTB	$D_i$	0.1	$D_{i,m}$	0.8	-1.6	0.4	0.0	-1.2	-0.2	0.8	-0.8	-0.2	-0.2	0.0	-0.5		0.0	3.3
	$U_i$	0.2	$U_{i,m}$	0.6	2.0	0.4	3.5	1.2	1.0	1.0	1.0	0.5	0.4	0.3	3.4		0.5	1.3
SMU	$D_i$	0.1	$D_{i,m}$	0.9	-1.6	0.5	0.0	-1.2	-0.2	0.8	-0.8	-0.1	-0.1	0.0	-0.4	0.0		3.3
	$U_i$	0.4	$U_{i,m}$	0.7	2.0	0.5	3.5	1.2	1.1	1.1	1.1	0.6	0.6	0.4	3.4	0.5		1.3
VNIOFI	$D_i$	-3.2	$D_{i,m}$	-2.4	-4.9	-2.9	-3.3	-4.5	-3.5	-2.5	-4.1	-3.5	-3.4	-3.3	-3.8	-3.3	-3.3	
	$U_i$	1.2	$U_{i,m}$	1.4	2.4	1.3	3.7	1.7	1.6	1.6	1.6	1.3	1.3	1.3	3.6	1.3	1.3	

Table A14. 1550 nm Unilateral and Bilateral Degrees of Equivalence (unit: %)

Lab <i>i</i>	Unilateral DoE		Lab <i>m</i>	BNM	CSIR	CSIRO	HUT	IFA	KRISS	NIM	NIST	NMi-VSL	NPL	NRC	OMH	PTB	SMU	VNIIOFI
BNM	$D_i$	-0.7	$D_{i,m}$		-3.1	-0.3	-0.6	-2.1	-0.7	0.2	-1.2	-1.0	-0.9	-0.8	2.0	-1.0	-1.0	2.9
	$U_i$	0.5	$U_{i,m}$		2.1	0.6	3.5	1.3	1.2	1.2	1.2	1.0	0.7	0.6	5.3	0.6	0.7	1.3
CSIR	$D_i$	2.4	$D_{i,m}$	3.1		2.8	2.5	1.0	2.4	3.3	1.9	2.1	2.2	2.3	5.1	2.1	2.1	6.0
	$U_i$	2.0	$U_{i,m}$	2.1		2.0	4.0	2.3	2.2	2.3	2.3	2.2	2.0	2.0	5.7	2.0	2.0	2.3
CSIRO	$D_i$	-0.4	$D_{i,m}$	0.3	-2.8		-0.3	-1.8	-0.4	0.5	-0.9	-0.7	-0.6	-0.5	2.3	-0.7	-0.7	3.2
	$U_i$	0.3	$U_{i,m}$	0.6	2.0		3.5	1.2	1.0	1.1	1.1	0.8	0.5	0.3	5.3	0.4	0.5	1.2
HUT	$D_i$	-0.1	$D_{i,m}$	0.6	-2.5	0.3		-1.5	0.0	0.9	-0.6	-0.4	-0.3	-0.2	2.7	-0.4	-0.3	3.6
	$U_i$	3.5	$U_{i,m}$	3.5	4.0	3.5		3.7	3.6	3.6	3.6	3.6	3.5	3.5	6.3	3.5	3.5	3.7
IFA	$D_i$	1.4	$D_{i,m}$	2.1	-1.0	1.8	1.5		1.4	2.3	0.9	1.1	1.1	1.3	4.1	1.1	1.1	5.0
	$U_i$	1.2	$U_{i,m}$	1.3	2.3	1.2	3.7		1.5	1.6	1.6	1.4	1.2	1.2	5.4	1.2	1.2	1.7
KRISS	$D_i$	0.0	$D_{i,m}$	0.7	-2.4	0.4	0.0	-1.4		0.9	-0.5	-0.4	-0.3	-0.1	2.7	-0.3	-0.3	3.6
	$U_i$	1.0	$U_{i,m}$	1.2	2.2	1.0	3.6	1.5		1.5	1.5	1.3	1.1	1.0	5.4	1.0	1.1	1.6
NIM	$D_i$	-0.9	$D_{i,m}$	-0.2	-3.3	-0.5	-0.9	-2.3	-0.9		-1.4	-1.2	-1.2	-1.0	1.8	-1.2	-1.2	2.7
	$U_i$	1.1	$U_{i,m}$	1.2	2.3	1.1	3.6	1.6	1.5		1.5	1.3	1.1	1.1	5.4	1.1	1.2	1.6
NIST	$D_i$	0.5	$D_{i,m}$	1.2	-1.9	0.9	0.6	-0.9	0.5	1.4		0.2	0.2	0.4	3.2	0.2	0.2	4.1
	$U_i$	1.1	$U_{i,m}$	1.2	2.3	1.1	3.6	1.6	1.5	1.5		1.3	1.1	1.1	5.4	1.1	1.2	1.6
NMi-VSL	$D_i$	0.3	$D_{i,m}$	1.0	-2.1	0.7	0.4	-1.1	0.4	1.2	-0.2		0.1	0.2	3.1	0.0	0.1	4.0
	$U_i$	0.8	$U_{i,m}$	1.0	2.2	0.8	3.6	1.4	1.3	1.3	1.3		0.9	0.8	5.3	0.8	0.9	1.4
NPL	$D_i$	0.2	$D_{i,m}$	0.9	-2.2	0.6	0.3	-1.1	0.3	1.2	-0.2	-0.1		0.1	3.0	-0.1	0.0	3.9
	$U_i$	0.3	$U_{i,m}$	0.7	2.0	0.5	3.5	1.2	1.1	1.1	1.1	0.9		0.4	5.3	0.4	0.6	1.3
NRC	$D_i$	0.1	$D_{i,m}$	0.8	-2.3	0.5	0.2	-1.3	0.1	1.0	-0.4	-0.2	-0.1		2.8	-0.2	-0.2	3.7
	$U_i$	0.2	$U_{i,m}$	0.6	2.0	0.3	3.5	1.2	1.0	1.1	1.1	0.8	0.4		5.3	0.3	0.5	1.2
OMH	$D_i$	-2.7	$D_{i,m}$	-2.0	-5.1	-2.3	-2.7	-4.1	-2.7	-1.8	-3.2	-3.1	-3.0	-2.8		-3.0	-3.0	0.9
	$U_i$	5.3	$U_{i,m}$	5.3	5.7	5.3	6.3	5.4	5.4	5.4	5.4	5.3	5.3	5.3		5.3	5.3	5.4
PTB	$D_i$	0.3	$D_{i,m}$	1.0	-2.1	0.7	0.4	-1.1	0.3	1.2	-0.2	0.0	0.1	0.2	3.0		0.0	3.9
	$U_i$	0.2	$U_{i,m}$	0.6	2.0	0.4	3.5	1.2	1.0	1.1	1.1	0.8	0.4	0.3	5.3		0.5	1.2
SMU	$D_i$	0.3	$D_{i,m}$	1.0	-2.1	0.7	0.3	-1.1	0.3	1.2	-0.2	-0.1	0.0	0.2	3.0	0.0		3.9
	$U_i$	0.4	$U_{i,m}$	0.7	2.0	0.5	3.5	1.2	1.1	1.2	1.2	0.9	0.6	0.5	5.3	0.5		1.3
VNIIOFI	$D_i$	-3.6	$D_{i,m}$	-2.9	-6.0	-3.2	-3.6	-5.0	-3.6	-2.7	-4.1	-4.0	-3.9	-3.7	-0.9	-3.9	-3.9	
	$U_i$	1.2	$U_{i,m}$	1.3	2.3	1.2	3.7	1.7	1.6	1.6	1.6	1.4	1.3	1.2	5.4	1.2	1.3	

Table A15. 1600 nm Unilateral and Bilateral Degrees of Equivalence (unit: %)

Lab <i>i</i>	Unilateral DoE		Lab <i>m</i>	BNM	CSIR	CSIRO	HUT	IFA	KRISS	NIM	NIST	NMi-VSL	NPL	NRC	OMH	PTB	SMU	VNIOFI
BNM	$D_i$	-0.6	$D_{i,m}$		-3.8	-0.3	0.0	-2.2	-0.9	0.3	-1.3	-1.0	-0.8	-1.0	1.4	-1.0	-0.8	3.4
	$U_i$	0.5	$U_{i,m}$		2.1	0.7	3.5	1.3	1.2	1.3	1.4	1.6	0.7	0.6	6.1	0.6	0.7	1.3
CSIR	$D_i$	3.2	$D_{i,m}$	3.8		3.5	3.7	1.6	2.8	4.1	2.5	2.8	3.0	2.8	5.2	2.7	3.0	7.1
	$U_i$	2.0	$U_{i,m}$	2.1		2.0	4.0	2.3	2.3	2.3	2.4	2.5	2.0	2.0	6.4	2.0	2.1	2.3
CSIRO	$D_i$	-0.3	$D_{i,m}$	0.3	-3.5		0.2	-1.9	-0.7	0.6	-1.0	-0.7	-0.5	-0.7	1.7	-0.8	-0.5	3.6
	$U_i$	0.3	$U_{i,m}$	0.7	2.0		3.5	1.2	1.1	1.3	1.3	1.5	0.5	0.4	6.1	0.4	0.6	1.2
HUT	$D_i$	-0.6	$D_{i,m}$	0.0	-3.7	-0.2		-2.1	-0.9	0.4	-1.2	-1.0	-0.8	-0.9	1.5	-1.0	-0.7	3.4
	$U_i$	3.5	$U_{i,m}$	3.5	4.0	3.5		3.7	3.6	3.7	3.7	3.8	3.5	3.5	7.0	3.5	3.5	3.7
IFA	$D_i$	1.6	$D_{i,m}$	2.2	-1.6	1.9	2.1		1.2	2.5	0.9	1.2	1.4	1.2	3.6	1.1	1.4	5.5
	$U_i$	1.2	$U_{i,m}$	1.3	2.3	1.2	3.7		1.6	1.7	1.7	1.9	1.3	1.2	6.2	1.2	1.3	1.7
KRISS	$D_i$	0.3	$D_{i,m}$	0.9	-2.8	0.7	0.9	-1.2		1.3	-0.3	-0.1	0.1	0.0	2.4	-0.1	0.2	4.3
	$U_i$	1.1	$U_{i,m}$	1.2	2.3	1.1	3.6	1.6		1.6	1.7	1.8	1.2	1.1	6.1	1.1	1.2	1.6
NIM	$D_i$	-0.9	$D_{i,m}$	-0.3	-4.1	-0.6	-0.4	-2.5	-1.3		-1.6	-1.3	-1.1	-1.3	1.1	-1.4	-1.1	3.0
	$U_i$	1.2	$U_{i,m}$	1.3	2.3	1.3	3.7	1.7	1.6		1.8	1.9	1.3	1.2	6.2	1.2	1.3	1.7
NIST	$D_i$	0.7	$D_{i,m}$	1.3	-2.5	1.0	1.2	-0.9	0.3	1.6		0.3	0.5	0.3	2.7	0.2	0.5	4.6
	$U_i$	1.3	$U_{i,m}$	1.4	2.4	1.3	3.7	1.7	1.7	1.8		1.9	1.4	1.3	6.2	1.3	1.4	1.7
NMi-VSL	$D_i$	0.4	$D_{i,m}$	1.0	-2.8	0.7	1.0	-1.2	0.1	1.3	-0.3		0.2	0.0	2.4	0.0	0.2	4.4
	$U_i$	1.4	$U_{i,m}$	1.6	2.5	1.5	3.8	1.9	1.8	1.9	1.9		1.5	1.5	6.2	1.5	1.5	1.9
NPL	$D_i$	0.2	$D_{i,m}$	0.8	-3.0	0.5	0.8	-1.4	-0.1	1.1	-0.5	-0.2		-0.2	2.2	-0.2	0.0	4.2
	$U_i$	0.4	$U_{i,m}$	0.7	2.0	0.5	3.5	1.3	1.2	1.3	1.4	1.5		0.5	6.1	0.5	0.6	1.2
NRC	$D_i$	0.4	$D_{i,m}$	1.0	-2.8	0.7	0.9	-1.2	0.0	1.3	-0.3	0.0	0.2		2.4	-0.1	0.2	4.3
	$U_i$	0.2	$U_{i,m}$	0.6	2.0	0.4	3.5	1.2	1.1	1.2	1.3	1.5	0.5		6.1	0.3	0.5	1.2
OMH	$D_i$	-2.0	$D_{i,m}$	-1.4	-5.2	-1.7	-1.5	-3.6	-2.4	-1.1	-2.7	-2.4	-2.2	-2.4		-2.5	-2.2	1.9
	$U_i$	6.0	$U_{i,m}$	6.1	6.4	6.1	7.0	6.2	6.1	6.2	6.2	6.2	6.1	6.1		6.1	6.1	6.2
PTB	$D_i$	0.4	$D_{i,m}$	1.0	-2.7	0.8	1.0	-1.1	0.1	1.4	-0.2	0.0	0.2	0.1	2.5		0.3	4.4
	$U_i$	0.3	$U_{i,m}$	0.6	2.0	0.4	3.5	1.2	1.1	1.2	1.3	1.5	0.5	0.3	6.1		0.5	1.2
SMU	$D_i$	0.2	$D_{i,m}$	0.8	-3.0	0.5	0.7	-1.4	-0.2	1.1	-0.5	-0.2	0.0	-0.2	2.2	-0.3		4.1
	$U_i$	0.4	$U_{i,m}$	0.7	2.1	0.6	3.5	1.3	1.2	1.3	1.4	1.5	0.6	0.5	6.1	0.5		1.3
VNIOFI	$D_i$	-4.0	$D_{i,m}$	-3.4	-7.1	-3.6	-3.4	-5.5	-4.3	-3.0	-4.6	-4.4	-4.2	-4.3	-1.9	-4.4	-4.1	
	$U_i$	1.1	$U_{i,m}$	1.3	2.3	1.2	3.7	1.7	1.6	1.7	1.7	1.9	1.2	1.2	6.2	1.2	1.3	

(Blank Page)